

# REPORT DOCUMENTATION PAGE

Form Approved  
OMB No. 0704-0188

Public reporting burden for this collection of information is estimated to average 1 hour per response, including the time for reviewing instructions, searching existing data sources, gathering and maintaining the data needed, and completing and reviewing the collection of information. Send comments regarding this burden estimate or any other aspect of this collection of information, including suggestions for reducing this burden, to Washington Headquarters Services, Directorate for Information Operations and Reports, 1215 Jefferson Davis Highway, Suite 1204, Arlington, VA 22202-4302, and to the Office of Management and Budget, Paperwork Reduction Project (0704-0188), Washington, DC 20503.

1. AGENCY USE ONLY (Leave blank) 2. REPORT DATE  
Feb 2000 3. REPORT TYPE AND DATES COVERED  
FINAL - 18 June 1997 - 29 Feb 2000

4. TITLE AND SUBTITLE  
"Investigating the Crevice Corrosion Behavior of Coated Stainless Steel in Seawater"

5. FUNDING NUMBERS  
Contract  
N00014-97-C-0216

6. AUTHOR(S)  
Robert M. Kain

7. PERFORMING ORGANIZATION NAME(S) AND ADDRESS(ES)  
LaQue Center for Corrosion Technology, Inc.  
702 Causeway Drive, P. O. Box 656  
Wrightsville Beach, NC 28480

8. PERFORMING ORGANIZATION  
REPORT NUMBER  
---

9. SPONSORING / MONITORING AGENCY NAME(S) AND ADDRESS(ES)  
Office of Naval Research  
800 N. Quincy Street  
Arlington, VA 22217-5660

10. SPONSORING / MONITORING  
AGENCY REPORT NUMBER  
---

11. SUPPLEMENTARY NOTES  
N/A

12a. DISTRIBUTION / AVAILABILITY STATEMENT  
UNLIMITED

12b. DISTRIBUTION CODE  
---

## 13. ABSTRACT (Maximum 200 words)

Normally, stainless steel is utilized without any type of coating whatsoever. However, there are occasions where coatings may be contemplated. One of present interest to the U.S. Navy is that associated with the use of antifouling coatings on ship hulls fabricated of non-magnetic, austenitic stainless steel. Testing in natural seawater has demonstrated that coatings can protect susceptible stainless steel from barnacle related crevice corrosion and localized corrosion at weldments. However, coating defects and damage create new areas for crevice corrosion to initiate. The risk of serious crevice corrosion damage to the substrate increases with the amount of bare metal exposed. Test results demonstrated that just a few square inches of bare stainless steel is sufficient to support the corrosion reactions producing penetrations in excess of 1.5 mm in less than six months. Even 6% Mo alloys are susceptible. Localized corrosion can be prevented by the use of cathodic protection, as demonstrated by testing with sacrificial zinc anodes. However, the apparent degree of polarization associated with zinc anodes may contribute to blistering and disbonding of the coating. Test results indicate that good surface preparation, expectedly, enhances bonding of the coating to the substrate. This degree of preparation also creates more optimum conditions for crevice corrosion propagation at sites which initiate.

14. SUBJECT TERMS  
stainless steel, crevice corrosion, coatings, antifouling, epoxy, seawater, testing, cathodic protection

15. NUMBER OF PAGES

16. PRICE CODE  
N/A

17. SECURITY CLASSIFICATION  
OF REPORT  
unclassified

18. SECURITY CLASSIFICATION  
OF THIS PAGE  
unclassified

19. SECURITY CLASSIFICATION  
OF ABSTRACT  
unclassified

20. LIMITATION OF ABSTRACT  
unlimited



**LaQUE CORROSION SERVICES**  
P.O. BOX 656 / Wrightsville Beach, NC 28480  
910-256-2271 FAX: 910-256-9816

**INVESTIGATING THE CREVICE CORROSION BEHAVIOR OF  
COATED STAINLESS STEEL IN SEAWATER  
(Contract N00014-97C-0216)**

***FINAL REPORT***

Prepared for

Office of Naval Research  
800 N. Quincy Street  
Arlington, VA 22217

Prepared by

Robert M. Kain  
LaQue Center for Corrosion Technology, Inc.  
702 Causeway Drive, P. O. Box 656  
Wrightsville Beach, NC 28480  
phone: 910/256-2271 fax: 910/256-9816  
email: info@laque.com web site: www.laque.com

**20000207 076**

February 2000

LaQUE CENTER FOR CORROSION TECHNOLOGY, INC.

**DQC QUALITY INSPECTED 1**



# REPORT DOCUMENTATION PAGE

Form Approved  
OMB No. 0704-0188

Public reporting burden for this collection of information is estimated to average 1 hour per response, including the time for reviewing instructions, searching existing data sources, gathering and maintaining the data needed, and completing and reviewing the collection of information. Send comments regarding this burden estimate or any other aspect of this collection of information, including suggestions for reducing this burden, to Washington Headquarters Services, Directorate for Information Operations and Reports, 1215 Jefferson Davis Highway, Suite 1204, Arlington, VA 22202-4302, and to the Office of Management and Budget, Paperwork Reduction Project (0704-0188), Washington, DC 20503.

1. AGENCY USE ONLY (Leave blank)		2. REPORT DATE Feb 2000	3. REPORT TYPE AND DATES COVERED FINAL - 18 June 1997 - 29 Feb 2000	
4. TITLE AND SUBTITLE "Investigating the Crevice Corrosion Behavior of Coated Stainless Steel in Seawater"			5. FUNDING NUMBERS Contract N00014-97-C-0216	
6. AUTHOR(S) Robert M. Kain				
7. PERFORMING ORGANIZATION NAME(S) AND ADDRESS(ES) LaQue Center for Corrosion Technology, Inc. 702 Causeway Drive, P. O. Box 656 Wrightsville Beach, NC 28480			8. PERFORMING ORGANIZATION REPORT NUMBER ---	
9. SPONSORING / MONITORING AGENCY NAME(S) AND ADDRESS(ES) Office of Naval Research 800 N. Quincy Street Arlington, VA 22217-5660			10. SPONSORING / MONITORING AGENCY REPORT NUMBER ---	
11. SUPPLEMENTARY NOTES N/A				
12a. DISTRIBUTION / AVAILABILITY STATEMENT UNLIMITED			12b. DISTRIBUTION CODE ---	
13. ABSTRACT (Maximum 200 words)  Normally, stainless steel is utilized without any type of coating whatsoever. However, there are occasions where coatings may be contemplated. One of present interest to the U.S. Navy is that associated with the use of antifouling coatings on ship hulls fabricated of non-magnetic, austenitic stainless steel. Testing in natural seawater has demonstrated that coatings can protect susceptible stainless steel from barnacle related crevice corrosion and localized corrosion at weldments. However, coating defects and damage create new areas for crevice corrosion to initiate. The risk of serious crevice corrosion damage to the substrate increases with the amount of bare metal exposed. Test results demonstrated that just a few square inches of bare stainless steel is sufficient to support the corrosion reactions producing penetrations in excess of 1.5 mm in less than six months. Even 6% Mo alloys are susceptible. Localized corrosion can be prevented by the use of cathodic protection, as demonstrated by testing with sacrificial zinc anodes. However, the apparent degree of polarization associated with zinc anodes may contribute to blistering and disbonding of the coating. Test results indicate that good surface preparation, expectedly, enhances bonding of the coating to the substrate. This degree of preparation also creates more optimum conditions for crevice corrosion propagation at sites which initiate.				
14. SUBJECT TERMS stainless steel, crevice corrosion, coatings, antifouling, epoxy, seawater, testing, cathodic protection			15. NUMBER OF PAGES	
			16. PRICE CODE N/A	
17. SECURITY CLASSIFICATION OF REPORT unclassified	18. SECURITY CLASSIFICATION OF THIS PAGE unclassified	19. SECURITY CLASSIFICATION OF ABSTRACT unclassified	20. LIMITATION OF ABSTRACT unlimited	



## TABLE OF CONTENTS

	<u>PAGE</u>
FOREWORD	i
EXECUTIVE SUMMARY	ii
EXPERIMENTALS DETAILS	1
RESULTS, DISCUSSION AND CONCLUSIONS	3
APPENDIX 1 -	Technical Paper "Crevice Corrosion Behavior of Coated Stainless Steel in Natural Seawater" by R.M. Kain
APPENDIX 2 -	Technical Paper "Use of Coatings to Assess the Crevice Corrosion Resistance of Stainless Steels in Warm Seawater" by R. M. Kain
APPENDIX 3 -	Atlas of Color Photographs
APPENDIX 4 -	Test Material Documentation
APPENDIX 5 -	Barrier and Antifouling Coatings 5a - Approved Coatings 5b - Product Information 5c - Coatings Application Details



## **FOREWORD**

Two technical papers (Appendices 1 and 2) have been prepared to describe the background, test preparations and results generated under this contract. For the purpose of this final report, the above are supplemented by an atlas of color photographs (Appendix 3) depicting the pre-test condition of test specimens, the applied coatings, exposure conditions, and the appearance of the various specimens after testing. Also provided are more elaborated details concerning the test materials, coatings selected, and the method of application.



## EXECUTIVE SUMMARY

The specific objective of the present research contract was to investigate the effect of barrier and antifouling coatings on the crevice corrosion behavior of stainless steel in natural seawater. Such research will ultimately benefit potential naval use of stainless steel for undersea devices, components or hulls of vessels for which austenitic stainless steels may be selected because of their non-magnetic properties. Offshore installations, coastal power utilities and other plants utilizing seawater may also benefit from this research.

The predominant failure mode for stainless steels in seawater is crevice corrosion. A test program to assess the influence of barrier and antifouling coatings systems on the crevice corrosion resistance of three different grades of austenitic stainless steels was devised and executed. The alloys tested were Type 316L (UNS S31603), the 22-13-5 alloy Nitronic-50 (UNS S20910) and the 20Cr-6Mo alloy AL6XN (UNS N08367). In addition to two epoxy barrier paint systems, antifouling coatings utilized for testing included a tributyltin-free polishing type system (ablative-Cu) and a biocide-free, low surface energy foul release (elastomeric) type system. Both welded and non-welded materials were tested. Welded specimens were tested in the fully coated condition, while non-welded specimens were either partially coated or prepared with intentionally scribed defects. Some flat specimens were exposed with unintentional coating defects along their edges. Other test variables included material surface finish, product form (sheet and pipe) and exposure conditions. A six-month test comprised exposure of partially coated (two area ratios of coated-to-bare metal) sheet and pipe specimens in controlled temperature (~85°F/30°C) filtered seawater. A longer term (12-month) test comprised exposure to ambient temperature natural seawater, with its complement of marine organisms. The latter test included specimens which were exposed with and without zinc anode protection. Key observations and conclusions are summarized below:

### **Bare Metal Behavior (one-year test)**

All of the bare stainless steel test panels were covered with tunicates (sea squirts), as well as with some barnacles and other crustaceans.



Welded Type 316L specimens exhibited crevice corrosion at barnacle sites, as well as localized pitting and tunneling attack which initiated at cut edges. They also suffered severe weld, adjacent fusion line and heat affected zone (HAZ) attack. When exposed with zinc anodes, the above material was fully resistant.

Welded Nitronic-50 also exhibited some barnacle related corrosion and edge attack, but no preferential weld-HAZ attack. Specimens with zinc anode attachments were fully resistant.

All uncoated AL6XN specimens exposed with or without zinc anodes were found to be fully resistant.

#### **Fully Coated Test Panels with Anodes (one-year test)**

No evidence of corrosion was found on any of the zinc protected, fully coated welded specimens, or fully coated non-welded specimens exposed with intentional or inadvertent defects.

Many of these cathodically protected specimens developed coating blisters, and a number experienced partial disbonding of the coating.

Coating disbondment was most apparent for those specimens coated with only epoxy barrier type paint to which marine growth became firmly attached.

It is quite likely that there is some optimum potential between that of zinc and freely corroding stainless steel that will not adversely affect the bonding.

Under the nominally quiescent test conditions, the ablative-Cu coated specimens developed only silt and slime-like fouling while those with the elastomeric type coating became encrusted with bryzoan. These results suggest that the barrier coating layers beneath the ablative-Cu coating provided effective insulation from the protected substrate, thus negating any significant loss of the ablative-Cu coating's antifouling properties due to polarization in the



electro-negative direction by the zinc. In contrast, the epoxy coated specimens were nearly fully covered with tunicates as well as some barnacles and other crustaceans.

#### **Fully Coated Non-welded Test Panels without Anodes (one-year test)**

When exposed without zinc anodes, no blistering developed in the coating and disbonding was limited to areas where crevice corrosion had developed. Except for superficial attack on one panel at a scribe site, the AL6XN specimens were otherwise unaffected. In contrast, several Type 316L and Nitronic-50 specimens incurred some "light" crevice attack adjacent to the scribe and at edge defect sites. These appeared mostly on those specimens with just the barrier coatings and those with the ablative-Cu applied over the two layers of epoxy.

#### **Partially Coated Test Panels without Anodes (six-month test)**

All three alloys tested incurred extensive crevice corrosion commencing at the coating interface with the bare metal portion of the specimens. However, variations in both affected area and depth of attack were found from side-to-side and specimen-to-specimen. Such variations are also often encountered in tests involving other types of crevice formers.

For Type 316L and Nitronic-50 there was a general trend that surfaces provided grit blasting were more affected than those left in the original mill 2B finish. It is believed that the greater adhesion afforded by the grit blasting helped to maintain some critical geometry which contributed to lateral propagation once initiation occurred.

Overall, AL6XN exhibited the greatest sensitivity to changes in exposed surface area. Affected crevice area and depth of attack diminished as the amount of exposed (cathodic) area was reduced.

#### **Partially Coated Pipe Specimens without Anodes (six-month test)**

Previous testing of alloy 625 (N06625) pipe had identified susceptibility to crevice corrosion under an epoxy barrier coating. In the present investigation, pipe samples of Type 316L stainless steel were partially coated with two different epoxy coating systems. One was the



1-coat brush applied type used previously on the alloy 625 pipe, and the other was the same 2-coat system applied to welded and non-welded test panels mentioned above.

All 24 pipes tested with the two different epoxy coating systems exhibited extensive crevice corrosion.

### **Overview**

Testing in natural seawater has demonstrated the propensity of crevice corrosion of stainless steels beneath coatings. When exposed without the benefit of cathodic protection, flat and curved surfaces of Type 316L initiated rapidly and incurred extensive propagation in most cases. More highly alloyed grades, including the 6Mo variety, were also seriously affected when the coating covered only a portion of the metal surface. Attack at defects in otherwise fully coated test panels was found to be minimal. However, it is conjectured that loss of coating adjacent to small defects could increase the risk of propagation. Obviously, the loss of larger areas of coating due to abrasion or other mishap should be cause for concern.

Because of the well documented susceptibility of stainless steel to crevice corrosion, it is highly probable that other alloys and alloy-coating system combinations would show similar behavior.



## **EXPERIMENTAL PROCEDURE**

Identification of the materials tested, specimen preparation, coatings application, and exposure conditions are summarized in the two reports located in Appendices 1 and 2. These are augmented by the pictorial description provided in the atlas of photographs in Appendix 3. For completeness of this final report, additional information related to the experimental procedure section of this final report are presented in Appendices 4 and 5.

### **Materials and Specimens**

Appendix 4 provides copies of the test material information sheets. Sheet test specimens were cut, welded, drilled, and stamped with permanent identification codes by Metal Samples Company, Munford, AL, from material in their inventory.

Pipe materials was acquired from a single heat of material and provided cut-to-length by another vendor. Pipe support holes were drilled in-house.

Additional testing of S20910 and N08367 was performed outside of the scope-of-work of this ONR contract. As-welded 1/2-inch thick plate test materials, identified in Appendix 2, were part of a separate test program conducted by the LaQue Center on behalf of Naval Surface Warfare Center - Carderock Division (NSWCCD). No information was provided concerning the actual chemistry of those two materials.

### **Surface Preparation**

All grit blasting described in the two reports was performed by a commercial shop principally involved with the application of thermal spray coatings. Fresh 80 mesh aluminum oxide was used to prepare the specimen surfaces for the coatings. Surface roughness of the mill-produced and grit blasted sheet materials is characterized in the Experimental Section of the Appendix 1 report and in Figures 1.1 to 4.3 in Appendix 3.

Prior to coating, the mill-produced and grit blasted surfaces were degreased with acetone. Next, those specimens intended to be tested with only part of the surface coated were masked



with 3M brand "best" paper and masking tape. As described in the Appendix 1 and Appendix 2 reports, respectively, sheet and pipe specimens were partially coated leaving 20% and 80% of the surface bare. In the case of the pipe samples, only the OD surfaces were coated.

### **Coating Systems**

A list of US Navy approved coatings was solicited from NAVSEA's Dr. Brenda Holmes (Appendix 5a). Ultimately, the LaQue Center selected an epoxy barrier paint system (Interguard®) and a polishing type antifouling coating (Interviron® BRA640), also known as an ablative-Cu type coating. Both are produced by Courtaulds Coatings - International Paint Company.

The LaQue Center also investigated and ultimately selected another antifouling coating (Intersleek®) from the same source. Intersleek is described in the product literature as both an "elastomeric foul release coating" and a "biocide-free, low surface energy foul release coating". Application of Intersleek required an intermediate tie coat. Product information sheets for all three coating systems cited above are found in Appendix 5b. Subsequent mention of these coatings in the two generated papers utilize only the generic identities "epoxy-barrier type", "ablative-Cu" and "elastomeric type".

After a careful review of the recommended paint mixing and spraying requirements, the coatings were applied at a nearby commercial auto body shop by a spray painter experienced with coating test panels for the LaQue Center. A dedicated spray room and dedicated spray equipment were provided. The only known deviation from the recommended procedure was in the use of a conventional spray gun over the airless type recommended on International Paint Co. literature for some of their coating products. Whereas the latter may be more conducive to spraying large ship hull surfaces, coating with the conventional spray gun provided more uniform coverage on the relatively small test panels. The step-by-step procedure used for coating the test panels and pipe systems is outlined in Appendix 5c.



In addition to tests with the three coating systems describe above, 12 pipe specimens were partially brush coated with another International product, Interlux®. This white, 2-part epoxy is the same paint that was utilized in earlier testing of nickel-base alloy 625 described by Hays (see reference 9 in Appendix 1 report).

### **Test Conditions**

Details of the seawater test conditions, including hydrology data, are also found in the two reports provided in Appendices 1 and 2. Photographic documentation of the pre-test condition of test specimens and arrangements for exposure are provided in Appendix 3.

## **RESULTS, DISCUSSION AND CONCLUSIONS**

Test results for the 12-month exposure of uncoated welded controls, fully coated welded panels and fully coated, but scribed, non-welded panels of S31603, S20910 and N08367, all with and without cathodic protection, are presented and discussed in the CORROSION/2000 (Paper No. 827) found in Appendix 1. That report also gives results from the 6-month test comprising partially coated panels of the same three materials. Photographic documentation is found in Appendix 3, Figures 1.1 to 37.3.

Results of the 6-month test comprising partially coated S31603 pipe specimens can be found in the report presented in Appendix 2, and Appendix 3, Figures 38.1 to 41.3. The (Appendix 2) report, which is to be presented in an ASTM Symposium on Marine Corrosion in Tropical Environments and published in ASTM STP 1399, also includes additional discussion on the three stainless steels tested for 6 months with 20% and 80% of the surfaces coated with the 2-layer epoxy system (see Appendix 3, Figures 26.1 to 29.3). Also presented is a summary of results from a related investigation on the crevice corrosion behavior of partially coated, welded S20910 and N08367 specimens which was conducted outside of the scope of this present ONR contract. As discussed in the Appendix 2 report, this latter group of specimens were prepared with a single layer of brush applied red epoxy coating (same as first coat in the principal investigation).



Both of the reports contain a number of conclusions derived from the testing of 292 specimens. The principal conclusion drawn is that there is a significant risk of crevice corrosion when partially coated stainless steel is exposed to natural seawater. Even the higher alloyed 6Mo grade incurred some attack in excess of 1 mm deep within 6 months. There is no reason to believe that other crevice corrosion susceptible stainless steels would not suffer attack under similar conditions. Moreover, coatings produced by other manufacturers are also likely to promote attack on these grades of stainless steel. Testing also revealed that crevice corrosion can initiate at defect sites on otherwise fully coated material. Although the observed propagation at these sites was considered superficial, more significant attack might result if the cathodic surface area is enlarged, due to coating loss at the original defect site.

Comparative testing of the three stainless steels with zinc anodes revealed that protection against crevice corrosion at coating defect sites was achievable. However, the apparent degree of polarization offered by the zinc anodes contributed to coating blisters and disbondment.

While zinc anodes were not included in the testing of partially coated panels, they were utilized on the uncoated controls and found to be effective in eliminating barnacle related crevice corrosion and exposed edge attack of S31603 and S20910. Moreover, S31603 was protected from weld and weld heat affect zone corrosion. Uncoated N08367 specimens were fully resistant when not coated and exposed for one year with and without zinc anodes.

### **REFERENCES**

The two reports included in Appendices 1 and 2 cite approximately 20 references which deal with crevice corrosion in general, and prior experience related to coatings. Most address stainless type alloy performance in natural seawater.



## **APPENDIX 1**

### **“Crevice Corrosion Behavior of Coated Stainless Steels in Natural Seawater”**

by  
Robert M. Kain

Paper #827 presented at CORROSION/2000  
NACE International T-7C Symposium on Marine Corrosion  
Orlando, FL, March 28, 2000



## **"Crevice Corrosion Behavior of Coated Stainless Steels in Natural Seawater"**

### ***ERRATA***

Page 6, 4th paragraph, line 2 - delete "%" after 11.

Page 6, 4th paragraph, line 4 - insert the underlined "Only a single scribed site on one of the elastomeric coated N08367 panels showed...crevice corrosion"



## CREVICE CORROSION BEHAVIOR OF COATED STAINLESS STEEL IN NATURAL SEAWATER

R. M Kain

LaQue Center for Corrosion Technology, Inc.  
702 Causeway Drive, P. O Box 656, Wrightsville Beach, NC 28480 USA

### ABSTRACT

Normally, stainless steels are utilized without any type of coating whatsoever. This report cites a few cases where coatings may be contemplated for use on stainless steels. Of particular interest is the use of various antifouling type coating systems applied over anticorrosion barrier coating systems for seawater service. Testing in natural seawater has demonstrated that coatings can protect susceptible stainless steel from barnacle related crevice corrosion and localized corrosion at weldments. However, coating defects and other unintentional or intentional interfaces with bare metal may create new areas for crevice corrosion to initiate. The risk of serious crevice corrosion damage to the substrate increases with the amount of bare metal exposed. Test results demonstrated that even a relatively small area of bare stainless steel is sufficient to support cathodic reactions that produce crevice corrosion penetrations in excess of 2 mm in less than six months. Even a 6% Mo alloy was susceptible. It was demonstrated that localized corrosion can be prevented by the use of cathodic protection from sacrificial zinc anodes. However, the degree of polarization associated with zinc anodes contributed to blistering and disbonding of the coating in some cases. The current test program did not investigate protection afforded by inorganic zinc-rich primers.

Keywords: stainless steel, crevice corrosion, natural seawater, coatings, antifouling, ablative-Cu, elastomeric, epoxy, cathodic protection, zinc anodes

### Copyright

©2000 by NACE International. Requests for permission to publish this manuscript in any form, in part or in whole must be in writing to NACE International, Conferences Division, P.O. Box 218340, Houston, Texas 77218-8340. The material presented and the views expressed in this paper are solely those of the author(s) and are not necessarily endorsed by the Association. Printed in U.S.A.



## INTRODUCTION

Over the past two decades there have been numerous investigations dealing with crevice corrosion and its effects on stainless steels and related alloys. Those addressing alloy behavior in seawater are important to naval and other marine interests. As described elsewhere<sup>1</sup>, previous work has covered the influence of alloy composition, surface finish, crevice geometry, area ratio and galvanic effects on crevice corrosion behavior. In addition, variations in seawater test location<sup>2</sup>, seawater temperature and exposure time<sup>3</sup>, and other factors such as chlorination, deaeration and stagnation have also been addressed<sup>4</sup>.

Previously, Sedriks<sup>5</sup> identified the types of crevices which appear to be problematic for seawater service. Most often these are deep-tight crevices of the type associated with metal-to-non-metal joints and other connections. Research has demonstrated that while such crevices are most likely to promote crevice corrosion of susceptible alloys, metal-to-metal crevices having the same geometry with respect to depth and tightness (gap parameter) can be equally or more severe.<sup>6</sup> This is attributed to two metal surfaces contributing to hydrolysis reactions within the crevices. Most crevice corrosion test programs reported in the open literature have dealt with metal-to-non-metal type crevices. These have included serrated and continuous annular-type washers, O-rings, strips, compression fittings and sleeves fashioned from PTFE, rubber and various plastic and vinyl type materials.<sup>7</sup>

In a few reported cases comprising actual in-service and testing conditions, crevice corrosion has been observed under coatings. Klein et al.,<sup>8</sup> for example, reported crevice corrosion of 6% Mo stainless alloy tubing (ID) at sites created accidentally by oversprayed epoxy paint coating applied to a condenser tube sheet. However, subsequent simulation tests in which ID surfaces of the same alloy tubing were partially coated did not produce any crevice attack in six months.<sup>8</sup> In contrast, application of the same coating on the OD surfaces of alloy 625 (N06625) pipes promoted accelerated corrosion in chlorinated seawater tests of 1-year duration.<sup>9</sup> However, as noted by Sedriks<sup>1</sup> this corrosion occurred at sites where the epoxy coating was contained within vinyl sleeves of the type known to produce attack of alloy 625 and other materials in the absence of an epoxy coating. Lee<sup>10</sup> and Kain<sup>11</sup> discussed problems with coatings associated with remote crevice corrosion testing of stainless steel and nickel-base alloys. Others<sup>12</sup> have also reported crevice corrosion of nickel-base alloys under coatings.

In the above examples, paint covered portions of the alloy surfaces, thereby creating situations where the coating-metal interface served as the mouth of the crevice. Larger, boldly exposed alloy surfaces served as effective cathodic areas to drive the crevice corrosion initiation and propagation process.

Except in a few cases, the main objectives of various testing programs were not to determine the effect of coatings on the crevice corrosion resistance of stainless steel. The present work is intended to help fill this apparent void. While stainless steels are used predominately without coatings, there are occasions where coatings have been or conceivably could be used. Coating of stainless steels has been suggested, for example, as one way to mitigate galvanic corrosion when stainless steel is the cathodic member of a dissimilar metal couple.<sup>13</sup> Use of stainless steel in seawater carries a risk of macrofouling, and the creation of natural crevice sites; for example, under barnacles which can attach in slowly moving or quiescent seawater.<sup>1</sup> Application of an antifouling paint system would prevent such attachments, and minimize fouling in general. However, in light of some earlier findings, the possibility exists that these coatings systems could promote crevice corrosion. This paper describes the preparation, coating and testing results for 180 stainless steel specimens exposed to natural seawater for up to one year.

## EXPERIMENTAL

### Materials/Specimens

Three grades of austenitic stainless steel were selected for testing, Type 316L (UNS S31603), a 6% Mo superaustenitic (UNS N08367) and a Cr-Ni-Mn-Mo variety (UNS S20910). Table 1 lists the actual chemical compositions of the sheet materials used for making the test specimens. Note that two heats of S31603 were



involved. A total of 60 panels measuring 4-inch x 12-inch x ~1/8-inch (100 mm x 400 mm x 3 mm) were cut and prepared for each stainless steel.

A total of 24 specimens of each alloy were butt welded by the tungsten inert gas (GTAW) process, leaving raised weld beads on both sides. Whereas, matching filler metal was used in welding of the S31603 and S20910 panels, alloy 625 (N06625) filler was used to weld the N08367 test panels. All 24 welded S31603 panels were from heat #1 material, while the remaining 36 non-welded panels were from heat #2 material.

Preparation. Each of the sheet metal panels were provided with one or two drilled 1/2-inch (13 mm) diameter holes to facilitate attachment of zinc anodes and/or identification tags. In addition, each panel was stamped with an identification code number.

All panel edges were rounded with a belt sander to enhance retention of the coatings that was subsequently applied. Panels were then degreased with acetone. Next, all surfaces of the welded panels were grit blasted with 80-mesh aluminum oxide to create a suitable surface anchor profile for enhanced coating adhesion. For the non-welded panels, one of the bold surfaces was intentionally left in the mill finish condition. This was accomplished by temporarily bonding two panels together with double-sided "carpet tape" and grit blasting the exposed surfaces. After separation, the specimens were scrubbed with a nylon bristle brush and rinsed with acetone to remove blasting dust and any residual adhesive from the tape. From this point onward the specimens were handled with gloves to prevent possible surface contamination.

Surface Roughness. Three specimens of each alloy were selected randomly for determination of surface roughness of the original mill finish, and the grit blasted surfaces. A hand-held digital surface roughness indicator (Rank Taylor Holson - Surtronic 10) was utilized. Table 2 gives the average surface roughness values based on nine measurements (three per panel side). As can be seen, grit blasting significantly enhanced the 2B mill-produced surfaces of the S31603 and S20910 material, but had minimal affect on the already rough N08367 mill surfaces.

Typically, a 2 to 3 mil (50 to 75  $\mu\text{m}$ ) anchor pattern profile is recommended (e.g., SSPC - SP10) in preparation for painting of carbon steel. The target profile for the stainless steel test panels was 1 to 2 mils (25 to 50  $\mu\text{m}$ ). Based on post-test cross-sectional metallographic examination of randomly selected specimens (see, for example, Figure 1), a profile of less than 1 mil (25.4  $\mu\text{m}$ ) was actually achieved for these stainless steels with the 80-mesh alumina grit blasting.

## Coating Systems

On vessels with carbon steel hulls, it is standard practice to apply an anti-corrosion barrier coating which is subsequently topcoated with antifouling paint. For the present series of tests, the barrier coating comprised two layers (gray over red) of a 2-part epoxy, applied by spraying. The generically identified antifouling coatings were an ablative copper (Cu) type (red) and a low surface energy elastomeric (black). These were spray applied over the barrier coating according to the manufacturers' recommendations. The elastomeric paint system comprised an intermediate tie coat applied over the second layer of barrier coating. Equal numbers of anticorrosion coated specimens were prepared with and without antifouling coating. Six welded sheet specimens of each alloy left in the uncoated condition.

## Preparation and Exposure of Fully Coated Panels for One-Year Test

All welded and non-welded panels intended for one-year exposure to natural seawater fouling conditions were fully coated. A pretest inspection, however, revealed the presence of coating "defects" on some specimen edges where paint coverage was more difficult and where "blind" sites were created at panel supports during spraying. Based on post-test, dry film thickness measurements on randomly selected panels, the thickness of the



two coats of epoxy was approximately 10 mils (250  $\mu\text{m}$ ). Total thickness of the ablative Cu and elastomeric paint systems (including the barrier coats) was approximately 15 mils (375  $\mu\text{m}$ ) and 20.5 mils (513  $\mu\text{m}$ ), respectively.

Intentional coating defects were created on both sides of the non-welded specimens by introducing a 8-inch (203 mm) long scribe through all layers of paint with a carbide tipped (lathe/shaper type) tool.

One-half of the total number of painted specimens intended for the one-year test were fitted with two 1-inch (25.4 mm) diameter zinc anodes, which were secured with S31600 stainless steel fasteners (Figure 2). A circular cutting tool was used to remove the layers of paint down to bare metal to facilitate mating with the anode surface.

Using porcelain insulators, the specimens were mounted on aluminum exposure racks (Figure 3). A total of six racks, each with 18 coated panels, and one rack with 18 uncoated, welded control specimens (9 with and 9 without anodes) were exposed. Each rack held one welded and one non-welded (with defect) panel of each of the three alloys and the three coating systems. Three racks held coated specimens protected by zinc anodes, and three more with freely corroding specimens. Each rack also held one PVC fouling control panel and one 90/10 CuNi (UNS C70600) antifouling control panel.

Conditions. The seven racks, containing a total of 126 stainless steel panels, were suspended about 18-inches below the seawater surface from the LaQue Center's test float located on Banks Channel, Wrightsville Beach, NC. Testing commenced in late summer at an ambient seawater temperature of 25.7°C. During the one-year period, temperatures ranged from 5.1°C to 29.6°C. The mean temperature was 13.4°C for the initial six months, and 18.2°C for the 12 months. Table 2 provides a summary of the seawater hydrology for the first and last six months of the test.

#### **Preparation and Exposure of Partially Coated Specimens for 6-Month Filtered Seawater Test**

A total of 54 specimens were masked and spray painted with the three coating systems described above, leaving 20% or 80% of the total surface bare, see Figure 4. The intention of the partial coating was two-fold; first, to create potential crevice sites at the bare metal-to-coating interface and second, to investigate effect of cathodic surface size on crevice corrosion behavior. This was intended to simulate coating damage or disbondment over small or large areas.

Conditions: Figure 5 shows the method of supporting the partially coated panels which were exposed in a 193 gal. (730 L) capacity polyethylene tank plumbed with PVC piping. Filtered (5  $\mu\text{m}$ ) seawater was continually introduced at a rate of 0.3 gpm (~1.1 L/min) which provided the equivalent of 2.2 complete changes daily. Quartz heaters were used during the colder months to maintain the seawater temperature above 25°C. The average temperature was 30.8°C during this 6-month test. A recirculation pump provided uniform heating within the tank.

The source seawater hydrology for this 6-month test was the same as that shown in Table 2 for the initial 6 months.

#### **Post-test Cleaning and Assessment**

Following an initial post-test inspection, the 6-month test specimens were washed using low pressure tap water and scrubbed with a nylon bristle brush to remove the accumulated corrosion products. This also resulted in the removal of some of the coatings, particularly those applied to the mill (2B finish) surfaces of the S31603 and S20910 specimens. A plastic scraper was used to remove additional areas of disbonded paint to facilitate inspection for crevice attack. Next, the bare metal portions of the panels were dipped in 30%  $\text{HNO}_3$  at room temperature to remove the calcareous deposits and reveal the specimen identification codes. Cleaning of the 12-month specimens was limited to removal of the accumulated fouling, brushing with tapwater and some scraping



around affected areas. In addition to measuring the affected area of each crevice site, maximum depths of attack were determined with a needle point dial depth indicator.

## RESULTS AND DISCUSSION

### Six-Month Test, Filtered Seawater

Testing in the filtered seawater tank initially provided an opportunity for in-situ inspection of the partially coated panels. Evidence of crevice corrosion at the paint-to-bare metal interfaces was detected on a number of specimens ranging from a few days to a few weeks. It was also apparent that calcareous mineral deposits were developing on the exposed, cathodic surfaces of the panels.

Figure 6 provides after-cleaning examples of crevice corrosion affecting the partially coated specimens. Tables 4 to 6 identify the surfaces which incurred crevice corrosion and provide data on propagation in terms of affected area and maximum depth of attack.

S31603. From Table 4, it can be seen that all 18 partially coated S31603 specimens exhibited some degree of attack on both the grit blasted and mill-produced 2B surfaces. Those specimens with only 20% paint coverage (larger cathodic surface exposed) generally incurred the most attack in terms of affected area. Results indicate no major differences in affected area relative to surface condition. However, for those panels with 80% paint coverage (smaller cathodic area), there was consistently less attack found on the mill-produced surfaces. Table 4 also shows that the Type 316L panels painted with the elastomeric antifouling system consistently exhibited less attack than those with the abrasive-Cu coating or just the anti-corrosion barrier coating.

Table 4 shows that depths of attack for the partially coated S31603 specimens ranged from 0.01 mm (slightly more than an etch) to over 2 mm in six months. The most reproducible results among replicate specimens is observed for the grit blasted surfaces 20% coated with the barrier and abrasive Cu systems, and the mill surfaces 80% coated with the barrier system.

N08367. From Table 5, it can be seen that 50% of the primary crevice sites created at the coating interfaces were found to be resistant. Most of these were present on the panels 80% coated. For those panels 20% coated, there were more resistant sites on the mill finished surfaces than on grit blasted surfaces. However, for those mill surfaces on which attack did initiate the affected areas were larger relative to the affected grit blasted surfaces. Overall, the affected areas on the grit blasted surfaces of N08367 panels were similar or smaller than those found on comparable S31603 surfaces. The data shown in Table 5 suggest that the overall resistance of N08367 to initiation and lateral propagation beneath the coating was independent of the coating system applied.

From Table 5, it can be seen that N08367 test panels incurred penetrations which ranged in depth from 0.01 mm to 1.25 mm. This is similar to the range observed over 60% of the sites on the S31603 panels. For the grit blasted surfaces, those with 80% paint coverage consistently exhibited the least penetration.

S20910. Crevice corrosion was also detected at all 36 coating/bare metal interfaces on the S20910 panels. The affected areas are indicated in Table 6. Overall, the mill surfaces, particularly those with 80% paint coverage, were the least affected. Panels with only 20% paint coverage may have been influenced by the applied coating. As with S31603, S20910 panels with the elastomeric system were on average more resistant to lateral propagation than those with either the abrasive-Cu system or the barrier coatings alone. Similar behavior is suggested by the data for mill-finish surfaces 80% coated.

Maximum depth of attack results for the partially coated S20910 specimens are also provided in Table 6. The overall range measured (<0.01 mm to 1.97 mm) was comparable to that noted above for S31603 panels. The deepest attack was found on grit blasted surfaces 20% coated with the barrier plus antifouling paints. With only



one exception, surfaces prepared by grit blasting exhibited deeper penetrations than those with the coating applied directly over the mill finish.

## One-Year Test Overview

All seven test racks described above were exposed from the LaQue Center's test float for one full year. One test rack, including the unprotected coated specimens mounted on it, was briefly removed after six months for an interim inspection. An appreciable amount of marine fouling was observed on test specimens with the epoxy barrier coating only. Under these nominally quiescent conditions, even the elastomeric coated panels were encapsulated in fouling, predominately encrusting bryzoa. The degree of fouling obscured visual inspection of the scribed defects without disturbance, except for the panels coated with the ablative Cu which exhibited no evidence of crevice corrosion.

In the ensuing six months, the degree of fouling increased, especially the development of tunicates (sea squirts), on the barrier coated specimens. It was observed that the presence of zinc anodes did not alter the antifouling characteristics of the ablative Cu coating. This is apparently due to effective isolation of barrier paint coatings. It is also conceivable that the Cu-containing coating was not sufficiently conductive to be influenced by the anodes.

Cathodic Disbondment. Removal of the tunicates from the cathodically protected barrier coated panels also resulted in removal of large areas of coating. While disbondment occurred on mill-produced and grit blasted surfaces for all three alloys, it was most prevalent on the S31603 and S20910 panels. Since there was little in the way of tunicate attachments on the elastomeric coated panels, and none on the ablative-Cu coated ones, any cathodic disbondment was not apparent on those specimens at this stage of the inspection. However, as described below, blistering of the coatings was detected.

## Final One-Year Inspection Results for Coated Specimens Without Zinc Anodes

Table 7 summarizes the after-cleaning inspection results for the 27 non-welded, coated specimens tested with intentional scribed defects. As shown, 11% of the 54 scribed areas were affected; most of the affected sites were on panels with the ablative-Cu coating applied over the barrier coating and mainly S31603 and S20910 test panels (see Figure 7). Only a single scribed site on the N08367 panels showed evidence of superficial crevice corrosion. Very shallow attack ( $\leq 0.01$  mm) was found at the affected scribe areas. This can be attributed to the insignificant cathodic surface area available to support crevice corrosion propagation. As indicated by the letter code E in Table 7, some specimens exhibited areas of superficial crevice attack extending inward from the panel edges. This attack may have initiated at some of the coating defect sites observed before exposure, or created at the porcelain insulator mounting locations.

Table 8 gives the after-cleaning inspection results for the 27 fully coated (without intentional defects) welded specimens exposed without cathodic protection from zinc anodes. No evidence of corrosion products, indicative of crevice corrosion, was found anywhere on these specimens, including locations associated with the specimen mounting sites. Moreover, there was no evidence of coating blisters or disbondment. Accordingly, the intact coatings were not removed to verify the absence of attack on the substrate.

## Final One-Year Inspection Results for Coated Specimens Exposed With Zinc Anodes

No evidence of crevice corrosion was detected on any of the fully coated specimens (with and without scribed or other defects) exposed with zinc anodes. However, coating blisters and some instances of coating disbondment were observed.



Table 9 summarizes the incidence of blistering and significant coating disbondment for the various substrates. It should be recalled that both surfaces of the welded specimens were grit blasted prior to coating, while non-welded specimens were blasted only on one surface. From Table 9, it is evident that the highest incidence of blistering occurred for specimens with the barrier and ablative-Cu coatings. Many of the specimens with only the barrier coating exhibited disbondment. However, disbondment was observed on only a few specimens with antifouling coatings which can be ascribed to prevention of tunicate attachments. Surface preparation and coating type notwithstanding, N08367 substrate exhibited the least coating disbondment. The S31603 panels exhibited the least number of surfaces with blisters. For S31603 and S20910 panels, there was a greater tendency for blistering on the as-produced mill surfaces than those grit blasted. On the other hand, surface preparation did not appear to influence large scale disbondment of the coating on these panels.

#### Uncoated Welded Specimens

As expected, all test panels cathodically protected with the zinc anodes were resistant to localized corrosion during the one-year test period. All three welded N08367 specimens exposed without zinc anodes were also fully resistant. In the case of unprotected S20910, several cases of barnacle related crevice corrosion and localized attack on specimen edges were found on two of the three welded specimens. In contrast, all three unprotected S31603 specimens exhibited barnacle related crevice attack on both surfaces, edge attack, and very extensive corrosion at the weld-to-base metal interface and adjacent heat affected zone (HAZ). An example of the barnacle and weld attack incurred by the S31603 specimens is shown in Figure 8. Several S31603 and S20910 panels also exhibited tunneling which propagated from edge pits.

### SUMMARY AND CONCLUSIONS

The predominant failure mode for stainless steels in seawater is crevice corrosion. A test program to assess the influence of barrier and antifouling coatings systems on the crevice corrosion resistance of three different grades of austenitic stainless steels was devised and executed. The alloys tested were UNS S31603, UNS S20910 and UNS N08367. In addition to epoxy barrier paint, antifouling coatings include ablative-Cu and a low surface energy elastomeric type system. Both welded and non-welded materials were tested. Welded specimens were tested in the fully coated condition while non-welded specimens were either partially coated or prepared with intentionally scribed defects. Other test variables included material surface finish and exposure conditions. A six-month test comprised exposure of partially coated (two area ratios of coated-to-bare metal) panels in warm, controlled temperature, filtered seawater. A longer term (12-month) test comprised exposure to ambient temperature natural seawater, with its complement of marine organisms. The latter test included specimens which were exposed with and without zinc anode protection. The following key observations and conclusions are presented:

#### Bare Metal Behavior (one-year test)

Welded S31603 specimens exhibited crevice corrosion at barnacle sites, localized pitting and tunneling attack originating at cut edges, as well as severe weld and adjacent fusion line/heat affected zone attack. When exposed with zinc anodes, S31603 was fully resistant.

Welded S20910 also exhibited some barnacle related corrosion and edge attack, but none at the weldment. Specimens with zinc anodes were fully resistant to corrosion.

All N08367 specimens exposed with or without zinc anodes were fully resistant to corrosion.



### **Partially Coated Sheet Specimens (six-month test)**

All three alloys tested incurred extensive crevice corrosion which initiated at the coating/bare metal interface. However, variations in both affected area and depth of attack were found from side-to-side and specimen-to-specimen. Such variations are also encountered in tests involving other types of crevice formers.

For S31603 and S20910 grit blasted surfaces were generally more affected than those with the original 2B mill finish. It is believed that the much better adhesion to grit blasted surfaces resulted in a more critical crevice geometry which contributed to lateral propagation of attack beneath the coating.

Exposed surface area appeared to have the greatest influence on N08367. Affected crevice area and depth of attack diminished as the amount of exposed (cathodic) area was reduced.

### **Fully Coated Specimens With Anodes (one-year test)**

No evidence of corrosion was found on any of the cathodically protected, fully coated welded specimens or fully coated non-welded specimens exposed with intentional or inadvertent defects.

Many of the cathodically protected specimens developed coating blisters and a number experienced partial disbonding of the coating.

Coating disbondment was most apparent for those specimens coated with only epoxy barrier type paint to which marine growth became firmly attached.

Under the nominally quiescent test conditions, the ablative-Cu coated specimens developed only silt and slime-like fouling while those with the elastomeric type coating became encrusted with bryzoa. These results indicate that antifouling characteristics of the ablative-Cu coating were not affected by the anodes attached to the substrate. In contrast, bare and epoxy coated specimens were nearly fully covered with tunicates (sea squirts), and some barnacles and other crustaceans.

### **Fully Coated Non-welded Specimens Without Anodes (one-year test)**

When exposed without zinc anodes, no blistering developed in the coating; and disbonding appeared to be limited to areas where crevice corrosion had developed. Except for superficial attack on one panel at a scribe site, the N08367 specimens were otherwise unaffected.

In contrast, several S31603 and S20910 specimens incurred very minor crevice attack adjacent to the scribe. This appeared mostly on those specimens with the ablative-Cu applied over the epoxy anticorrosion barrier.

### **General Comments**

It remains uncertain if stainless steel prepared with other surface treatments or coated with an inorganic zinc primer beneath the epoxy barrier coating would have behaved significantly differently.

### **REFERENCES**

1. A. J. Sedriks, *Corrosion of Stainless Steels*, 2nd edition, Chapter 5 - Crevice Corrosion, Wiley-Interscience Publication, John Wiley & Sons, Inc., 1996.
2. R. M. Kain, *Journal of Testing & Evaluation*, (Sept. 1990): p. 309.



3. R. M. Kain, "Evaluation of Crevice Corrosion Susceptibility," CORROSION/96, Research Symposium, (Houston, TX: NACE International, 1996).
4. R. M. Kain, A. Zeuthen, J. Maurer, "Localized Corrosion Resistance of Stainless Type Materials in Aerated, Deaerated, and Stagnant Sulfide Bearing Seawater", CORROSION/97, paper no. 423, (Houston, TX: NACE International, 1997)
5. A. J. Sedriks, International Metals Review 27, (1982): p. 321.
6. J. W. Oldfield, W. H. Sutton, British Corrosion Journal 13, (1978): p. 104.
7. ASTM G78-95 Standard Guide for Crevice Corrosion Testing of Iron-Base and Nickel-Base Stainless Alloys in Seawater and Other Chloride Containing Aqueous Environments, Vol. 03.02, (West Conshohocken, PA: American Society for Testing and Materials).
8. P. A. Klein, C. D. Krause, C. L. Friant, R. M. Kain, "A Localized Corrosion Assessment of 6% Molybdenum Stainless Steel Condenser Tubing at the Calvert Cliffs Nuclear Power Plant," CORROSION/94, paper no. 490, (Houston, TX: NACE International, 1994).
9. R. A. Hays, "Alloy 625 Crevice Corrosion Countermeasures Program: Evaluation of Concentric Pipe and Metal-to-Metal Gap Specimens", Report NO. CDNSWC-SME-92/53, Carderock Division of the Naval Surface Warfare Center, Annapolis, MD, January 1993.
10. T. S. Lee, *ASTM STP 727*, (West Conshohocken, PA: American Society for Testing and Materials, 1979), pp. 43-68.
11. R. M. Kain, Materials Performance 23, 2(1983): p. 24.
12. J. M. Kroughman and F. P. Ijjeseling, *Proceedings of 5th International Congress on Marine Corrosion and Fouling*, Barcelona, Spain, May 1980, p. 214.
13. F. L. LaQue, *Marine Corrosion - Causes and Prevention*, Chapter 6. Galvanic Corrosion, (New York, NY: Wiley-Interscience, John Wiley & Sons, 1975), p. 185.

### ACKNOWLEDGMENTS

Testing described was originally funded by the Office of Naval Research, Contract N00014-97-C-0216, Dr. Robert Pohanka, Administrator. The author expresses appreciation to co-workers at the LaQue Center who participated in the testing and reporting of this program.

**TABLE 1**  
**COMPOSITION OF MATERIALS TESTED**

UNS Designation	Chemical Composition (wt%)									
	C	Cr	Ni	Mo	Si	Mn	N	Cu	S	P
S31603 <sup>1</sup>	0.010	16.49	10.17	2.06	0.38	1.79	0.034	0.29	0.013	0.030
S31603 <sup>2</sup>	0.018	16.42	10.23	2.10	0.48	1.89	0.04	--	0.001	0.028
N08367	0.017	20.48	23.90	6.22	0.39	0.35	0.21	0.21	0.0004	0.021
S20910	0.048	20.98	14.20	2.15	0.34	6.28	0.22	--	0.010	0.022

<sup>1</sup> heat #1 used exclusively for welded specimens

<sup>2</sup> heat #2



**TABLE 2**  
**AVERAGE SURFACE ROUGHNESS**

	S31603		S20910		N08367	
	Ra (μin)	Ra (μm)	Ra (μin)	Ra (μm)	Ra (μin)	Ra (μm)
mill-finish	13.4	0.3	3.4	<0.1	100.2	2.5
grit blasted	77.0	1.9	59.5	1.5	105.6	2.6

**TABLE 3**  
**SOURCE SEAWATER HYDROLOGY<sup>1</sup>**

	Initial 6 Months <sup>2</sup>	Final 6 Months
Temperature °C <sup>3</sup>	25.4 - 7.6	9.5 - 28.9
Dissolved O <sub>2</sub> (mg/L)	5.6 - 9.8	4.6 - 9.0
Percent Saturation	81 - 100	72 - 100
pH	7.8 - 8.1	7.6 - 8.0
Salinity (g/L)	26.2 - 36.1	28.2 - 39.7
Chlorinity (g/L)	14.5 - 19.8	15.6 - 22.0
Sulfate (mg/L)	1950 - 2800	2160 - 2480
Conductivity (mmhos/cm)*	32.5 - 45.4	32.5 - 52.6
Total Fe (mg/L)*	0.038 - 0.162	0.033 - 0.235
Copper ( mg/L)*	<0.001 - 0.002	0.001
Ammonia (mg/L)*	<0.05	<0.05 - 0.06
Sulfide (mg/L)*	<0.005	<0.005

<sup>1</sup> Weekly, except monthly where indicated \*

<sup>2</sup> Corresponds also to 6-month filtered seawater test

<sup>3</sup> Temperature at sampling time



**TABLE 4**  
**CREVICE CORROSION INITIATION AND PROPAGATION BEHAVIOR OF PARTIALLY COATED**  
**S31603 STAINLESS STEEL PANELS IN SIX-MONTH FILTERED SEAWATER TEST AT 30°C**

Coating System	Affected Crevice Area (cm <sup>2</sup> )					
	20% Paint Coverage			80% Paint Coverage		
	Panel Code	Grit Blasted Surface	Mill Surface	Panel Code	Grit Blasted Surface	Mill Surface
A) Barrier	04	36.0	33.5	04	29.5	5.8
	05	35.0	29.5	05	26.8	15.0
	06	53.5	52.5	06	26.0	2.8
	avg.	41.5	38.5	avg.	27.4	7.8
B) Barrier +	10	35.0	43.0	11	32.0	7.0
Ablative-Cu	11	36.5	40.0	12	27.0	2.5
	12	41.5	31.5	13	21.0	30.0
	avg.	37.7	38.2	avg.	26.7	13.2
C) Barrier +	16	28.0	26.5	09	8.0	7.0
Elastomeric	17	25.5	28.0	16	14.5	6.5
	18	28.0	16.5	17	17.0	6.3
	avg.	24.5	23.7	avg.	13.2	6.6

Coating System	Maximum Depth (mm)					
	20% Paint Coverage			80% Paint Coverage		
	Panel Code	Grit Blasted Surface	Mill Surface	Panel Code	Grit Blasted Surface	Mill Surface
A) Barrier	04	1.58 (E)	1.71	04	0.43	0.10
	05	1.72 (E)	0.30	05	1.83	0.01
	06	1.61	0.53	06	2.13	0.02
B) Barrier +	10	1.24	0.95	11	1.35	0.04
Ablative-Cu	11	1.10	1.12	12	1.41	0.01
	12	1.21	0.26	13	0.20	0.42
C) Barrier +	16	0.82	1.25	09	0.20	0.26
Elastomeric	17	0.52	1.61	16	2.10	0.05
	18	0.51	1.70	17	1.77	0.16

(E) Denotes perforation within 1/2-inch (13 mm) of edge



**TABLE 5**  
**CREVICE CORROSION INITIATION AND PROPAGATION BEHAVIOR OF PARTIALLY**  
**COATED N08367 PANELS IN SIX-MONTH FILTERED SEAWATER TEST AT 30°C**

Coating System	Affected Crevice Area (cm <sup>2</sup> )					
	20% Paint Coverage			80% Paint Coverage		
	Panel Code	Grit Blasted Surface	Mill Surface	Panel Code	Grit Blasted Surface	Mill Surface
A) Barrier	04	6.8	52.0	04	0.0	0.0
	05	15.0	0.0	05	0.0	0.0
	06	1.0	25.3	06	0.6	0.0
B) Barrier +	10	0.0	0.0	10	0.0	0.0
Ablative-Cu	11	17.3	0.0	11	0.0	28.5
	12	2.0	0.0	12	0.6	0.0
C) Barrier +	16	16.5	45.0	16	0.0	0.0
Elastomeric	17	0.0	0.0	17	17.5	10.3
	18	7.0	53.0	18	0.0	29.0

Coating System	Maximum Depth (mm)					
	20% Paint Coverage			80% Paint Coverage		
	Panel Code	Grit Blasted Surface	Mill Surface	Panel Code	Grit Blasted Surface	Mill Surface
A) Barrier	04	0.05	0.96	04	0.00	0.00
	05	0.93	0.00	05	0.00	0.00
	06	*	0.75	06	0.20	0.00
B) Barrier +	10	0.00	0.00	10	0.00	0.00
Ablative-Cu	11	1.25	0.00	11	0.00	0.50
	12	0.63	0.00	12	0.40	0.00
C) Barrier +	16	0.58	0.53	16	0.00	0.00
Elastomeric	17	0.00	0.00	17	0.01	0.20
	18	0.07	0.57	18	0.00	0.22

\* Measurable attack limited to within 1/2-inch (13 mm) of panel edge.



**TABLE 6**  
**CREVICE CORROSION INITIATION AND PROPAGATION BEHAVIOR OF PARTIALLY**  
**COATED S20910 PANELS IN SIX-MONTH FILTERED SEAWATER TEST AT 30°C**

Coating System	Affected Crevice Area (cm <sup>2</sup> )					
	20% Paint Coverage			80% Paint Coverage		
	Panel Code	Grit Blasted Surface	Mill Surface	Panel Code	Grit Blasted Surface	Mill Surface
A) Barrier	04	22.5	37.5	04	20.5	15.5
	05	54.5	30.0	05	38.0	4.5
	06	45.0	37.5	06	25.5	19.5
	avg.	40.7	35.0	avg.	28.0	13.2
B) Barrier +	10	39.0	26.8	10	36.5	6.5
Ablative-Cu	11	33.5	37.5	11	26.5	10.5
	12	36.0	8.5	12	42.0	4.5
	avg.	36.2	24.3	avg.	35.0	7.2
C) Barrier +	13	24.0	9.3	16	21.8	1.7
Elastomeric	16	23.0	9.8	17	23.5	1.7
	17	23.8	13.8	18	27.5	1.6
	avg.	23.6	10.9	avg.	24.3	1.7

Coating System	Maximum Depth (mm)					
	20% Paint Coverage			80% Paint Coverage		
	Panel Code	Grit Blasted Surface	Mill Surface	Panel Code	Grit Blasted Surface	Mill Surface
A) Barrier	04	0.15	1.05	04	1.07	0.26
	05	1.15	0.50	05	0.59	0.00*
	06	0.24	0.73	06	0.16	0.13
B) Barrier +	10	1.97	0.55	11	0.68	<0.01
Ablative-Cu	11	1.23	1.39	12	0.89	0.04
	12	1.46	0.11	13	0.84	<0.01
C) Barrier +	13	1.84	0.29	16	0.78	0.08
Elastomeric	16	1.42	0.60	17	0.91	0.00*
	17	1.32	0.42	18	0.60	0.00*

\* Measurable attack within 1/2-inch (13 mm) of panel edge



**TABLE 7**  
**RESULTS FOR NON-WELDED, COATED AND SCRIBED SPECIMENS EXPOSED**  
**FOR ONE YEAR WITHOUT CATHODIC PROTECTION FROM ZINC ANODES**

Coating	Substrate Alloy	Specimen Number	Observed Rust Indicative of Crevice Corrosion at Scribe		Coating Blisters
			Front (blasted)	Back (mill)	
Barrier	S31603	7	None	None (E)	None
		8	None	None	None
		9	None	Yes (D)	None
	N08367	25	None	None	None
		26	None	None	None
		27	None	None	None
	S20910	44	None (E)(D)	None	None
		45	Yes (E)(D)	None	None
		46	None	Yes (D)	None
Barrier + Ablative-Cu	S31603	63	None (E)	None (E)	None
		64	Yes	None	None
		65	Yes	None	None
	N08367	81	None	None	None
		82	Yes x	None	None
		83	None	None	None
	S20910	100	None (E)	None (E)	None
		101	Yes	None	None
		102	Yes	None	None
Barrier + Elastomeric	S31603	119	None	Yes v	None
		120	None	None	None
		121	None	None	None
	N08367	137	None	None	None
		138	None	None	None
		139	None	Yes x	None
	S20910	156	Yes ✓	None	None
		157	None	None	None
		158	None	None	None

E = attack found at panel edge

D = delamination associated with crevice corrosion



**TABLE 8**  
**SUMMARY OF RESULTS FOR FULLY COATED, WELDED SPECIMENS EXPOSED**  
**FOR ONE YEAR WITHOUT CATHODIC PROTECTION FROM ZINC ANODES**

Coating	Substrate Alloy	Specimen Number	Observed Rust Indicative of Crevice Corrosion		Coating Blisters
			Front (blasted)	Back (mill)	
Barrier	S31603	1	None	None	None
		2	None	None	None
		3	None	None	None
	N08367	19	None	None	None
		20	None	None	None
		21	None	None	None
	S20910	38	None	None	None
		39	None	None	None
		40	None	None	None
Barrier + Ablative-Cu	S31603	57	None	None	None
		58	None	None	None
		59	None	None	None
	N08367	75	None	None	None
		76	None	None	None
		77	None	None	None
	S20910	94	None	None	None
		95	None	None	None
		96	None	None	None
Barrier + Elastomeric	S31603	113	None	None	None
		114	None	None	None
		115	None	None	None
	N08367	131	None	None	None
		132	None	None	None
		133	None	None	None
	S20910	150	None	None	None
		151	None	None	None
		152	None	None	None



**TABLE 9**  
**NUMBER OF CATHODICALLY PROTECTED SPECIMEN SURFACES EXHIBITING**  
**BLISTERING AND/OR COATING DISBONDMENT IN ONE-YEAR SEAWATER TEST**

Alloy	Condition	Observed Blistering			Disbondment-Substrate Revealed		
					Barrier	Barrier + Ablative-Cu	Barrier + Elastomeric
		Barrier	Ablative-Cu	Elastomeric	Barrier	Ablative-Cu	Elastomeric
<i>Welded Materials<sup>1</sup></i>							
S31603	blasted	5/6	6/6	2/6	4/6	0/6	0/6
N08367	blasted	5/6	6/6	3/6	2/6	0/6	0/6
S20910	blasted	5/6	6/6	6/6	5/6	0/6	0/6
<i>Non-Welded Materials<sup>1</sup></i>							
S31603	blasted	0/3	2/3	1/3	2/3	1/3	0/3
	mill	2/3	2/3	2/3	3/3	0/3	0/3
N08367	blasted	2/3	1/3	3/3	2/3	0/3	0/3
	mill	2/3	2/3	1/3	0/3	0/3	0/3
S20910	blasted	3/3	1/3	2/3	2/3	0/3	1/3
	mill	3/3	2/3	2/3	1/3	0/3	1/3

<sup>1</sup> All resistant to crevice corrosion

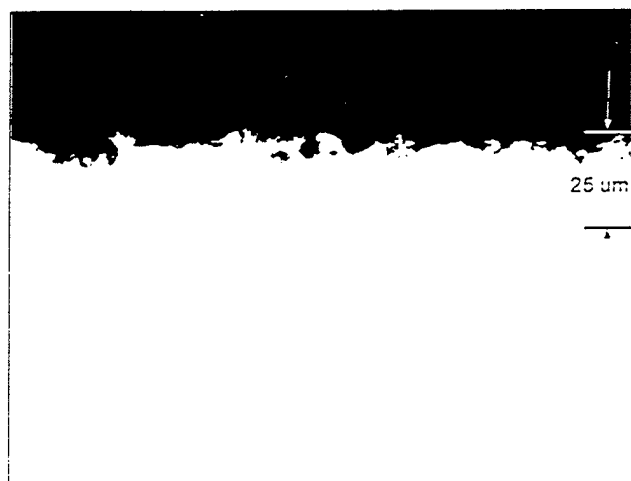


FIGURE 1 - Cross-sectional view (original magnification 500X) showing surface profile created by grit blasting the stainless steel test panels (shown N08367).

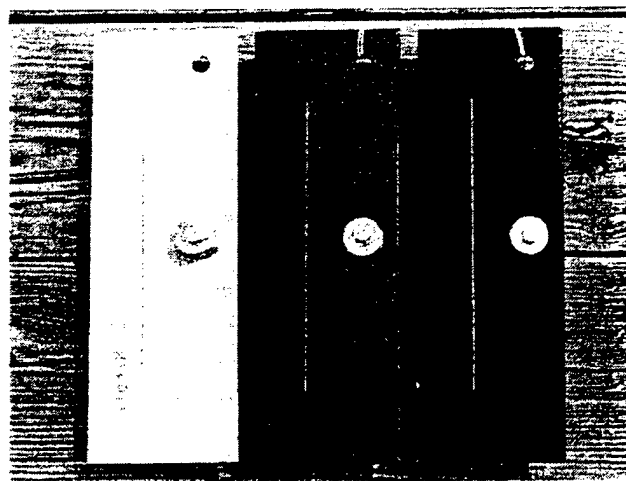


FIGURE 2 - Representative view of fully coated test panels with zinc anodes. Non-welded specimens shown have intentionally scribed "defects".



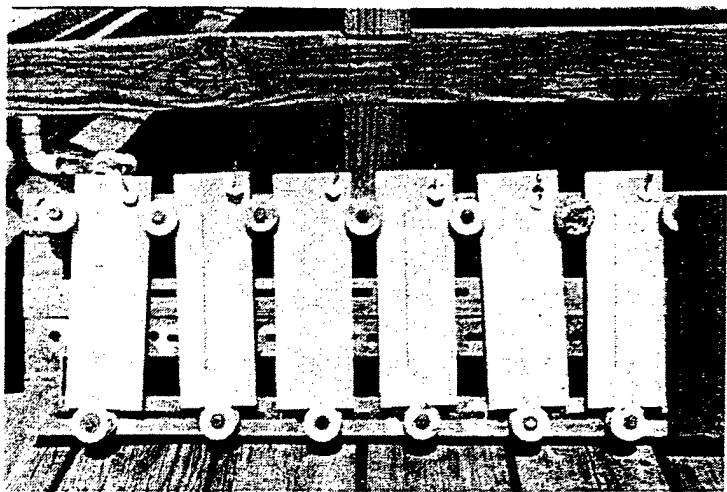


FIGURE 3 - Partial view of test rack containing fully coated, welded specimens and fully coated, non-welded specimens with scribed "defect" in gray barrier coating; shown one for each alloy without zinc anodes.

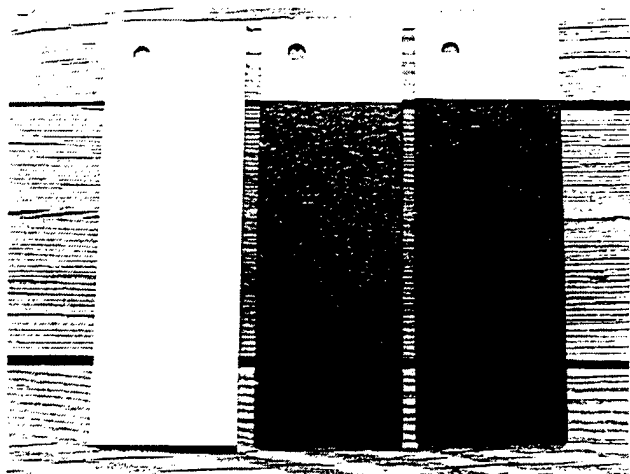
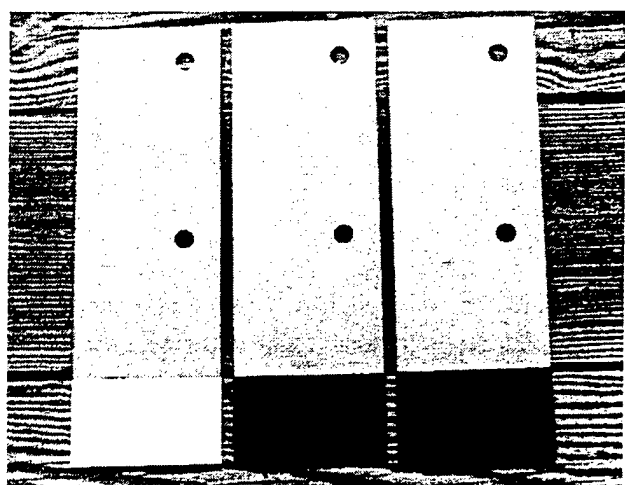


FIGURE 4 - Representative views of partially coated test panels (top) 20% coated (80% bare), and (bottom) 80% coated (20% bare).



FIGURE 5 - Partially coated test specimens on support fixture ready for exposure in filtered seawater tank.



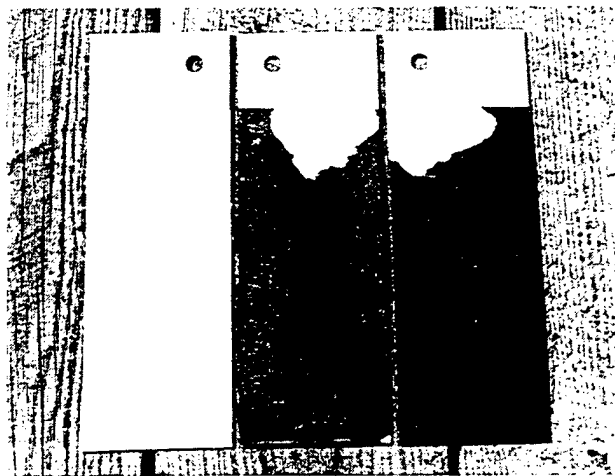
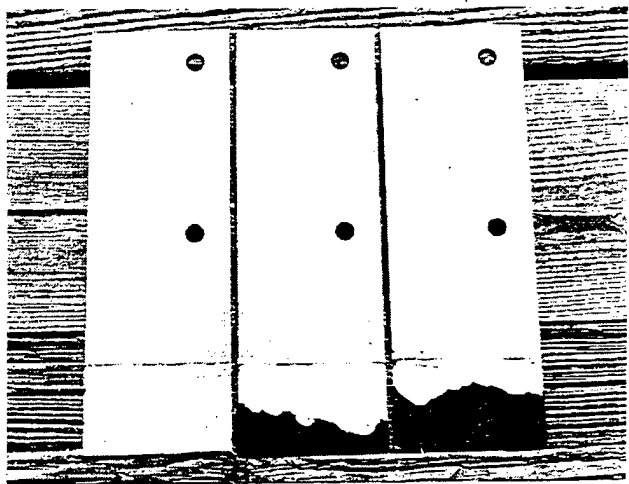
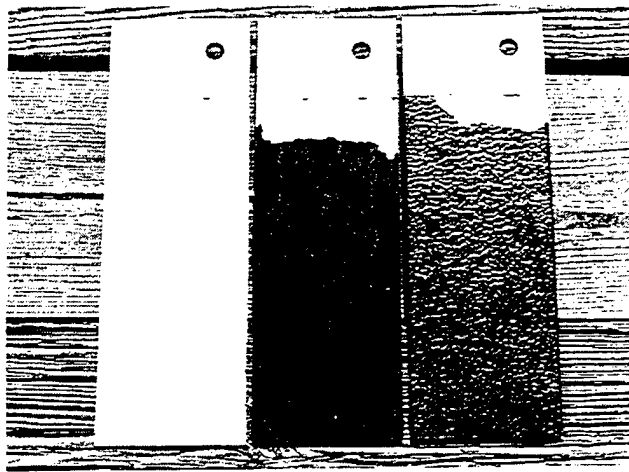


FIGURE 6 - Examples of crevice corrosion affecting partially coated stainless steel with (left to right) barrier coating and antifouling ablative-Cu and elastomeric type coating. (Top) S31603 (80% coated), (center) S20910 (20% coated), and (bottom) N08367 (80% coated).

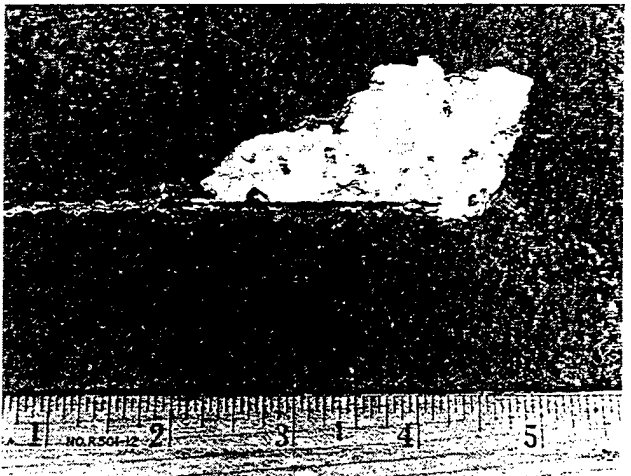
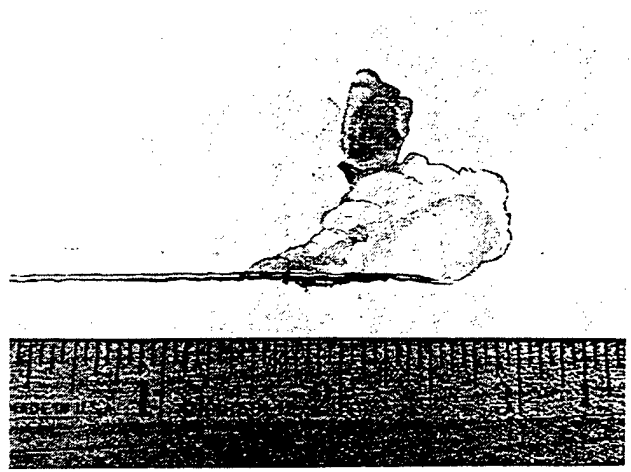


FIGURE 7 - Example of crevice corrosion at scribed location on (top) S20910 test panel with epoxy barrier system and (bottom) S31603 test panel with ablative-Cu system.

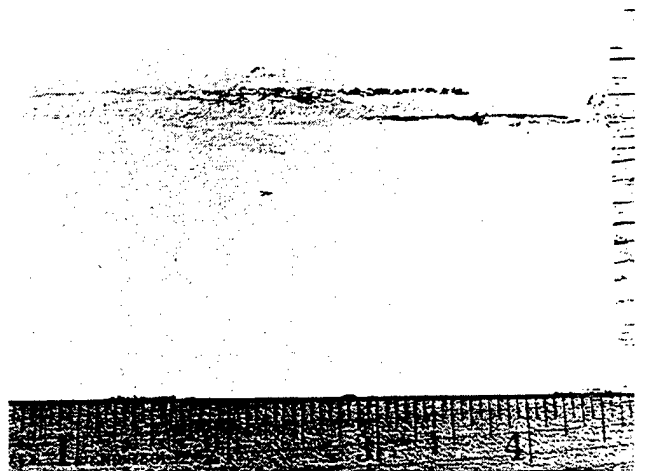


FIGURE 8 - Localized corrosion damage to uncoated S31603 test panel exposed to seawater for 12 months.



**APPENDIX 2**

**“Use of Coatings to Assess the  
Crevice Corrosion Resistance of Stainless Steel in Warm Seawater”  
(unedited)**

by  
Robert M. Kain

To be presented at ASTM G.1  
Symposium on Marine Corrosion in Tropical Environments  
Orlando, FL, November 13-14, 2000

Edited paper scheduled for publication in  
ASTM STP 1399 “Marine Corrosion in Tropical Environments”  
S. W. Dean, G. Hernandez-Duque Delgadillo, and J. B. Bashman, Editors



Robert M. Kain<sup>1</sup>

## **Use of Coatings to Assess the Crevice Corrosion Resistance of Stainless Steels in Warm Seawater**

---

**Reference:** Kain, R. M., "Use of Coatings to Assess the Crevice Corrosion Resistance of Stainless Steels in Warm Seawater," *Marine Corrosion in Tropical Environments*, ASTM STP 1399, S. W. Dean, G. Hernandez-Duque Delgadillo, and J. B. Bushman, Eds., American Society for Testing and Materials, West Conshohocken, PA, 2000.

**Abstract:** This paper focuses on the utility of epoxy-type coatings for testing the crevice corrosion resistance of a variety of stainless type alloys in warm, natural seawater. Details of surface preparation, coating application and exposure to 30°C seawater for periods of up to six months are provided. Testing comprised exposure of UNS S31603, UNS N08367 and UNS S20910 in one or more of the following forms: pipe, sheet, welded plate. Results are discussed in terms of alloy resistance to crevice corrosion initiation and propagation. The attributes of coatings as a crevice former are reviewed. While alloy N08367 was clearly the most resistance to crevice corrosion initiation at coating sites, it suffered intense attack in some cases.

**Key Words:** warm seawater, crevice corrosion, coatings, austenitic stainless steel

### **Introduction**

In the absence of cathodic protection, crevice corrosion is the most problematic issue affecting stainless steel utilization in seawater [1]. The problem is particularly acute in warm natural seawater where the cathodic process is enhanced by the ennobling effects of biological films which form on stainless steel surfaces [2]. Although crevice corrosion can occur in cold seawater, propagation of attack is generally greater in warm seawater. Susceptibility is not limited just to the common "300 series" grades (e.g., UNS S30400/ S30403 and UNS S31600/ S31603). Under certain conditions, higher alloyed duplex and austenitic stainless steels, including "super" varieties are also susceptible [3-9]. Even 9 to 15 percent molybdenum containing nickel-base alloys (e.g., UNS N06625 and UNS N01276) are not completely immune [5, 7, 9]. Testing and modeling based research has shown that crevice corrosion is more likely to occur when crevices are deep and tight [10-12]. Crevices may be of the metal-to-metal or metal-

---

<sup>1</sup> Senior Corrosion Scientist, LaQue Center for Corrosion Technology, Inc., P. O. Box 656, Wrightsville Beach, NC 28480



to-nonmetal type. Variations in alloy behavior can result from differences in crevice geometry, and due to other environmental and metallurgical factors described elsewhere [11,12].

ASTM Standard Guide for Crevice Corrosion Testing of Iron-base and Nickel-base Stainless Alloys in Seawater and Other Chloride-Containing Aqueous Environments (G78-95) describes a number of different types of non-metallic crevice devices which have been used to investigate crevice corrosion. Presently, G78 does not address the use of coatings as crevice formers.

Coatings have been implicated with the failure of "20Cr-6Mo" alloy condenser tubes [6]. While not intentionally coated, overspray from a condenser tube sheet coating operation produced crevices which lead to the tube failures. Problems with crevice corrosion affecting partially coated stainless steel and nickel alloy electrochemical test specimens have been reported by several researchers [13,14]. The use of "coatings" to investigate crevice corrosion resistance has been proposed previously. Celis et al. [14], for example, proposed testing of crevice corrosion susceptibility by a photomasking technique capable of producing various size crevice-forming dots on the stainless steel test surfaces. The technique, however, relied on potentiostatic polarization in a simple 0.1 M KCl solution.

Earlier, Degerbeck and Gille [16] described simple immersion trials conducted with a crevice former of dried plastic from a felt tip pen. Some of the attributes described for this technique included:

- a constant critical geometry
- no need for a fixture
- applicable to convex, concave and uneven surfaces (e.g., weldments)
- crevice area can be varied
- simple to make specimens

Besides the inadvertent coating issue described previously, there are occasions where stainless steel might be intentionally coated. Coating of stainless steel has been suggested, for example, as one way to mitigate galvanic corrosion when stainless steel is the cathodic member of a couple [17]. In some applications, there may be need to coat stainless steel with an antifouling type paint, to minimize fouling in general and to preclude barnacle-related crevice corrosion. The behavior of three different grades of stainless steel when fully and partially coated with epoxy barrier paints and antifouling type paints, in a recent test program, are reported elsewhere [8].

This paper discusses three series of tests that were directly and indirectly related to reference [8]. Results of two of these have not been published previously. Tests were performed on three diverse grades of austenitic stainless steel: Type 316L (UNS S31603), AL6XN™ (N08367) and a Cr-Ni-Mn-Mo alloy (UNS S20910). N08367 is the nitrogen-containing version of the "20Cr-6Mo" alloy (UNS N08366) which had suffered crevice corrosion under the epoxy paint over-spray mentioned earlier.

---

AL6XN™ is a registered trademark of Allegheny Ludlum Corporation, Brackenridge, PA



## Experimental

### Materials and Specimens

Table 1 gives the nominal compositions for the three alloys tested. As will be described later, different product forms from different heats of material were tested.

Testing included exposure of 2-inch (50.8 mm) diameter pipe specimens of S31603, 1/8-inch (~3 mm) sheet specimens of all three alloys, and 1/2-inch (12.7 mm) plate specimens of S20910 and N08367. Surface preparation and coating details are described in the specific test series sections.

Table 1 - Nominal Composition of Test Materials

UNS	Weight Percent							
Designation		Fe	Cr	Ni	Mo	Mn	S*	N
S31603 <sup>1</sup>	0.030	Base	16.0-18.0	10.0-14.0	2.0-3.0	2.0*	0.03	--
S20910 <sup>2</sup>	0.06	Base	20.5-23.5	11.5-13.5	1.5-3.0	4.0-6.0	0.03	0.22-0.4
N08367 <sup>3</sup>	0.03	Base	20.0-22.0	23.5-25.5	6.0-7.0	2.0*	0.03	0.18-0.25
N06625 <sup>4</sup>	0.10	5.0*	20.0-23.0	Base	8.0-10.0	0.5*	0.015	--

\* denotes maximum

<sup>1</sup> Type 316L, <sup>2</sup> 22-13-5 alloy, <sup>3</sup> AL6XN

<sup>4</sup> alloy 625, used as filler metal for welded N08367 specimens in Series 3

### Environments

All three test series described below were conducted in constantly refreshed, recirculated, filtered (5-10  $\mu$ m), natural seawater at an average temperature of 30°C  $\pm$  2°C. Table 2 provides weekly hydrology data. Series 1 and Series 2 ran concurrently for 60 days. Subsequent Series 3 tests also ran up to 60 days, but with interim removal of some specimens.

Table 2 - Weekly Source Seawater Hydrology

	Series 1 and 2	Series 3
Temperature °C <sup>1</sup>	25.4 - 7.6	29.4 - 14.9
Dissolved O <sub>2</sub> (mg/L)	5.6 - 9.8	4.7 - 8.0
Percent Saturation	81 - 100	72 - 90
pH	7.8 - 8.1	7.7 - 8.0
Salinity (g/L)	26.2 - 36.1	25.8 - 35.6
Chlorinity (g/L)	14.5 - 19.8	14.5 - 20.4

<sup>1</sup> temperature at sampling time



## Series 1 --- Pipe Tests

As noted elsewhere [9], crevice corrosion of alloy 625 (UNS N06625) was found beneath epoxy paint which had been applied to the OD of 3-inch (25.4 mm) schedule 40 pipe. The coated areas had been inserted into sections of clear vinyl tubing and clamped in place to form a "piping system" handling natural seawater. A series of tests was subsequently performed to assess if epoxy paint, without the overlaying vinyl tubing would promote crevice corrosion. As described below, several test variables were considered.

### *Procedure*

Type 316L (UNS S31603) was selected as the crevice-corrosion-susceptible control material. A total of twenty-four 12-inch (305 mm) long sections of 2-inch schedule 40 pipe were prepared. Twelve of the specimens were blasted with clean, 80-mesh aluminum oxide to prepare the surface for coating application. The other 12 were left in the as-produced mill finish. Subsequently, the outside diameter (OD) of the pipe specimens was partially coated with epoxy paint, leaving either 20% or 80% of OD surface uncoated. The bare inside diameter (ID) surfaces were included in determining the cathode to crevice area ratios. The interface between the epoxy and the bare metal section was considered to be the crevice mouth. An equal number of pipes were coated with two different epoxy paint systems. One system comprised a dual-layer coating of conventionally sprayed epoxy (gray over red) identical to that used in another study (Coating I) [8]. The total dry film thickness was about 10 mils (250  $\mu\text{m}$ ). The second system comprised a one-coat brush applied (~20 mils or 500  $\mu\text{m}$ ) layer of a two-part epoxy paint of the type used in the earlier testing of the alloy N06625 pipe (Coating II). Both coating systems were produced by the same company. Specimens were tested in triplicate. A typical pre-test view of the coated pipes is shown in Figure 1. The specimens were exposed to warm, filtered seawater for six months in the same large test tank containing a number of other coated specimens reported in reference [8].

### *Results and Observations*

While the depth of the seawater test tank precluded a thorough in-situ inspection of all specimens, it was apparent from the easily visible specimens that crevice corrosion had initiated on some within a few days. Post-test inspection revealed that 18 specimens had incurred extensive crevice corrosion at the primary site, i.e., where the paint created an interface with the bare OD, and also at the edge of the paint at the other end. For the remaining six specimens, the attack was confined at the latter sites. In one case, the attack too close to the pipe end precluded accurate measurements.

Figure 2 provides a representative view of the specimens after cleaning. The poor paint adhesion on the mill surface may have influenced the crevice corrosion process for some specimens. The paint was much more adherent to the grit blasted surfaces. For these, coating disbondment was observed only at areas affected by crevice corrosion.



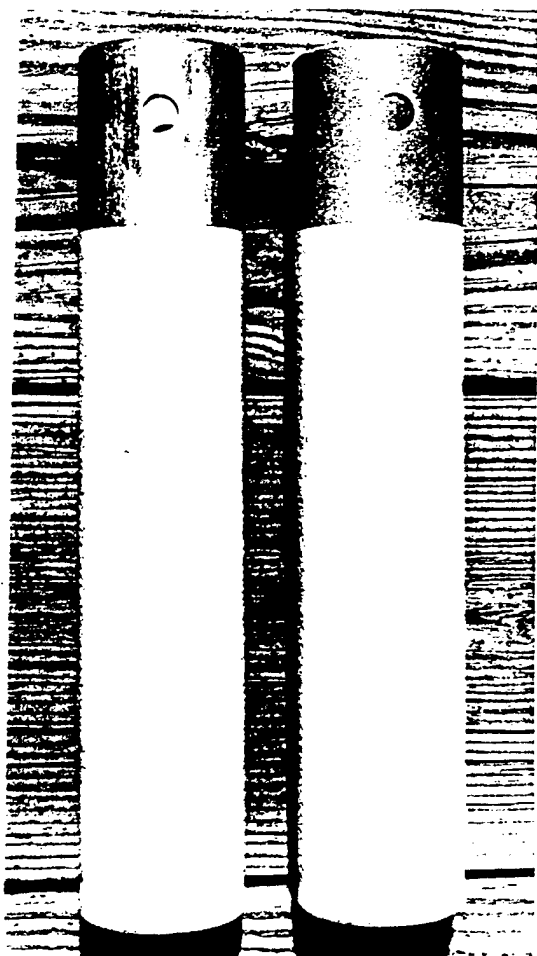


*Figure 1 - Pre-test view of coated S31603 pipe. Shown (left) as-produced and (right) grit blasted pipe specimens with 80% of OD surfaces coated with spray applied epoxy.*



*Figure 2 - Examples of crevice corrosion which developed on partially coated S31603 pipe exposed to warm seawater for 6 months. Shown triplicates of grit blasted pipe specimens with brush-applied epoxy paint on 20% of OD surface.*

In addition to visual appearance, the quantitative extent of lateral and maximum depth of attack are commonly used to characterize crevice corrosion resistance. Differences in initiation times, as well as other factors, can influence crevice corrosion propagation results. Table 3 gives the maximum depth of penetration results for 23 specimens. It is evident that values ranged from 0.53 mm to 3.85 mm. The minimum and maximum values were measured for two specimens of the triplicate specimens sprayed with two coats of epoxy on 20 percent of the original mill surface. The third specimen was resistant to attack at the primary crevice site, but did crevice corrode at the painted end. The result in Table 3 also illustrate that there was greater variability in the specimen-to-specimen maximum depths of attack for those specimens with either coating system applied to 20 percent of the pipe OD surface. Conversely, those with the smallest cathodic surfaces, i.e., 80 percent paint covered, exhibited the least variability.



Table 4 gives average and standard deviation data for all 23 specimens, and for sub-sets of 11 or 12 specimens grouped according to surface preparation, paint application and area coverage. The overall average and standard deviation values were 1.73 mm and 0.88 mm, respectively. While the differences in the average value is greatest for the grit blasted versus mill-finish surfaces, the greatest difference in standard deviation is observed for the two coating types. Considering that the maximum depths of attack (Table 3) differed by an order of magnitude, the average values shown in Table 4 indicate a fair degree of reproducibility. Somewhat surprisingly, the set with the brush applied coating exhibited the lowest standard deviation value, while that with the spray applied coating exhibited the greatest. Again, the latter data were influenced by the "rogue" behavior of some specimens with 80 percent of the bare mill-produced surface exposed to seawater.

Table 3 - Maximum Depth of Penetration Incurred by Partially Coated UNS S31603 Stainless Steel Pipe Specimens in Six-Month Filtered Seawater Test at 30°C

Coating System	Maximum Depth (mm)							
	20% Paint Coverage*				80% Paint Coverage*			
	Pipe No.	Grit Blasted	Pipe No.	Mill Finish	Pipe No.	Grit Blasted	Pipe No.	Mill Finish
Coating I (Sprayed)	1	1.05	1	**	1	1.27	1	2.85 <sup>1</sup>
	2	0.95	2	0.53	2	0.57	2	2.75 <sup>1</sup>
	3	2.45	3	3.85	3	0.82	3	2.35 <sup>1</sup>
Coating II (Brushed)	1	1.68	1	1.35	1	2.30	1	1.51 <sup>1</sup>
	2	2.42	2	2.40	2	2.15	2	1.45 <sup>1</sup>
	3	2.05	3	1.76	3	1.82	3	1.13 <sup>1</sup>

\* Based on OD surface area

\*\* Attacked but not measurable

<sup>1</sup> Denotes deepest attack at primary interface site

Table 4 - Summary of UNS S31603 Pipe Specimen Test Results

Total Conditions Considered	Total Number of Specimens	Maximum Depth of Attack (mm)	
		Average Value	Standard Deviation
All	23	1.73	0.88
Coating I	11	1.77	1.12
Coating II	12	1.84	0.43
Grit Blasted	12	1.63	0.67
Mill Finish	11	1.99	0.95
20% OD Coverage	11	1.86	0.92
80% OD Coverage	12	1.75	0.74





Figure 3 - Pre-test view of partially coated stainless steel sheet specimens (same coating system as in Figure 1).

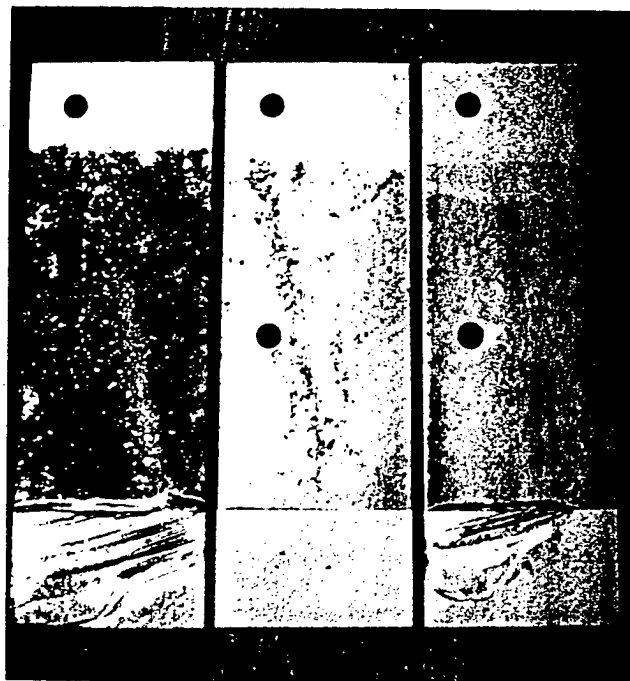


Figure 4 - Examples of crevice corrosion which developed under coating on sheet specimens. Shown N08367 with 20% of original mill surface coated

### Series 2 --- Flat Plate Tests

Results of a much larger test program comprising 180 fully and partially coated flat stainless steel specimens have been reported elsewhere [8]. Again, those tests comprised the three alloys (S31603, S20910 and N08367) listed in Table 1, and three types of coatings (epoxy-barrier paint, ablative copper and elastomeric); the latter two are antifouling coatings. In each case, the flat panels were coated with two layers of spray applied epoxy (gray over red). Other test variables included weldments, surface condition, coating defects and the effects of sacrificial protection with zinc anodes. Because of the relationship between the previously described pipe test, and other tests described later in this paper, only the results for the referenced tests comprising panels partially coated with two layers of sprayed-applied epoxy are reviewed in detail.

Figure 3 shows the typical pre-test appearance of the 4-inch x 12-inch (100 x 300 mm) test panels with 20% and 80% paint coverage, or conversely 80% and 20% bare metal, respectively. As reported previously, one surface of each panel was grit blasted



with 80-mesh aluminum oxide while the other was left in its mill finish condition. For S31603 and S20910, the mill finish was a standard 2B. In the case of N08307, the mill finish was much coarser and approached the surface roughness achieved by the grit blasting. Triplicate specimens were exposed for each alloy-paint coverage combination. Testing was performed concurrently with the previously described pipe test specimens in 30°C seawater for six months.

### Results and Observations

Tables 5 and 6 summarize the results from the referenced testing of stainless steel panels with 20% and 80% epoxy barrier paint coverage. In Table 5, material performance is compared in terms of crevice corrosion initiation and lateral propagation (affected area). For each stainless steel tested, the data base comprises a total of 12 crevice sites, i.e., two per specimen. That data shows that all available sites on the two lower molybdenum-containing alloys, S31603 and S20910, were attacked. In contrast, only 50 percent of the primary interface sites on the "6Mo" alloy (N08367) panels were attacked. Figure 4 shows the post-test condition of N08367 panels tested with 20% paint coverage. No significant difference in the affected areas was observed between S31603 and S20910. Both alloys consistently exhibited larger affected areas at sites associated with grit blasted surfaces versus those with the original 2B finish. This was most apparent for those panels with the least cathodic surface area, i.e., 80% paint coverage. In addition to enhanced resistance to initiation, N08367 exhibited greater resistance to lateral propagation, particularly when the cathode surface area was relatively small (i.e., 20% of total).

Table 5 - Crevice Corrosion Resistance of Three Stainless Steels Partially Coated with an Epoxy Type Barrier Paint and Exposed to Warm Seawater for Six Months

Material	Affected Crevice Area (cm <sup>2</sup> )					
	20% Paint Coverage			80% Paint Coverage		
	Panel Code	Grit Blasted Surface	Mill Surface	Panel Code	Grit Blasted Surface	Mill Surface
S31603	04	36.0	33.5	04	29.5	5.8
	05	35.0	29.5	05	26.8	15.0
	06	53.5	52.5	06	26.0	2.8
	avg.	41.5	38.5	avg.	27.4	7.8
S20910	04	22.5	37.5	04	20.5	15.5
	05	54.5	20.0	05	38.0	4.5
	06	45.0	37.5	06	25.5	19.5
	avg.	40.7	31.9	avg.	28.0	13.2
N08367	04	6.8	52.0	04	0.0	0.0
	05	15.0	0.0	05	0.0	0.0
	06	1.0	25.3	06	0.6	0.0
	avg.	7.6	27.2 <sup>1</sup>	avg.	0.6	0.00

<sup>1</sup> Average of #04 and #06



Table 6 provides additional propagation results comparing the maximum depths of penetration. Because of the possible influence of edge effects, penetrations within 1/2-inch (13 mm) of the edges are not included. As indicated by (E), through-plate penetrations were found within this zone on two of the S31603 specimens. Considerable variations in the maximum depth values for some sets of specimens are apparent. The reduction in the affected area and maximum depth of attack for S31603 and S20910 specimens with 80% paint coverage in the 2B surface is likely attributed to the combination of smaller cathodic surface area and poor adhesion of the coating. Independent of surface preparation and epoxy paint coverage factors, S31600 exhibited the greatest average depth of attack (0.92 mm) and the most variability (std. dev. 0.82 mm) among the three alloys tested. Both S20910 and N08367 were nominally 40 to 50 percent lower in this regard.

Table 6 - Maximum Depth of Crevice Corrosion Incurred by Three Stainless Steels Partially Coated with an Epoxy Type Barrier Paint and Exposed to Warm Seawater for Six Months

Material	Maximum Depth (mm)					
	20% Paint Coverage			80% Paint Coverage		
	Panel Code	Grit Blasted Surface	Mill Surface	Panel Code	Grit Blasted Surface	Mill Surface
S31603	04	1.58 (E)	1.71	04	0.43	0.10
	05	1.72 (E)	0.30	05	1.83	0.01
	06	1.61	0.53	06	2.13	0.02
	avg.	1.64	0.85	avg.	1.46	0.04
S20910	04	0.15	1.05	04	1.07	0.26
	05	1.15	0.50	05	0.59	0.00*
	06	0.24	0.73	06	0.16	0.13
	avg.	0.51	0.76	avg.	0.61	0.20
N08367	04	0.05	0.96	04	0.00	0.00
	05	0.93	0.00	05	0.00	0.00
	06	0.00*	0.75	06	0.20	0.00
	avg.	0.49	0.86	avg.	0.20	0.00

\* Measurable attack within 1/2-inch (13 mm) of panel edge

The above testing clearly demonstrate the susceptibility of a range of stainless steel compositions to crevice corrosion when partially coated and exposed to natural seawater. The reference document [8] has shown that the same materials were fully resistant if they were coated in total, and exposed without defects. Specimens exposed with intentional and inadvertent defects, but protected with zinc anodes were also fully resistant in a one-year test. However, the degree of cathodic protection imposed caused paint blisters to form and promoted coating disbondment, particularly on 2B mill surfaces.



### Series 3 --- Cruciform Specimens

#### *Procedure*

The effects of coating on the crevice corrosion resistance of N08367 and S20910 were also investigated in a third series of seawater tests. In this case, 35 specimens of each material were exposed. Testing was performed on cruciform shaped welded specimens as depicted in Figure 5. The nominal cross arm dimensions were 4" x 4" x 1/2" (100 mm x 100 mm x 12.7 mm) and 4" x 8" x 1/2" (100 mm x 200 mm x 12.7 mm). While the S20910 cruciforms were welded with like metal filler; alloy N06625 filler was used to weld the N08367 cruciforms. The specimens had been prepared for a mechanical test, but were utilized as a convenient "multi-crevice" type specimen to incorporate the effects of crevice corrosion.

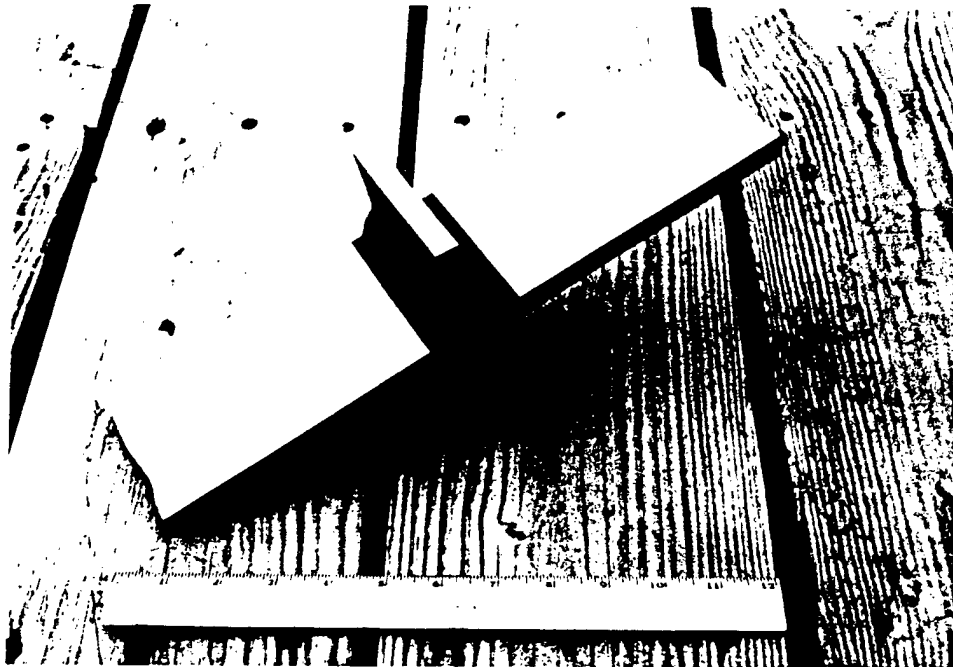


*Figure 5 - Pre-test view of partially coated welded cruciform specimen with multiple crevice sites.*

Prior to coating, all surfaces were blasted with clean, 80-mesh aluminum oxide. The coating was the same as the first coat in the previous pipe and panel tests, but brush applied as a single coat. For this series, it was the intent to provide a large boldly exposed surface area of stainless steel. Accordingly, only the weldment and a small overlap area on the base metal shown in Figure 5 was coated. As discussed later, the overlap area on the N08367 specimens was intentionally varied. When completed, each specimen had two potential crevice sites in each quadrant of the cruciform, or eight all together. The full complement of 35 specimens, therefore, had a total of 280 crevice



sites per alloy. As discussed later, a number of N08367 specimens were reblasted, recoated and re-exposed, thus providing even more data. The short length crevices produced on the edges of the specimens were not included in the subsequent evaluation. It is noted, however, that some attack did occur at these sites.

### *UNS S20910 Testing and Results*

All 35 of S20910 cruciform specimens were prepared with the epoxy coating covering the weldment and 1/16 - 1/8 inch (~1.6 mm - 3.2 mm) of the base metal from the weld toe. The specimens were divided for exposure in two shallow seawater test troughs approximately 10 inches (250 mm) deep. These exposure conditions provided an opportunity for in-situ inspection of the upward-facing surface crevice sites. Within three days, attack was detected at 31 visible sites on 25 of the specimens. By day seven, attack was detected at 50 visible sites on 30 of the specimens. Five affected specimens were removed for evaluation after 10 days, 12 more after 30 days and another 6 after 45 days. The remaining 12 were tested for a full 60 days. At each interim removal, there was a conscious attempt to select specimens exhibiting varying degrees of propagation. Test duration notwithstanding, all 35 specimens crevice corroded within 60 days. Moreover, 76 percent of the primary interface sites were affected. Table 7 includes a summary of the incidence of attack. Had all 35 specimens been exposed for the full 60 days, the total number of affected sites may have been greater. It is perhaps a more significant observation to note the substantial number of sites which did initiate in the relatively brief exposure time.

Figure 6 shows a representative view of an attacked S20910 cruciform specimen after only 10 days' exposure. Subsequent propagation beneath the coating affected the base-metal heat affected zone, and, in most cases, a significant portion of the weld metal. Albeit varying in length, the attack was continuous along the interface on most surfaces. In a few cases, however, two or three discrete sites of initiation had propagated. As shown in Table 7, the average length of the attacked sites increased somewhat with test duration.

Table 7 - Summary of Results for UNS S20910 Welded Cruciform Specimens

Test Duration (days)	Number of Specimens Exposed	Percent of Sites Attacked	Average Length of Attacked Sites (mm)	Maximum Depth of Attack (mm)*			Percent of All Sites ≥0.50 mm
				Overall Range	Average Value	Std. Dev.	
10	5	58	32	0.48 to 1.61	0.90	0.27	96
30	12	77	44	0.09 to 1.65	0.84	0.34	85
45	6	85	42	0.17 to 1.84	0.73	0.37	78
60	12	77	48	<0.01 to 2.21	0.76	0.41	78

\* Base metal-heat affected zone measurements





*Figure 6 - Example of crevice corrosion affecting welded S20910 cruciform specimen after only 10 days exposure to warm seawater.*

Table 7 also provides depth of penetration data for the S20910 cruciform specimens. Because of the geometry of the specimens, accurate measurements were limited to the base metal-heat affected zone regions within the crevice site. Again, there were considerable site-to-site differences in the maximum depths of attack incurred. Those specimens exposed for 60 days exhibited the broadest range of attack values (std. dev. 0.41 mm). Conversely, those exposed for only 10 days exhibited the least degree of variability (std. dev. 0.27 mm). It is observed from Table 7 that the absolute values for maximum depth increase (exponentially) with time. On the other hand, the average value of the maximum depth determinations, and the percent of all sites with attack depths  $\geq 0.50$  mm decreased with time.

#### *N08367 Testing and Results*

A total of 27 welded N08367 cruciform specimens were prepared and exposed in the same manner described above for S20910. In contrast to the behavior described for S20910, only two specimens (two sites) exhibited attack within the first three days of exposure. After seven days, only one site on each of five N08367 specimens was found to be corroding. By the end of 30 days, the total had increased to nine specimens with one affected site each. These were allowed to continue in test for another 30 days (total 60 days), while the 18 resistant ones were removed for subsequent re-exposure.

At the conclusion of the 60-day test, a total of 20 affected sites were found on the nine specimens. This constitutes 28 percent of the 72 potential sites for initiation. The average length of the attack across the width of the specimen was 54 mm; slightly



more than that found at the S20910 sites. In each case, the alloy N06625 weldment was also attacked. While not quantified by depth measurement, the weld attack shown, for example, in Figure 7 was significant. For the above nine specimens, base metal-heat affected zone depth of attack near the weld toe ranged from 0.12 mm to 2.77 mm (max.). Eighty percent of the sites measured  $\geq 0.50$  mm. The average maximum value and standard deviation value for the preceding were 1.37 mm and 0.82 mm, respectively.



*Figure 7 - Example of crevice corrosion affecting weld metal (N06625) used for joining N08367 cruciform specimen and exposed to warm seawater for 60 days.*

The previously mentioned 18 resistant specimens were reblasted and re-coated; this time with a paint overlap of 1/8-inch to 3/16-inch (3.2 mm - 4.8 mm) from the weld toe. In-situ inspection revealed attack at one site after 19 days. With the one exception, no other evidence of attack was found during or after the course of a 54-day exposure to warm seawater. The length and maximum depth of attack at the sole affected site was 40 mm and 1.55 mm, respectively; not far from the average values for the nine sites attacked in the preceding test.



Eight other N08367 cruciform specimens were also tested for periods ranging from 30 to 52 days. Four each were coated with 1/4-inch (~6.4 mm) to 1/2-inch (~12.7 mm) overlaps from the weld toe. Some attack was again observed within the first three days of exposure. Notwithstanding the differences in coating overlap and exposure time, 52 percent of the 64 crevice sites on these eight specimens initiated. The overall penetration range was 0.07 mm to 1.73 mm. The absolute maximum was associated with a specimen prepared with 1/2-inch overlaps and exposed for 30 days. The average and standard deviation values for the 33 affected sites were 0.60 mm and 0.41 mm, respectively.

### **Summary and Conclusions**

The propensity for stainless steels to suffer crevice corrosion in warm seawater has been reviewed. Particular attention has been given to crevice conditions associated with epoxy type coatings applied to different grades of stainless steel in several product forms. Based on the testing and evaluation of 124 test specimens with a combined total of 752 crevice sites, a number of conclusions can be drawn. These are expressed below as they relate to crevice corrosion testing and to the performance of stainless steels in warm seawater.

- Epoxy coating can be used as a crevice former for the purpose of testing the crevice corrosion resistance of different grades of stainless steel. While both coat-systems utilized were produced by the same manufacturer, there is no reason to suspect that similar coatings produced by manufacturers would affect stainless steel any differently.
- This type of crevice former can be applied to flat as well as curved and irregular surfaces and requires no fixturing or some standard torquing.
- Epoxy coatings are suitable for testing the crevice corrosion resistance of as-deposited weldments, mill-produced and surface treated material.
- Consideration for including epoxy coating as another type of crevice former in ASTM G-78 is recommended.
- The effects of cathodic surface area can be investigated by varying the amount of coverage by the coating.
- Unlike some other types of crevice-forming devices having fixed dimensions, the true depth of a crevice formed by a coating is not readily apparent. Moreover, as crevice corrosion propagates, the crevice gap may change, for example, due to coating disbondment.
- Epoxy coating is suitable for long-term exposure to seawater within the normal ambient temperature range. Present research has not evaluated its performance above 30°C.
- It has been demonstrated that austenitic stainless steels such as S31603 and the manganese-containing grade S20910 are highly susceptible to crevice corrosion when partially coated with epoxy.
- While the "26Cr-6Mo" grade tested (N08367) was also found to be susceptible, its overall resistance to crevice corrosion initiation was substantially greater. However, once initiated, significant propagation occurred even for this alloy.



- As might be expected, the N08367 was more sensitive to area ratio effects than the more susceptible grades. Test results for N08367 appear to complement field experience with a related alloy, for example, when inadvertently oversprayed with epoxy.
- Related work reported elsewhere [8] demonstrated the resistance of fully coated stainless steel, while at the same time noting that small defects in the coating provided sites for initiation. Overall, crevice corrosion susceptibility and the extent of attack increased with increased bare metal (i.e., cathodic) surface.
- If coatings are to be used on large stainless steel structures, e.g., ship hulls, exposure of bare metal due to coating damage could result in attack at the interface between the coating and any exposed metal.
- Related testing has demonstrated that crevice corrosion can be prevented by the use of cathodic protection. It has been reported elsewhere [8] that the potential associated with the use of sacrificial zinc anodes can cause blistering and, in some cases, coating disbondment.
- Attack of alloy 625 (N06625) weldments associated with N08367 cruciform specimens confirmed that these alloys are susceptible to attack beneath epoxy coatings. Moreover, it has been demonstrated that the coating need not be "held" in place, e.g., by a vinyl sleeve or other mechanism, in order for crevice corrosion to initiate.

### Acknowledgment

The author expresses his appreciation for assistance provided by co-workers at the LaQue Center for Corrosion Technology, Inc. Also recognized are Mr. Chip Becker and Mr. Dave Kihl of the Carderock Division - Naval Surface Warfare Center for providing the cruciform test specimens. Portions of the testing described were funded by the Office of Naval Research under Contract N00014-97-C-0216.

### References

- [1] Sedriks, A. J., *Corrosion of Stainless Steels, 2nd edition*, Chapter 5- Crevice Corrosion, Wiley-Interscience Publication, John Wiley & Sons, Inc., 1996.
- [2] Mollica, A., Trevis, et al., *Corrosion*, Vol. 45, No. 1, 1989, p. 48-56.
- [3] Aylor, D. M., Hays, R. A., Kain, R. M., and Ferrara, R. J. "Crevice Corrosion Performance of Candidate Naval Ship Seawater Valve Materials in Quiescent and Flowing Natural Seawater," Paper No. 99329, CORROSION/99, NACE International, Houston, TX, 1999.
- [4] Zeuthen, A. W. and Kain, R. M., "Crevice Corrosion Testing of Austenitic, Superaustenitic, Superferritic and Superduplex Stainless Type Alloys in Seawater," *Corrosion Testing in Natural Waters, ASTM STP 1300*, ASTM ASTM, West Conshohocken, PA, 1997, pp. 91-108.



- [5] Kain, R. M., "Evaluation of Crevice Corrosion Susceptibility," Research Symposium, CORROSION/96, NACE International, Houston, TX, 1996.
- [6] Klein, P. A., Krause, C. D., Friant, C. L., and Kain, R. M., "A Localized Corrosion Assessment of 6% Molybdenum Stainless Steel Condenser Tubing at the Calvert Cliffs Nuclear Power Plant," Paper No. 490, CORROSION/94, NACE International, Houston, TX, 1994.
- [7] Kroughman, J. M. and Ijjeseling, F. P., *Proceedings of 5th International Congress on Marine Corrosion and Fouling*, Barcelona, Spain, May 1980, p. 214.
- [8] Kain, R. M., "Crevice Corrosion Behavior of Coated Stainless Steel in Natural Seawater," Paper No. 00827, CORROSION/2000, NACE International, Houston, TX, 2000.
- [9] Hays, R. A., "Alloy 625 Crevice Corrosion Countermeasures Program: Evaluation of Concentric Pipe and Metal-to-Metal Gap Specimens," Report No. CDNSWC-SME-92/53, Carderock Division - Naval Surface Warfare Center, West Bethesda, MD, January 1993.
- [10] Sedriks, A. J., *International Metals Review*, Vol. 27, 1982, p. 321.
- [11] Oldfield, J. W., and Sutton, W. H., *British Corrosion Journal*, Vol. 13, 1978, p. 104.
- [12] Kain, R. M., *ASM Metals Handbook*, 9th ed., Vol. 13, ASM International, Metals Park, OH, 1987, pp. 109-112.
- [13] Lee, T. S., "A Method of Quantifying the Initiation and Propagation Stages of Crevice Corrosion," *Electrochemical Corrosion Testing, ASTM STP 727*, ASTM, West Conshohocken, PA, 1979, pp. 43-68.
- [14] Kain, R. M., *Materials Performance*, Vol. 23, No. 2, 1983, p. 24.
- [15] Celis, J. P., Roos, J. R., Kinawy, N. and Ruelle, C. Della, *Corrosion Science*, Vol. 26, 1986, pp. 237-254.
- [16] Degerbeck, J. and Gille, I., *Corrosion Science*, Vol. 19, 1979, pp. 1113-1114.
- [17] LaQue, F. L., *Marine Corrosion - Causes and Prevention*, Chapter 6 - Galvanic Corrosion, Wiley-Interscience, John Wiley & Sons, New York, 1975, p. 185.



### **APPENDIX 3**

This atlas contains color reproductions of photographs which are intended to familiarize the reader with the preparation and ultimate seawater exposure of 204 coated and non-coated test specimens, and their crevice corrosion behavior. A general guide identifying 17 related groups of photographs is provided. This is supplemented with an index listing the subject matter for each of the 122 views contained in 41 figure pages. The index also provides photo-negative file information. Finally, each photograph is accompanied by a brief caption.



## **GUIDE TO PHOTOGRAPHS DOCUMENTING PREPARATION AND TESTING OF COATED STAINLESS STEEL TEST PANELS AND PIPES**

Figures 1.1 to 4.3 characterize the shape and surface condition of the test specimens.

Figures 5.1 to 9.3 characterize the coating applied and show examples of intentional and other coating defects.

Figures 10.1 to 11.2 show the technique for attaching zinc anodes.

Figures 11.3 to 14.3 provide representative pretest views of uncoated and coated test panels mounted on racks for a 1-year exposure to natural seawater.

Figure 15.1 shows the test location.

Figure 15.2 to 18.3 show the extent of fouling incurred after 6 months and 12 months exposure from the test float.

Figures 19.1 to 19.3 show examples of coating disbondment and blistering found on the zinc anode protected specimens after 1 year.

Figures 20.1 to 22.3 provide examples of corrosion affecting the various materials at coating defect sites.

Figures 23.1 and 23.2 document attack found on uncoated Type 316L welded test panels.

Figures 24.1 to 24.3 provide pre-test views of partially coated specimens intended for 6 months exposure to filtered seawater at 30°C.



Figures 25.1 to 25.3 provide examples of the condition of the specimens following 6 months exposure in the test tank.

Figures 26.1 to 29.3 show the partially cleaned appearance of test panels with the epoxy barrier paint system.

Figures 30.1 to 33.3 show similar views of test panels with the ablative-Cu antifouling coating.

Figures 34.1 to 37.1 show similar views of test panels with the low surface energy elastomeric coating.

Figures 38.1 to 39.2 provide pretest views of the partially coated Type 316L pipe specimens.

Figures 39.3 to 40.3 show representative views of the partially coated pipes after removal, and with some cleaning.

Figures 41.1 to 41.3 show typical after cleaning views of the Type 316L pipes which had been partially coated and exposed to filtered seawater for 6 months.



## PHOTOGRAPHIC DOCUMENTATION INDEX

Figure No.	Subject	Photo-Negative Reference
	Surface Appearance of Specimens	
1.1	Typical 2B for S31603/S20910	97334-20A
1.2	Mill surface of N08367	97344-6
1.3	Representative grit blasted surface	97334-16A
2.1	Typical welded specimen	97293-19
2.2	Welded and non-welded specimens (3 alloys)	97310-4
2.3	Specimen with second hole for anode attachment	97345-8
	Photomicrographs of Randomly Selected Specimens (cross-sectional views at 500X)	
3.1	S31603 mill produced	31603-500M
3.2	S20910 mill produced	20910-500M
3.3	N08367 mill produced	08367-500M
4.1	S31603 grit blasted	31603-500GB
4.2	S20910 grit blasted	20910-500GB
4.3	N08367 grit blasted	08367-500GB
	Applied Coatings - Typical Surface Appearance	
5.1	Gray 2nd layer of epoxy	97344-9
5.2	Ablative-Cu topcoat	97344-18
5.3	Black elastomeric topcoat	97344-23
	Cross-sectional Views of Coating on Randomly Selected N08367 Panels with Grit Blasted Surfaces at 100X	
6.1	2 layer epoxy system	08367-100EP
6.2	3 layer ablative-Cu system	08367-100ACU
6.3	4 layer elastomeric system	08367-100EL
	Examples of Pretest Coating Defects	
7.1	First coat epoxy revealed	97346-12
7.2	Different sample	97346-8
7.3	Topcoat of epoxy revealed beneath ablative-Cu coat	97346-16
8.1	Tie coat revealed beneath elastomeric coat	97346-25



	Typical Pretest Views	
8.2	Welded specimens with 3 different paint systems	97346-3
8.3	Non-welded specimens with scribed defects	97347-24
	Photomacrographs (8X) of Scribed Areas	
9.1	2 layer epoxy systems	97350-2
9.2	3 layer ablative-Cu system	97350-9
9.3	4 layer elastomeric system	97350-13
	Attachment of Zinc Anodes	
10.1	Prepared area at lower hole in panel (see Figure 2.3)	97345-1
10.2	Two anodes secured with Type 316 stainless steel fasteners	97348-1
10.3	Overall view of completed specimens (welded)	97347-17
11.1	Non-welded and scribed specimens	97348-9
11.2	Insulation of anode and specimen from test rack	97356-4
11.3	Mounted control specimens (Left to right) S31603, N08367, S20910 uncoated welded specimens with and without anodes attached	97357-20
	Typical Pretest Views of Coated Welded and Non-welded Specimens (left to right: (in pairs) S31603, N08367 and S20910)	
12.1	Epoxy coated specimens	97349-14
12.2	Ablative-Cu coated specimens	97349-16
12.3	Elastomeric coated specimens	97351-2
	Same as Above With Anodes Attached	
13.1	Epoxy coated specimens	97357-4
13.2	Ablative-Cu coated specimens	97357-6
13.3	Elastomeric coated specimens	97357-9
	Overall View of Pretest Test Racks	
14.1	Uncoated control rack with triplicate specimens of each alloy with and without anodes (PVC panel and 90/10 panels in 7th and 14th position from left)	97357-13
14.2	One of three similar racks containing coated specimens of all 3 alloys without anodes	97351-4
14.3	Same as above - with anodes	97356-9
15.1	Deployment of test racks from float located on Banks Channel, Wrightsville Beach, NC	97358-12



	As-removed Appearance of Test Racks	
15.2	Epoxy coated panels exposed without anodes for 6 months	48144-23
15.3	Similar panels after 12 months	98593-4A
16.1	Ablative-Cu coated panels exposed without anodes for 6 months	98145-3A
16.2	Close-up view of typical corrosion-free scribed area at 6 months (September-March)	98145-8A
16.3	Similar panels after 12 months	98593-8A
17.1	View of affected 1-year S31603 scribed panels after water rinsing	98590-17A
17.2	Panels with elastomeric topcoat exposed for 6 months	98145-11A
17.3	Similar panels after 12 months	98593-9A
	Overall View of Test Racks after 1-Year Exposure	
18.1	Uncoated control panels	98591-10A
18.2	Typical appearance of coated panels without anodes	98587-20
18.3	Typical view of coated panels with anodes	98587-14
	Selected Post-Test Views	
19.1	Disbondment of epoxy coating on mill produced surface of panel exposed with zinc anodes	98589-3
19.2	Blistering of ablative-Cu system on welded panel with zinc anodes	98607-8A
19.3	Disbondment of elastomeric coating from tie coat on zinc anode protected panel	98589-17
20.1	Example of crevice corrosion originating and edge defect site on epoxy coated S31603 test panel (grit blasted surface)	98734-4A
20.2	Example of crevice corrosion on grit blasted surface at scribed area of epoxy coated S20910 test panel	98734-6A
20.3	Example of attack at edge defect on ablative-Cu coated S20910 test panel	98602-16A
21.1	Rust developed at scribed site on elastomeric coated S20910 test panel (grit blasted surface)	98602-20A
21.2	Same as above - at scribed site on ablative-Cu coated S3160 test panel	98600-10A
21.3	Same as Fig. 21.2 after removal of loosened paint layers	98734-2A
22.1	Only confirmed case of attack found at scribed sites on coated N08367 test panel (elastomeric)	98600-21A
22.2	Attack at scribed site of ablative-Cu coated S20910 test panel	98600-8A
22.3	Same as Fig. 22.2 after removal of loosened paint layers	98734-0A



23.1	View of uncoated/unprotected welded S31603 test panel. (S20910 exhibited similar barnacle related attack, but no weld-HAZ corrosion.)	98734-10A
23.2	Magnified view (8X) of weld-HAZ corrosion on another S31603 test panel	98744-14
23.3	Blank	--
	View of Partially Coated Test Panels Before 6-Month Exposure to 30°C Filtered Seawater	
24.1	Typical appearance of panels with 20% paint coverage (both sides); bare grit blasted surfaces shown in this view. (NOTE: No anodes were attached on any panel in this series.)	97345-9
24.2	Typical appearance of panels with 80% paint coverage (both sides); bare mill surfaces shown in this view.	97345-13
24.3	Typical specimen mounting arrangement for seawater tank exposure.	97358-17
	Examples of As-removed Appearance of Partially Coated Test Panels After 6 Months	
25.1	S31603 with 80% coverage by epoxy system	98142-16
25.2	S20910 with 20% coverage with ablative-Cu system	98141-12A
25.3	N08367 with 20% coverage with elastomeric system	98140-14
	Post-Test Views of Partially Cleaned Test Panels Showing Extent of Crevice Corrosion Beneath Coatings and Calcareous Deposition on Cathodic Surfaces --- Portion of Same Acid Cleaned to Reveal Specimen Identification Codes	
	<i>20% of Grit Blasted Surface Coated with Epoxy</i>	
26.1	S31603	98168-9A
26.2	S20910	98170-2A
26.3	N08367	98172-1
	<i>20% of Mill Surfaces Coated with Epoxy</i>	
27.1	S31603	98168-12A
27.2	S20910	98170-7A
27.3	N08367	98172-6
	<i>80% of Grit Blasted Surface Coated with Epoxy</i>	
28.1	S31603	98168-0A
28.2	S20910	98170-11A
28.3	N08367	98172-10



	<i>80% of Mill Surface Coated with Epoxy</i>	
29.1	S31603	98168-4A
29.2	S20910	98170-14A
29.3	N08367	98172-15
	<i>20% of Grit Blasted Surface Coated with Ablative-Cu System</i>	
30.1	S31603	98168-16A
30.2	S20910	98170-17A
30.3	N08367	98172-19
	<i>20% of Mill Surface Coated with Ablative-Cu System</i>	
31.1	S31603	98168-20A
31.2	S20910	98170-20A
31.3	N08367	98172-24
	<i>80% of Grit Blasted Surface Coated with Ablative-Cu System</i>	
32.1	S31603	98169-0A
32.2	S20910	98171-2A
32.3	N08367	98173-1A
	<i>80% of Mill Surface Coated with Ablative-Cu System</i>	
33.1	S31603 (bulk of paint removed with a plastic scraper)	98169-3A
33.2	S20910	98171-4A
33.3	N08367	98173-4A
	<i>20% of Grit Blasted Surface Coated with Elastomeric System</i>	
34.1	S31603	98169-7A
34.2	S20910	98171-8A
34.3	N08367	98173-11A
	<i>20% of Mill Surface Coated with Elastomeric System</i>	
35.1	S31603	98169-11A
35.2	S20910	98171-11A
35.3	N08367	98173-15A
	<i>80% of Grit Blasted Surface Coated with Elastomeric System</i>	
36.1	S31603	98169-16A
36.2	S20910	98171-19A
36.3	N08367	98173-19A



	<i>80% of Mill Surface Coated with Elastomeric System</i>	
37.1	S31603	98169-20A
37.2	S20910	98171-23A
37.3	N08367	98173-24A
	<i>Examples of Partially Coated S31603 Pipe Specimens Before 6 Months Exposure to 30°C Filtered Seawater</i>	
38.1	20% of OD coated with 2-layer epoxy system (left) mill surface and (right) grit blasted	97345-24
38.2	Same as Fig. 38.1, but with 80% of OD coated	97345-20
38.3	20% of OD coated with 1-layer of brush applied epoxy (type used elsewhere) (left) mill surface and (right) grit blasted	97347-6
39.1	Same as Fig. 38.3, but with 80% of OD coated	97347-1B
39.2	Arrangement for exposure of partially coated pipe specimens in seawater tank	97358-23
39.3	Example of the condition of S31603 pipe specimens after 6 months exposure	98144-12
	<i>Post-test Appearance of Partially Cleaned Pipe Specimens Showing Crevice Corrosion Under Coating and Calcareous Deposition on OD Cathodic Surfaces</i>	
40.1	3 pipes with 80% of grit blasted surface coated with 2-layer epoxy system	98175-4A
40.2	3 pipes with 20% of grit blasted surface coated with 2-layer epoxy system	98174-16A
40.3	3 pipes with 80% of grit blasted surface with brush applied coat of white epoxy	98174-8A
	<i>Examples of Fully Cleaned Specimens Showing Extent of Crevice Corrosion Under Epoxy Coating</i>	
41.1	3 pipes with grit blasted surfaces coated (20%) with 2-layer system	98190-15A
41.2	Same as Fig. 41.1, but with 1-coat brush applied system	98189-22
41.3	3 pipes with mill surfaces coated (80%) with 1-coat brush applied system	98190-3A



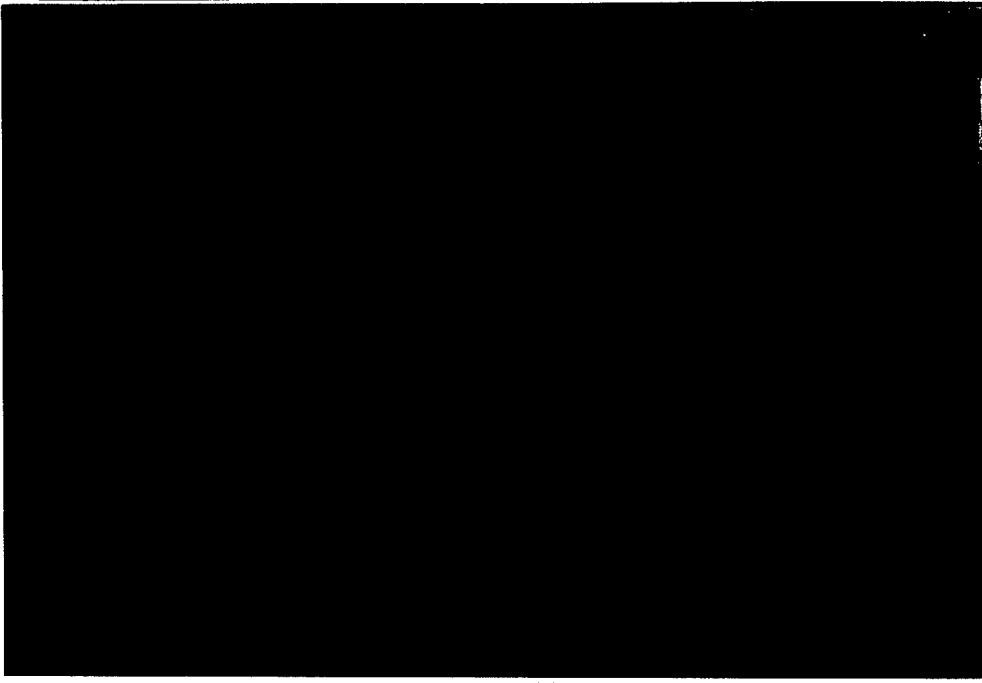


Figure 1.1  
Mill surface of S31603 and S20910

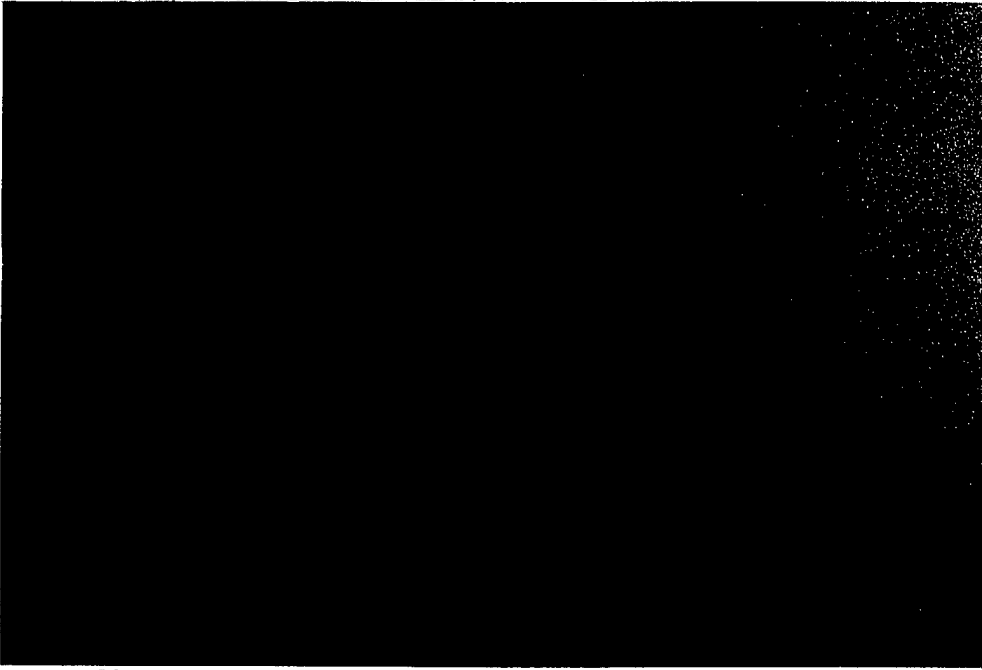


Figure 1.2  
Mill Surface of N08367

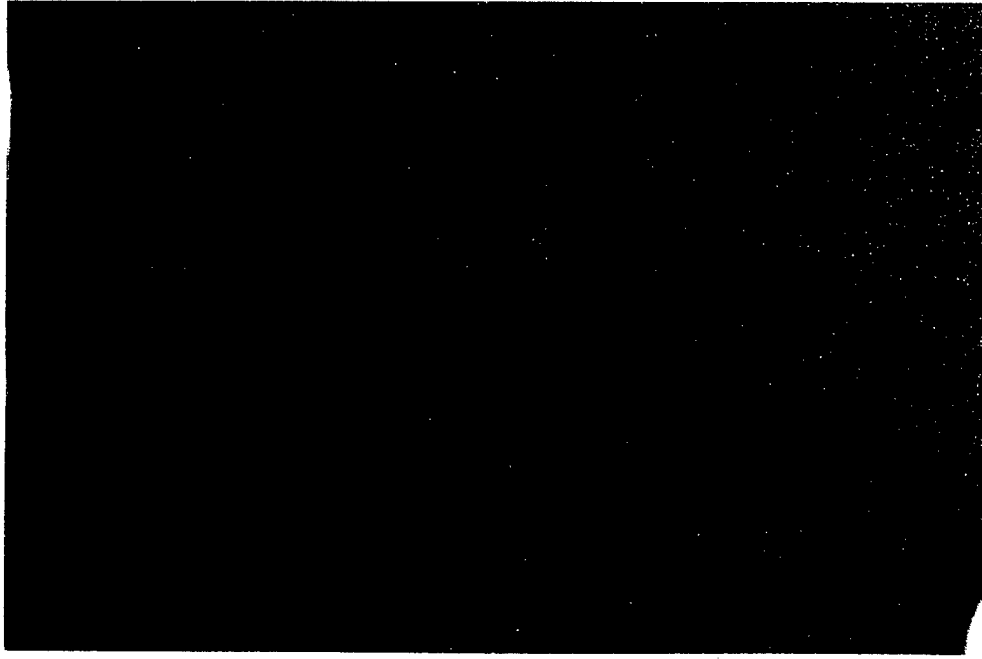


Figure 1.3  
Typical grit blasted surface



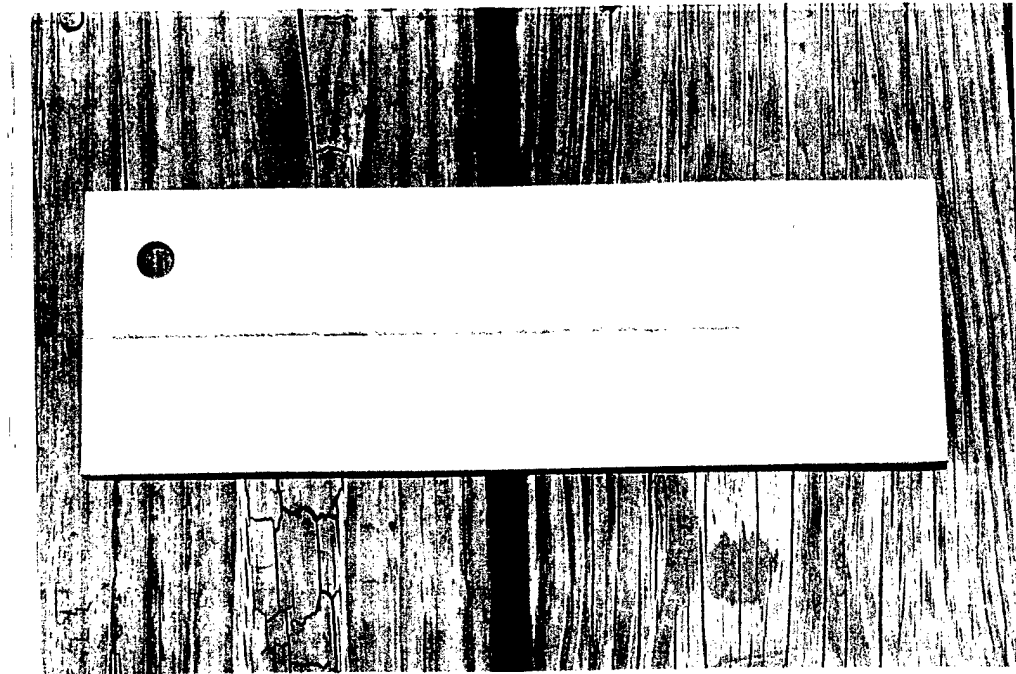


Figure 2.1  
Grit blasted welded test panel

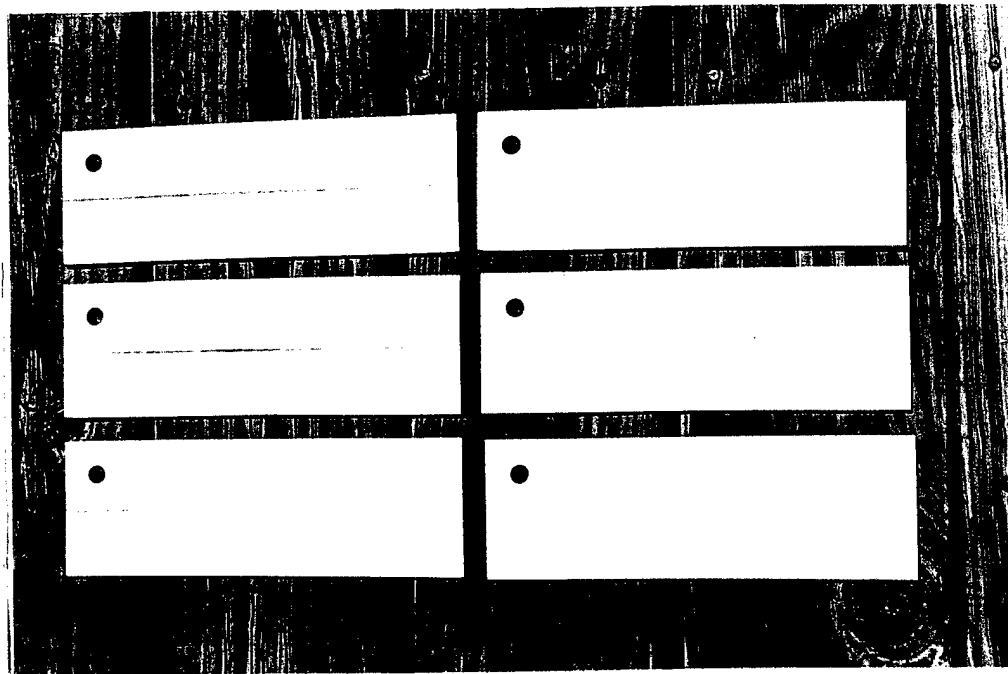


Figure 2.2  
Grit blasted welded and non-welded  
test panels

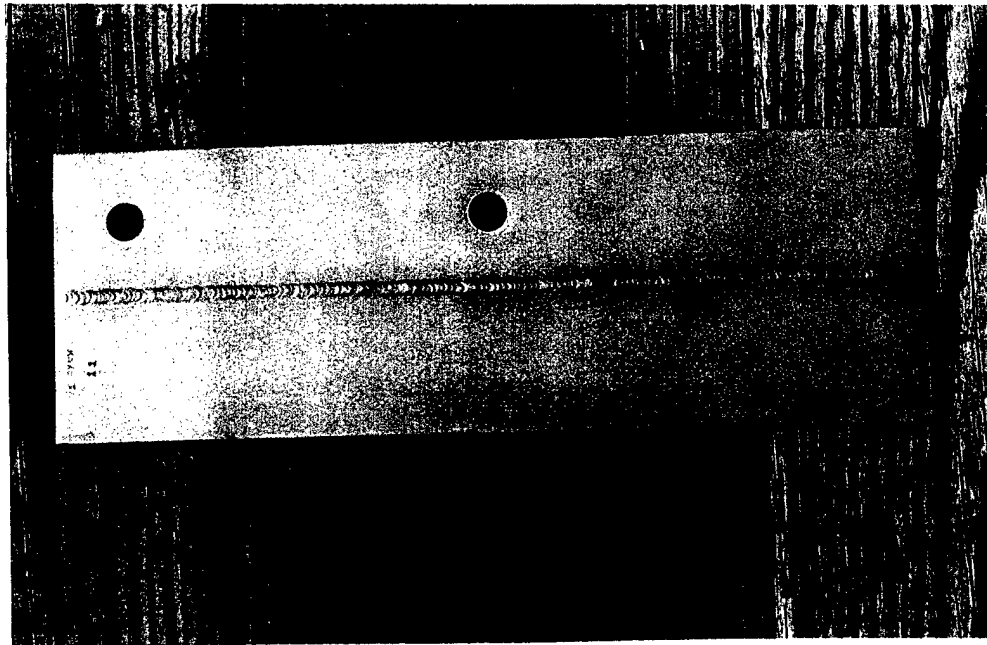


Figure 2.3  
Test panel with additional hole for  
anode attachment





Figure 3.1  
X-section of S31603 mill surface @  
500X

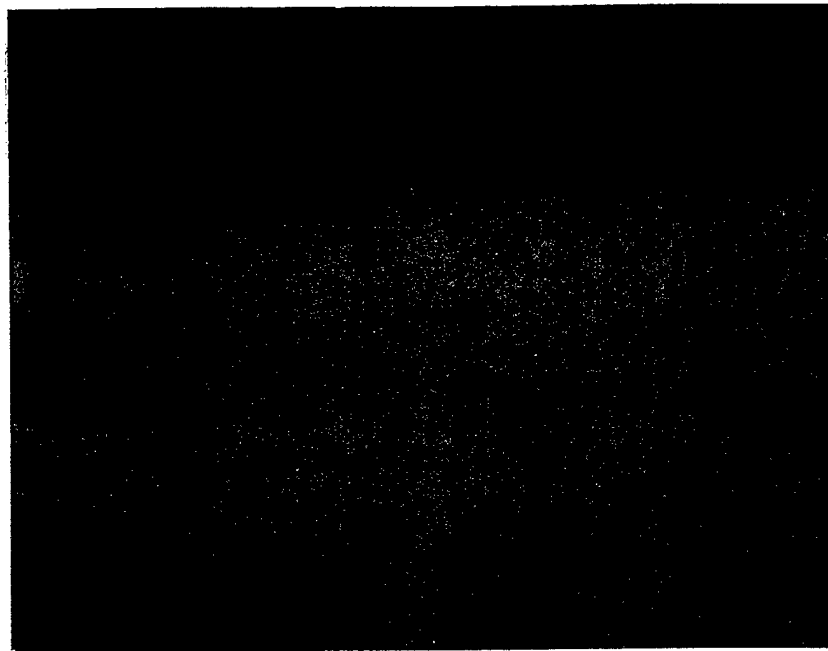


Figure 3.2  
X-section of S20910 mill surface @  
500X

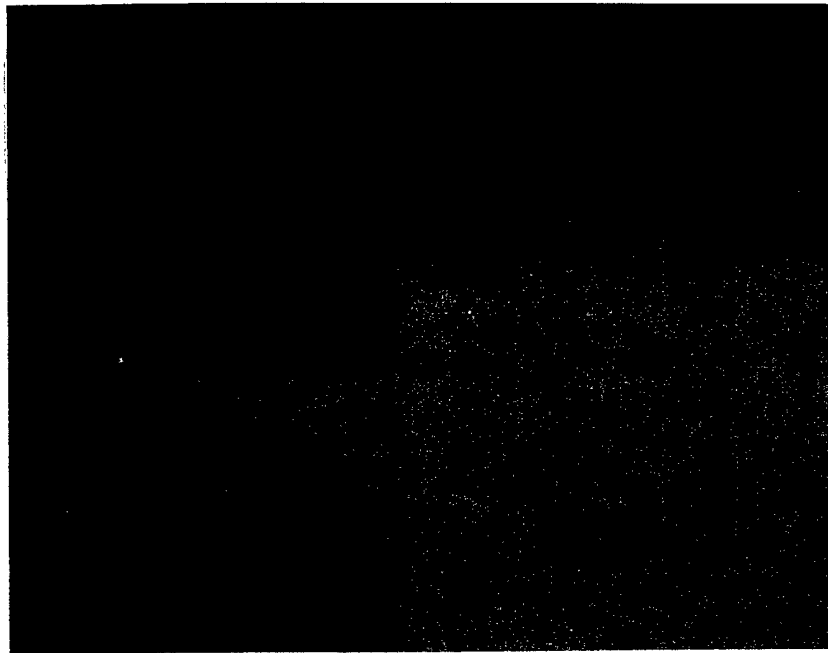


Figure 3.3  
X-section of N08367 mill surface @  
500X



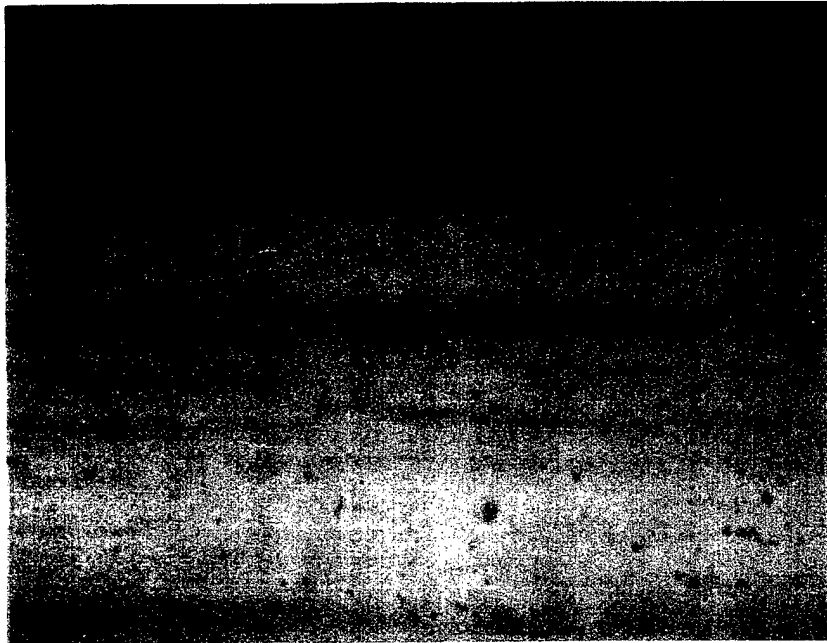


Figure 4.1  
X-section of S31603 grit blasted  
surface @ 500X

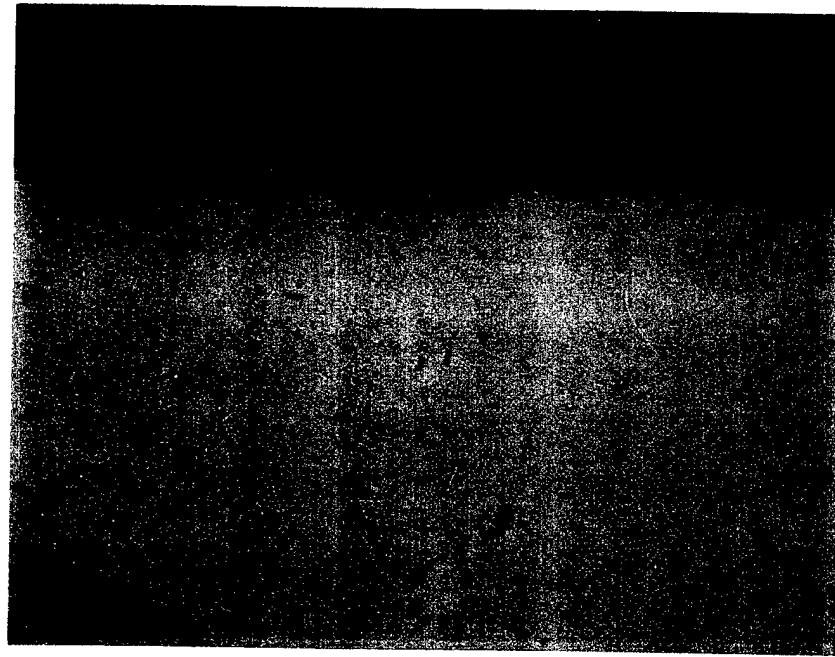


Figure 4.2  
X-section of S20910 grit blasted  
surface @ 500X

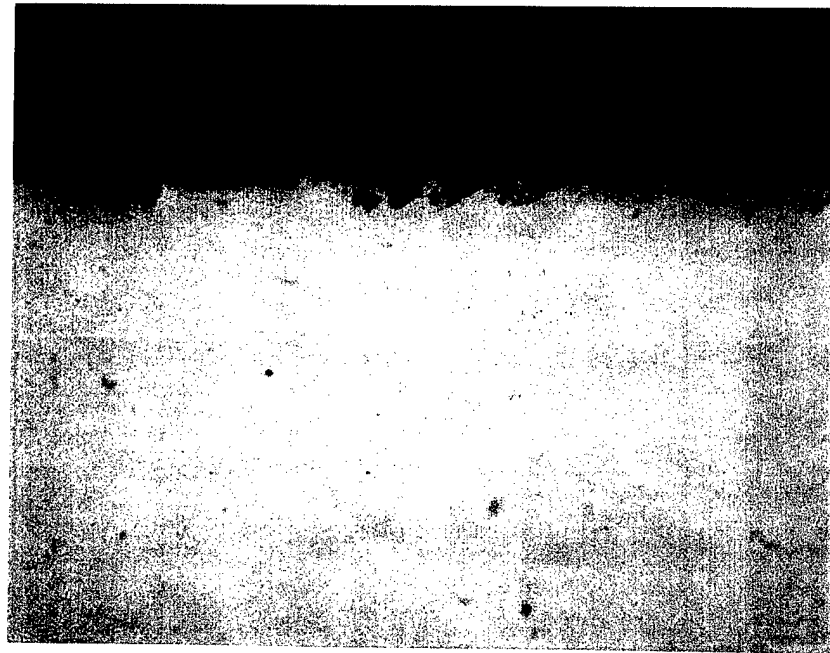


Figure 4.3  
X-section of N08367 grit blasted  
surface @ 500X



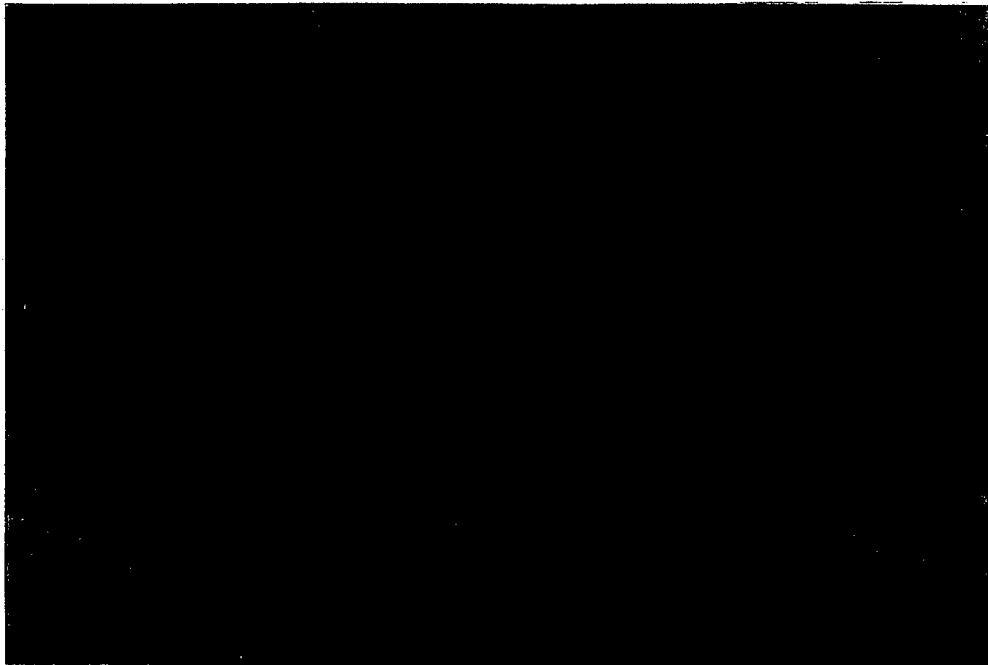


Figure 5.1  
Appearance of sprayed epoxy  
topcoat



Figure 5.2  
Appearance of sprayed ablative-Cu  
topcoat

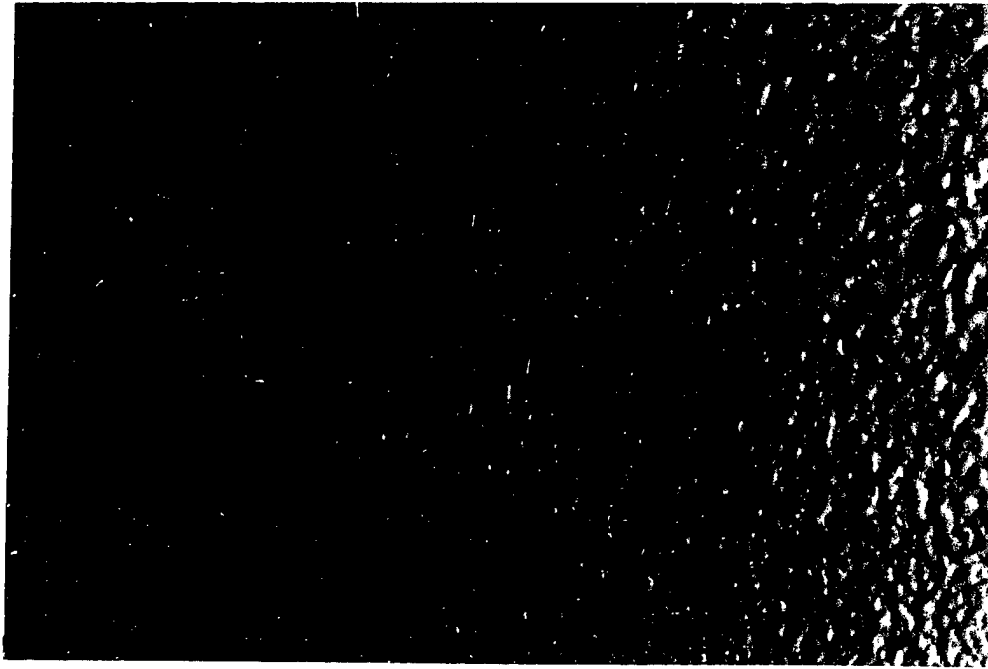


Figure 5.3  
Appearance of sprayed elastomeric  
topcoat





after  
test  
x-section

(1)  
(2)

Figure 6.1  
X-section of 2-layer epoxy system @  
100X



after  
test  
x-section

(1)  
(2)  
(3)

Figure 6.2  
X-section of 3-layer ablative-Cu  
system @ 100X



after  
test  
x-section

(1)  
(2)  
(3)  
(4)

Figure 6.3  
X-section of 4-layer elastomeric  
system @ 100X



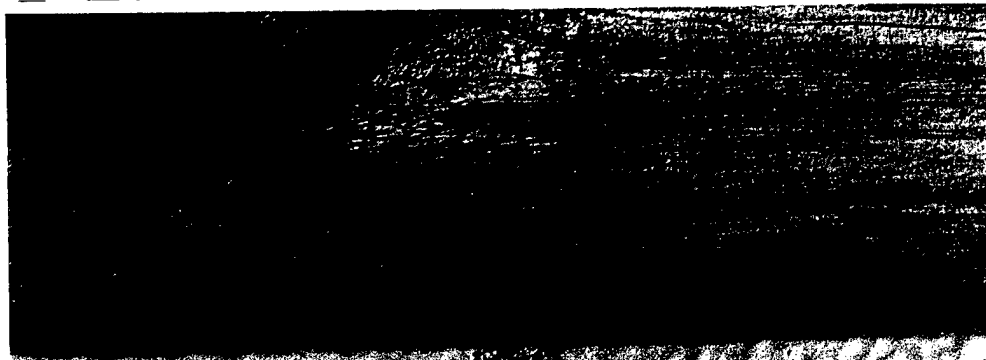


Figure 7.1  
Example of edge defect in top layer  
of epoxy coating

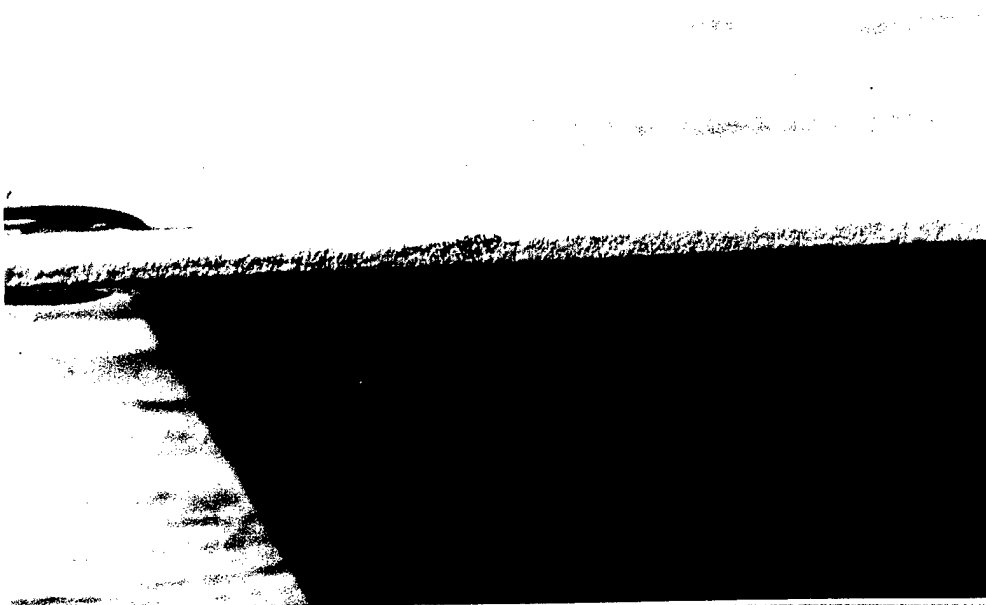


Figure 7.2  
Edge view of coating defect

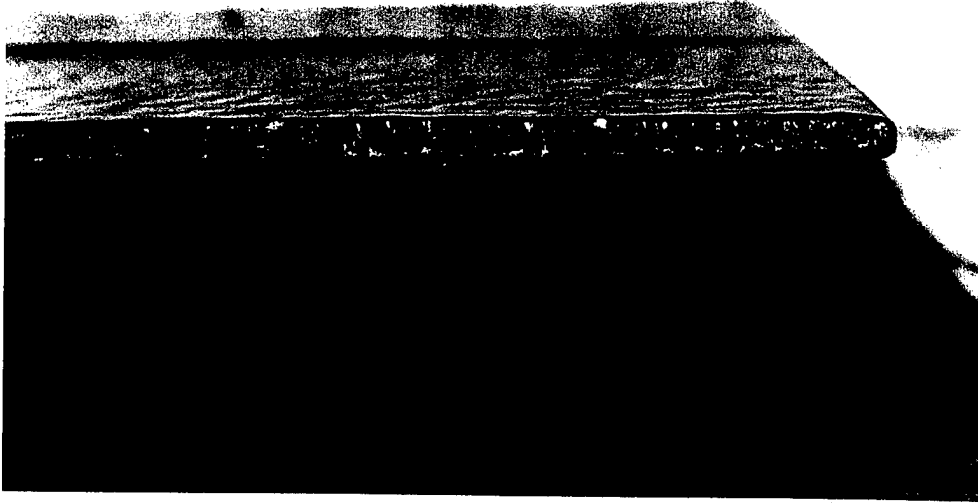


Figure 7.3  
Example of edge defect in ablative-  
Cu topcoat



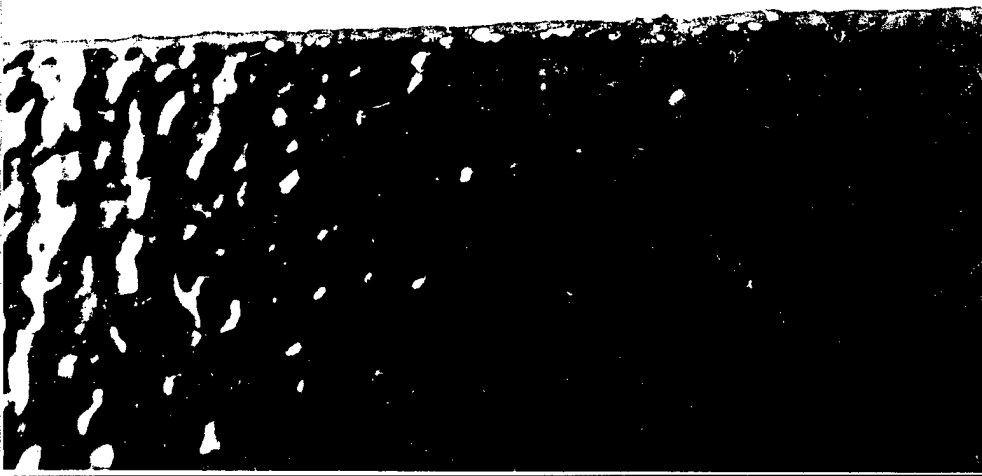


Figure 8.1  
Example of defect in elastomeric  
topcoat

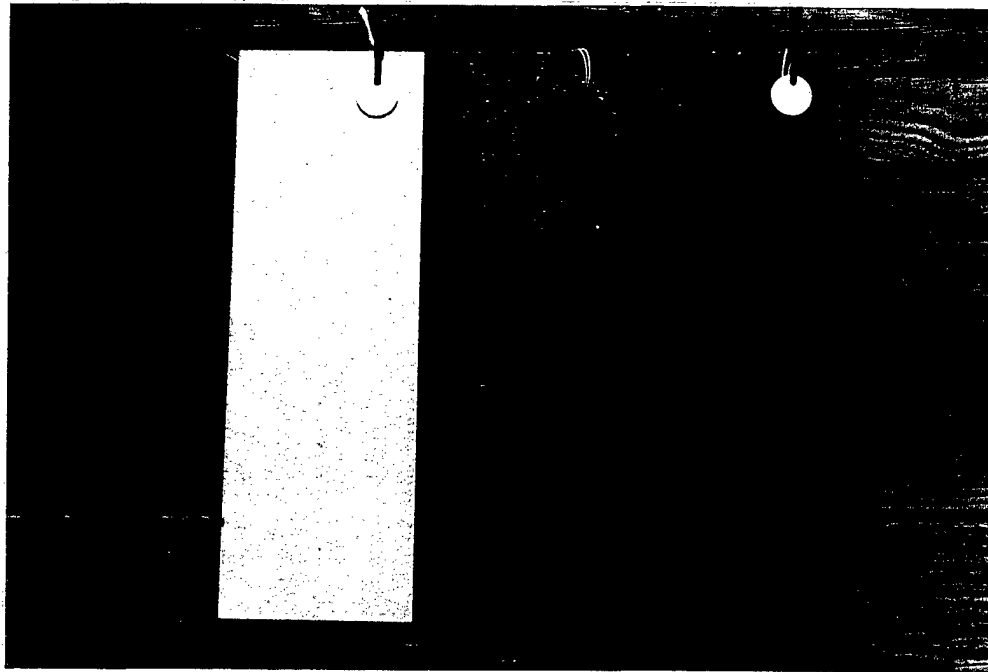


Figure 8.2  
Typical appearance of fully coated  
welded panels

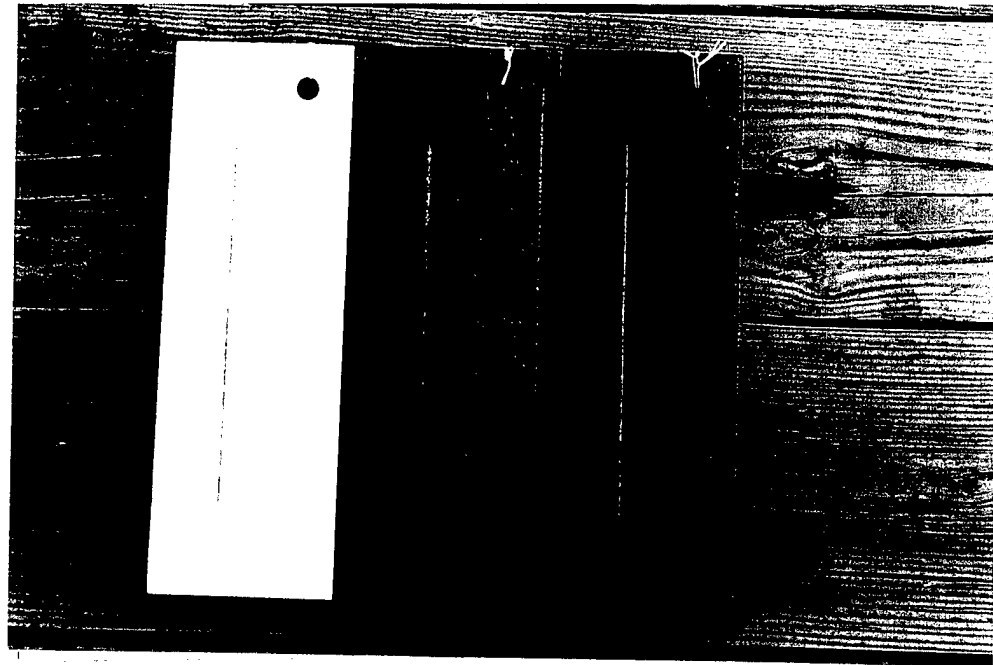


Figure 8.3  
Typical appearance of coated and  
scribed non-welded panels



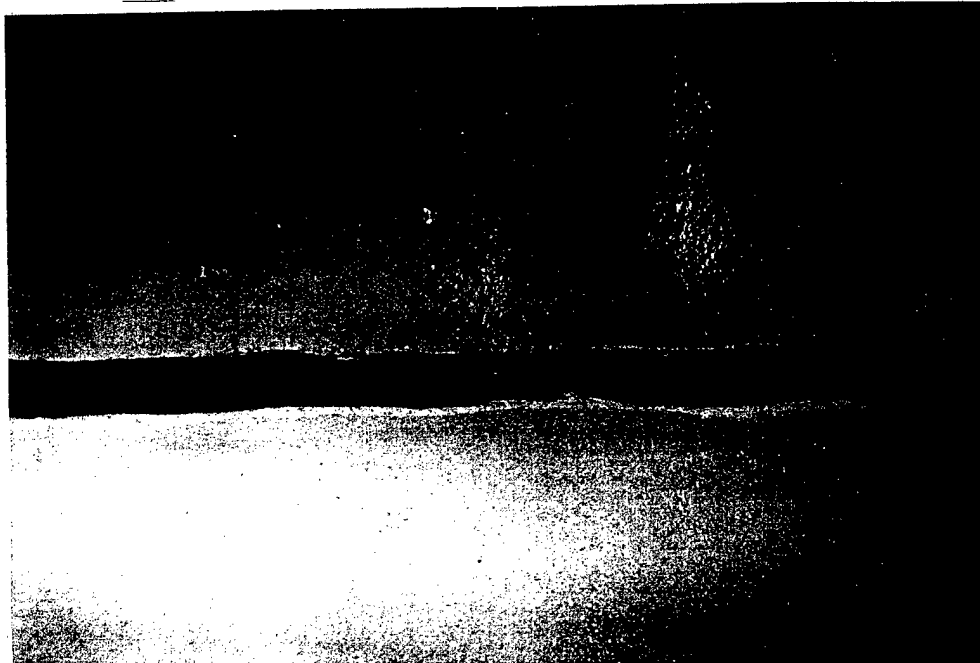


Figure 9.1  
View of scribed defect in epoxy  
coated panel @ 8.5X

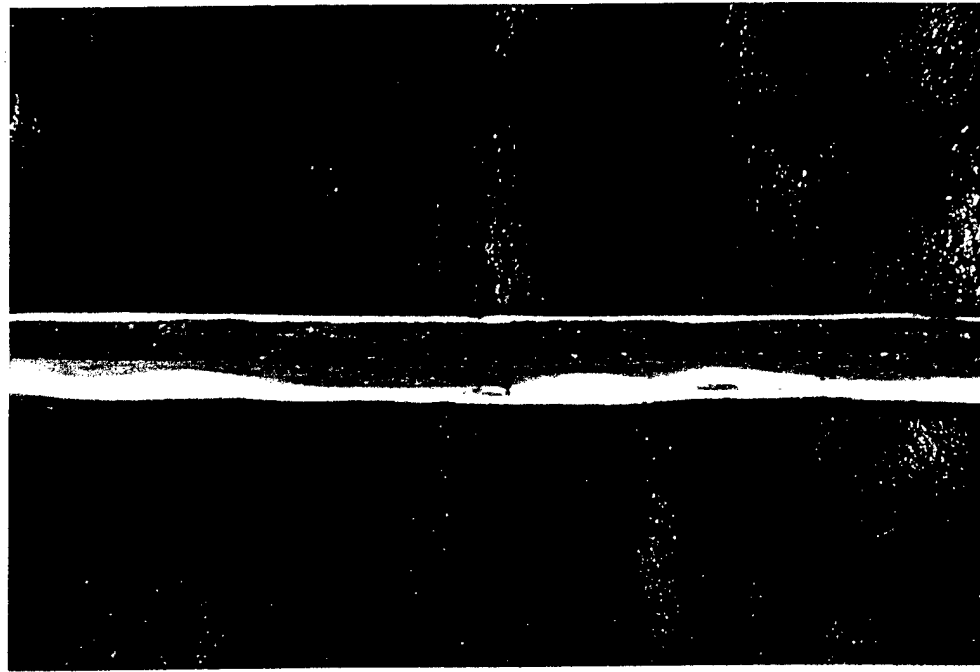


Figure 9.2  
View of scribed defect in ablative-Cu  
coated panel @ 8.5X

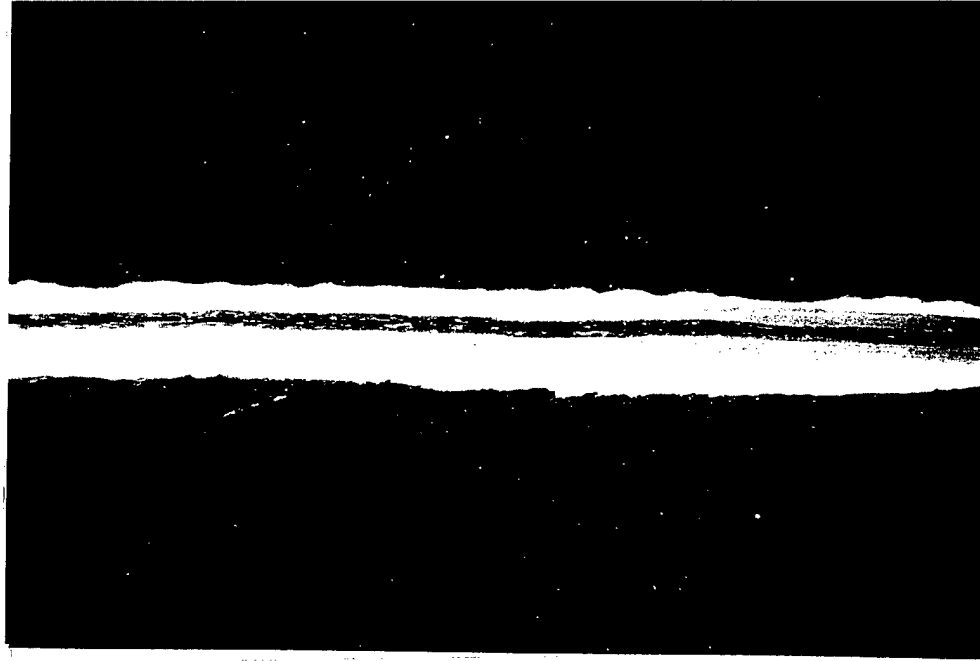


Figure 9.3  
View of scribed defect in elastomeric  
coated panel @ 8.5X



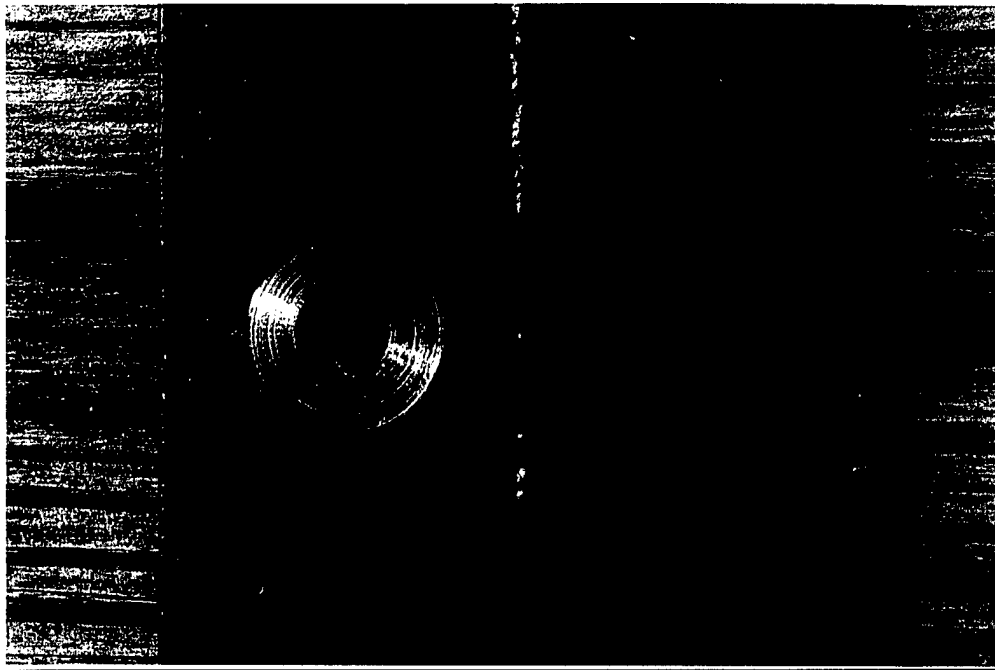


Figure 10.1  
Site preparation for Zn anode

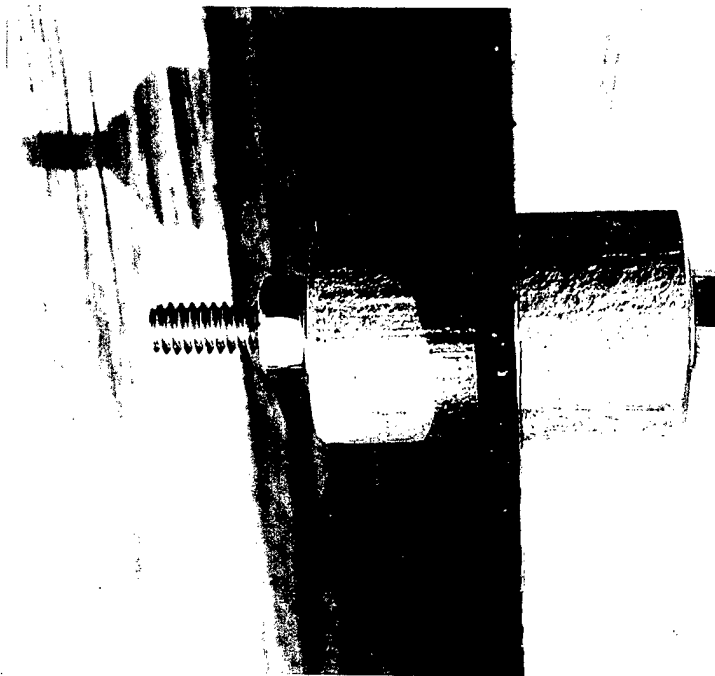


Figure 10.2  
Dual anodes attached with Type 316  
fastener

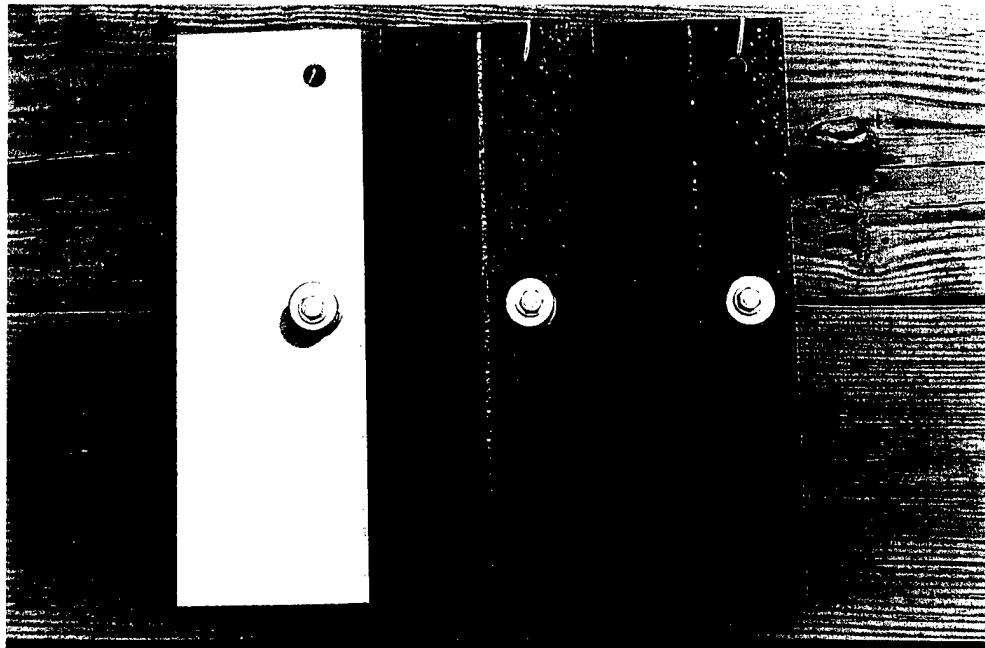


Figure 10.3  
Typical view of welded and coated  
test panels with anodes



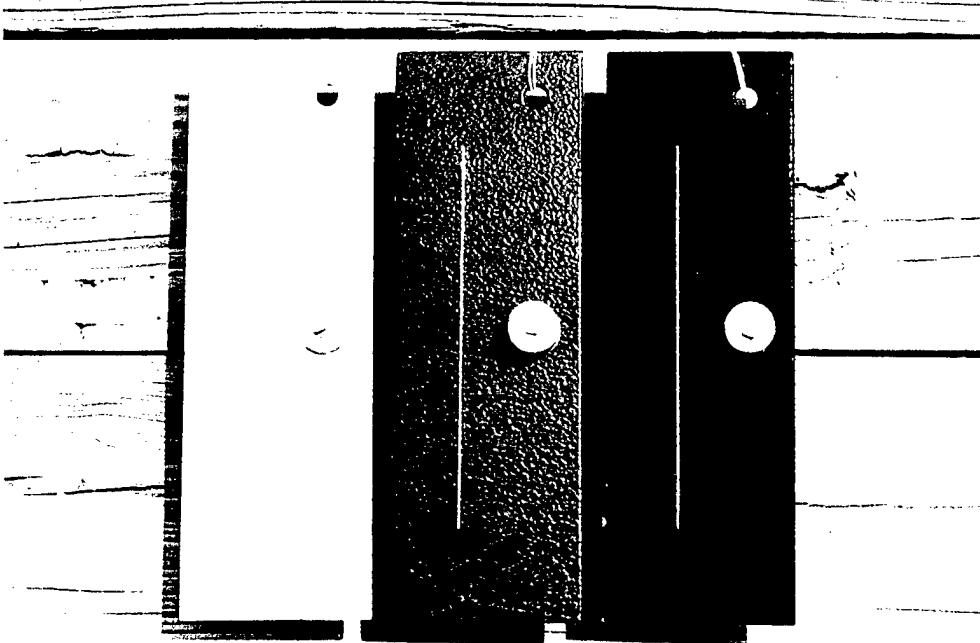


Figure 11.1  
Typical view of non-welded and  
coated panels with zinc anodes



Figure 11.2  
Test panel and anode electrical  
isolation from exposure rack

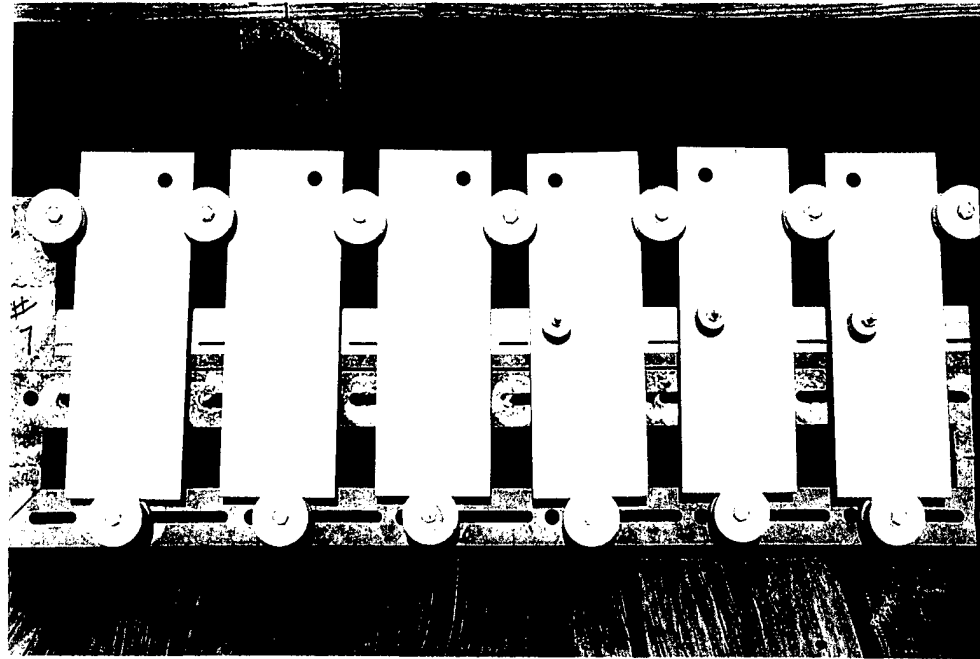


Figure 11.3  
View of uncoated welded controls  
with and without zinc anodes



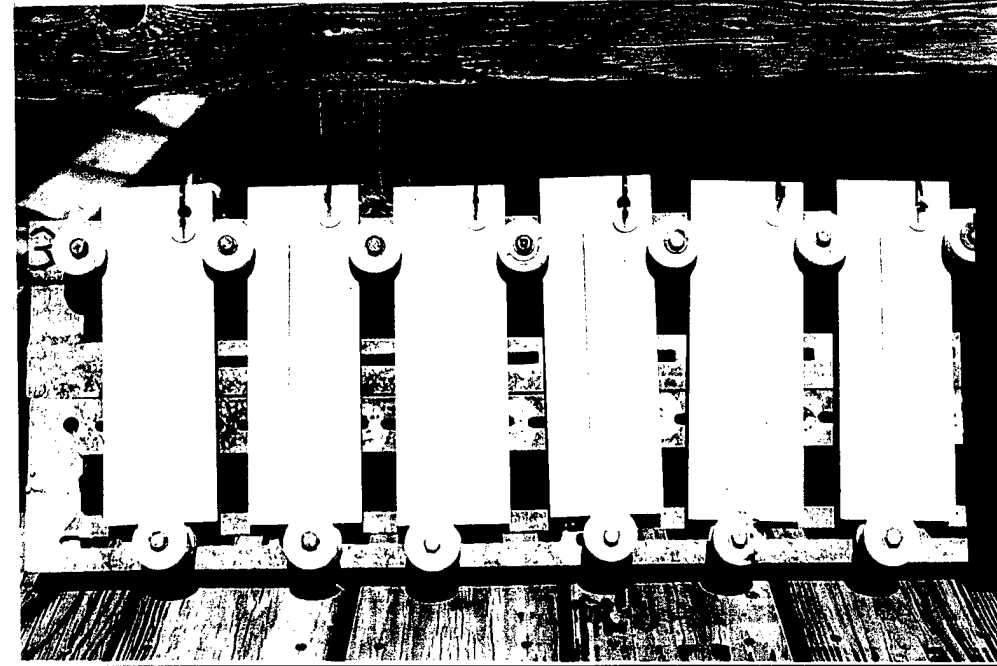


Figure 12.1  
One set of epoxy coated welded and  
non-welded panels of 3 alloys  
mounted for 1 year exposure without  
CP

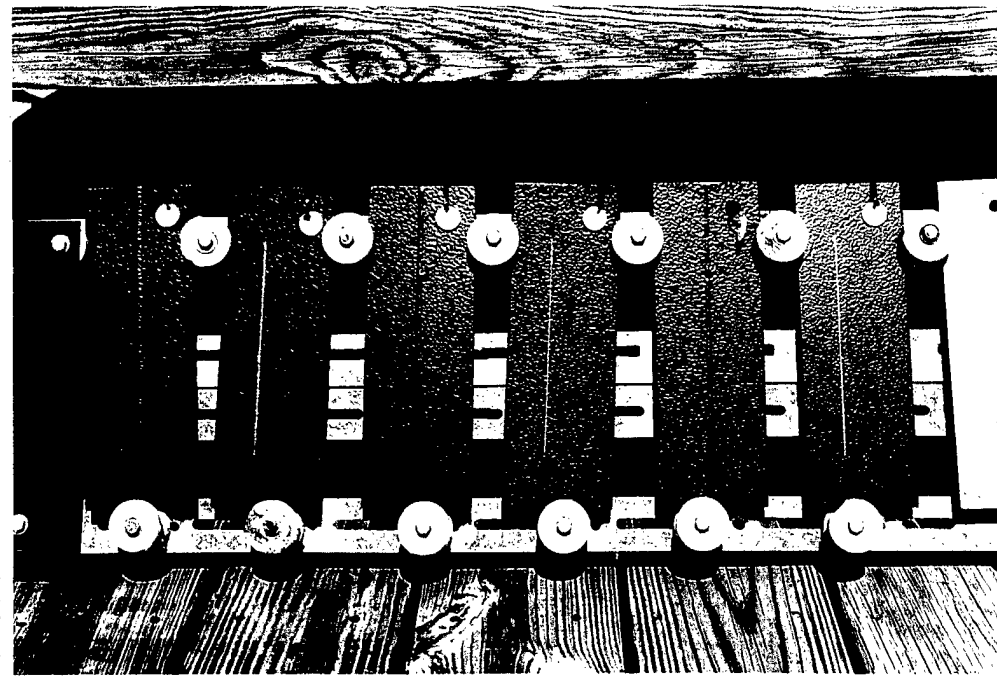


Figure 12.2  
Same as Fig. 12.1, but with ablative-  
Cu coating system

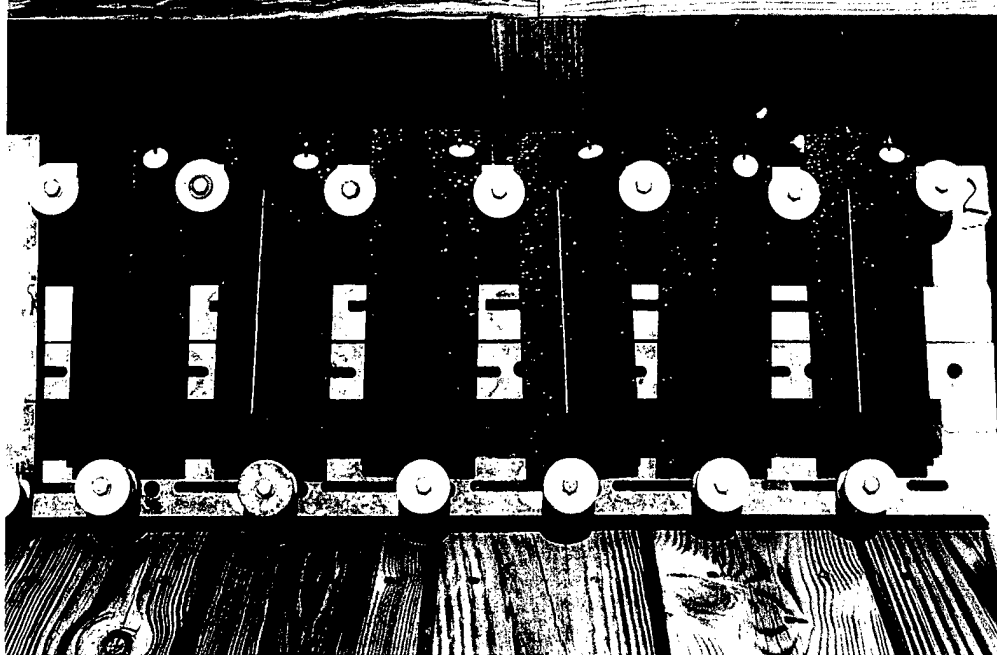


Figure 12.3  
Same as Fig. 12.1, but with  
elastomeric coating system



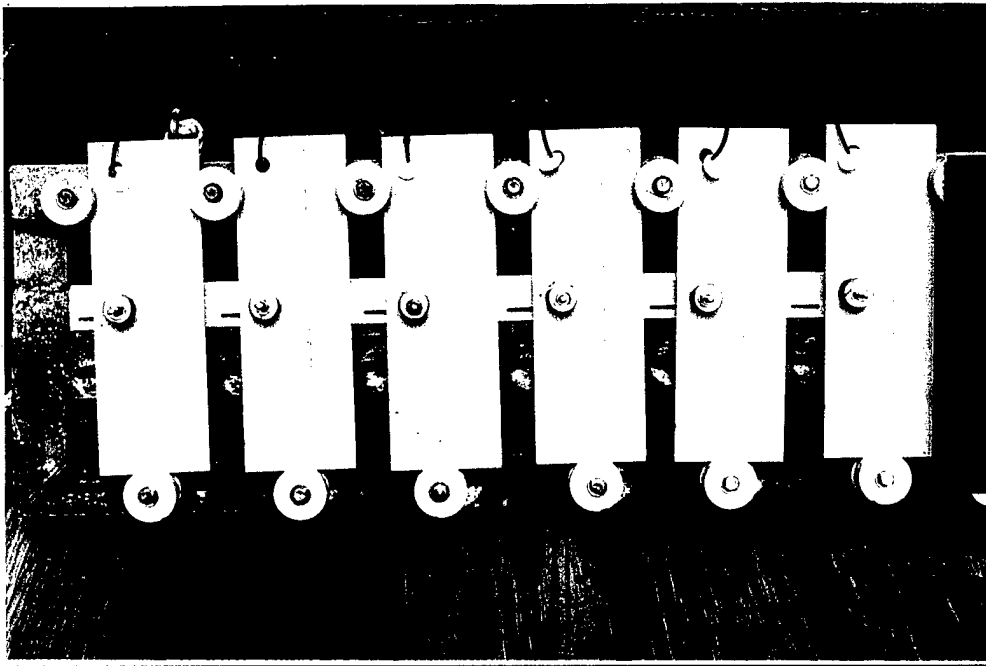


Figure 13.1  
Same as Fig. 12.1, but with Zn  
anodes

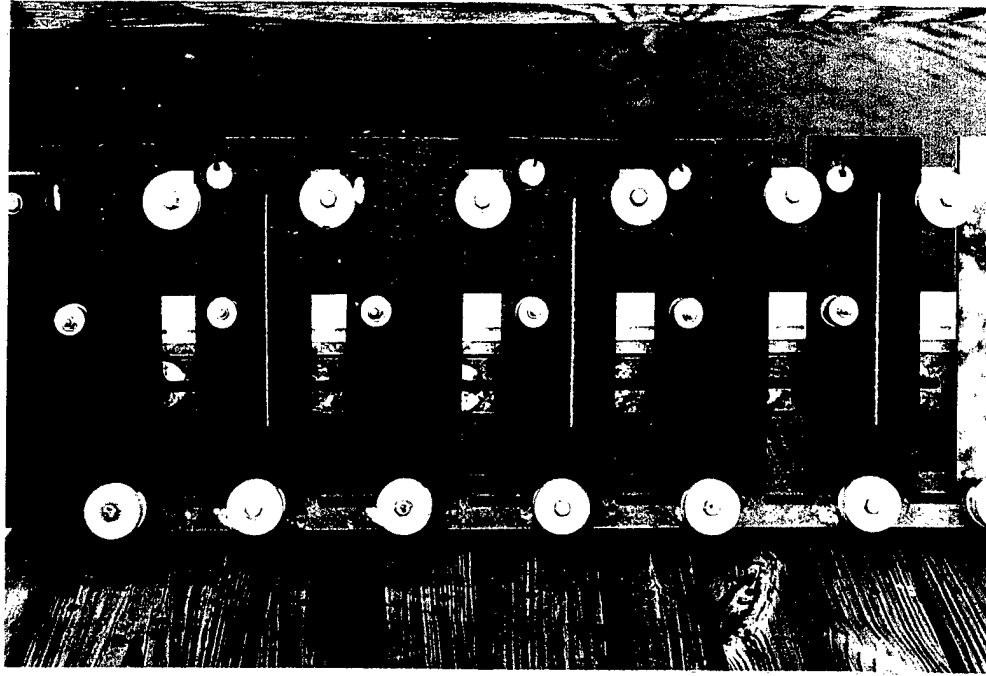


Figure 13.3  
Same as Fig. 12.2, but with Zn  
anodes

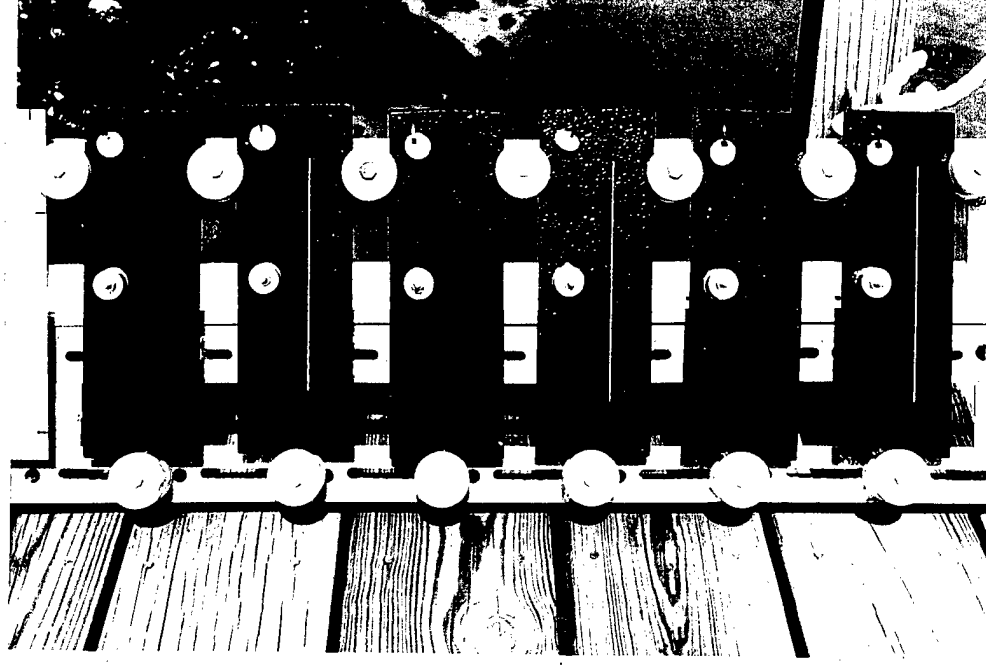


Figure 13.3  
Same as Fig. 12.3, but with Zn  
anodes



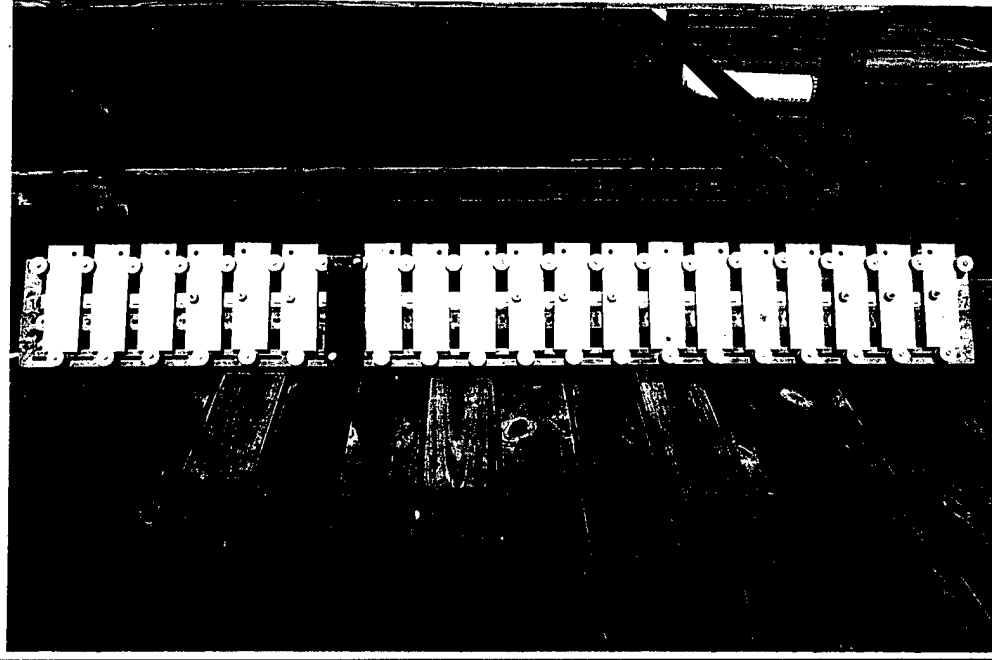


Figure 14.1  
Overall view of test rack with  
uncoated controls with and without  
CP



Figure 14.2  
Overall view of test rack with coated  
panels for exposure without CP

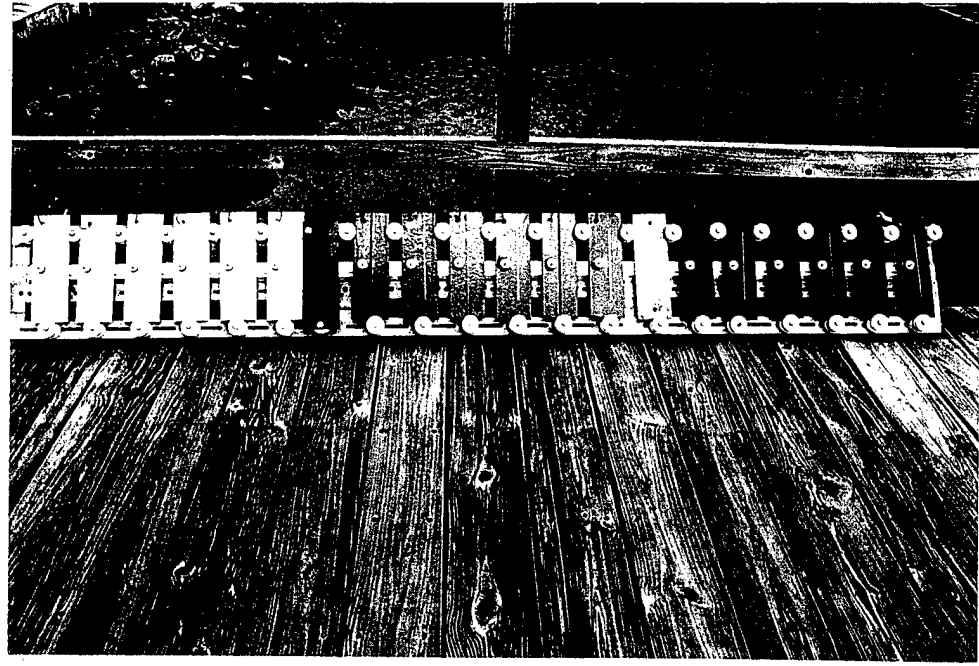


Figure 14.3  
Same as Fig. 14.2, but with Zn  
anodes





Figure 16.3  
Typical view of ablative-Cu coated  
panels - 12 months exposure without  
CP

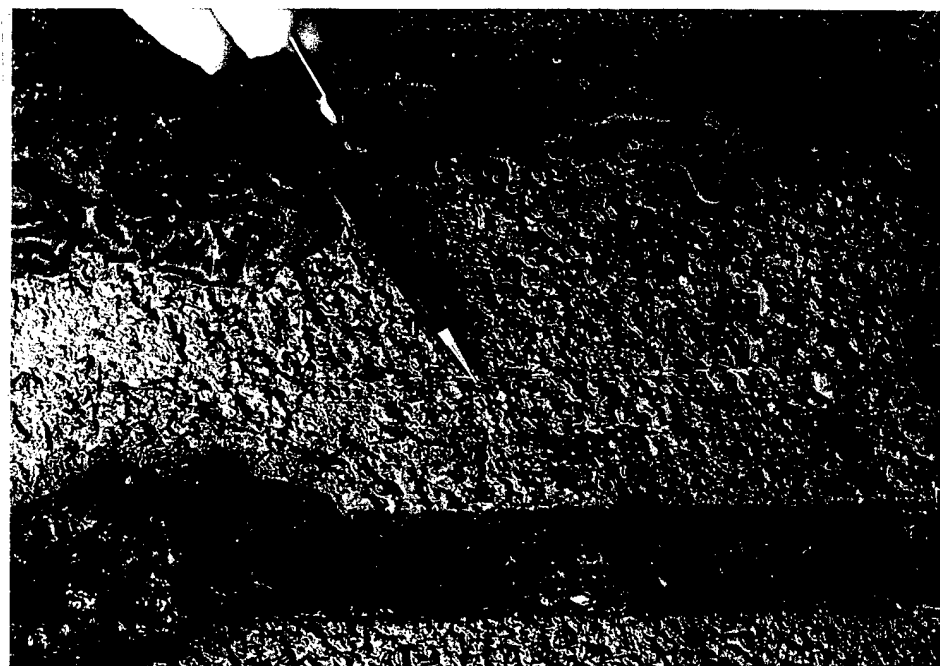


Figure 16.2  
Close-up view of resistant scribe site  
on panel inspected at 6 months

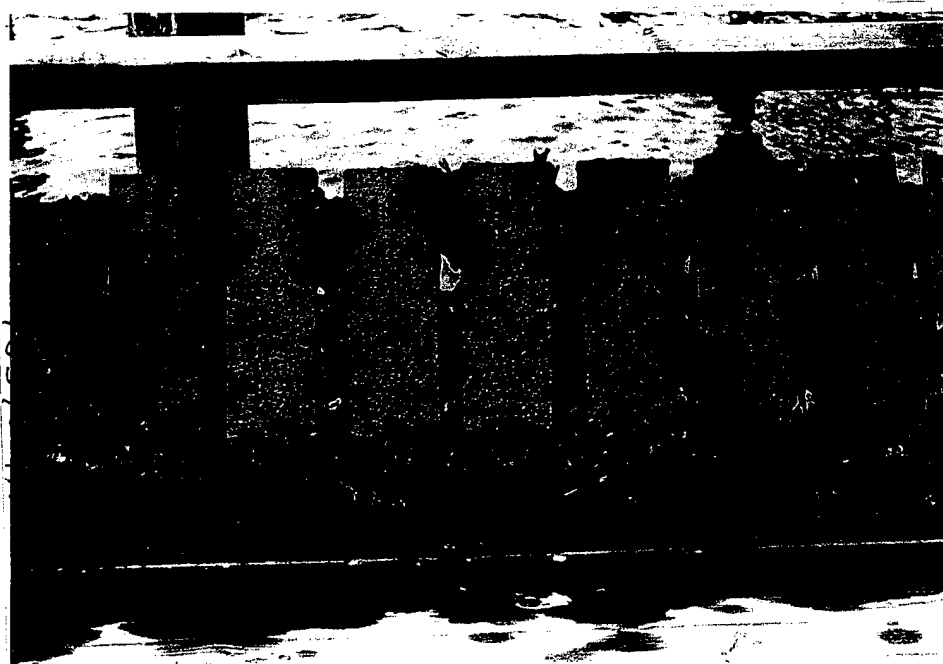


Figure 16.1  
Appearance of ablative-Cu coated  
panels - 6 months exposure without  
CP





Figure 18.1  
Overall view of test rack with  
uncoated controls - 12 months  
AV0005196



Figure 18.2  
Typical view of racks (1 of 3) with  
coated panels - exposed without CP  
for 12 months



Figure 18.3  
Typical view of racks (1 of 3) with  
coated panels exposed with CP  
for 12 months





Figure 19.1  
Epoxy coating disbondment on mill  
surface of S31603 panel with CP

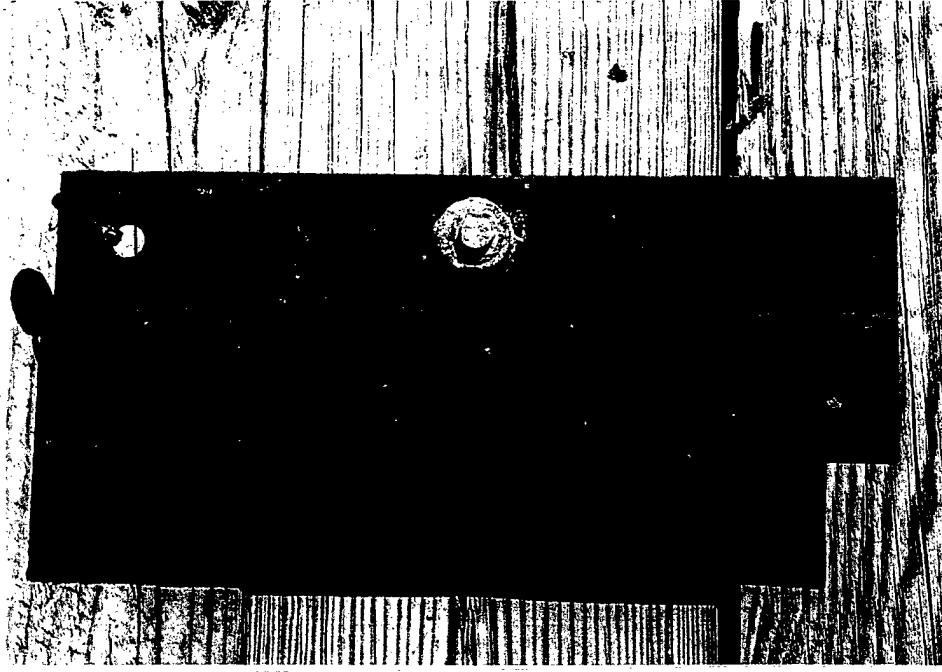


Figure 19.2  
Representative view of blisters on  
ablative-Cu coated panel with CP



Figure 19.3  
Evidence of elastomeric coating  
disbonding





Figure 20.1  
Attack at edge defect site on epoxy  
coated S31603 panel (blasted  
surface)

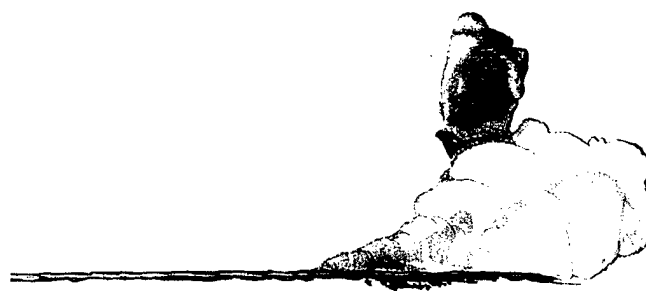


Figure 20.2  
Attack at scribe site on epoxy coated  
S20910 panel (blasted surface)

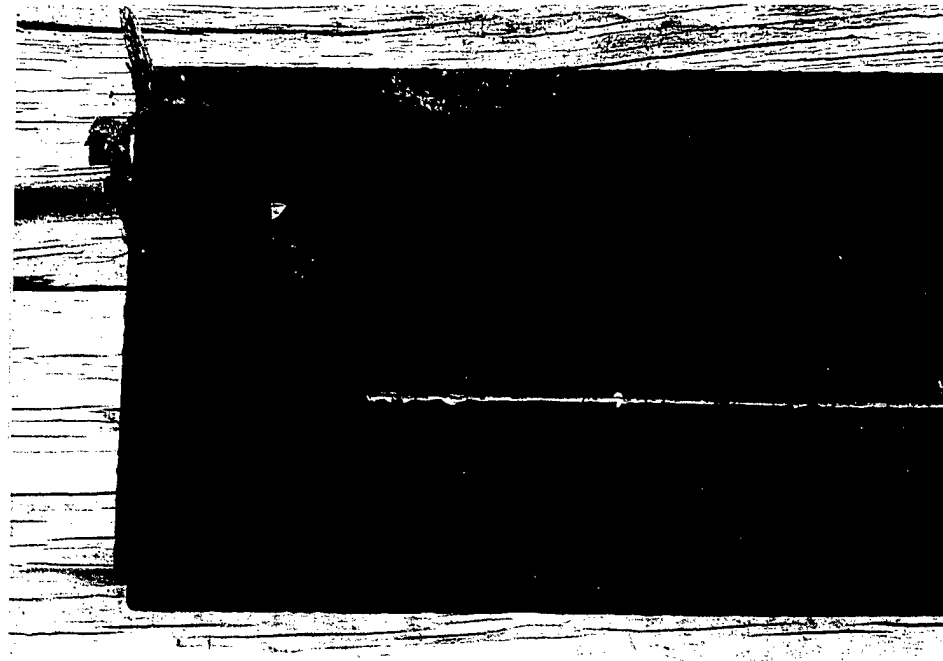


Figure 20.3  
Attack at edge defect on ablative-Cu  
coated S20910 panel



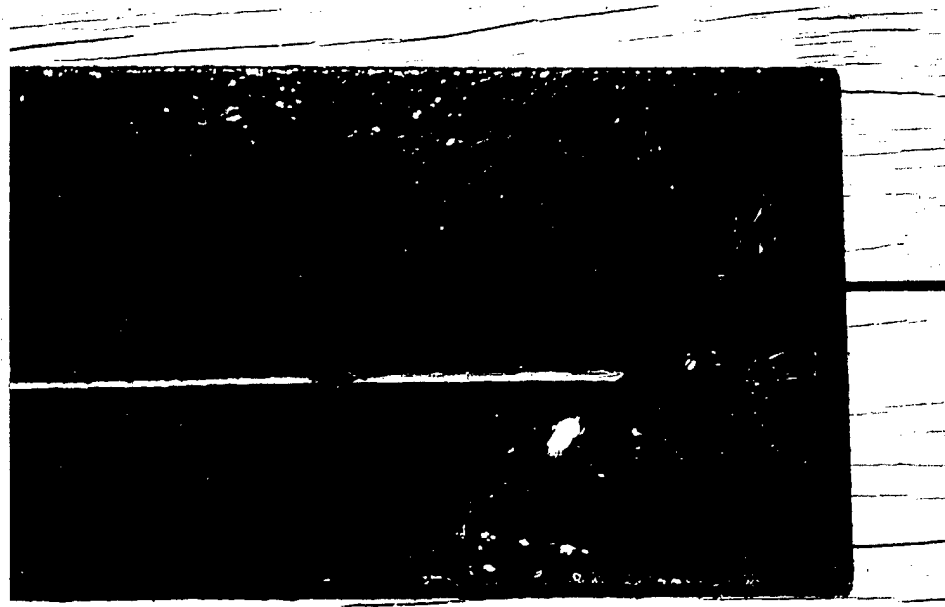


Figure 21.1  
Attack at scribed site on elastomeric  
coated S20910 panel

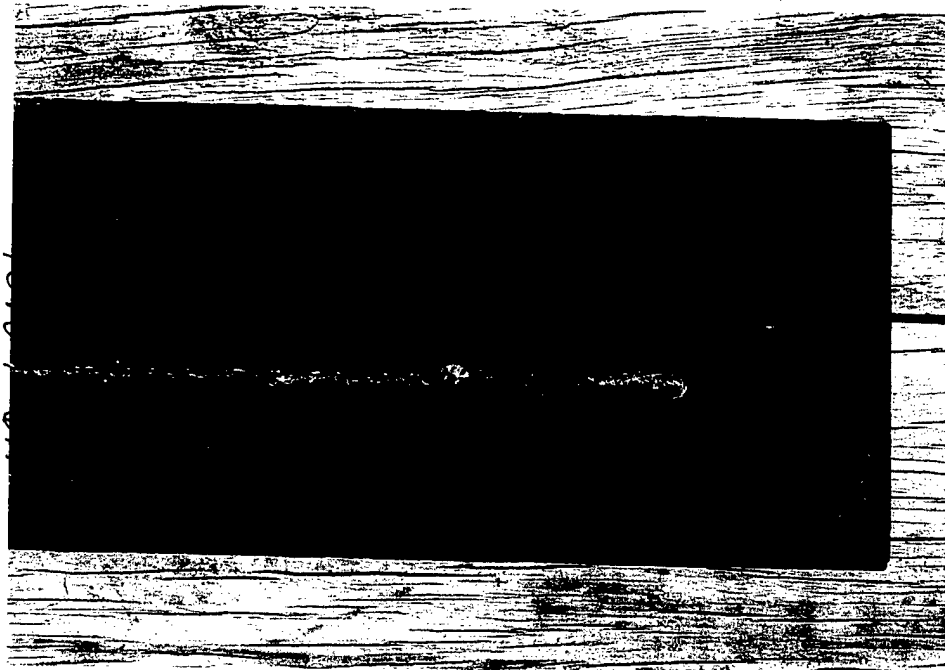


Figure 21.2  
Attack at scribed site on ablative-Cu  
coated S31603 panel

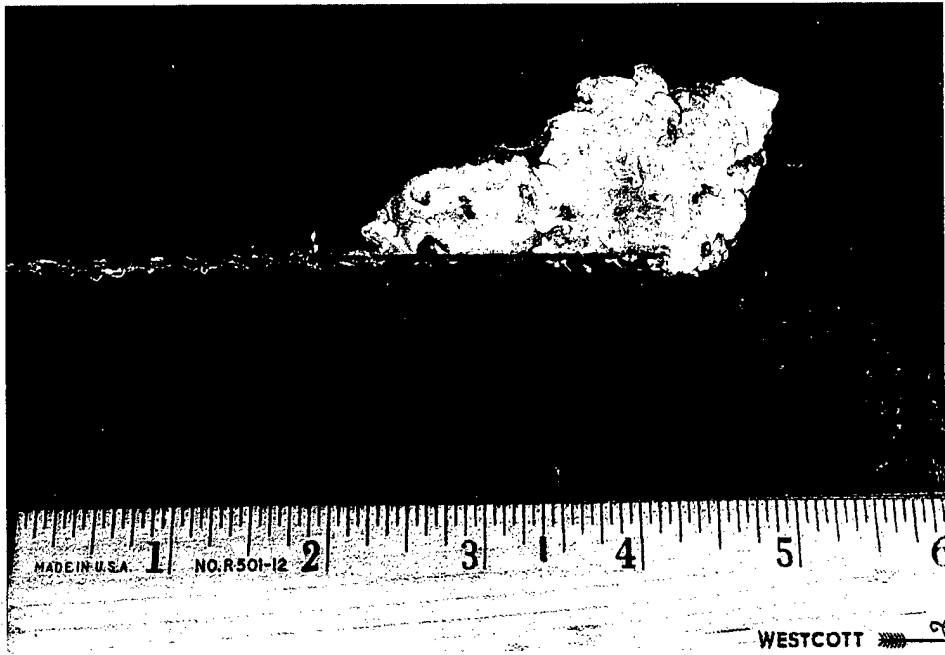


Figure 21.3  
Same as Fig. 21.2, but with  
disbonded coating removed



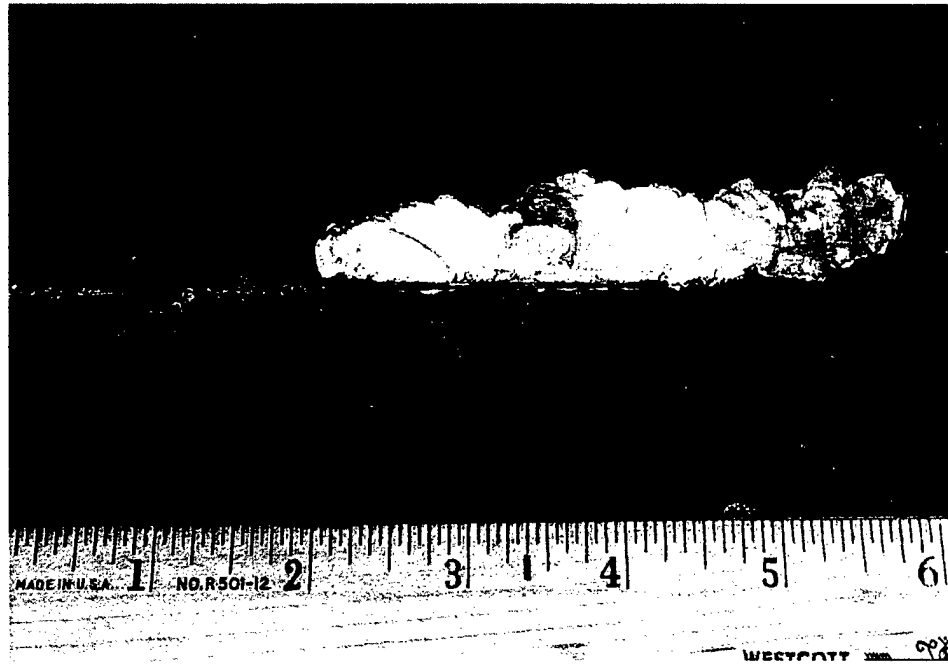


Figure 22.3  
Same as Fig. 22.2, but with  
disbonded coating removed

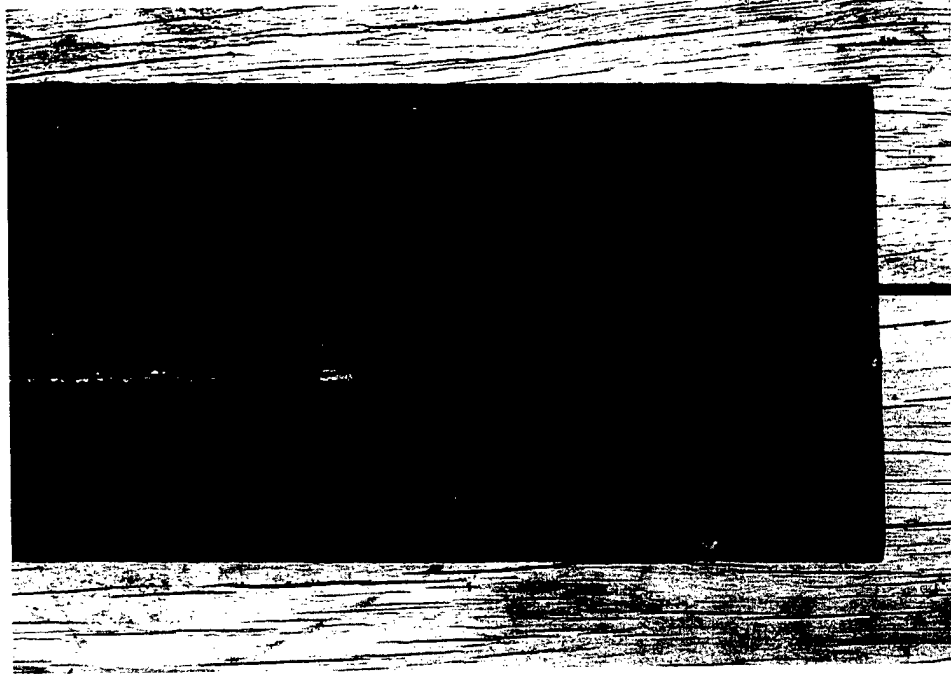


Figure 22.2  
Attack at scribed site on ablative-Cu  
coated S20910 panel



Figure 22.1  
Only confirmed attack at scribe sites  
on N08367 panels



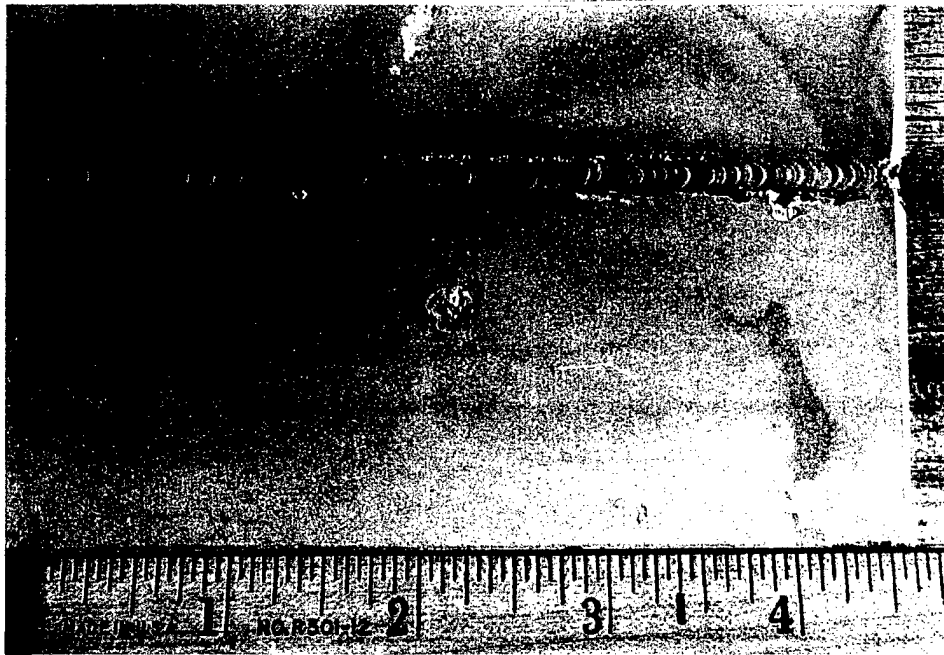


Figure 23.1  
Barnacle site and weld-HAZ attack  
on uncoated S31603 panel

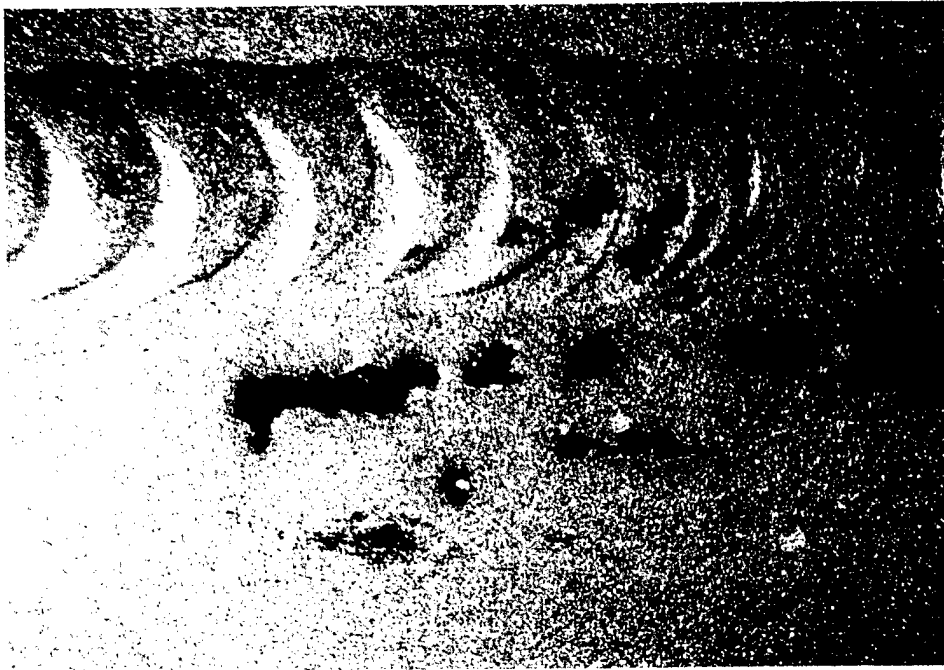


Figure 23.2  
Close-up view of weld-HAZ attack  
on another S31603 panel (8.5X)

Figure 23.3  
Blank



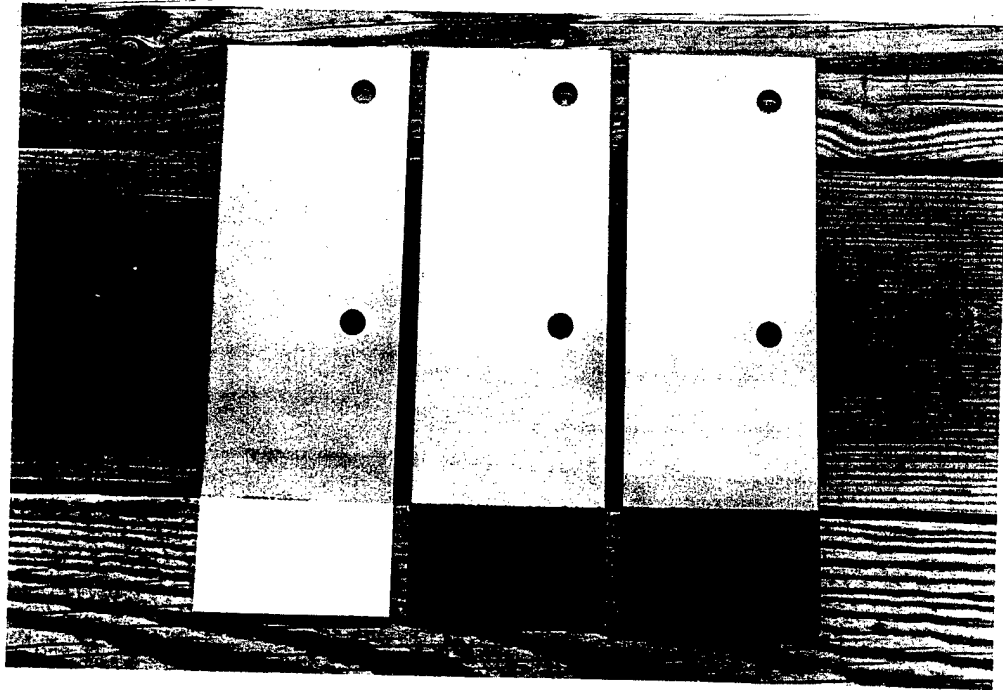


Figure 24.1  
Panels with 20% of surface area  
coated (grit blasted side shown)

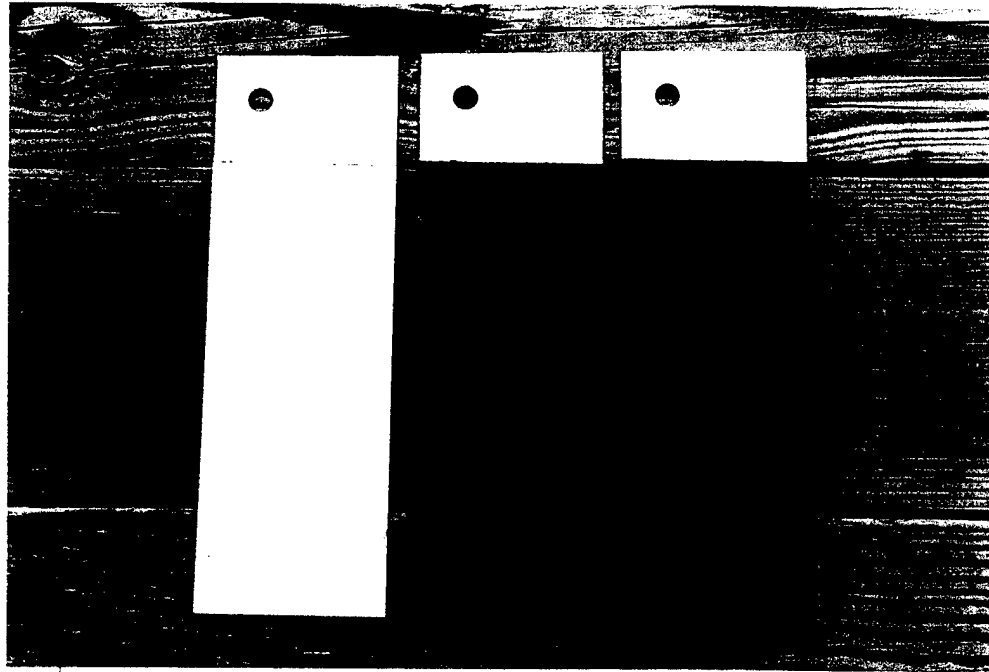


Figure 24.2  
Panels with 80% of surface area  
coated (mill surface side shown)



Figure 24.3  
Exposure arrangement for 6-month  
filtered seawater test



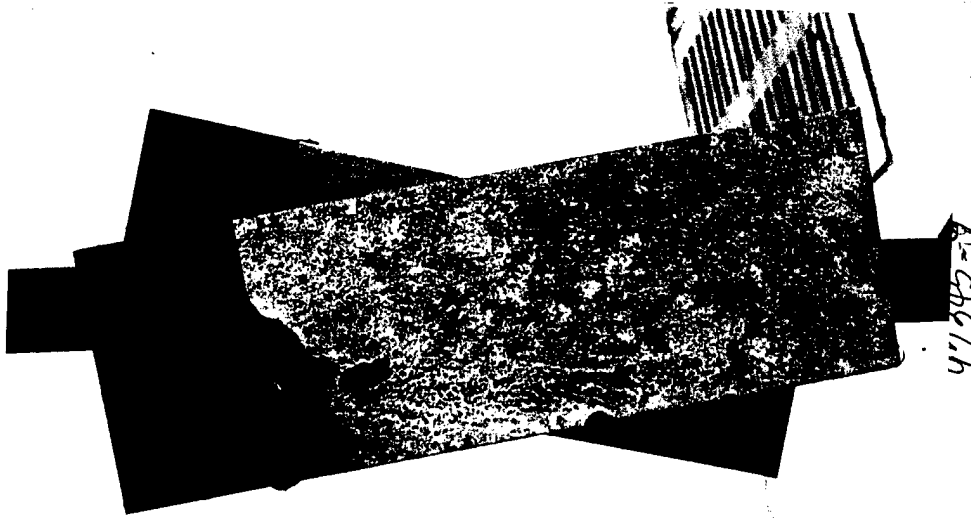


Figure 25.1  
Attack of S3 1603 panel with 80%  
epoxy coverage

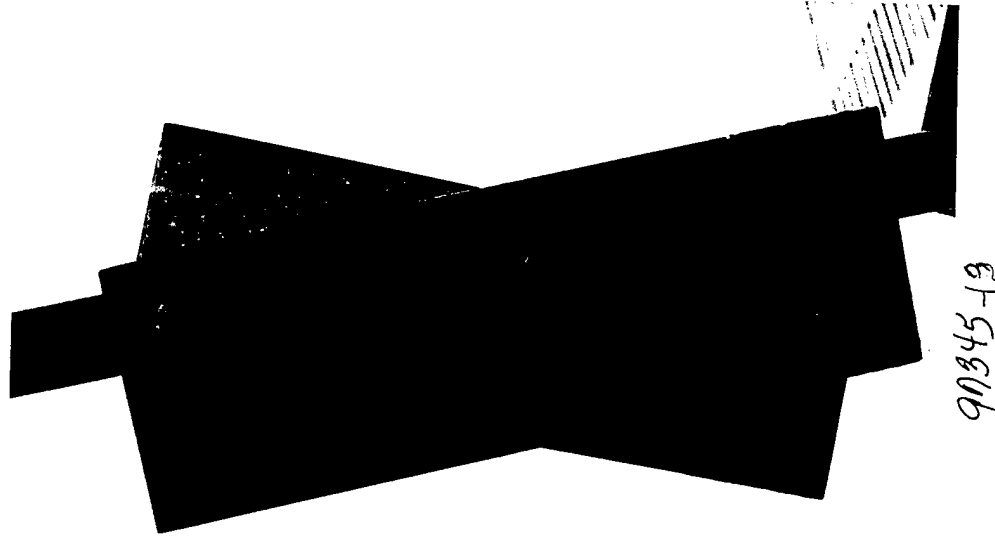


Figure 25.2  
Attack of S20910 panel with 20%  
ablative-Cu coverage

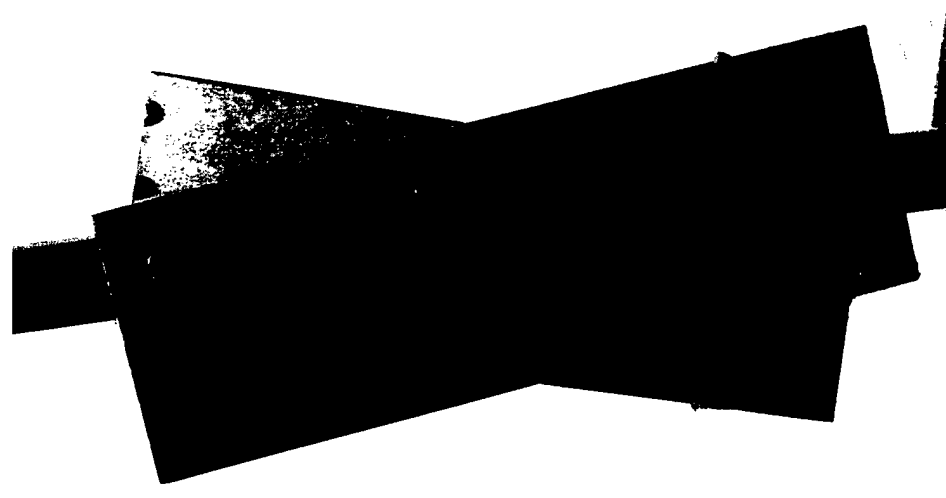


Figure 25.3  
Attack of N08367 panel with 20%  
elastomeric coverage



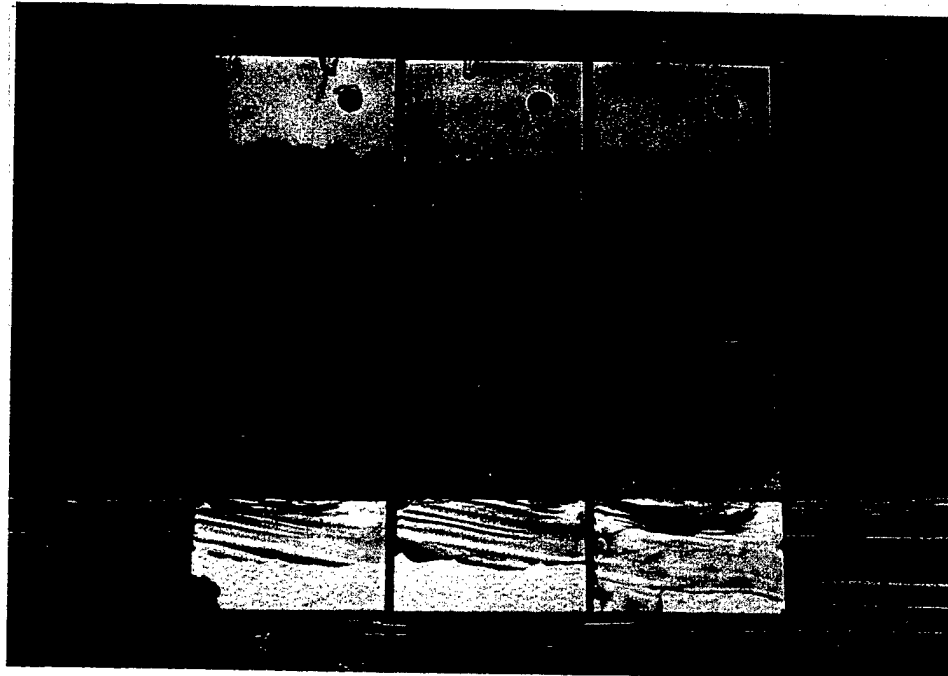


Figure 26.1  
Material - Surface: S31603 - blasted  
Coating - Area: epoxy - 20%

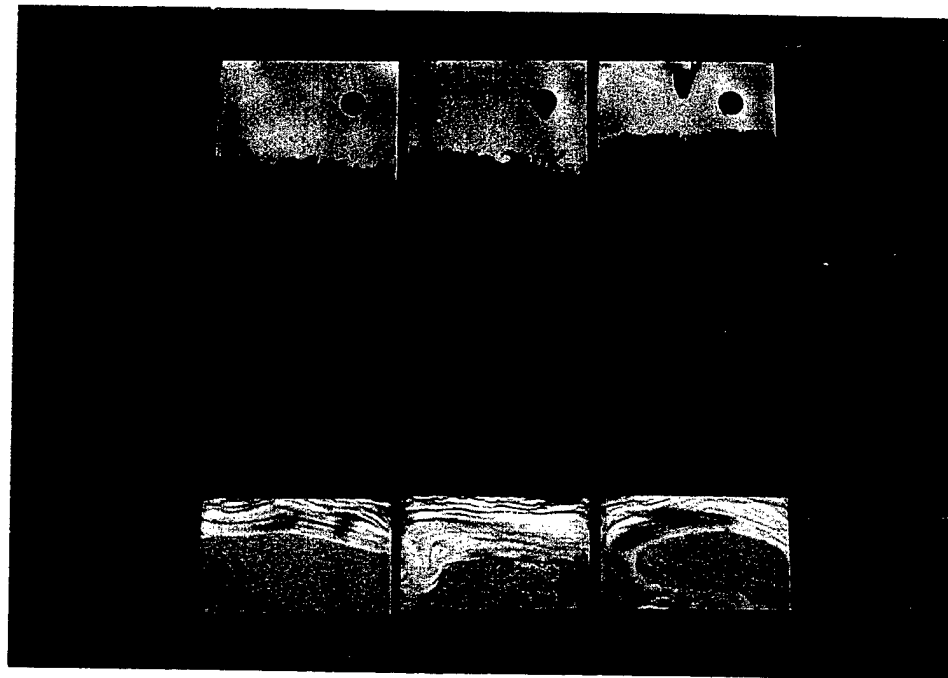


Figure 26.2  
Material - Surface: S20910 - blasted  
Coating - Area: epoxy - 20%

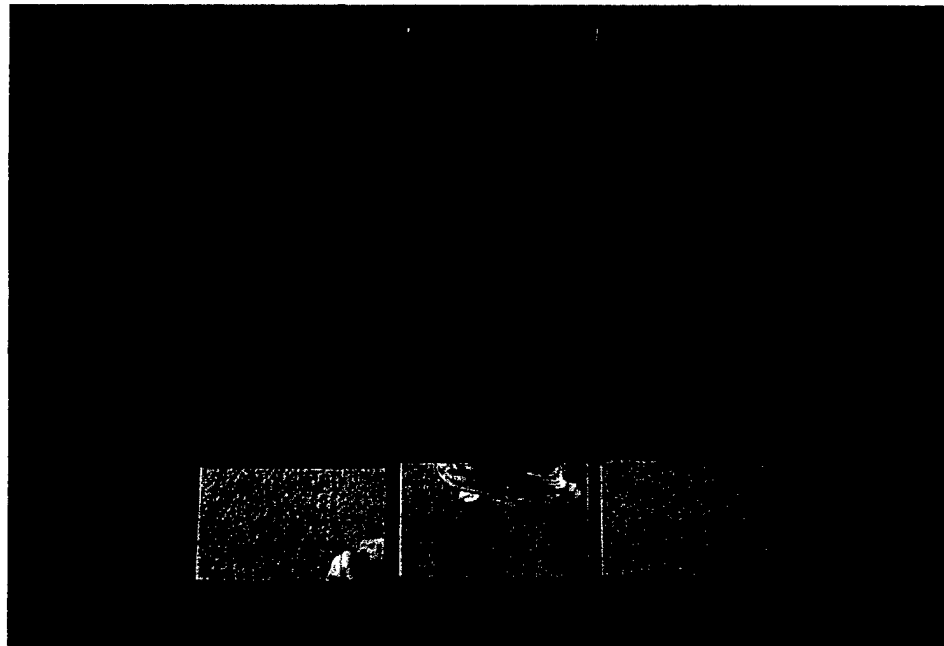


Figure 26.3  
Material - Surface: N08367 - blasted  
Coating - area: epoxy - 20%



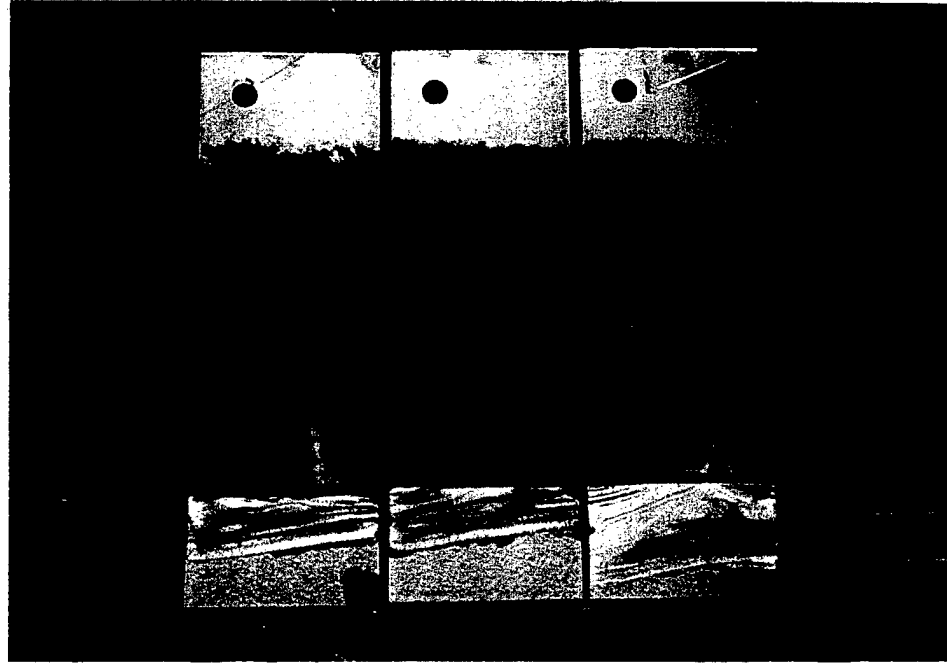


Figure 27.1  
Material - Surface: S31603 - mill  
Coating - Area: epoxy - 20%

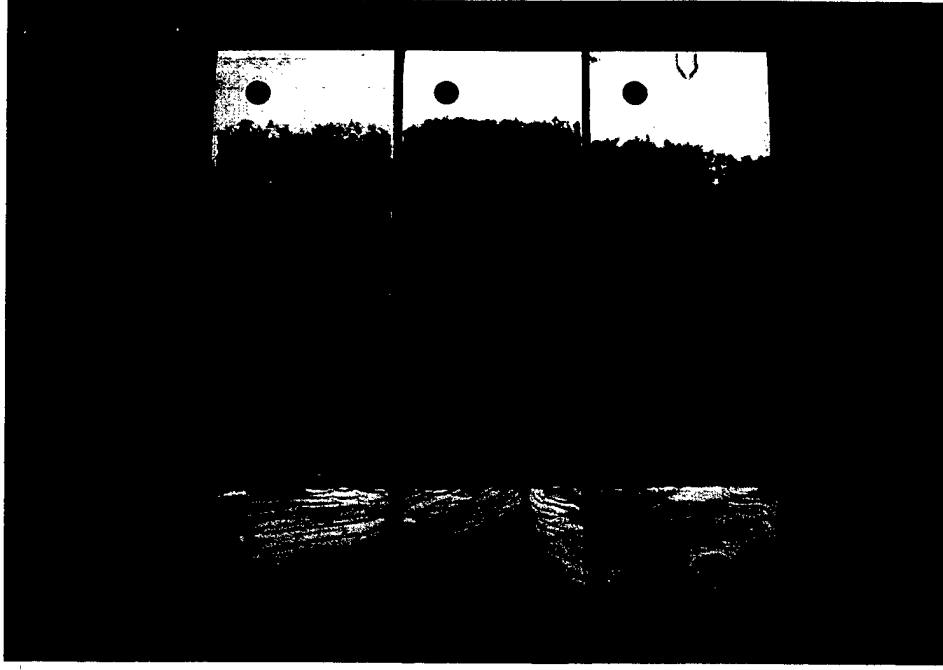


Figure 27.2  
Material - Surface: S20910 - mill  
Coating - Area: epoxy - 20%

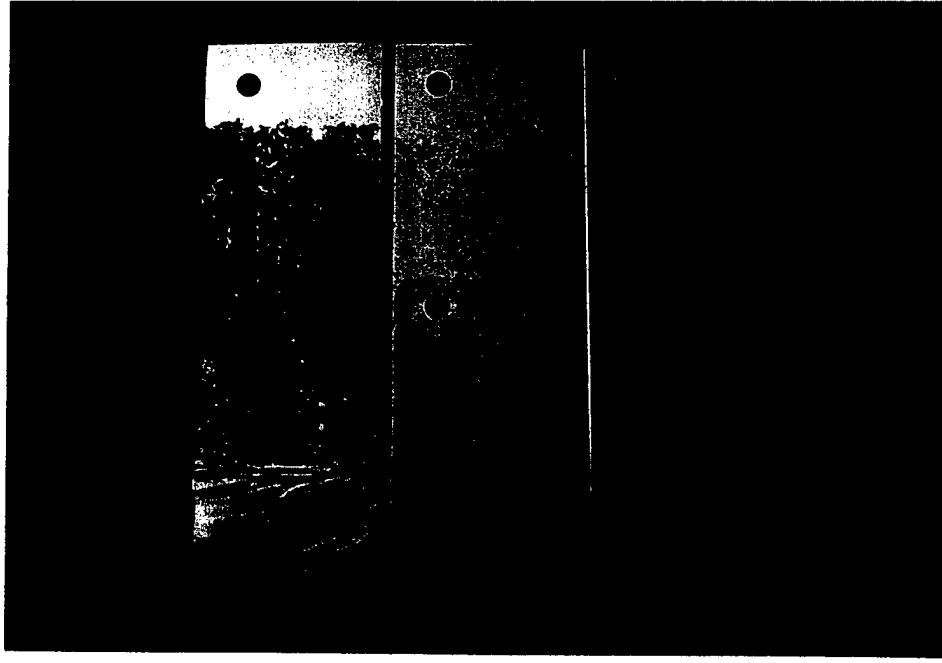


Figure 27.3  
Material - Surface: N08367 - mill  
Coating - Area: epoxy - 80%



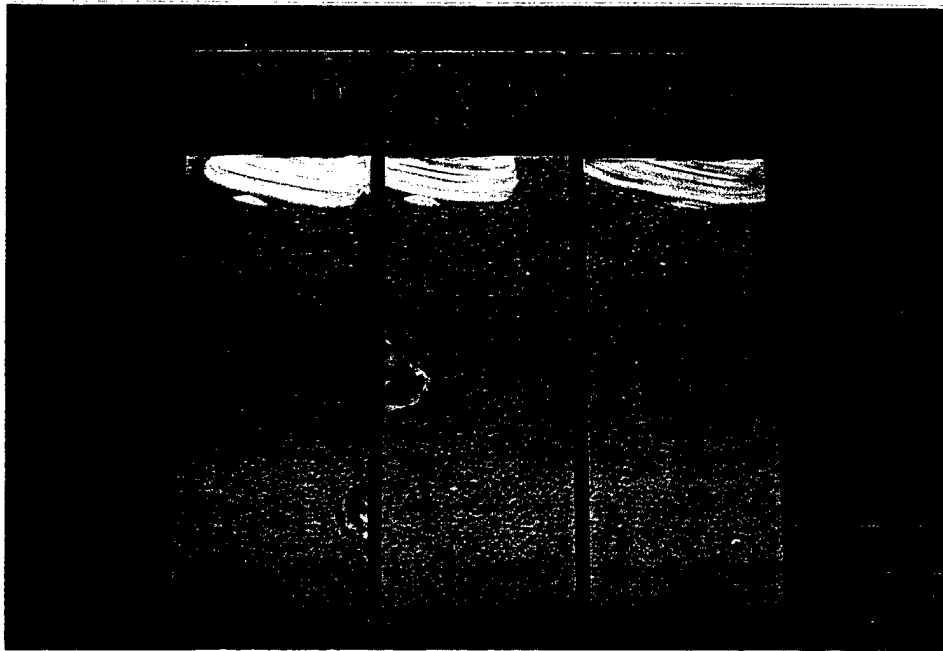


Figure 28.1  
Material - Surface: S31603 - blasted  
Coating - Area: epoxy - 80%

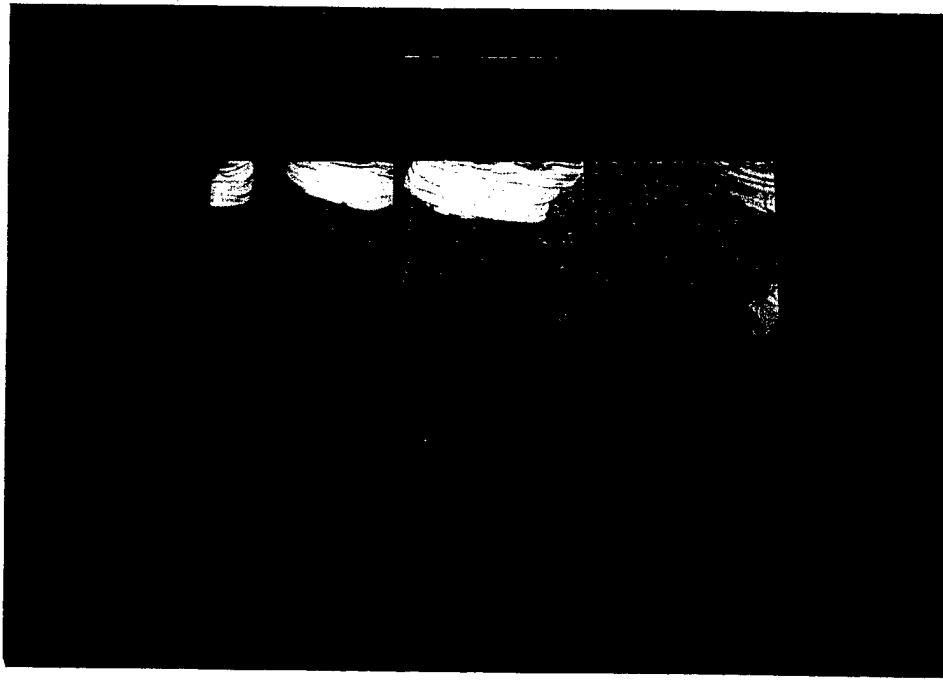


Figure 28.2  
Material - Surface: S20910 - blasted  
Coating - Area: epoxy - 80%

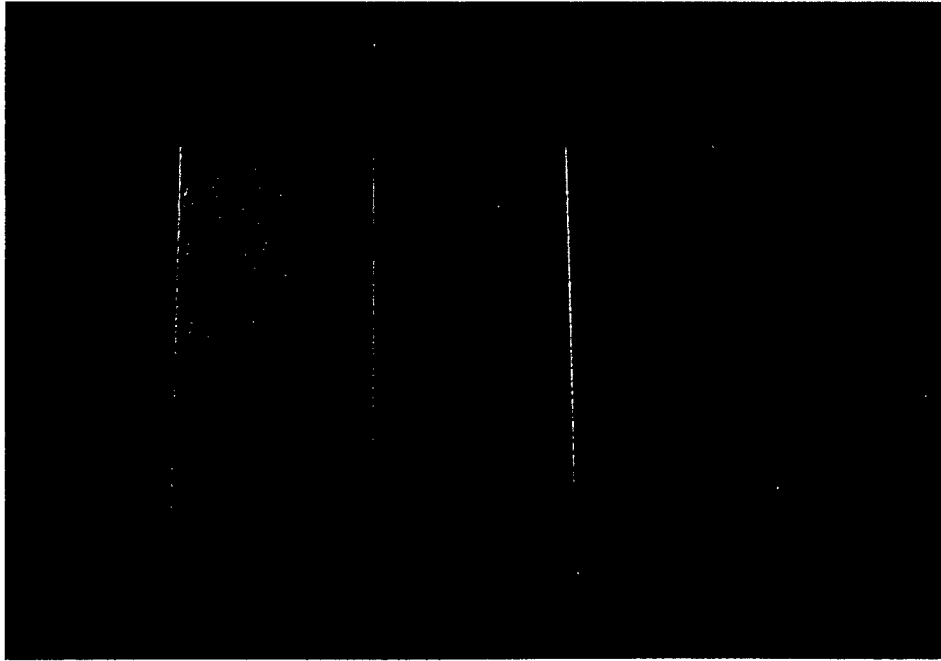


Figure 28.3  
Material - Surface: N08367 - blasted  
Coating - Area: epoxy - 80%



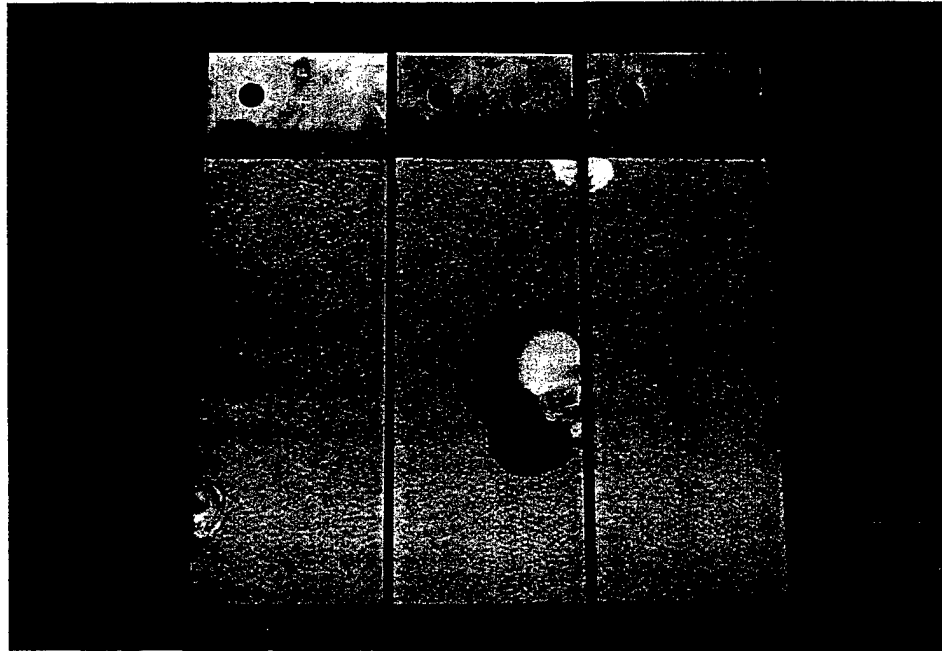


Figure 29.1  
Material - Surface: S31603 - mill  
Coating - Area: epoxy - 80%

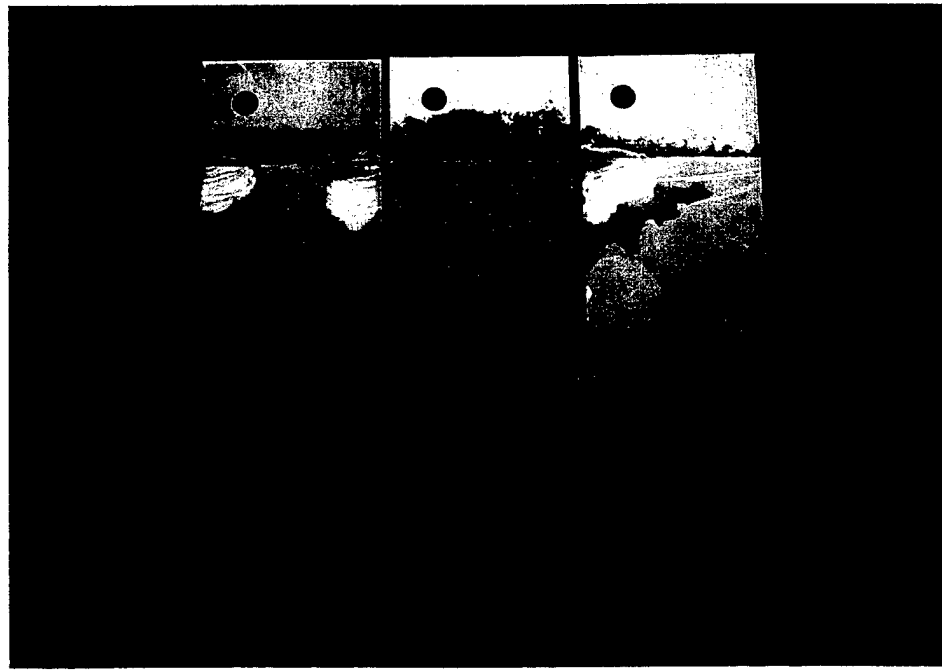


Figure 29.2  
Material - Surface: S20910 - mill  
Coating - Area: epoxy - 80%

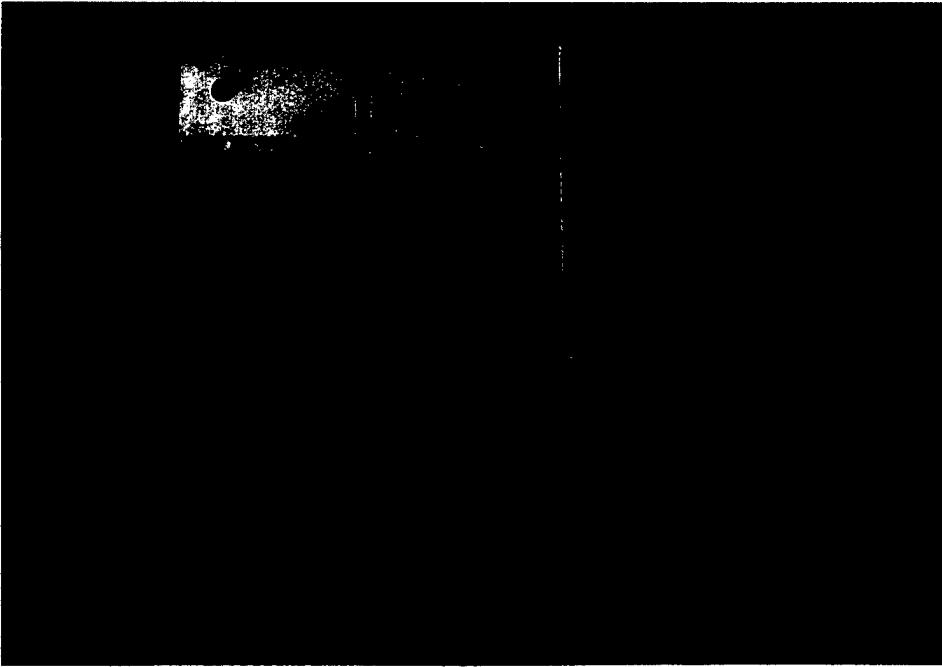


Figure 29.3  
Material - Surface: N08367 - mill  
Coating - Area: epoxy - 80%



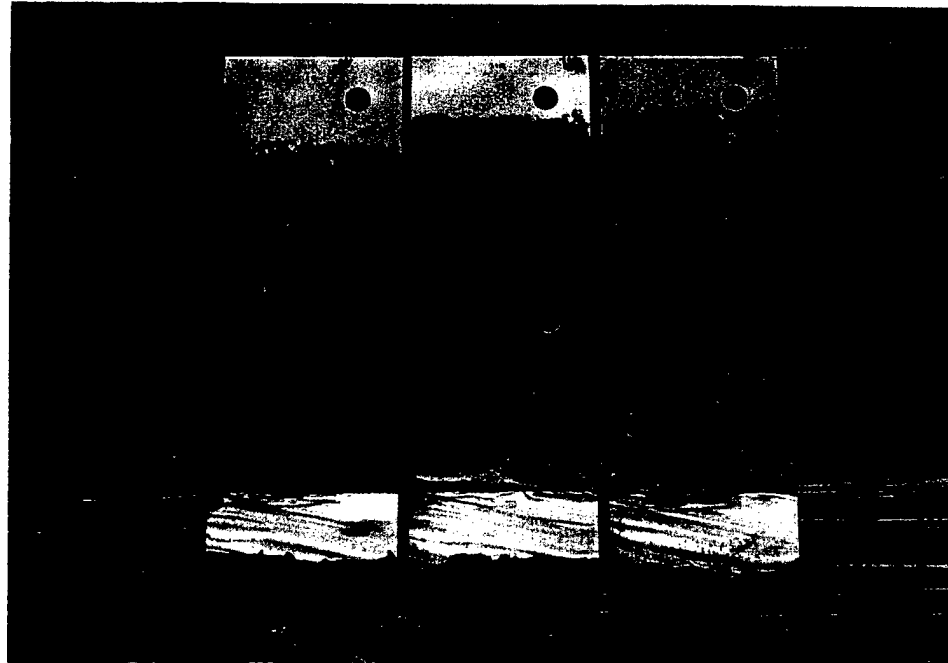


Figure 30.1  
Material - Surface: S31603 - blasted  
Coating - Area: ablative-Cu - 20%

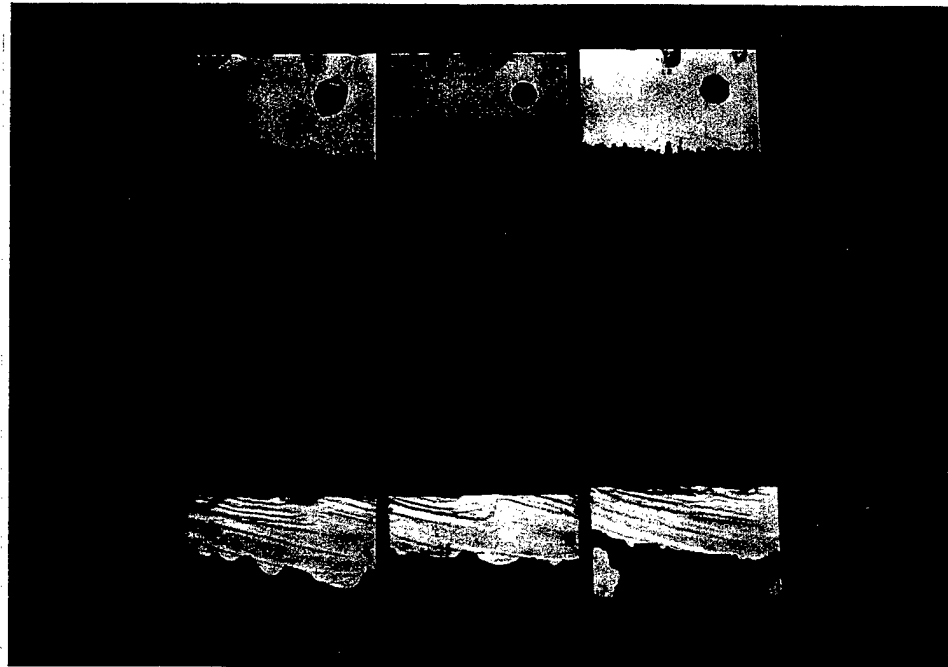


Figure 30.2  
Material - Surface: S20910 - blasted  
Coating - Area: ablative-Cu - 20%



Figure 30.3  
Material - Surface: N08367 - blasted  
Coating - Area: ablative-Cu - 20%



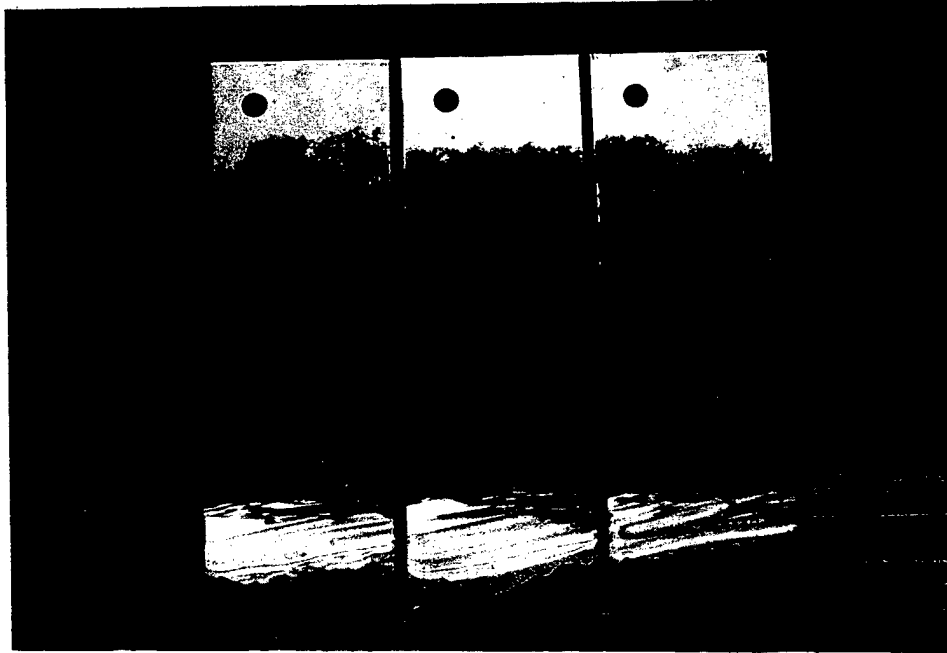


Figure 31.1  
Material - Surface: S31603 - mill  
Coating - Area: ablative-Cu - 20%

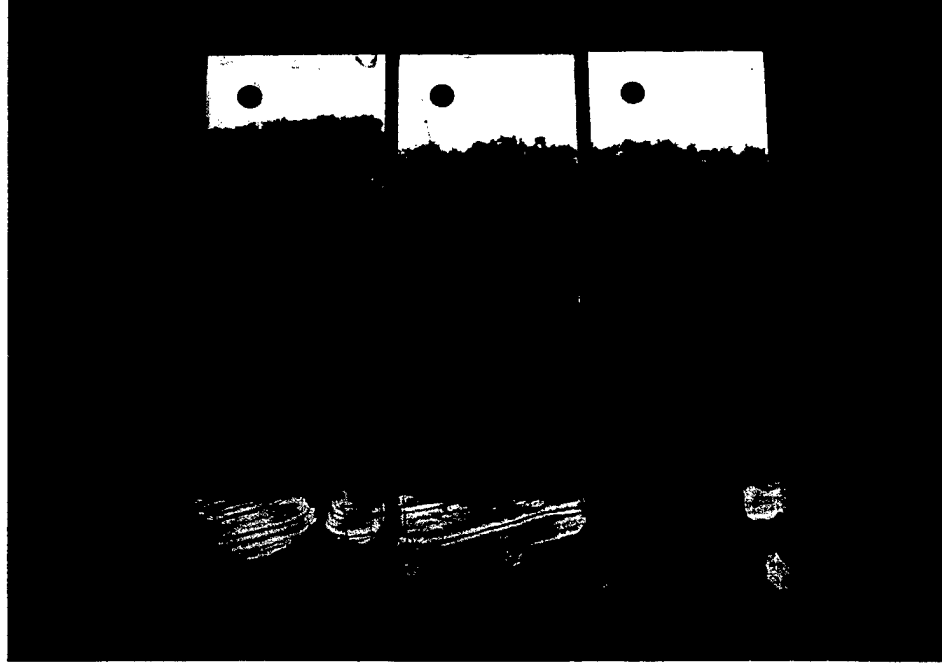


Figure 31.2  
Material - Surface: S20910 - mill  
Coating - Area: ablative-Cu - 20%

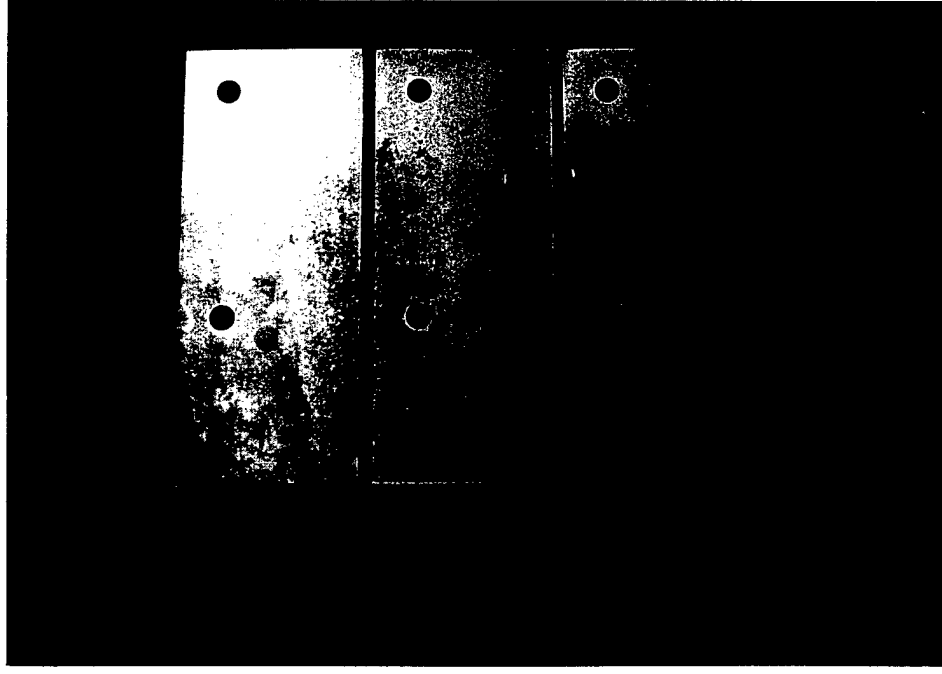


Figure 31.3  
Material - Surface: N08367 - mill  
Coating - Area: ablative-Cu - 20%



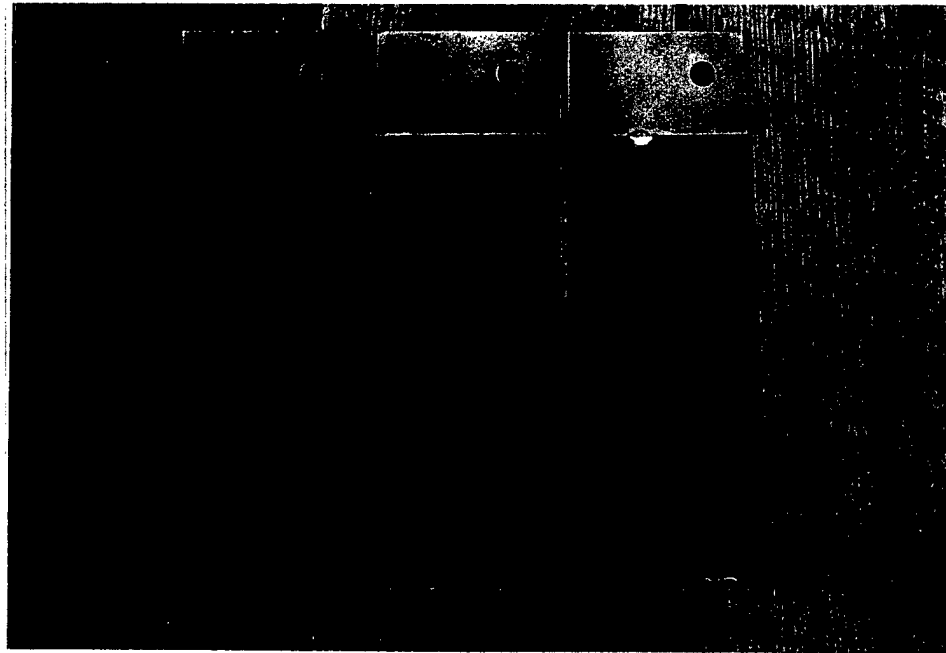


Figure 32.3  
Material - Surface: N08367 - blasted  
Coating - Area: ablative-Cu - 80%

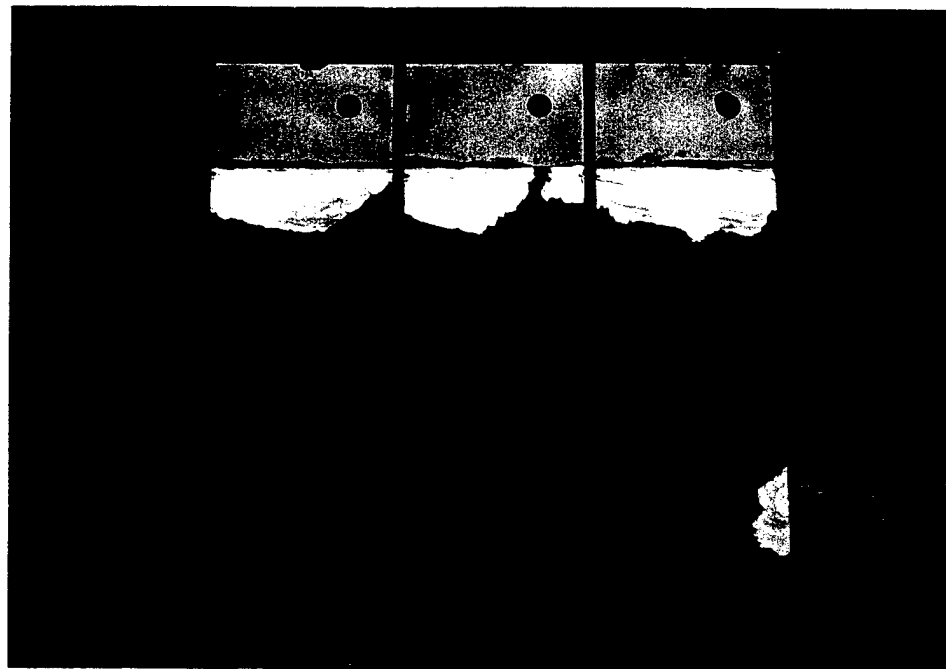


Figure 32.2  
Material - Surface: S20910 - blasted  
Coating - Area: ablative-Cu - 80%

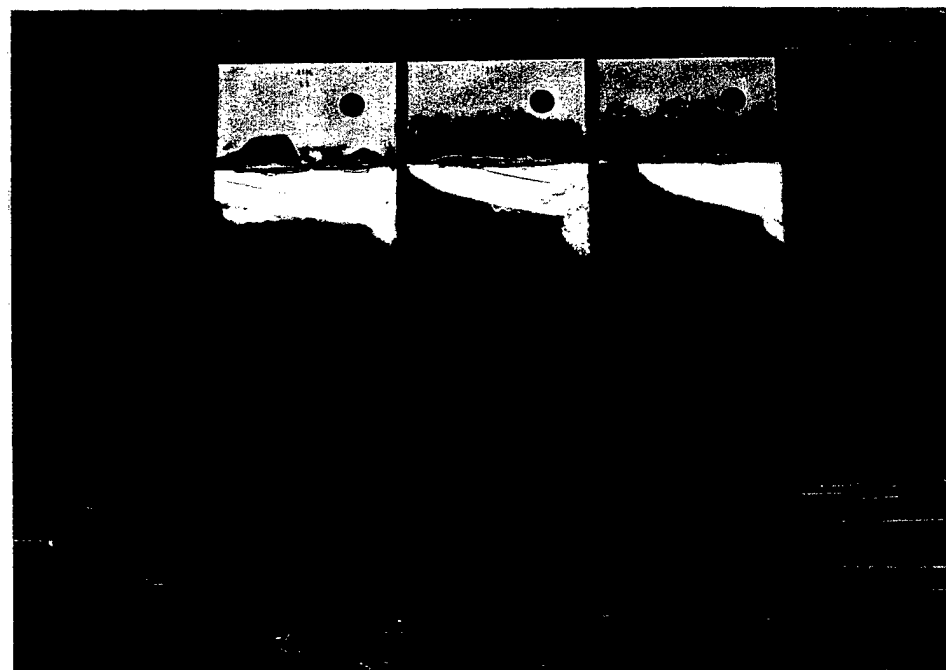


Figure 32.1  
Material - Surface: S31603 - blasted  
Coating - Area: ablative-Cu - 80%





Figure 33.1  
Material - Surface: S31603 - mill  
Coating - Area: ablative-Cu - 80%

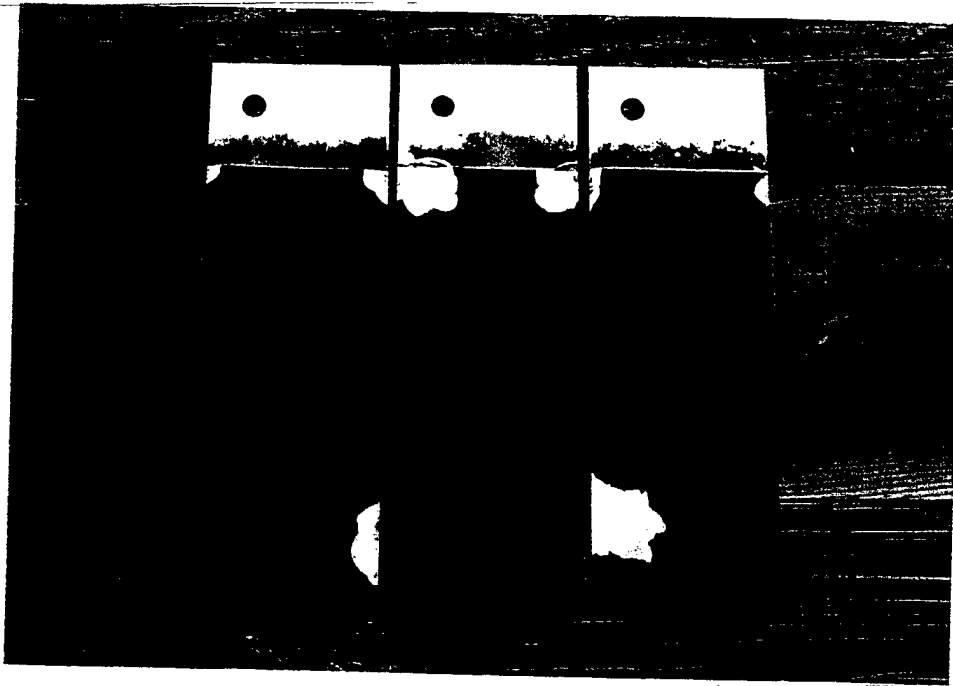


Figure 33.2  
Material - Surface: S20910 - mill  
Coating - Area: ablative-Cu - 80%

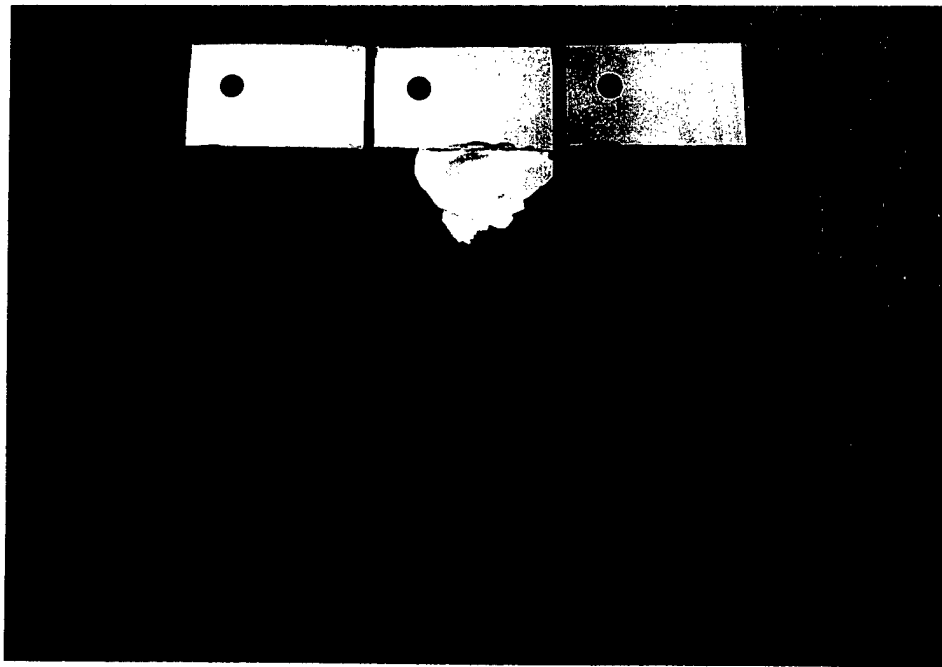


Figure 33.3  
Material - Surface: N08367 - mill  
Coating - Area: ablative-Cu - 80%





Figure 34.1  
Material - Surface: S31603 - blasted  
Coating - Area: elastomeric - 20%

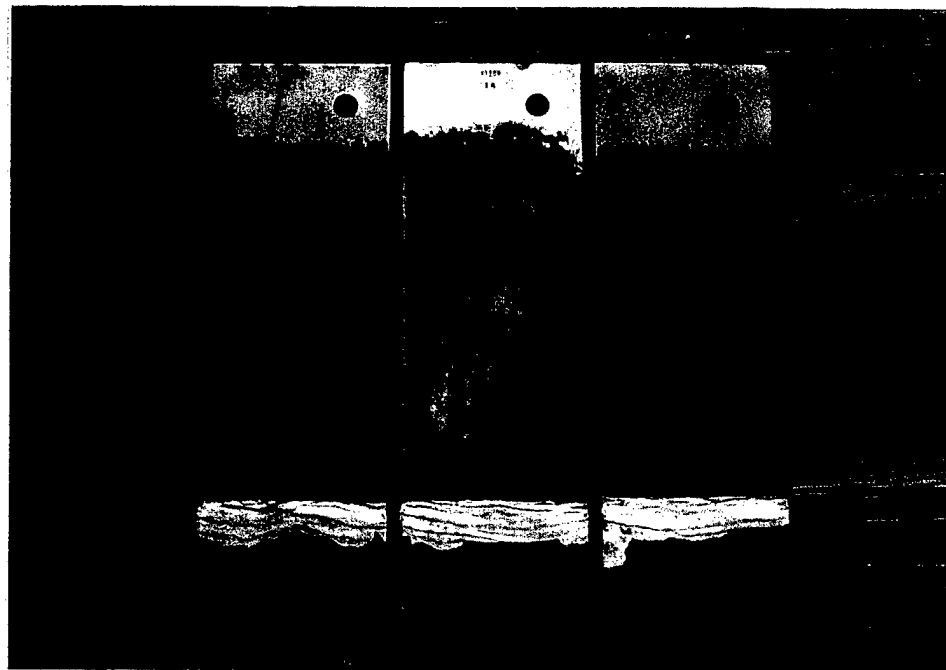


Figure 34.2  
Material - Surface: S20910 - blasted  
Coating - Area: elastomeric - 20%

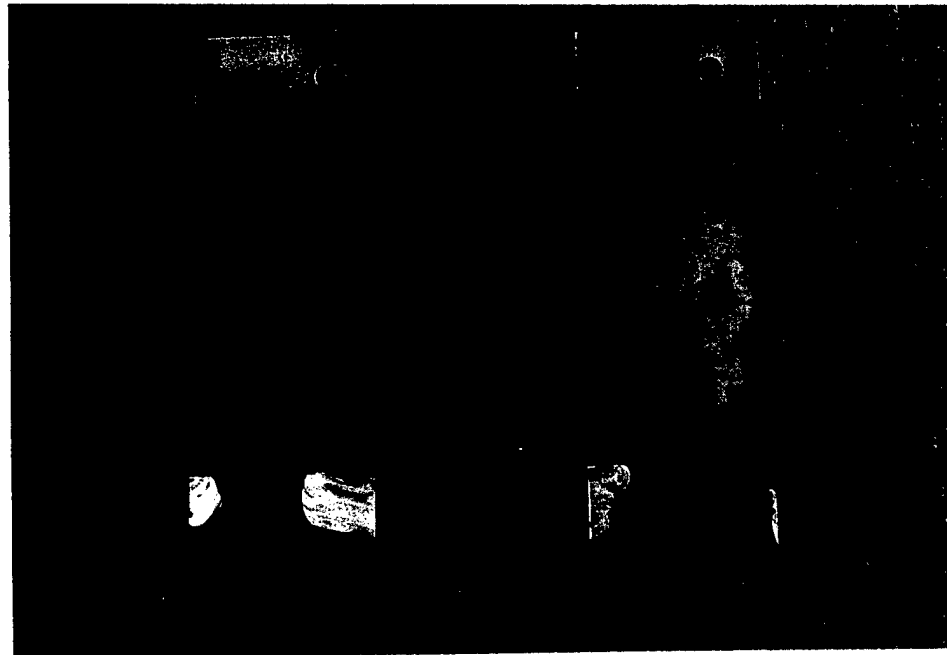


Figure 34.3  
Material - Surface: N08367 - blasted  
Coating - Area: elastomeric - 20%





Figure 35.1  
Material - System: S31603 - mill  
Coating - Area: elastomeric - 20%

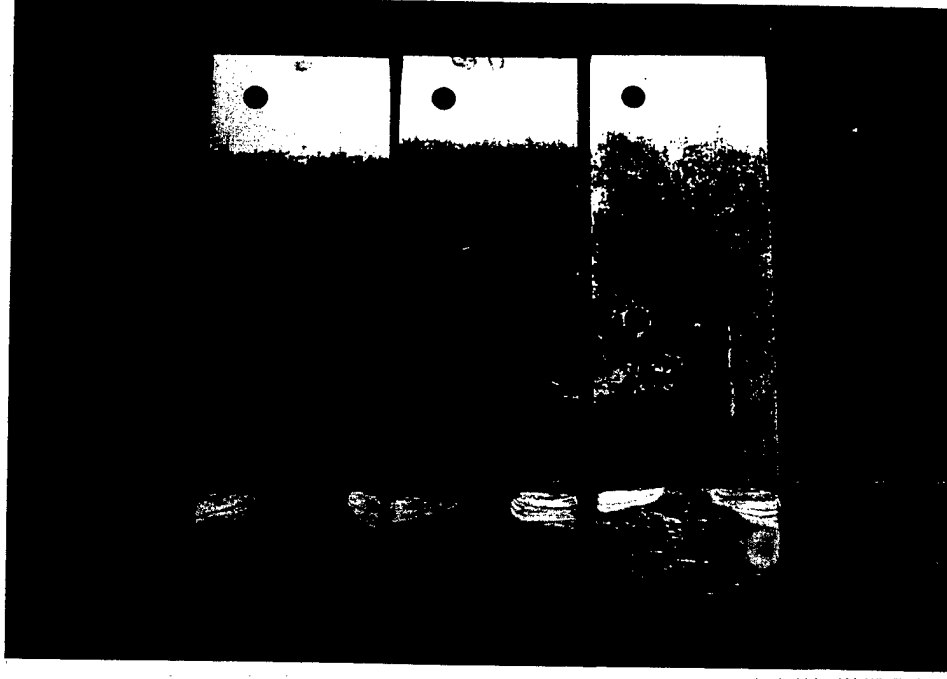


Figure 35.2  
Material - System: S20910 - mill  
Coating - Area: elastomeric - 20%

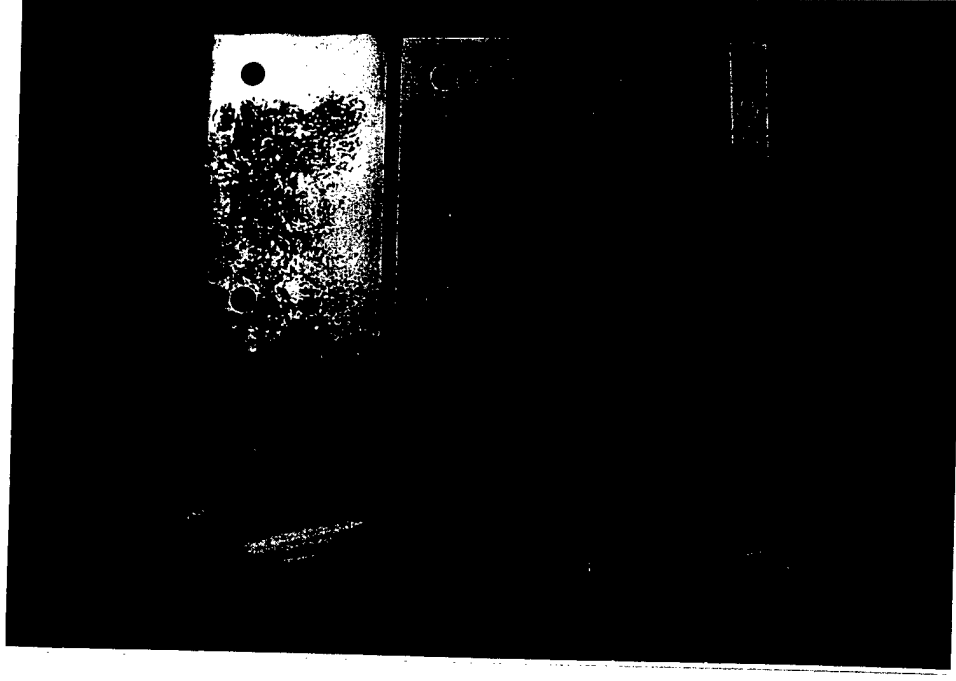


Figure 35.3  
Material - System: N08367 - mill  
Coating - Area: elastomeric - 20%



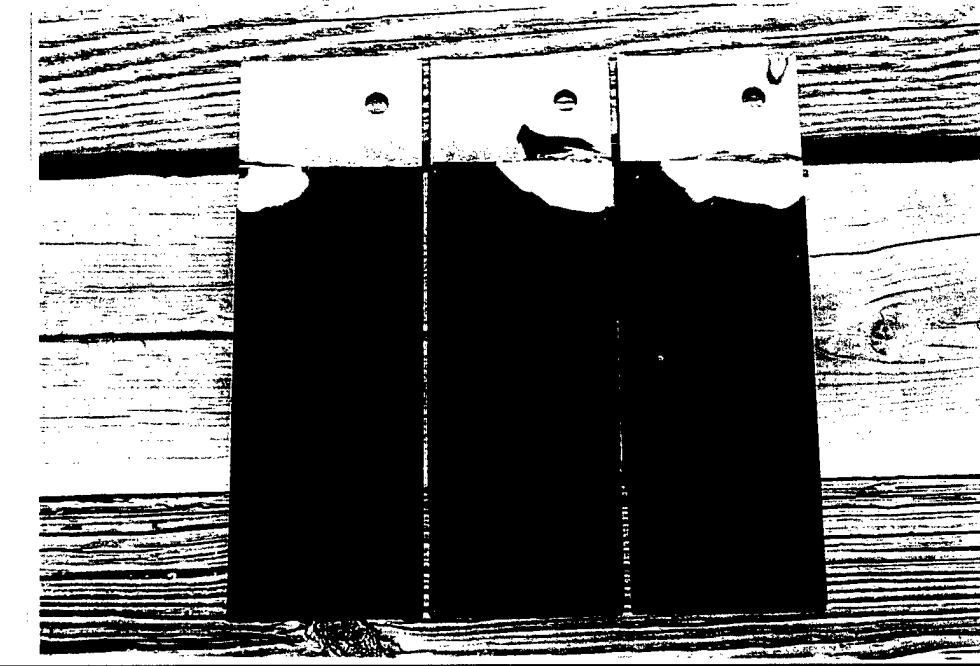


Figure 36.1  
Material - System: S31603 - blasted  
Coating - Area: elastomeric - 80%

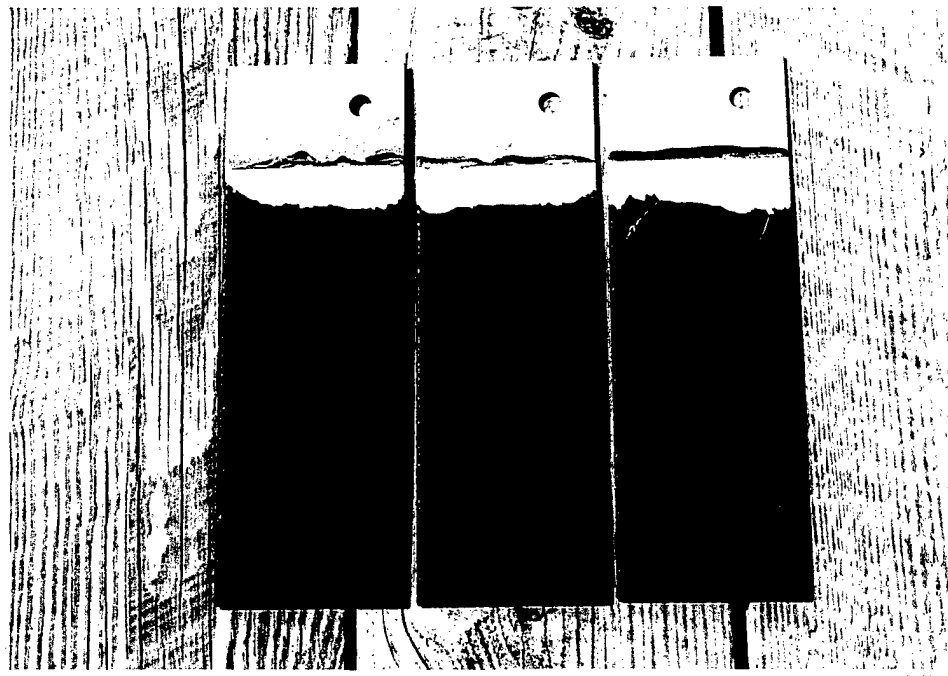


Figure 36.2  
Material - System: S20910 - blasted  
Coating - Area: elastomeric - 80%

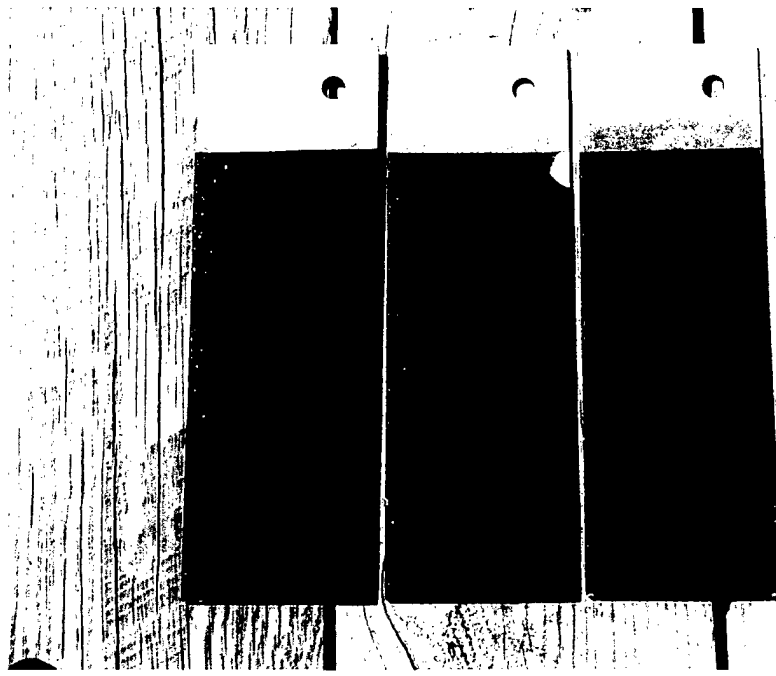


Figure 36.3  
Material - System: N08367 - blasted  
Coating - Area: elastomeric - 80%



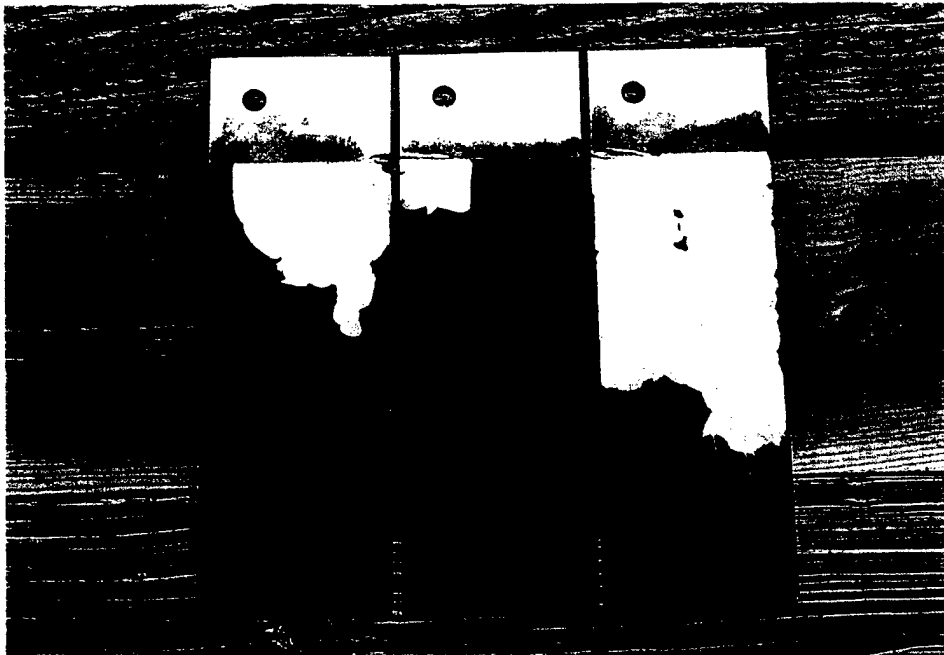


Figure 37.1  
Material - System: S31603 - mill  
Coating - Area: elastomeric - 80%

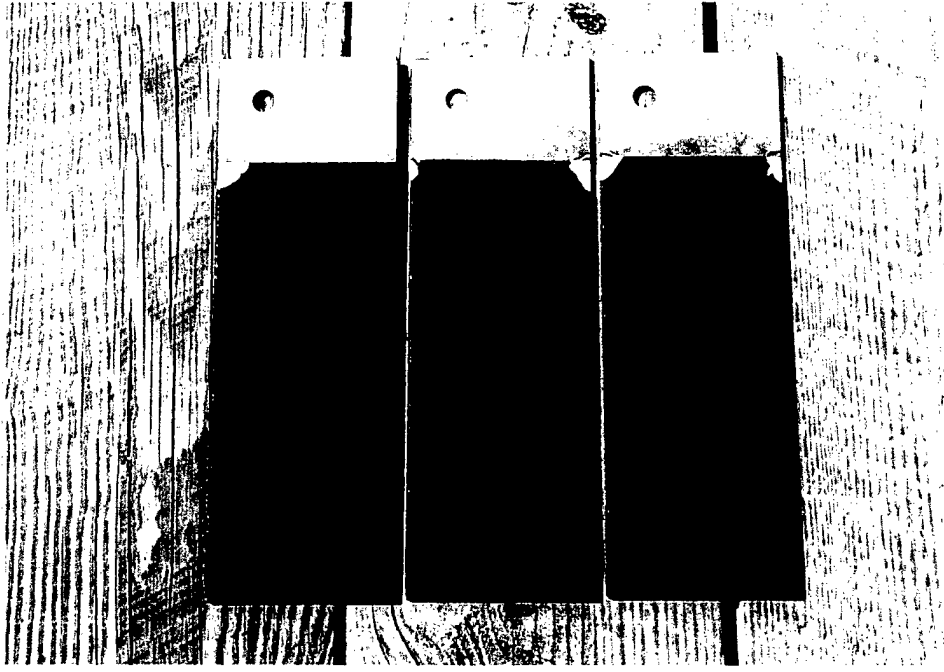


Figure 37.2  
Material - System: S20910 - mill  
Coating - Area: elastomeric - 80%

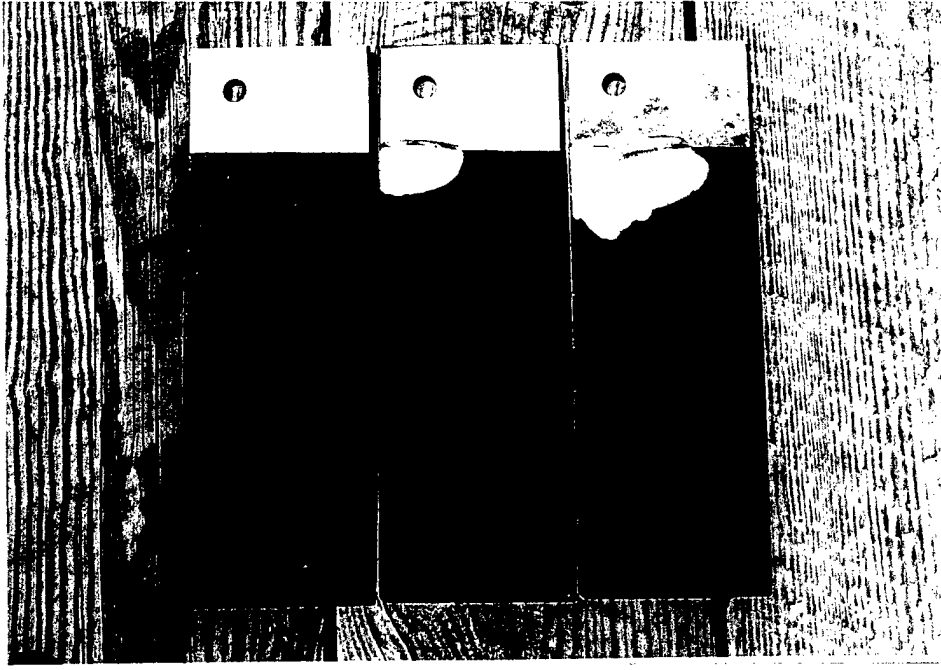


Figure 37.3  
Material - System: N08367 - mill  
Coating - Area: elastomeric - 80%



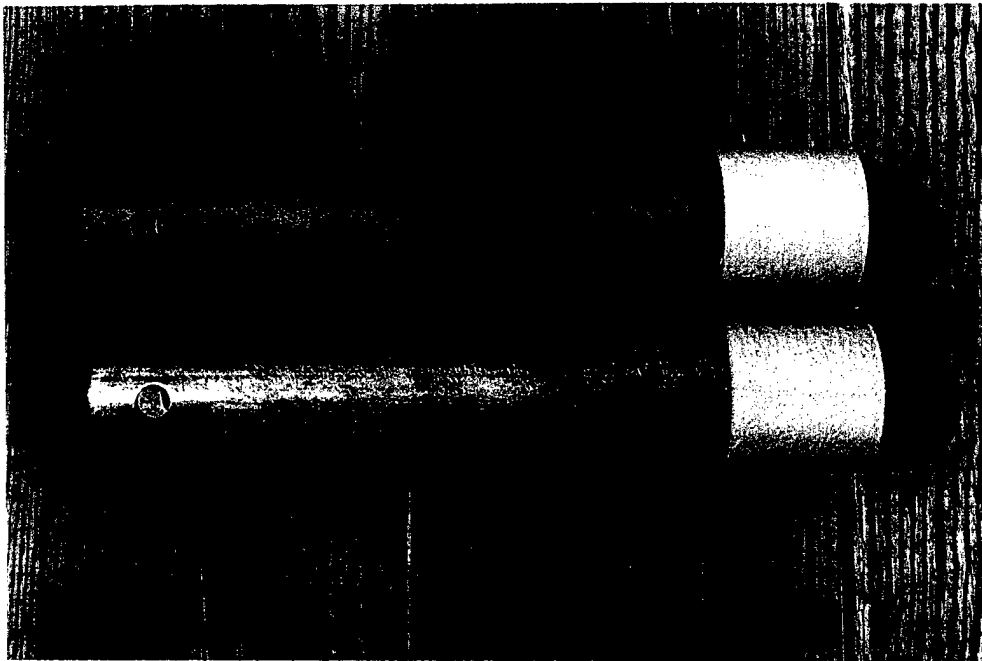


Figure 38.1  
Mill and blasted S31603 with 20%  
epoxy (2-layer)

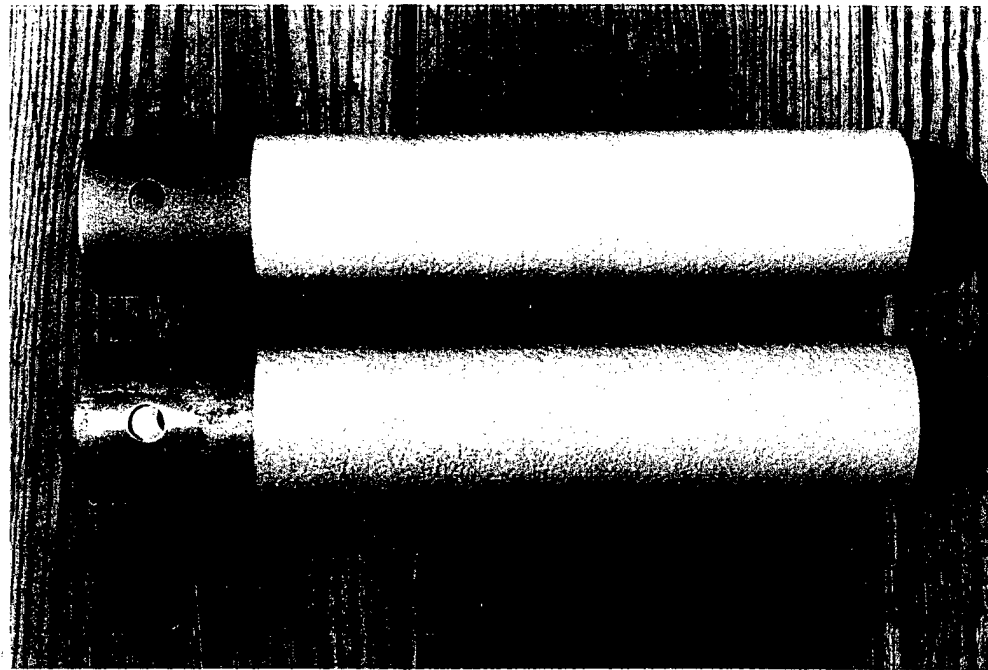


Figure 38.2  
Mill and blasted S31606 with 80%  
epoxy (2-layer)

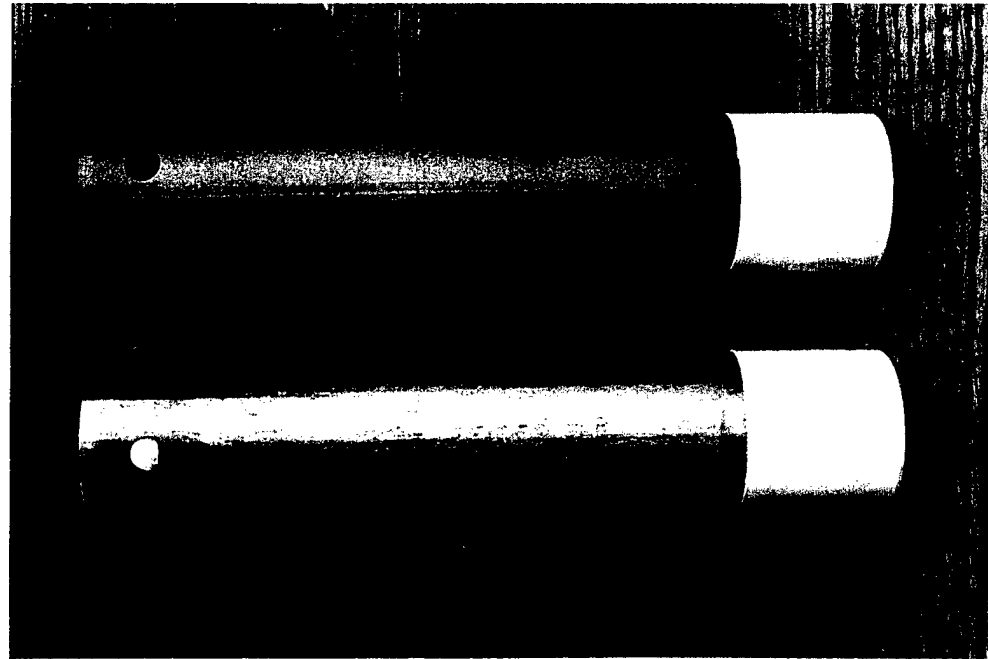


Figure 38.3  
Mill and blasted S31603 with 20%  
epoxy (1-layer)



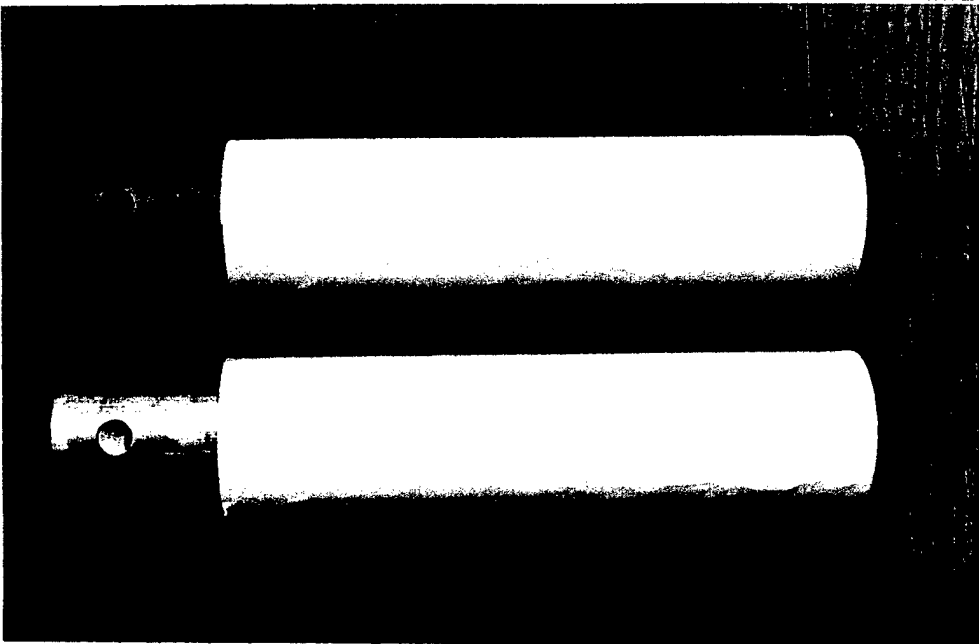


Figure 39.1  
Mill and blasted S31603 with 80%  
epoxy (1-layer)



Figure 39.2  
Exposure arrangement for 6-month  
filtered seawater test

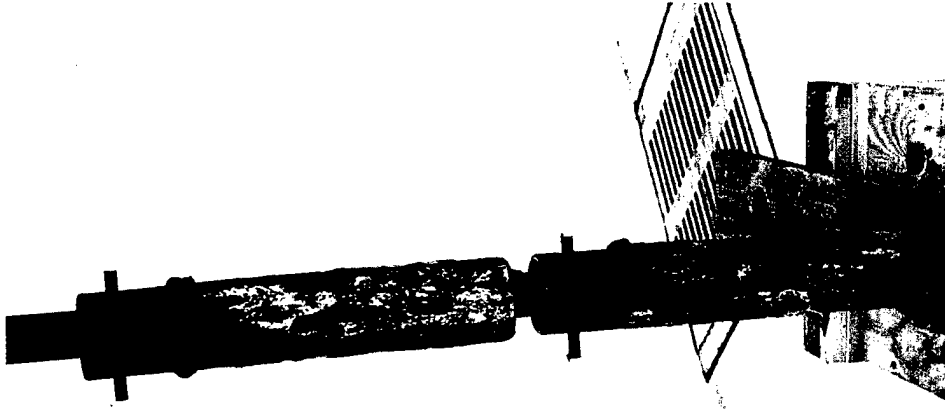


Figure 39.3  
Typical as-removed view



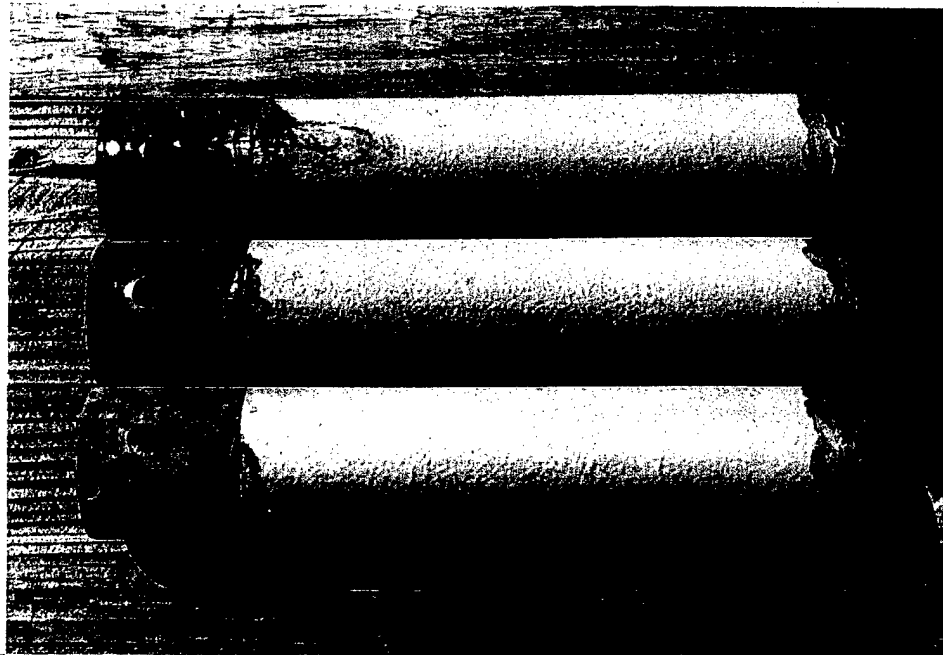


Figure 40.1  
3 grit blasted pipes with 80% epoxy  
(2-layer)

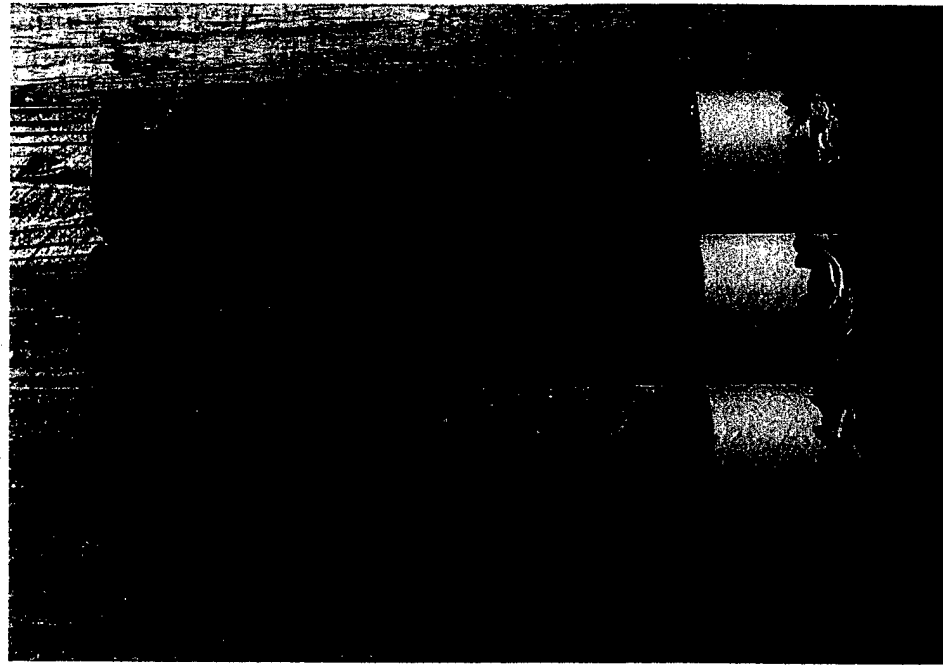


Figure 40.2  
3 grit blasted pipes with 20% epoxy  
(2-layer)

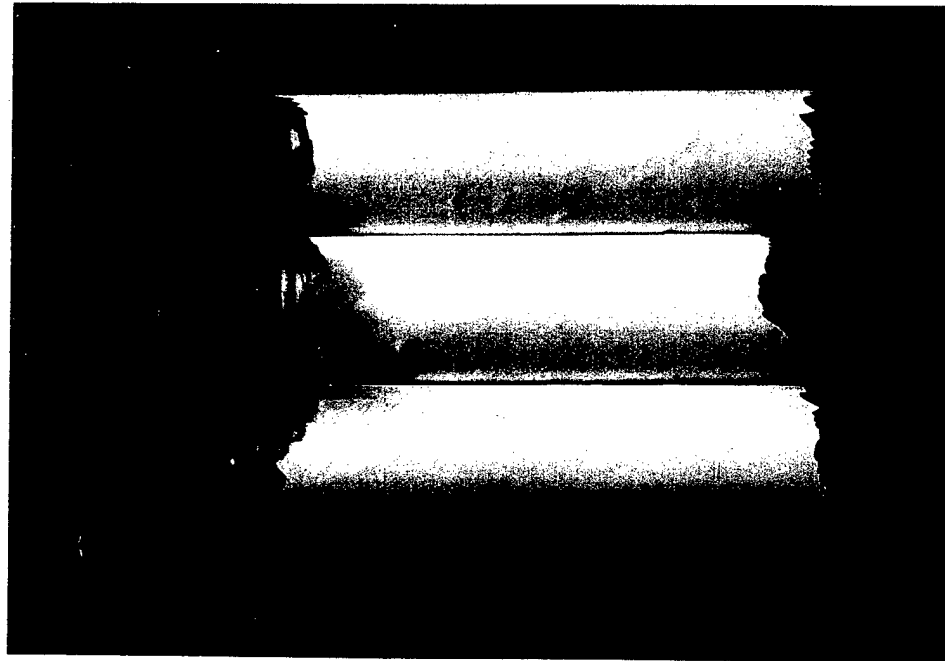


Figure 40.3  
3 grit blasted pipes with 80% epoxy  
(1-layer)



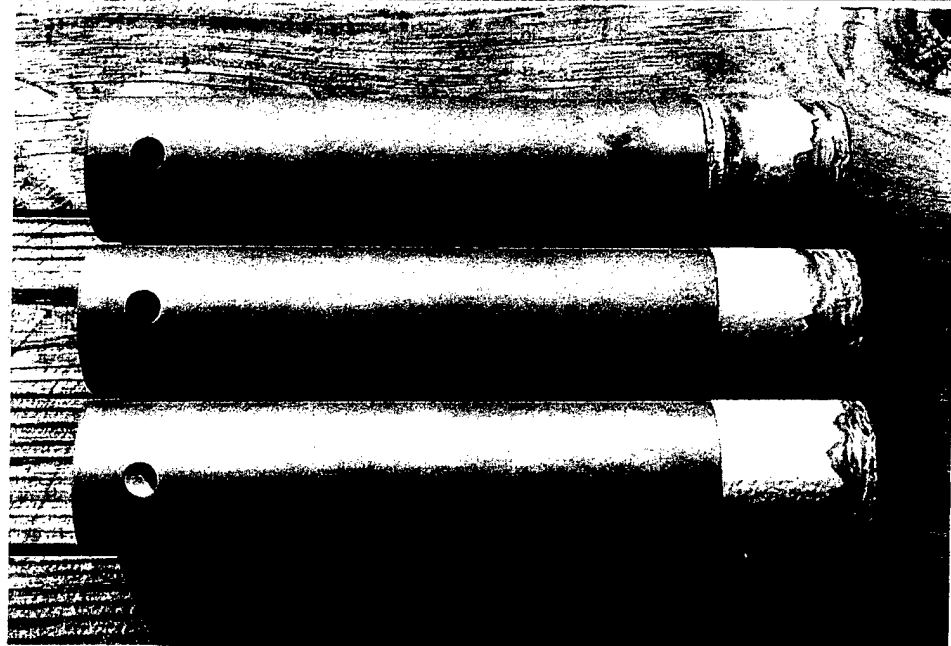


Figure 41.1  
3 grit blasted pipes with 20% epoxy  
(2-coat), after cleaning

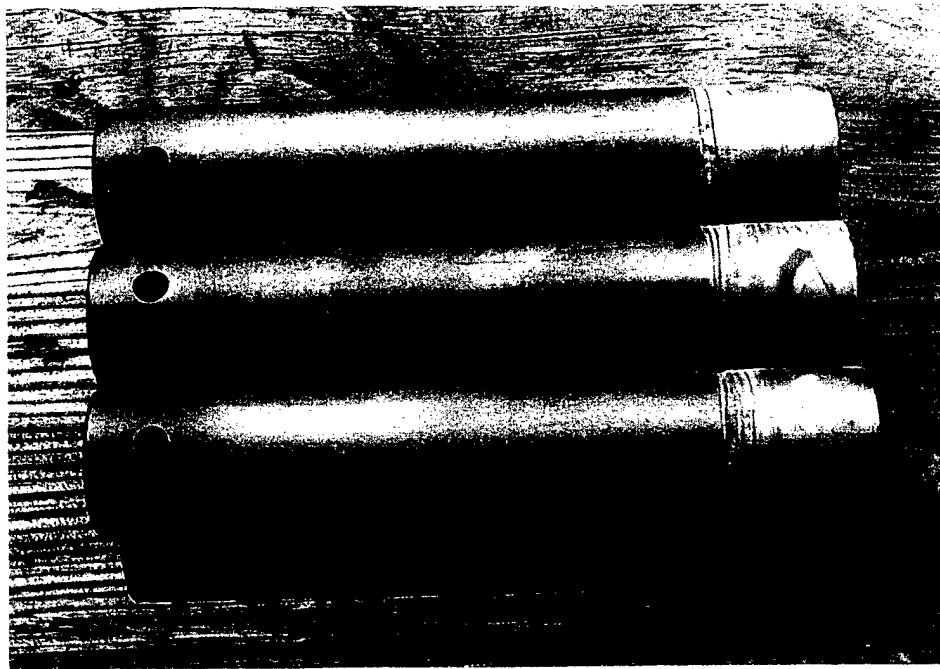


Figure 41.2  
3 grit blasted pipes with 20% epoxy  
(1-coat), after cleaning

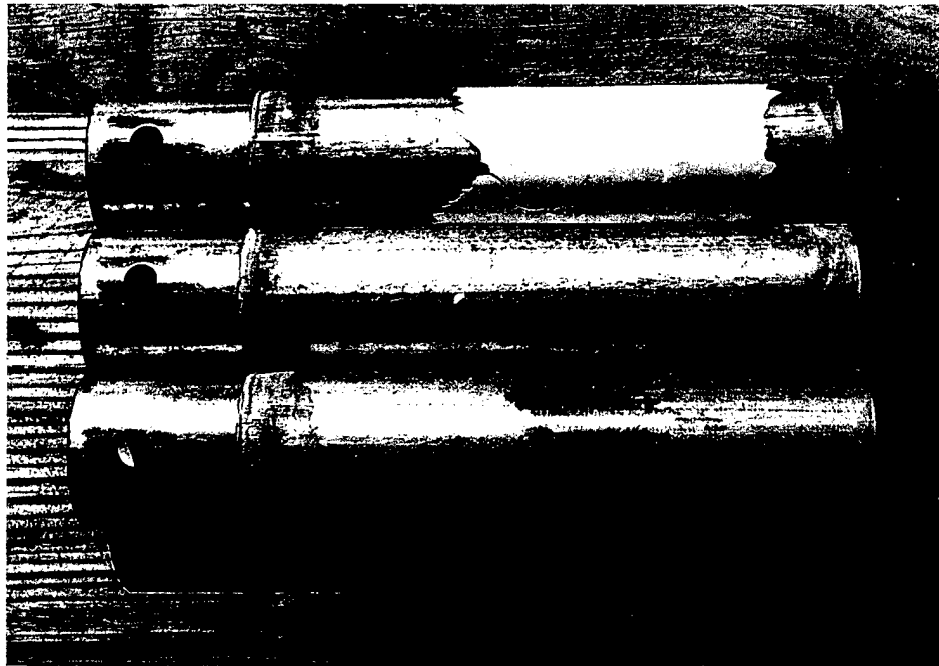


Figure 41.3  
3 mill pipes with 80% epoxy (1-  
coat), after cleaning



## **APPENDIX 4**

### **Test Materials**

#### **Chemical Composition and Properties**



## MATERIAL TEST REPORT

DATE : 07/16/97

PAGE : 1

ORDER: 20391

Metal Samples Company

P.O. Box 8

152 Metal Samples Road

Munford, AL 36268

Ph. (205)358-4202 Fx. (205)358-4515

Customer: 01318 LAQUE CENTER / CORROSION TECHNOLOGY  
Your PO#: 9182

Lot No. L708 Mill: J&L SPECIALTY Our Order Line No. 1  
Description: 316L .125" X 48"X 120"(4 PCS)  
Notes: FILLER 316L #L717

## Chemical Properties:

C:0.010	Co:0.140	Cr:16.490	Cu:0.290
Fe:BALANCE	Mn:1.790	Mo:2.060	N:0.034
Ni:10.170	P:0.030	S:0.013	Si:0.380

## Physical Properties:

Tensile-PSI:81,900 Yield-PSI:44,000  
Hardness:RB 80

Lot No. L708 Mill: J&L SPECIALTY Our Order Line No. 4  
Description: 316L .125" X 48"X 120"(4 PCS)  
Notes: FILLER 316L #L717

## Chemical Properties:

C:0.010	Co:0.140	Cr:16.490	Cu:0.290
Fe:BALANCE	Mn:1.790	Mo:2.060	N:0.034
Ni:10.170	P:0.030	S:0.013	Si:0.380

## Physical Properties:

Tensile-PSI:81,900 Yield-PSI:44,000  
Hardness:RB 80

Lot No. M383 Mill: ALLEGHENY LUDLUM Our Order Line No. 2  
Description: AL6X+N.125" X 22" X 147"(2)  
Notes: FILLER I625 #H858

## Chemical Properties:

C:0.017	Cr:20.450	Cu:0.210	Fe:BALANCE
Mn:0.350	Mo:6.220	N:0.210	Ni:23.900
P:0.021	S:0.0004	Si:0.390	

## Physical Properties:

Tensile-PSI:106,000 Elong-%:48.0



## MATERIAL TEST REPORT

DATE : 07/16/97

PAGE : 2

ORDER: 20391

Metal Samples Company

P.O. Box 8

152 Metal Samples Road

Munford, AL 36268

Ph. (205)358-4202 Fx. (205)358-4515

Customer: 01318 LAQUE CENTER / CORROSION TECHNOLOGY  
Your PO#: 9182

Lot No. M383 (Continued...)

Yield-PSI:50,500

Condition:ANLD

Hardness:RB 87

Lot No. M383 Mill: ALLEGHENY LUDLUM

Our Order Line No. 5

Description: AL6X+N.125" X 22" X 147"(2)

Notes: FILLER I625 #H858

## Chemical Properties:

C:0.017

Cr:20.450

Cu:0.210

Fe:BALANCE

Mn:0.350

Mo:6.220

N:0.210

Ni:23.900

P:0.021

S:0.0004

Si:0.390

## Physical Properties:

Tensile-PSI:106,000

Elong-%:48.0

Yield-PSI:50,500

Condition:ANLD

Hardness:RB 87

Lot No. M382 Mill: ARMCO

Our Order Line No. 3

Description: NIT50 .125" X 48.75" X 120"

Notes: FILLER NIT50 #K244

## Chemical Properties:

C:0.048

Cr:20.980

Mn:6.280

Mo:2.150

N:0.220

Nb:0.010

Ni:14.200

P:0.022

S:0.011

Si:0.340

V:0.180

## Physical Properties:

Tensile-PSI:111,000

Elong-%:40.0

Yield-PSI:55,100

Lot No. M382 Mill: ARMCO

Our Order Line No. 6

Description: NIT50 .125" X 48.75" X 120"

Notes: FILLER NIT50 #K244

## Chemical Properties:



## MATERIAL TEST REPORT

DATE : 07/16/97

PAGE : 3

ORDER: 20391

Metal Samples Company

P.O. Box 8

152 Metal Samples Road

Munford, AL 36268

Ph. (205)358-4202 Fx. (205)358-4515

Customer: 01318 LAQUE CENTER / CORROSION TECHNOLOGY  
Your PO#: 9182

Lot No. M382 (Continued...)

C:0.048	Cr:20.980	Mn:6.280	Mo:2.150
N:0.220	Nb:0.010	Ni:14.200	P:0.022
S:0.011	Si:0.340	V:0.180	

## Physical Properties:

Tensile-PSI:111,000 Elong-%:40.0  
Yield-PSI:55,100

Lot No. L708 Mill: J&amp;L SPECIALTY

Our Order Line No. 7

Description: 316L .125" X 48"X 120"(4 PCS)

Item: 011590125 316L .125"

## Chemical Properties:

C:0.010	Co:0.140	Cr:16.490	Cu:0.290
Fe:BALANCE	Mn:1.790	Mo:2.060	N:0.034
Ni:10.170	P:0.030	S:0.013	Si:0.380

## Physical Properties:

Tensile-PSI:81,900 Yield-PSI:44,000  
Hardness:RB 80

Lot No. M383 Mill: ALLEGHENY LUDLUM

Our Order Line No. 8

Description: AL6X+N.125" X 22" X 147"(2)

## Chemical Properties:

C:0.017	Cr:20.450	Cu:0.210	Fe:BALANCE
Mn:0.350	Mo:6.220	N:0.210	Ni:23.900
P:0.021	S:0.0004	Si:0.390	

## Physical Properties:

Tensile-PSI:106,000 Elong-%:48.0  
Yield-PSI:50,500 Condition:ANLD  
Hardness:RB 87

Lot No. M382 Mill: ARMCO

Our Order Line No. 9

Description: NIT50 .125" X 48.75" X 120"

## Chemical Properties:

C:0.048	Cr:20.980	Mn:6.280	Mo:2.150
---------	-----------	----------	----------



## MATERIAL TEST REPORT

DATE : 07/16/97

PAGE : 4

ORDER: 20391

Metal Samples Company

P.O. Box 8

152 Metal Samples Road

Munford, AL 36268

Ph. (205)358-4202 Fx. (205)358-4515

Customer: 01318

LAQUE CENTER / CORROSION TECHNOLOGY

Your PO#: 9182

Lot No. M382 (Continued...)

N:0.220

Nb:0.010

Ni:14.200

P:0.022

S:0.011

Si:0.340

V:0.180

## Physical Properties:

Tensile-PSI:111,000

Elong-%:40.0

Yield-PSI:55,100

Lot No. K304 Mill: ALLEGHENY LUDLUM

Our Order Line No. 10

Description: 316L .125" X 48" X 1

## Chemical Properties:

C:0.018

Cr:16.420

Fe:BALANCE

Mn:1.890

Mo:2.100

N:0.040

Ni:10.230

P:0.028

S:0.001

Si:0.480

## Physical Properties:

Tensile-PSI:85,500

Elong-%:56.0

Yield-PSI:38,800

Condition:ANLD

Hardness:80.HRB

Lot No. M383 Mill: ALLEGHENY LUDLUM

Our Order Line No. 11

Description: AL6X+N.125" X 22" X 147"(2)

## Chemical Properties:

C:0.017

Cr:20.450

Cu:0.210

Fe:BALANCE

Mn:0.350

Mo:6.220

N:0.210

Ni:23.900

P:0.021

S:0.0004

Si:0.390

## Physical Properties:

Tensile-PSI:106,000

Elong-%:48.0

Yield-PSI:50,500

Condition:ANLD

Hardness:RB 87

Lot No. M382 Mill: ARMCO

Our Order Line No. 12

Description: NIT50 .125" X 48.75" X 120"

## Chemical Properties:

C:0.048

Cr:20.980

Mn:6.280

Mo:2.150

N:0.220

Nb:0.010

Ni:14.200

P:0.022



MATERIAL TEST REPORT

DATE : 07/16/97

PAGE : 5

ORDER: 20391

Metal Samples Company

P.O. Box 8

152 Metal Samples Road

Munford, AL 36268

Ph. (205)358-4202 Fx. (205)358-4515

Customer: 01318

LAQUE CENTER / CORROSION TECHNOLOGY

Your PO#: 9182

Lot No. M382 (Continued...)

S:0.011

Si:0.340

V:0.180

Physical Properties:

Tensile-PSI:111,000

Elong-%:40.0

Yield-PSI:55,100

=====

We certify that the Material Test Report is correct to the best of our knowledge and that the material supplied meets your required P.O. specifications.

THANK YOU, Quality Control Dept.

*Larry Braden (RL)*

=====





DMV STAINLESS France  
SERVICE QUALITÉ  
R.P. 10-21501 Aubrey Cedex

CERTIFICAT DE RECEPTION B  
INSPECTION CERTIFICATE B  
ABNAHMEPRUFZEUGNIS B  
EN 10204 - 3.1.B

9655879

Page  
Sheet/Seite  
1/2

(7) R4K  
2609 J03

CLIENT TAD USA INC  
Purchaser / Besteller  
COMMANDE No D003780 PO H015521/9 No COMMANDE USINE G2533808D  
Order Nr / Besteller Nr (Identification Fourniture/Certificat)  
SUBORDER / ITEM

TYPE DE PRODUIT Tubes sans soudure Finis à chaud Série pipe Hypertrempé Décapé  
Seamless Pipes/Tubes Hot finished Pipe series Annealed Pickled  
Nahtlose Stahlrohre Warmgefertigt Série pipe Abgeschreckt Gebeizt

NUANCES ET SPECIFICATIONS / Grade and Specifications / Stahlsorte und Liefervorschriften

TP316L

ASTM A 312/ASME SA 312/94B - ASTM A 376/ASME SA 376/93 - NACE MR 0175

MARQUAGE/MARKING/MARKIERUNG : DMV -F- TP316L/TP316 - ASTM A312/ASMESA312-  
ASTM A376 / ASME SA376 - 2" NPS.SCH 40S-HEAT PP521-SEAMLESS-1900PSI-FRANCE

QUANTITE / Quantity / Liefermenge

DIMENSIONS (Diam. X Ep. X Lg(mm)) / Size / Abmessung

Nombre  
150

M  
1045.43

Kg  
5662

60.30 x 3.91  
SIZE 2" SCH 40S

6110 / 7620  
20.04' TO 25.00'

Total length 3029.89 Feet Total weight 12482.35 lbs

CARACTERISTIQUES CHIMIQUES / Chemical Analysis / Chemische Zusammensetzung

Elaboration / Melting Process / Erzeugungsart

ACIER ELECTRIQUE / ELECTRIC STEEL / ELECTROSTAHL

	C	Mn	P	S	Si	Ni	Cr	Mo	Co		
MINI											
MAXI	0.035	2.00	0.040	0.030	0.75	10.00	16.00	2.00	0.20		
						15.00	18.00	3.00			
Coulée / Heat											
PP521	0.019	1.91	0.019	0.0040	0.35	11.20	16.91	2.10	0.08		

CARACTERISTIQUES MECANQUES ET METALLURGIQUES / Mechanical and Metallurgical Properties / Mechanische und Metallurgische Kennwerte

	Re. à 0.2 Ys 0.2 STRECKGRENZE PSI	Rm TENSILE TEST BIEGESTICHUNG PSI	A ELONGATION DEFORM 2"	APLATISSEMENT FLATTENING RINGFALTY	DURETE HARDNESS TEST BAHRT	CORROSION CORROSION KORROSION
CONDITIONS IMPOSEES	MINI 25000	MINI 70000	MINI 35		NACEMR0175 <= 22HRC	MIL/P/ 24691-3
S065	36695	80522	48.3	BON-OK-OB	<= 18	BON-OK-OB
S066	32779	80543	51.7	BON-OK-OB	<= 18	BON-OK-OB
S067	34954	78880	48.6		<= 18	BON-OK-OB
S068						BON-OK-OB
S069						BON-OK-OB
S070						BON-OK-OB

SUITE PAGE 2/2

Stainless Pipe & Ftgts. Date 07/30/97

LAQUE CENTER FOR

Cust PO- 9244

Shpr No- C74209

2 S40 SMLS PIPE 316L

DMV STAINLESS France Certifié ISO9002 - LRQA N° 926478





## **APPENDIX 5**

- 5a - Products Qualified Under Military Specification MIL-P-24647  
Paint System, Anticorrosive and Antifouling, Ship Hull
- 5b - International Paint Company product literature
- 5c - Coating Application Procedure Utilized for Flat Test Panels and Pipes



**APPENDIX 5a**

**Products Qualified Under Military Specification MIL-P-24647  
Paint System, Anticorrosive and Antifouling, Ship Hull**



QUALIFICATIONS CERTIFIED  
APRIL 1996

QPL-24647-3  
2 April 1996  
SUPERSEDING  
QPL-24647-2  
29 January 1993

QUALIFIED PRODUCTS LIST  
OF  
PRODUCTS QUALIFIED UNDER MILITARY SPECIFICATION

MIL-P-24647

PAINT SYSTEM, ANTICORROSIVE AND ANTIFOULING, SHIP HULL

This list has been prepared for use by or for the Government in the acquisition of products covered by the subject specification and such listing of a product is not intended to and does not connote endorsement of the product by the Department of Defense. All products listed herein have been qualified under the requirements for the product as specified in the latest effective issue of the applicable specification. This list is subject to change without notice; revision or amendment of this list will be issued as necessary. The listing of a product does not release the contractor from compliance with the specification requirements.

THE ACTIVITY RESPONSIBLE FOR THIS QUALIFIED PRODUCTS LIST IS THE NAVAL SEA SYSTEMS COMMAND, SEA 03R42, 2531 JEFFERSON DAVIS HWY, ARLINGTON, VA 22242-5160.

GOVERNMENT DESIGNATION	MANUFACTURER'S DESIGNATION	TEST OR QUALIFICATION REFERENCE	MANUFACTURER'S NAME AND ADDRESS
Type I	Coat 1 FPL274/FPA327 AC (Red) 5 mils MDFT	NSTM 39086-	Courtaulds Coatings
Class 1A	Coat 2 FPJ034/FPA327 AC (Gray) 5 mils MDFT	BD-ST-M-000/	International Paint
Grades A&B	or	Chapter 631,	6001 Antoine Drive
Applica- tion 1	Coat 1 FPL274/FCA321 Low Temp AC*(Red) 5 mils MDFT	Change 8, Table 631-39	Houston, TX 77091
	Coat 2 FPJ034/FCA321 Low Temp AC*(Gray) 5 mils MDFT	& NAVSEA Ltr Ser 03M1/089	Plants: 6001 Antoine Drive Houston, TX 77091
	* For use at temperatures below 40°F plus	of 12 Aug 94	2270 Morris Avenue Union, NJ 07083
	Coat 3 BRA642 AF(Black) 5 mils MDFT		
	Coat 4 BRA640 AF(Red) 5 mils MDFT		

AMSC N/A

FSC 8010

DISTRIBUTION STATEMENT A Approved for public release; distribution unlimited



QPL-24647-3

GOVERNMENT DESIGNATION	MANUFACTURER'S DESIGNATION	TEST OR QUALIFICATION REFERENCE	MANUFACTURER'S NAME AND ADDRESS
Type I Class 1A Grades A&B Application 2	Coat 1 FPL274/FPA327 AC (Red) 5 mils MDFT Coat 2 FPJ034/FPA327 AC (Gray) 5 mils MDFT or Coat 1 FPL274/FCA321 Low Temp AC*(Red) 5 mils MDFT Coat 2 FPJ034/FCA321 Low Temp AC*(Gray) 5 mils MDFT * For use at temperatures below 40°F plus Coat 3 BRA642 AF(Black) 5 mils MDFT Coat 4 BRA642 AF(Black) 5 mils MDFT	NSTM S9086- BD-ST-M-000/ Chapter 631, Change 8, Table 631-39 & NAVSEA Ltr Ser 03M1/089 of 12 Aug 94	Courtaulds Coatings International Paint 6001 Antoine Drive Houston, TX 77091 Plants: 6001 Antoine Drive Houston, TX 77091 2270 Morris Avenue Union, NJ 07083
Type I Class 1A Grades A&B Application 1	Coat 1 KHA303/KHA062 AC (Red) 5 mils MDFT Coat 2 KHA302/KHA062 AC (Gray) 5 mils MDFT or Coat 1 KHA303/KHA414 Low Temp AC*(Red) 5 mils MDFT Coat 2 KHA302/KHA414 Low Temp AC*(Gray) 5 mils MDFT * For use at temperatures below 40°F plus Coat 3 BRA642 AF(Black) 5 mils MDFT Coat 4 BRA640 AF(Red) 5 mils MDFT	NSTM S9086- BD-ST-M-000/ Chapter 631, Change 8, Table 631-39 & NAVSEA Ltr Ser 03M1/089 of 12 Aug 94	Courtaulds Coatings International Paint 6001 Antoine Drive Houston, TX 77091 Plants: 6001 Antoine Drive Houston, TX 77091 2270 Morris Avenue Union, NJ 07083
Type I Class 1A Grades A&B Application 2	Coat 1 KHA303/KHA062 AC (Red) 5 mils MDFT Coat 2 KHA302/KHA062 AC (Gray) 5 mils MDFT or Coat 1 KHA303/KHA414 Low Temp AC*(Red) 5 mils MDFT Coat 2 KHA302/KHA414 Low Temp AC*(Gray) 5 mils MDFT * For use at temperatures below 40°F plus Coat 3 BRA642 AF(Black) 5 mils MDFT Coat 4 BRA642 AF(Black) 5 mils MDFT	NSTM S9086- BD-ST-M-000/ Chapter 631, Change 8, Table 631-39 & NAVSEA Ltr Ser 03M1/089 of 12 Aug 94	Courtaulds Coatings International Paint 6001 Antoine Drive Houston, TX 77091 Plants: 6001 Antoine Drive Houston, TX 77091 2270 Morris Avenue Union, NJ 07083



QPL-24647-3

GOVERNMENT DESIGNATION	MANUFACTURER'S DESIGNATION	TEST OR QUALIFICATION REFERENCE	MANUFACTURER'S NAME AND ADDRESS
Type I Class 3A Grades A&B Application 1	Coat 1 BRA 640 AF (Red) 5 mils MDFT Coat 2 BRA 640 AF (Red) 5 mils MDFT or Coat 1 BRA 642 AF (Black) 5 mils MDFT Coat 2 BRA 640 AF (Red) 5 mils MDFT	Technical Handbook S6360- AD-HBK-010/SHT Maintenance & Repair for Submarines, Table 5-2 and NAVSEA Ltr Ser 5141/028 of 22 Feb 91	Courtaulds Coatings International Paint 6001 Antoine Drive Houston, TX 77091 Plants: 6001 Antoine Drive Houston, TX 77091 2270 Morris Avenue Union, NJ 07083
Type I Class 3A Grades A&B Application 2	Coat 1 BRA 642 AF (Black) 5 mils MDFT Coat 2 BRA 642 AF (Black) 5 mils MDFT or Coat 1 BRA 640 AF (Red) 5 mils MDFT Coat 2 BRA 642 AF (Black) 5 mils MDFT	Technical Handbook S6360- AD-HBK-010/SHT Maintenance & Repair for Submarines, Table 5-2 and NAVSEA Ltr Ser 5141/028 of 22 Feb 91	Courtaulds Coatings International Paint 6001 Antoine Drive Houston, TX 77091 Plants: 6001 Antoine Drive Houston, TX 77091 2270 Morris Avenue Union, NJ 07083
Type I Class 1A Grades A Application 1	Coat 1 Devran 230 AC (Red) 5 mils MDFT Coat 2 Devran 230 AC (Gray) 5 mils MDFT or Coat 1 Devco Bar Rust 235 Low Temp AC* (Red) 5 mils MDFT Coat 2 Devco Bar Rust 235 Low Temp AC* (Gray) 5 mils MDFT *May also be used at temperatures above 40°F plus Coat 3 Devco ABC#3 AF(Black) 5 mils MDFT Coat 4 Devco ABC#3 AF(Red) 5 mils MDFT	NSTM S9086- BD-ST-M-000/ Chapter 631, Change 8, Table 631-39 and NAVSEA Ltr Ser 03M1/090 of 12 Aug 94	Devco Coatings Co. 4000 Dupont Circle P.O. Box 7600 Louisville, KY 40207 Plants: 9155 River Road Pennsauken, NJ 08110 2625 Durahart Street Riverside, CA 92502
Type I Class 1A Grades A Application 2	Coat 1 Devran 230 AC (Red) 5 mils MDFT Coat 2 Devran 230 AC (Gray) 5 mils MDFT or Coat 1 Devco Bar Rust 235 Low Temp AC* (Red) 5 mils MDFT Coat 2 Devco Bar Rust 235 Low Temp AC* (Gray) 5 mils MDFT *May also be used at temperatures above 40°F plus Coat 3 Devco ABC#3 AF(Black) 5 mils MDFT Coat 4 Devco ABC#3 AF(Black) 5 mils MDFT	NSTM S9086- BD-ST-M-000/ Chapter 631, Change 8, Table 631-39 & NAVSEA Ltr Ser 03M1/090 of 12 Aug 94	Devco Coatings Co. 4000 Dupont Circle P.O. Box 7600 Louisville, KY 40207 Plants: 9155 River Road Pennsauken, NJ 08110 2625 Durahart Street Riverside, CA 92502



QPL-24647-3

GOVERNMENT DESIGNATION	MANUFACTURER'S DESIGNATION	TEST OR QUALIFICATION REFERENCE	MANUFACTURER'S NAME AND ADDRESS
Type I Class 3A Grades A Application 1	Coat 1 Devran 223AF Coat 2 Devoe ABC#3 AF (Red) Coat 3 Devoe ABC#3 AF (Red)	3-4 mils MDFT 3-4 mils MDFT 3-4 mils MDFT	Technical Handbook S6360- AD-HBK-010/SHT Maintenance & Repair for Submarines, Table 5-2
			Devoe Coatings, Co. 4000 Dupont Circle P.O. Box 7600 Louisville, KY 4020 Plants: 9155 River Road Pennsauken, NJ 08110 2625 Durahart St. Riverside, CA 92502
Type I Class 1A Grades A Application 2 40207	Coat 1 Devran 223AF Coat 2 Devoe ABC#3 AF (Black) Coat 3 Devoe ABC#3 AF (Black)	3-4 mils MDFT 3-4 mils MDFT 3-4 mils MDFT	Technical Handbook S6360- AD-HBK-010/SHT Maintenance & Repair for Submarines, Table 5-2
			Devoe Coatings, Co. 4000 Dupont Circle P.O. Box 7600 Louisville, KY Plants: 9155 River Road Pennsauken, NJ 08110 2625 Durahart St. Riverside, CA 92502
Type I Class 1A Grades A Application 1	Coat 1 Hempadur 4515-5063 AC (Red) Coat 2 Hempadur 4515-1148 AC (Gray) or Coat 1 Hempadur 4514-5063 Low Temp AC* (Red) Coat 2 Hempadur 4514-1148 Low Temp AC* (Gray)	5 mils MDFT 5 mils MDFT 5 mils MDFT 5 mils MDFT	Hempel Test Rpt. dated 20 Dec 91 and NAVSEA Ltr Ser 03M1/091 of 12 Aug 94 77028
			Hempel Coatings (USA), Inc. 6901 Cavalcade Houston, TX 77028 Plant: 6901 Cavalcade Houston, TX
	*For use at temperatures below 50°F plus		
	Coat 3 Olympic 7660-1999 AF (Black) Coat 4 Olympic 7660-5111 AF (Red)	5 mils MDFT 5 mils MDFT	

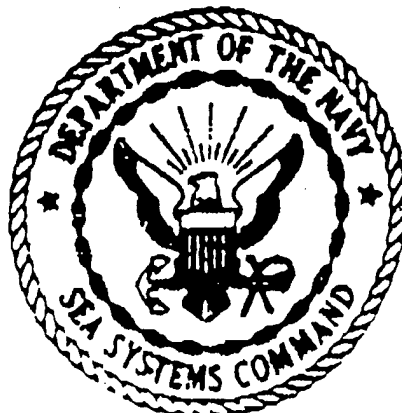


QPL-24647-3

GOVERNMENT DESIGNATION	MANUFACTURER'S DESIGNATION	TEST OR QUALIFICATION REFERENCE	MANUFACTURER'S NAME AND ADDRESS
Type I	Coat 1 Hempadur 4515-5063 AC (Red)	Hempel Test	Hempel Coatings
Class 1A	5 mils MDFT	Rpt. dated	(USA), Inc.
Grades A	Coat 2 Hempadur 4515-1148 AC (Gray)	20 Dec 91	6901 Cavalcade
Application 2	5 mils MDFT	and NAVSEA	Houston, TX 77028
	or	Ltr Ser	Plant:
	Coat 1 Hempadur 4514-5063 Low Temp AC* (Red)	03M1/091 of	6901 Cavalcade
	5 mils MDFT	12 Aug 94	Houston, TX
	Coat 2 Hempadur 4514-1148 Low Temp AC* (Gray)		77028
	5 mils MDFT		
	*For use at temperatures below 50°F		
	plus		
	Coat 3 Olympic 7660-1999 AF (Black) 5 mils MDFT		
	Coat 4 Olympic 7660-1999 AF (Black) 5 mils MDFT		



## NAVAL SEA SYSTEMS COMMAND



FOR TRANSMITTAL OF UNCLASSIFIED MATERIAL ONLY

FACSIMILE TRANSMITTAL SHEET

MATERIALS ENGINEERING GROUP

CODE SEA 03M12.5 FROM DR. BRENDA S. HOLMES  
2531 JEFFERSON DAVIS HIGHWAY  
ARLINGTON, VA 22242-5160

TELEPHONE 703-602-0213 X123 FAX 703-602-0247E-MAIL ADDRESS HOLMES\_BRENDA@HQ.NAVSEA.NAVY.MILDATE 24 Feb 97

TO

Bob Kain

TELEPHONE NUMBER

Le Que Corrosion

FAX NUMBER

910-256-9816

SUBJECT

QPL for 11/W Hull

THIS PAGE 1 OF \_\_\_\_



**APPENDIX 5b**

**International Paint Company Product Literature**



**X International,****Intergard<sup>®</sup>  
universal  
FP series/FPA327****Marine Coatings  
Product Data Sheet**

<b>Product Description</b>	A two pack epoxy anticorrosive	
	<ul style="list-style-type: none"> <li>• Surface tolerant</li> <li>• Self priming</li> </ul>	<ul style="list-style-type: none"> <li>• High build, up to 8 mils (200 microns) in one coat</li> <li>• Available in a limited range of colors</li> </ul>
<b>Intended Uses</b>	A universal anticorrosive for use on:	
	<ul style="list-style-type: none"> <li>• Underwater hulls</li> <li>• Above water areas</li> </ul>	<ul style="list-style-type: none"> <li>• Internal areas including ballast tanks</li> <li>• Marine vessels, barges and offshore structures</li> </ul>
<b>Product Information</b>	Volume Solids	80%
	Typical Thickness Dry Film	4 mils equivalent to 5.0 mils wet (100 microns equivalent to 125 microns wet)
	Theoretical Coverage	321 sq. ft./U.S. gallon (at stated volume solids and typical thickness) (385 sq. ft./imp. gallon) (7.89 sq. m./litre)
	Practical Coverage	Allow appropriate loss factors.
	Regulatory Data	VOC 1.58 lbs./gal. (190 g/l).
<b>Application Details</b>	Mix Ratio	4 volumes FP series to 1 volume FPA327.
	Method of Application	
	Airless Spray	Recommended <ul style="list-style-type: none"> <li>- Tip range 25-33 thou. inch.</li> <li>- Total output fluid pressure 2500 p.s.i. (175 kg/sq. cm.)</li> </ul>
	Brush or Roller	For small areas only
	Conventional Spray	Suitable.
	Thinner	Not normally recommended. In exceptional circumstances use GTA415 (max. 5% by volume).
	Cleaner	GTA415.
	Pot Life	41°F ( 5°C) - 8 hours 73°F (23°C) - 4 hours 95°F (35°C) - 2 hours
	Drying Times	
	Substrate Temperature	
		Touch Dry
		Hard Dry
		Overcoating Interval Intergard FP series/FPA327 by
		Self Intergard FAJ034/FAA262
		Interthane CC and Intergard EC series
		Intersheen LA
		Min. Max. Min. Max. Min. Max.
		41°F ( 5°C) 10 hrs 24 hrs 16 hrs 3 mos 16 hrs 2 mon 16 hrs 4 days
		73°F (23°C) 4 hrs 8 hrs 6 hrs 2 mos 6 hrs 1 mon 6 hrs 2 days
		95°F (35°C) 2 hrs 4 hrs 3 hrs 1 mon 3 hrs 7 days 3 hrs 24 hrs
<b>Storage and Handling</b>	Storage	Store in cool, dry conditions.
	Pack Size	
	FP series	4 gallons in 5 gallon container
	FPA327	1 gallon in 1 gallon container
	Flash Point	Greater than 100°F (38°C) for both components and mixed paint.



## Specification and Surface Preparation

Intergard FP series/FPA327 should be used in accordance with the specifications given in the Marine Product Specification Manual.

- Fresh water wash to remove all dirt and salt contamination.
- Degrease according to SSPC-SP1 solvent cleaning.

### NEWBUILDING

- Where necessary, remove weld spatter and smooth weld seams and sharp edges.
- Clean welds and damaged shop primer by blasting to near white metal SSPC-SP10 or Sa2½ Swedish Standard SIS 05 59 00 or by power tooling to SSPC-SP3.
- For intact zinc shop primers power tool to P12 JSRA SPSS 1975, or abrasive sweep.

### MAJOR REFURBISHMENT

- Blast clean to SSPC-SP10 or Sa2½.

### UPGRADING

- Hard grit sweep.

### REPAIR

- Prepare bare areas of steel by blasting to SSPC-SP10 or Sa2½ or by power tooling to SSPC-SP3 or S12 Swedish Standard SIS 05 59 00.
- Feather or chip back surrounding area to a sound edge.
- Overlap onto the existing coats by 1 inch.
- For blasted areas, Intergard FP series/FPA327 should be applied before oxidation occurs.
- Ensure the total area is clean and dry prior to application.

## Limitations

This product will not cure adequately below 41°F (5°C). For maximum performance, the curing temperature should be above 50°F (10°C). Optimum performance is achieved when Intergard FP series/FPA327 is applied over blasted steel.

## Safety Precautions

Prior to use, consult the appropriate Material Safety Data Sheet for detailed health and safety information. Minimum safety precautions in dealing with all paints are:

- Take precautions to avoid skin and eye contact (i.e. gloves, goggles, face mask, barrier creams, etc.)
- Provide adequate ventilation.
- If the product comes in contact with the skin, wash thoroughly with lukewarm water and soap or suitable industrial cleanser. If the eyes are contaminated flush with water (minimum 10 minutes) and obtain medical attention at once.
- Since these products contain flammable materials, keep away from sparks and open flames. No smoking should be permitted in the area.
- Observe all precautionary notices on containers.

## Worldwide Availability

It is the policy of International to supply this product worldwide. However, in certain countries, product modifications may be required in order to comply with legislation or particular local conditions. Where this occurs, an alternative sales code and data sheet is used. This product is available only in the USA and Canada.

## Definitions

<b>Tolerances</b>	The numerical information quoted in this data sheet is subject to normal manufacturing tolerances.
<b>Practical Coverage</b>	Practical coverage can vary depending on application conditions, the geometrical complexity of the structure, the weather conditions, etc.
<b>Volume Solids</b>	The volume solids figure given in this data sheet is the percentage of dry film obtained from a given wet film thickness under specified application rate and conditions. ASIM D2697-73 (Reapproved 1979) at 77°F (25°C) and 7 days cure.
<b>Overcoating Intervals</b>	The intervals given assume preparation consistent with good painting practice.

## Disclaimer

The information contained herein is intended solely to acquaint you with these products and is not intended to be exhaustive. This information is subject to modification from time to time without further notice. Further, the information does not constitute and shall not be interpreted or construed to constitute an express warranty or a recommendation by International of the products' suitability or fitness for a particular purpose or application. IMPLIED WARRANTIES OF FITNESS FOR A PARTICULAR PURPOSE AND OF MERCHANTABILITY ARE EXCLUDED. INTERNATIONAL SHALL NOT UNDER ANY CIRCUMSTANCES BE LIABLE FOR NEGLIGENCE.







# Interviron® BRA640

## Polishing Antifouling

### INTENDED USES

For superior performance, tributyltin free, polishing antifouling. As a multiple coat system for extended in-service periods.

### PRODUCT DESCRIPTION

A high performance, tributyltin free, polishing antifouling. Enhanced biocide release mechanism. Prevents coating build-up. At subsequent drydockings, it is only necessary to top up the system. Low VOC.

### PRODUCT INFORMATION

<b>Color</b>	BRA640-Red, BRA641-Blue, BRA642-Black; BRA643-Ocean Green
<b>Finish/Sheen</b>	Semi-Gloss (ASTM D-523)
<b>Converter</b>	One pack
<b>Volume Solids</b>	62% ± 2% (ASTM D-2697)
<b>Mix Ratio</b>	One pack
<b>Flash Point</b>	79°F (26°C) (Setaflash) (ASTM D-3278)
<b>Film Thickness</b>	4.0 mils (102 microns) dry specified equivalent to 6.5 mils (165 microns) wet 4.0-5.0 mils (102-127 microns) dry practical range equivalent to 6.5-8.1 mils (165-206 microns) wet
<b>Theoretical Coverage</b>	248 sq. ft./gal. (4.0 mils (102 microns) DFT) Allow appropriate loss factors.

### APPLICATION DETAILS

<b>Method</b>	Airless spray, brush or roller
<b>Induction/Sweat-in Time</b>	Not applicable
<b>Thinner</b>	Not recommended. If necessary use GTA007, see thinning section.
<b>Cleaner</b>	GTA007
<b>Pot Life</b>	Not applicable

	(ASTM D 1640 7.5.1)	Overcoating Interval By		Minimum drying time* before flooding (for 2x5 mil (125 microns) DFT coats)
		Self	Minimum Maximum	
Drying Time (hours)		(ASTM D-1640 7.8)		
Substrate Temperature	Touch			
41°F (5°C)	12	24	Indefinite	3 days
73°F (23°C)	6	12	Indefinite	2 days
95°F (35°C)	4	6	Indefinite	1 day

\*Refer to your International Representative for minimum drying time before flooding at higher dry film thicknesses and to Limitations section for maximum recommended atmospheric exposure time before flooding.

### REGULATORY DATA

<b>VOC</b>	2.8 lb/gal (336 g/l) as supplied
<b>EPA</b>	Federal EPA Registration No. 2693-142 For specific state registrations contact your International Representative See Page 4 for additional Regulatory Data.
<b>MIL SPEC</b>	MIL-P-24647B, Type I, CL IA, Gr A & B, Applications 1 & 2



## Interviron® BRA640

Polishing Antifouling

### SYSTEMS AND COMPATIBILITY

Consult your International Representative for the system best suited for surfaces to be protected.

### LIMITATIONS

Apply in good weather when air and surface temperatures are above 35°F (2°C). Surface temperature must be at least 5°F (3°C) above dew point. For optimum application properties, bring material to 70-80°F (21-27°C) temperature range prior to mixing and application. Unmixed material (in closed containers) should be maintained in protected storage between 40 and 100°F (4-38°C).

Prolonged atmospheric exposure of this product may detract from antifouling performance. Recommended maximum exposure time before flooding:

Temperate conditions 28 days

Tropical conditions 7 days

These times may be extended under certain conditions. Contact your local International Representative for advice.

Technical and application data herein is for the purpose of establishing a general guideline of the coating and proper coating application procedures. Test performance results were obtained in a controlled laboratory environment and International makes no claim that the exhibited published test results, or any other tests, accurately represent results actually found in all field environments. As application, environmental and design factors can vary significantly, due care should be exercised in the selection, verification of performance, and use of the coating.

### SURFACE PREPARATION

Paint only clean, dry surfaces. Remove all grease, oil, soluble contaminants and other detrimental foreign matter by "solvent cleaning" (SSPC-SP1).

*New Construction:* Dependent on yard procedures, consult International.

*Unpainted surfaces:* Prepare surface and apply recommended primer. Apply one or more coats of Interviron BRA640 as specified. (Consult the relevant primer data sheet for surface preparation and overcoating information.)

*Recoating and Upgrading of approved systems:* Use controlled close high pressure fresh water washing (3,000 psi, 211 kg/sq. cm.) to clean the entire area, and remove any leached layer at the surface of the existing antifouling system.

Repair corroded areas with the recommended anticorrosive primer and apply a spot coat of Interviron BRA640 within the overcoating interval specified for the primer (consult relevant primer data sheet).

Apply the specified number of full coats of Interviron BRA640.



**Interviron® BRA640**

Polishing Antifouling

MIXING	This material is a one component coating. Always mix thoroughly with a power agitator before application.
APPLICATION	<p>Apply by airless spray only. Application by other methods, brush or roller, may require more than one coat and is suggested for small areas only or initial stripe coating. Apply 6.5 mils (166 microns) wet which will yield 4.0 mils (102 microns) dry film thickness. Consult the following equipment recommendations or utilize suitable equal.</p> <p><b>Equipment</b> <i>Brush:</i> Use appropriate size China bristle brush. <i>Roller:</i> Use All Purpose Roller Cover 3/8" pile smooth to medium. Prewash roller cover to remove loose fibers prior to use. <i>Airless Spray:</i> Minimum 28:1 ratio pump; .021" - .026" (533-660 microns) orifice tip; 3/8" ID high pressure material hose; 60 mesh tip filter.</p>
THINNING	DO NOT THIN BEYOND YOUR STATE'S COMPLIANCY. Material is supplied at spray viscosity and normally does not need thinning. If thinning is necessary, thin up to a maximum of 4 ounces (118 ml) per gallon with International GTA007 Thinner.
WORK STOPPAGES AND CLEANUP	Clean all equipment immediately after use with International GTA007 Thinner. Spray equipment requires flushing with this solvent. It is good working practice to periodically flush out spray equipment during the course of the working day. Frequency will depend upon factors such as amount sprayed, temperature and elapsed time including work stoppages. Monitor material condition.
WELDING	In the event welding or flame cutting is performed on metal coated with this product, do so in accordance with instruction in ANSI/ASC Z49.1 "Safety in Welding and Cutting."
SAFETY	<p>Prior to use, obtain and consult the Material Safety Data Sheet for this product concerning health and safety information. Read and follow all precautionary notices on the Material Safety Data Sheet and container label. If you do not fully understand these warnings and instructions or if you cannot strictly comply with them, do not use this product. Proper ventilation and protective measures must be provided during application and drying to keep solvent vapor concentrations within safe limits and to protect against toxic or oxygen deficient hazards. Actual safety measures are dependent on application methods and work environment.</p> <p>Medical Advisory Number 1-800-854-6813.</p>
WORLDWIDE AVAILABILITY	It is the policy of International to supply this product worldwide. However in certain countries, product modifications may be required in order to comply with legislation or particular local conditions. Where this occurs, an alternative sales code and data sheet are used.



**Interviron® BRA640**

Polishing AntiFouling

**REGULATORY DATA**

It is a violation of federal law to use this product in a manner inconsistent with its labeling.

Refer to container label for information concerning Precautionary Statements, Directions for Use and Storage and Disposal

**UNIT SIZE**

*This product can be made available in other pack sizes.  
Consult International for details.*

**5 Gallon Unit (18.9 l)****UNIT SHIPPING WEIGHT****98 lb (44.5 kg)****UN SHIPPING No: 1263****STORAGE**

*Store in cool, dry conditions.*

**Shelf Life**

One year minimum from date of manufacture when maintained in protected storage at 40-100°F (4-38°C). Subject to reinspection thereafter.

*All representations and statements concerning the product(s) in this data sheet are accurate to the best of International's knowledge. Any statements herein are not intended to be specific recommendations or warranties of any product, combination of products or fitness for any particular purpose. Any warranty, if given, or specific Terms and Conditions of Sale are contained in International's Terms and Conditions of Sale. You should request a copy of this document and review it carefully.*

*Interviron is a registered trademark.*

General Offices 6001 Antoine, Houston, Texas 77091  
Tel: (713) 682-1711  
Medical Advisory Number 1-800-854-6813

**COURTAULDS  
COATINGS**PI5011.2  
8/96





# Intersleek® Tie Coat

**International**  
Marine Coatings

## Elastomeric Polymer

**INTENDED USES** As a tie coat between epoxy anticorrosives and Intersleek finish to ensure maximum system performance.

**PRODUCT DESCRIPTION** A three component elastomeric coating.

**PRODUCT INFORMATION**

<b>Color</b>	BXA386-Light Gray
<b>Finish/Sheen</b>	Semi-Gloss (ASTM D-523)
<b>Converter</b>	BXA390 & BXA391
<b>Volume Solids</b>	59% ± 2% (ASTM D - 2697)
<b>Mix Ratio</b>	0.4:0.5:0.1 by volume
<b>Flash Point</b>	BXA386 93°F (34°C); BXA390 99°F (37°C); BXA391 74°F (23°C); Mixed paint 90°F (32°C) (Setaflash) (ASTM D-3278)
<b>Film Thickness (SSPC-PA2)</b>	4.0 mils (102 microns) dry specified, equivalent to 6.8 mils (173 microns) wet 3.0-5.0 mils (76-127 microns) dry practical range equivalent to 5.1-8.5 mils (130-216 microns) wet
<b>Theoretical Coverage</b>	237 sq. ft./gal. (4.0 mils (102 microns) DFT) Allow appropriate loss factors.

**APPLICATION DETAILS**

<b>Method</b>	Airless spray or brush
<b>Induction/Sweat-in Time</b>	Not required
<b>Thinner</b>	GTA007. Not normally required.
<b>Cleaner</b>	GTA007
<b>Pot Life</b>	2 hrs @ 50°F (10°C)/1 hr @ 73°F (23°C)/30 mins @ 95°F (35°C)

	(ASTM D 1640 7.5.1)	(ASTM D 1640 7.7)	Overcoating Interval By Intersleek Finish (ASTM D-1640 7.8)	
Drying Time (hours)	Touch	Handle	Minimum	Maximum
50°F (10°C)	4	8	12	1 week
73°F (23°C)	2	5	6	1 week
95°F (35°C)	1	3	3	1 week

## REGULATORY DATA

**VOC**

2.8 lb/gal (336 g/l) as supplied (EPA Method 24)



**Intersleek® Tie Coat**

Elastomeric Polymer

**SYSTEMS AND  
COMPATIBILITY**

Consult your International Representative for the system best suited for surfaces to be protected.

**LIMITATIONS**

Apply in good weather when air and surface temperatures are above 41°F (5°C). Surface temperature must be at least 5°F (3°C) above dew point. For optimum application properties, bring material to 70-80°F (21-27°C) temperature range prior to mixing and application. Unmixed material (in closed containers) should be maintained in protected storage between 40 and 100°F (4-38°C).

Care should be taken to avoid overspray on to conventionally coated areas.

All equipment must be thoroughly cleaned prior to use and before reuse with other materials, to prevent contamination.

Liquids used to clean up Intersleek Tie Coat must not be allowed to contaminate other paints.

Technical and application data herein is for the purpose of establishing a general guideline of the coating and proper coating application procedures. Test performance results were obtained in a controlled laboratory environment and International makes no claim that the exhibited published test results, or any other tests, accurately represent results actually found in all field environments. As application, environmental and design factors can vary significantly, due care should be exercised in the selection, verification of performance, and use of the coating.

**SURFACE PREPARATION**

Paint only clean, dry surfaces. Remove all grease, oil, soluble contaminants and other detrimental foreign matter by "solvent cleaning" (SSPC-SP1).

*Unpainted surfaces:* Prepare surface and apply recommended primer. Apply a coat of Intersleek Tie Coat as specified. (Consult the relevant primer data sheet for surface preparation and overcoating information.).



## Intersleek® Tie Coat

Elastomeric Polymer

### MIXING

Material is supplied in 3 containers as a unit. Always mix a complete unit in the proportions supplied. (1) Agitate Part A with a power agitator. (2) Combine entire contents of Part A and B and mix thoroughly with a power agitator; (3) Add entire contents of Part C and mix thoroughly with a power agitator.

### APPLICATION

Apply by airless spray. Application by brush may require more than one coat and is suggested for small areas only. Strain material through a minimum 60 mesh screen before application. Apply at 6.8 mils (173 microns) wet which will yield 4.0 mils (102 microns) dry film thickness. Consult the following equipment recommendations or utilize suitable equal.

#### Equipment

*Brush:* Use appropriate size China bristle brush.

*Airless Spray:* Minimum 28:1 ratio pump; .017"-.019" (425-475 microns) orifice tip; 3/8" ID high pressure material hose; 60 mesh tip filter.

### THINNING

DO NOT THIN BEYOND YOUR STATE'S COMPLIANCY. Material is supplied at spray viscosity and normally does not need thinning. If thinning is necessary, thin up to a maximum of 4 ounces (118 ml) per gallon with International GTA007 Thinner.

### WORK STOPPAGES AND CLEANUP

Clean all equipment immediately after use with International GTA007 Thinner. Spray equipment requires flushing with this solvent. It is good working practice to periodically flush out spray equipment during the course of the working day. Frequency will depend upon factors such as amount sprayed, temperature and elapsed time including work stoppages. Monitor material condition. Do not exceed pot life limitations.

### WELDING

In the event welding or flame cutting is performed on metal coated with this product, do so in accordance with instruction in ANSI/ASC Z49.1 "Safety in Welding and Cutting."

### SAFETY

Prior to use, obtain and consult the Material Safety Data Sheet for this product concerning health and safety information. Read and follow all precautionary notices on the Material Safety Data Sheet and container label. If you do not fully understand these warnings and instructions or if you cannot strictly comply with them, do not use this product. Proper ventilation and protective measures must be provided during application and drying to keep solvent vapor concentrations within safe limits and to protect against toxic or oxygen deficient hazards. Actual safety measures are dependent on application methods and work environment.

Medical Advisory Number 1-800-854-6813.

### WORLDWIDE AVAILABILITY

It is the policy of International to supply this product worldwide. However, in certain countries, product modifications may be required in order to comply with legislation or particular local conditions. Where this occurs, an alternative sales code and data sheet are used.



## Intersleek® Tie Coat

Elastomeric Polymer

**UNIT SIZE**

*This product can be made available in other pack sizes.  
Consult International for details.*

Part A: BXA386  
Part B: BXA390  
Part C: BXA391

1 Gallon Unit (3.8 l)

1 Gallon (short-filled)  
Half Gallon (short-filled)  
1 Pint (short-filled)

**UNIT SHIPPING WEIGHT**

10.1 lb (4.6 kg)

**UN SHIPPING NO: 1263****STORAGE**

*Store in cool, dry conditions.*

**Shelf Life**

Six months minimum from date of manufacture when maintained in protected storage at 40-100°F (4-38°C). Subject to reinspection thereafter.

*All representations and statements concerning the product(s) in this data sheet are accurate to the best of International's knowledge. Any statements herein are not intended to be specific recommendations or warranties of any product, combination of products or fitness for any particular purpose. Any warranty, if given, or specific Terms and Conditions of Sale are contained in International's Terms and Conditions of Sale. You should request a copy of this document and review it carefully.*

*Intersleek is a registered trademark.*

General Offices 6001 Antoine, Houston, Texas 77091  
Tel: (713) 682-1711  
Medical Advisory Number 1-800-854-6813



COURTAULDS  
COATINGS

PI5217.1  
5/96



# Intersleek® Finish

**International.**  
Marine Coatings

## Elastomeric Foul Release Coating

### INTENDED USES

As a biocide-free, low surface energy foul release coating. Easy clean characteristics. Particularly suited for use on underwater hulls of aluminum vessels.

### PRODUCT DESCRIPTION

A three component elastomeric finish with excellent foul release characteristics. Low VOC.

### PRODUCT INFORMATION

<b>Color</b>	BXA816-Haze Gray; BXA819-Black
<b>Finish/Sheen</b>	Gloss
<b>Converter</b>	BXA820 & BXA821
<b>Volume Solids</b>	72% ± 2%
<b>Mix Ratio</b>	9.75 to 1 to 0.25 by volume
<b>Flash Point</b>	BXA816 101°F (38°C); BXA821 78°F (26°C); BXA822 77°F (25°C); Mixed paint 85°F (29°C) (Setaflash) (ASTM D-3278)
<b>Film Thickness (SSPC-PA2)</b>	6.0 mils (152 microns) dry specified equivalent to 8.3 mils (211 microns) wet 5.0-7.0 mils (127-178 microns) dry practical range equivalent to 6.9-9.7 mils (175-246 microns) wet
<b>Theoretical Coverage</b>	192 sq. ft./gal. (6.0 mils (152 microns) DFT) Allow appropriate loss factors.

### APPLICATION DETAILS

<b>Method</b>	Airless spray or brush
<b>Induction/Sweat-in Time</b>	Not required
<b>Thinner</b>	GTA007. Not normally required.
<b>Cleaner</b>	GTA007
<b>Pot Life</b>	2 hrs @ 50°F (10°C)/1 hr @ 73°F (23°C)/30 mins @ 95°F (35°C)

	(ASTM D 1640 7.5.1)	(ASTM D 1640 7.7)	Overcoating Interval By Self (ASTM D-1640 7.8)	
Drying Time (hours)	Touch	Handle	Minimum	Maximum
50°F (10°C)	8	10	12	*
73°F (23°C)	3	5	6	*
95°F (35°C)	1	3	3	*

\*May be overcoated after prolonged exposure provided surface is in good clean condition. Contact your International Representative for advice.

### REGULATORY DATA

#### VOC

2.1 lb/gal (254 g/l) as supplied (EPA Method 24)



## Intersleek® Finish

Elastomeric Foul Release Coating

### SYSTEMS AND COMPATIBILITY

Consult your International Representative for the system best suited for surfaces to be protected.

### LIMITATIONS

Apply in good weather when air and surface temperatures are above 41°F (5°C). Surface temperature must be at least 5°F (3°C) above dew point. For optimum application properties, bring material to 70-80°F (21-27°C) temperature range prior to mixing and application. Unmixed material (in closed containers) should be maintained in protected storage between 40 and 100°F (4-38°C).

Care should be taken to avoid overspray on to conventionally coated areas.

All equipment must be thoroughly cleaned prior to use and before reuse with other materials, to prevent contamination.

Liquids used to clean up Intersleek Finish must not be allowed to contaminate other paints.

Technical and application data herein is for the purpose of establishing a general guideline of the coating and proper coating application procedures. Test performance results were obtained in a controlled laboratory environment and International makes no claim that the exhibited published test results, or any other tests, accurately represent results actually found in all field environments. As application, environmental and design factors can vary significantly, due care should be exercised in the selection, verification of performance, and use of the coating.

### SURFACE PREPARATION

Paint only clean, dry surfaces. Remove all grease, oil, soluble contaminants and other detrimental foreign matter by "solvent cleaning" (SSPC-SP1).

*Unpainted surfaces:* Prepare surface and apply recommended priming system. Apply a coat of Intersleek Finish over Intersleek Tie Coat as specified. (Consult the relevant primer data sheet for surface preparation and overcoating information.).



**Intersleek® Finish**

Elastomeric Foul Release Coating

**MIXING**

Material is supplied in 3 containers as a unit. Always mix a complete unit in the proportions supplied. (1) Agitate Part A with a power agitator, (2) Combine entire contents of Part A and B and mix thoroughly with a power agitator; (3) Add entire contents of Part C and mix thoroughly with a power agitator.

**APPLICATION**

Apply by airless spray. Application by brush may require more than one coat and is suggested for small areas only. Strain material through a minimum 60 mesh screen before application. Apply at 8.3 mils (211 microns) wet which will yield 6.0 mils (152 microns) dry film thickness. Consult the following equipment recommendations or utilize suitable equal.

**Equipment**

*Brush:* Use appropriate size China bristle brush.

*Airless Spray:* Minimum 28:1 ratio pump; .017"-.019" (425-475 microns) orifice tip; 3/8" ID high pressure material hose; 60 mesh tip filter.

**THINNING**

**DO NOT THIN BEYOND YOUR STATE'S COMPLIANCY.** Material is supplied at spray viscosity and normally does not need thinning. If thinning is necessary, thin up to a maximum of 4 ounces (118 ml) per gallon with International GTA007 Thinner.

**WORK STOPPAGES  
AND CLEANUP**

Clean all equipment immediately after use with International GTA007 Thinner. Spray equipment requires flushing with this solvent. It is good working practice to periodically flush out spray equipment during the course of the working day. Frequency will depend upon factors such as amount sprayed, temperature and elapsed time including work stoppages. Monitor material condition. Do not exceed pot life limitations.

**WELDING**

In the event welding or flame cutting is performed on metal coated with this product, do so in accordance with instruction in ANSI/ASC Z49.1 "Safety in Welding and Cutting."

**SAFETY**

Prior to use, obtain and consult the Material Safety Data Sheet for this product concerning health and safety information. Read and follow all precautionary notices on the Material Safety Data Sheet and container label. If you do not fully understand these warnings and instructions or if you cannot strictly comply with them, do not use this product. Proper ventilation and protective measures must be provided during application and drying to keep solvent vapor concentrations within safe limits and to protect against toxic or oxygen deficient hazards. Actual safety measures are dependent on application methods and work environment.  
Medical Advisory Number 1-800-854-6813.

**WORLDWIDE  
AVAILABILITY**

It is the policy of International to supply this product worldwide. However, in certain countries, product modifications may be required in order to comply with legislation or particular local conditions. Where this occurs, an alternative sales code and data sheet are used.



**Intersleek® Finish**

Elastomeric Foul Release Coating

**UNIT SIZE**

*This product can be made available in other pack sizes.  
Consult International for details.*

**1 Gallon Unit (3.79 l)**

Part A: BXA816 or BXA819 1 Gallon (short-filled)  
Part B: BXA820 1 Quart (short-filled)  
Part C: BXA821 Half Pint (short-filled)

**UNIT SHIPPING WEIGHT****8.6 lb (3.9 kg)****UN SHIPPING NO: 1263****STORAGE***Store in cool, dry conditions.***Shelf Life**

Six months minimum from date of manufacture when maintained  
in protected storage at 40-100°F (4-38°C). Subject to reinspection  
thereafter.

*All representations and statements concerning the product(s) in this data sheet are accurate to the best of International's knowledge. Any statements herein are not  
intended to be specific recommendations or warranties of any product, combination of products or fitness for any particular purpose. Any warranty, if given, or specific  
Terms and Conditions of Sale are contained in International's Terms and Conditions of Sale. You should request a copy of this document and review it carefully.*

*Intersleek is a registered trademark.*

General Offices 6001 Antoine, Houston, Texas 77091  
Tel: (713) 682-1711  
Medical Advisory Number 1-800-654-6813

**COURTAULDS  
COATINGS**PI5213.1  
5/96





# EPOXY BARRIER-KOTE 404/414

## PRODUCT DESCRIPTION

EPOXY BARRIER-KOTE 404/414 is a multi-purpose two part epoxy primer for use above and below the waterline. EPOXY BARRIER-KOTE 404/414 is an excellent undercoater for INTERTHANE PLUS. EPOXY BARRIER-KOTE 404/414 is used as a sanding surfacer to smooth rough layup and to resurface cracked and crazed gelcoat. EPOXY BARRIER-KOTE 404/414 should also be used over clear epoxies to eliminate the effects of amine blush.

## TECHNICAL DATA

NUMBER OF COMPONENTS:	2
MIXING RATIO:	3:1 by volume as supplied
INDUCTION TIME:	20 minutes
POT LIFE:	4 hours
COLOR:	White
FINISH:	Matte
SOLVENT:	Brush: BRUSHING SOLVENT 2333N Spray: REDUCING SOLVENT 2316N
REDUCTION LIMIT:	25%
WIPE DOWN SOLVENT:	Bare Fiberglass - SOLVENT WASH 202 Painted Surfaces - N/A
CLEAN UP SOLVENT:	REDUCING SOLVENT 2316N
METHOD OF APPLICATION:	Brush, Roll or Spray
V.O.C.:	Less than 380 grams per liter as supplied (kit)
VOLUME SOLIDS:	55%
PRACTICAL COVERAGE:	450 sq. ft/gal (brush) yields 2.0 mils D.F.T. 375 sq. ft/gal (spray) yields 2.0 mils D.F.T.
RECOMMENDED APPLIED THICKNESS:	4.0 mils wet film thickness per coat
FLASH POINT:	81°F
SHIPPING DOCUMENTATION REQUIRED:	ORM-D consumer commodity all pack sizes

## DRYING TIMES

TEMP (°F)	TOUCH DRY	OVERCOATING TIME (SELF) (MINIMUM)	LAUNCH TIME	
			MIN	MAX
50°-60°	3 Hours	12 Hours	N/A	N/A
60°-80°	2 Hours	8 Hours	N/A	N/A
80°-95°	1 Hour	6 Hours	N/A	N/A

## APPLICATION TEMPERATURE LIMITS

	PRODUCT (°F)	AMBIENT (°F)	SUBSTRATE (°F)
Minimum	50°	50°	50°
Maximum	85°	95°	85°

## APPLICATION DATA-SPRAY

EQUIPMENT	PRESSURE (PSI)	TIP SIZE
Airless	2500-3000	21 thou. inch
Pressure Pot	8-10 Pot 50-65 Tip	70-85 thou. inch
Syphon Cup	N/A	N/A



# EPOXY BARRIER-KOTE 404/414

## **SURFACE PREPARATION:**

Surface should always be clean, dry and properly prepared prior to painting. All surfaces should be wiped clean with a cloth dampened with either **BRUSHING SOLVENT 2333N** or **REDUCING SOLVENT 2316N**.

## **LEAD KEEL SYSTEM:**

Surface should be blasted to bright metal (if blasting is not possible, grind with 36 grit discs). Apply one very thin coat of **VINY-LUX PRIME WASH 353/354**. Allow to dry approximately 1 hour but no more than 24 hours and apply **EPOXY BARRIER-KOTE 404/414**.

If fairing is required, apply 1 coat **EPOXY BARRIER-KOTE PRIMER 404-414**. After overnight dry, apply fairing compound utilizing **EPOXY SURFACING AND FAIRING COMPOUND 417A/418B** as required. This should be followed by three coats of **EPOXY BARRIER-KOTE PRIMER WHITE 404/414**, allow an overnight dry between each coat and sand with 120 grit paper. Apply 1 thin coat of **FIBERGLASS NO-SANDING PRIMER AL200** as a tie coat prior to application of antifouling paint.

If fairing is not required, three coats of **404/414** should be applied following the **VINY-LUX PRIME WASH 353/354**. Apply 1 thin coat of **FIBERGLASS NO-SANDING PRIMER AL200** as a tie coat prior to application of antifouling paint. See appropriate labels for finish coat application.

## **STEEL OR CAST IRON KEEL SYSTEM:**

Systems for applying **BARRIER-KOTE PRIMER 404/414** to steel or cast iron are identical to the lead keel system with the exception of applying 2 coats of **STEEL EPOXY PRIMER 402/414** instead of the 1 coat of **VINY-LUX PRIME WASH 353/354**.

## **CLEAR EPOXY SYSTEM:**

Scrub the surface of the clear epoxy with a stiff bristle brush and soap and water to remove amine blush. Rinse with fresh water. When dry, sand with 80 grit production sandpaper. Wipe sanding residue off with **BRUSHING SOLVENT 2333N** or **SPRAYING SOLVENT 2316N**.

## **SAFETY PRECAUTIONS:**

Prior to use, consult the appropriate Material Safety Data Sheet for detailed health and safety information. Minimum safety precautions in dealing with all paints are:

- (a) Take precautions to avoid skin and eye contact (i.e. gloves, goggles, face mask, barrier creams, etc.).
- (b) Provide adequate ventilation.
- (c) If the product comes in contact with the skin, wash thoroughly with lukewarm water and soap or suitable industrial cleaner. If the eyes are contaminated flush with water (minimum 10 minutes) and obtain medical attention at once.
- (d) Since these products contain flammable materials, keep away from sparks and open flames. No smoking should be permitted in the area.
- (e) Observe all precautionary notices on containers.

## **DISCLAIMER:**

The performance of any marine paint or coating depends on many factors outside the control of Courtaulds Coatings Inc., including surface preparation, proper application, and environmental conditions. Therefore, Courtaulds Coatings, Inc. cannot guarantee this product's suitability for your particular purpose or application. **IMPLIED WARRANTIES OF FITNESS FOR A PARTICULAR PURPOSE AND OR MERCHANTABILITY ARE EXCLUDED. COURTAULDS COATINGS SHALL NOT, UNDER ANY CIRCUMSTANCES, BE LIABLE FOR INCIDENTAL OR CONSEQUENTIAL DAMAGES.** By Purchase or use of this product, buyer agrees that the sole exclusive remedy, if any, is limited to the refund of the purchase price or replacement of the product at Courtaulds Coatings option.



**APPENDIX 5c**

**Coating Application Procedure Utilized for Flat Test Panels and Pipes**



**Coating Application Procedure**  
**Prepared for Fully and Partially Coated Test Panels and Pipes**

**Epoxy coated specimens without antifouling topcoats:**

- Initial set of 54 flat panels (18 per alloy) were mounted horizontally on a wooden support rack. The panels actually rested on two finishing nails with a stand-off block behind.
- The exposed surfaces (Side A) were then spray coated with 5 mils wet film thickness (WFT) of Interguard FPL274 (red)/FPA327 epoxy barrier paint.
- When dried, the panels were flipped to expose and spray coat Side B.
- When dried, Side B was spray coated with 5 mils (WFT) of Interguard FPJ034 (gray)/FPA327 epoxy barrier paint.
- When dried, the panels were flipped to expose and apply the second coat of epoxy to Side A.
- 12 pipe specimens first received the Interguard red coat and then the gray coat, as described above.
- 12 other pipe specimens received one "heavy" brush applied coating of white Interlux epoxy.

**Epoxy coated specimens with ablative-Cu antifouling topcoats:**

- Another set of 54 panels were mounted on the rack and were spray painted, one side at a time, with the Interguard red epoxy.
- Side B of each was then spray coated with 5 mils (WFT) of the Interguard gray epoxy.
- While the above was still soft-to-the-thumb, a 6.5 mil (WFT) coat of Interviron BRA640 (red ablative-Cu paint was applied.
- When dried, the panels were flipped to apply the second coat of epoxy and the BRA460 to Side A.



*Epoxy coated specimens with elastomeric type antifouling coating:*

- A third set of 54 panels were mounted on the rack and were spray painted one side at a time with the InterGuard red epoxy.
- Side B of each was then spray coated with the layer of InterGuard gray epoxy.
- While the above was still soft, a 6.7 mil (WFT) coat of light gray Intersleek tie coat (BXA386/390/391) was sprayed.
- When dried, the panels were flipped for coating of Side A with the second layer of epoxy and the tie coat.
- When dried, Side A was topcoated with 8.3 mils (WFT) of black Intersleek elastomeric polymer (BXA816/20/821).
- When dried, the panels were flipped a final time for topcoating of Side B with the Intersleek coating.

NOTE: The coating thickness cited are those recommended by the coatings' manufacturer. Trial samples were sprayed and tested with a wet film thickness gauge to establish the desired result. There was no attempt made to verify the actual coating thickness applied to each test panel or pipe. As noted in the Appendix 1 report, the dry film thickness of the coating on several randomly selected specimens was determined after the seawater exposure. Cross-sectional views of a sample of each of the three coating systems are shown in Appendix 3, Figures 6.1 to 6.3. Pre-exposure inspection of the coating panels revealed evidence of incomplete topcoat coverage on the edges of some panels. Examples are shown in Appendix 3, Figures 7.1 to 8.1.



# CFD Research Corporation

215 Wynn Dr. • Huntsville, Alabama 35805 • Tel.: (256) 726-4800 • FAX: (256) 726-4806 • info@cfdr.com



## AIR TURBO ROCKET FOR MINIMUM COST HIGH SPEED VEHICLE PROPULSION

### Final Report

By

John A. Bossard

December 1999

CFDRC Report No. 8202/3

Sponsored by  
Defense Advanced Research Projects Agency  
DARPA/TTO  
ARPA Order Nr. D611  
Amdt. Nr.: 56  
Issued by U.S. Army Missile Command under  
Contract No: DAAH01-99-C-R178  
DARPA Project Manager: Mr. Bill Friday  
CFDRC Project Manager: Mr. Matthew E. Thomas (met@cfdr.com)

The Contractor, CFD Research Corporation, hereby declares that, to the best of its knowledge and belief, the technical data delivered herewith under Contract No. DAAH01-99-C-R178 is complete, accurate, and complies with all requirements of the contract.

Date: December 29, 1999

CFDRC Project Manager: Matthew E Thomas

The views and conclusions contained in this document are those of the authors and should not be interpreted as representing the official policies, either express or implied, of the Defense Advanced Research Projects Agency or the U.S. Government.

Distribution <sup>authorized</sup> limited to U.S. Government agencies only; Test and Evaluation; July 1999. Other requests for this document must be referred to Commander, U.S. Army Aviation and Missile Command, ATTN: AMSAM-RD-WS-DP, Redstone Arsenal, AL 35898-5248.

20000207 070

DRG QUALITY INSPECTED 1



## **PREFACE**

This report is the Phase I Final Report under DARPA contract DAAH01-99-C-R178. The report summarizes pertinent ATR development efforts and states the approach and objectives of the project. Each objective of this effort was met or exceeded as related to the original proposal.

Mr. Matthew E. Thomas was the project manager and Dr. John Bossard was the principal investigator for CFD Research Corporation (CFDRC). Valuable assistance from Mr. John Bergmans, Mark Ostrander and Robert Myers of CFDRC was critical to program success. Dr. Kirk Christensen supported selected ATR system model code development and simulations. Valuable assistance was obtained from Mr. Mike Lloyd of Lockheed Martin Vought Systems regarding AFSS systems. The final typescript was accurately prepared by Mrs. Stephanie Cameron.



## SUMMARY

The Air Turbo Rocket (ATR) engine concept was evaluated for use in several DoD mission and vehicle concepts which have emerged from DARPA initiatives. These missions and vehicles were specifically chosen because they place severe constraints on currently available propulsion systems, such as turbojets and rocket motors, and may require the use of more innovative, higher-performing propulsion systems such as the ATR. The numerous advantages of the ATR, such as its high thrust-to-weight, high Isp, deep throttling, and potential for low-cost fabrication, became obvious during these evaluations, and served to highlight the need for this system.

Three basic missions were evaluated: a small, low cost anti-cruise missile mission, a scramjet-boost mission, and the use of the ATR in the Advanced Fire Support System (AFSS) concept. Details of the mission simulations are reported in the missions section.

The performance of the actual ATR engine was also evaluated in detail during this Phase I effort. Two different engine sizes were analyzed. For the anti-cruise missile and AFSS missions, an ATR which possessed a 3-inch diameter compressor was evaluated, referred to as the 3-inch ATR. For the scramjet-boost mission, a 6-inch ATR engine design was evaluated. This engine is based on CFDRC's baseline ATR demonstrator engine which was delivered to the U.S. Army AMCOM in December of 1998. Performance results from these engines are discussed in the ATR propulsion analysis section.

Lastly, the actual layout of the ATR engine was considered, and resulted in the development of engineering drawings for the 3-inch engine, and the fabrication of a full-scale model of this engine. The evaluation of cost/producibility issues associated with the ATR engine was initiated, but it quickly became obvious that without a specific mission for the ATR, these issues could not be meaningfully addressed.

In summary, all tasks proposed in the original SBIR proposal were completed, and major program objectives were met or exceeded. The major conclusion from this Phase I effort was that the ATR engine is an extremely promising candidate for next-generation tactical missile propulsion, and further development of ATR engine technology should be pursued.



## 1.0 INTRODUCTION

This final report summarizes work completed on the DARPA Phase I SBIR program entitled "Air-Turbo-Rocket for Minimum Cost High Speed Vehicle Propulsion". The Phase I effort was completed during the time period of 4/21/99 through program completion on 10/30/99. The objective of this effort was to ascertain the suitability of the Air Turbo Rocket (ATR) Engine for a variety of tactical missile applications, and reinvigorate an interest in the ATR for future propulsion needs.

## 2.0 BACKGROUND

The Air-Turbo-Rocket is an airbreathing propulsor in which incoming air is compressed by a turbine-driven single stage compressor. In the Solid Propellant Air Turbo Rocket (SPATR), shown schematically in Figure 1, the turbine is driven by the fuel-rich gases from a solid propellant gas generator (SPGG). These gases, on exiting the turbine, mix with the compressor discharge air and burn in a combustor, producing thrust. Despite its inherent simplicity, the SPATR offers a diverse array of characteristics, including high thrust/weight (20-100 Lbf/Lbm) and thrust/frontal area (1000-10,000 lb/ft<sup>2</sup>) ratios, throttleability, and a wide speed-altitude operating envelope such as shown in Figure 2. First-order performance characteristics and overall combustor stoichiometry of the ATR is determined by the propellant used in the SPGG, and the performance of the turbomachinery. Liquids (monopropellants and bipropellants), solids, and hybrids with greatly diverse properties can be considered for use in an ATR, allowing an engine to be optimally designed for a given mission.<sup>1-5</sup> If a liquid propellant is used, the gas generator can be part of the main engine (along with a pump), or external. When a solid propellant is used, the gas generator is independent of the main engine and air flowpath, with hot gases entering directly into the turbine. This separation of the gas generator from the engine air flowpath allows considerable flexibility in vehicle performance and configuration.

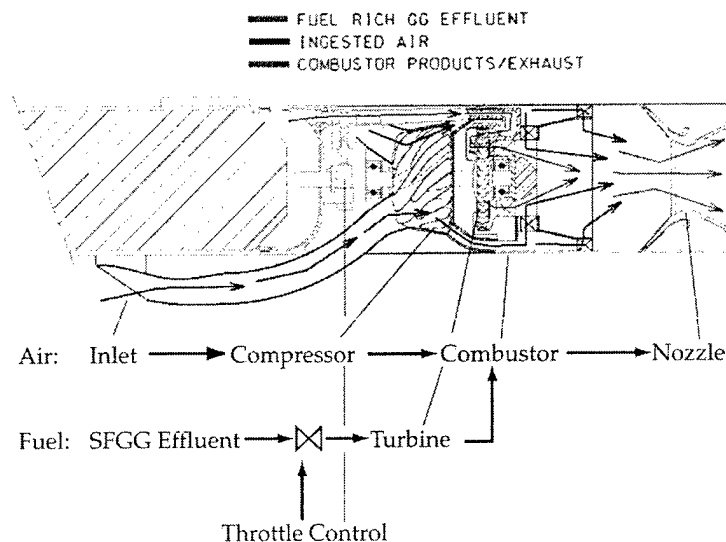
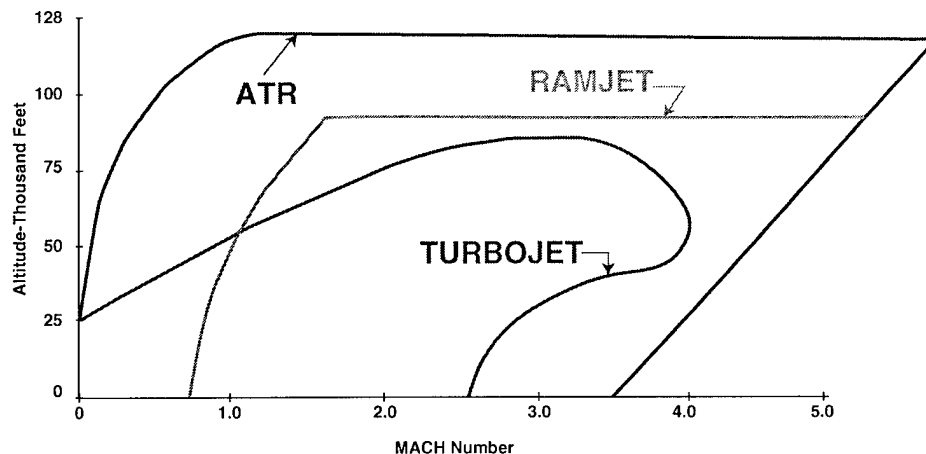


Figure 1. SPATR Propulsion Schematic





*Figure 2. Airbreathing Propulsion System Operating Envelopes*

Although solids can be more difficult to tailor and throttle, they offer simplicity, reliability, and high density and with performance comparable to that available from liquids in many applications. Since the SPATR does not depend solely on the heating value of the propellant to generate good performance, a wide variety of qualified solid propellants could find use in ATRs. In fact, for SPATR applications where  $I_{sp}$  can be traded for thrust coefficient or engine weight, propellants may be favored that have high stoichiometric ratios with air up to about 0.3 and corresponding low heating values down to about 5000 Btu/lbm. In addition, the SPATR propulsion system offers low debris and plume signatures during mission operation as compared to a solid rocket. This feature has significant tactical and strategic implications associated with launch location and corresponding plume signature tracking for numerous military applications.

## **2.1 SPATR Technology Advantages**

As Figure 3 shows, an SPATR can exhibit thrust-vs-speed dependency in which specific thrust rises sharply from dry-turbojet-like values below about Mach 0.5 to perhaps five times this value at Mach 2. Thrust may continue to rise at higher speeds, depending on propellant selection, turbomachinery capability, burner stoichiometry, control scheme, etc. Since the fuel entering the burner of an SPATR will consist of hot gases such as hydrogen, carbon monoxide, methane, and ammonia and the combustor operates well above ram recovery pressures, the combustor performance of a SPATR at altitude can be expected to be considerably superior to that of a ramjet.



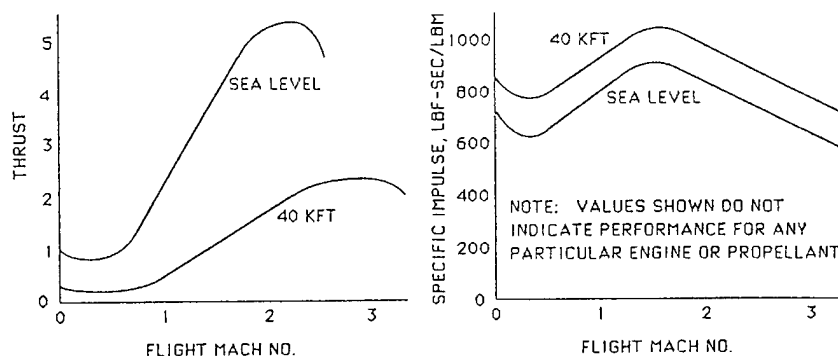


Figure 3. Typical Variations in Thrust and Specific Impulse with Flight Speed for an SPATR

Net Isp depends mainly on burner stoichiometry and propellant heating value, with some flight speed variation up to Mach 2, beyond which it drops (Figure 3). Even for propellants with rather low heating values, the Isp can range from 500 to 1000 lbf-sec/lbm. This range is comparable to the combined boost-sustained Isp delivered by hydrocarbon ramjet vehicles.<sup>6</sup> Thrust from SPATRs is generally large enough such that no boost propulsion is required in many launch environments (including rail launch).

Selection of the propellant and compressor pressure ratio (CPR) are critical and inextricably bound together in the design of an SPATR. The CPR, together with secondary influences such as compressor and turbine efficiencies, establishes the propellant flow required to drive the compressor and, therefore, the propellant/air ratio in the burner. The combustor temperature rise that results from this propellant/air ratio must be appropriate to the engine and flight envelope selected. For example, selecting a SPATR with a high CPR (e.g., 4:1) to get high thrust coefficients, and a high heating-value propellant (e.g., methane) to get high Isp, can result in an inferior overall propellant/air ratio. This SPATR would deliver excellent thrust coefficients, but moderate Isp, because some of the fuel will exit the nozzle unburned. The designer may also compromise on the propellant heating value to gain somewhere else, such as propellant density, or turbine drive capability (low molecular weight). Numerous system studies<sup>7-10</sup>, and U.S. Army AMCOM test experience<sup>11-12</sup>, indicate that a reduction in combustor mixture ratio (MRC) at a constant combustor pressure increases specific impulse. Conversely, an increased MRC reduces Isp but increases available thrust. This trend is summarized from a global aspect in Figure 4 and is one reason the SPATR possesses the capability to be implemented in a diverse array of missions.



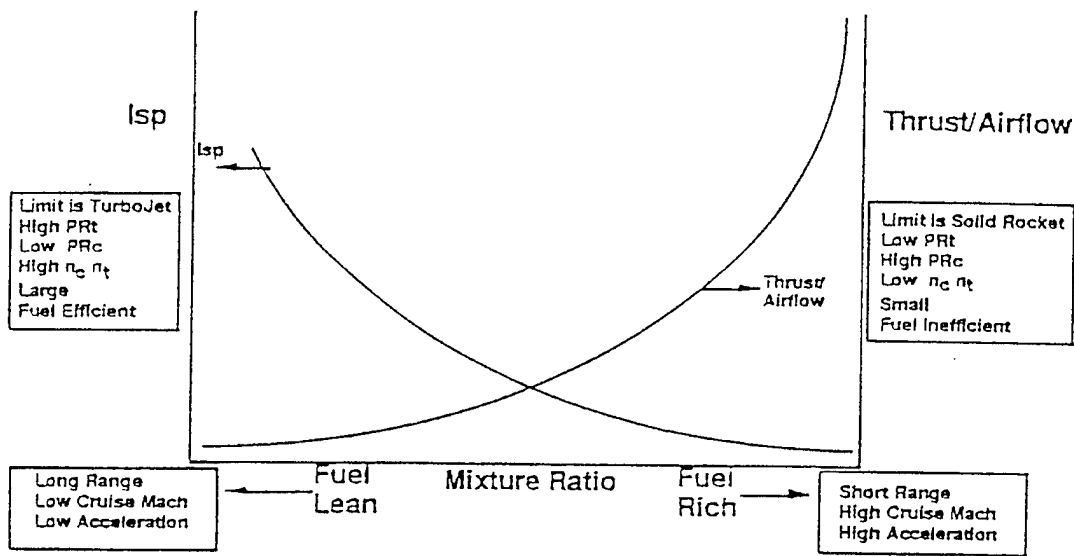


Figure 4. ATR Engine Performance Trends

In summary, Table 1 identifies why the ATR may be an optimum propulsion plant due to its inherent flexibility for numerous tactical missile as compared with alternative propulsion systems

Table 1. Supersonic Propulsion System Tradeoff

Parameter	Liquid Fueled Ramjet	Ducted Rocket	Turbojet	Solid Rocket Motor	ATR
Low Cost Potential Relative to SRM	Yes	Yes	No	Yes	Yes
Booster Not Required	No	No	No	Yes	Yes
Subsonic Loiter	No	No	Yes	No	Yes
Solid Propellant Fuel Source	No	Yes	No	Yes	Yes
Supersonic Cruise	Yes	Yes	Yes	Yes	Yes
Excellent $I_{sp}$ at All Flight Conditions	No	No	Yes	No	Yes
Turboelectric Power	No	No	Yes	No	Yes

## 2.2 Recent SPATR Propulsion Research

Over the years, numerous research studies have been completed on the SPATR; however, a satisfactory demonstration of a high-performance SPATR has yet to be completed. Recent research which most directly relates to this research is presented here to assist in justifying the activity completed during this SBIR effort.



### 2.2.1 U.S. Air Force

The SPATR performance study summarized in Figure 5 focused on the thrust/Isp tradeoff in a 10 inch HARM class missile airframe.<sup>13,14</sup> In the estimates shown in Figure 5b the influence of different levels of turbomachinery and propellant technology on ATR performance is summarized. Each turbomachinery type represented an available technology. The lowest turbomachinery technology level was associated with the aircraft starter industry which combines nominal impulse turbine blading with a turbocharger radial compressor. The second level was turbomachinery composed of a liquid rocket high impulse turbine and a turbocharger compressor. The final level of performance can be achieved by combining a customized radial flow compressor and impulse turbine technology. The SPATR propellants utilized in this study are briefly described below.

- a. Low energy MG-712, a well characterized Hercules formulation currently used in variable flow ducted rocket propulsion systems.
- b. Medium energy ARC428, an Atlantic Research Corporation (ARC) formulation incorporating fluorinated graphite and amorphous boron in a cross-linked polystyrene matrix currently being refined for implementation in the USAF VFDR propulsion system.
- c. A high energy ARC formulation (formulation designator not available) which produces approximately 60% gaseous  $H_2$  and 40% gaseous methane at the expense of a very low yield by mass (3-15% by mass).

The performance of this SPATR propulsion configuration in the HARM and the Sparrow has also been considered. The HARM trajectory results indicate that the use of an  $H_2$ -generating solid with a 35% gas yield in the SPGG (realistic maximum of 10%) provides maximum range, while ARC428 in the SPGG produces considerably higher flight Mach numbers (up to Mach 3.09) with an excellent range. Further study has revealed that the maximum  $H_2$  yield is only about 10%, thereby making this family of propellants unsuitable for further consideration in an SPATR.



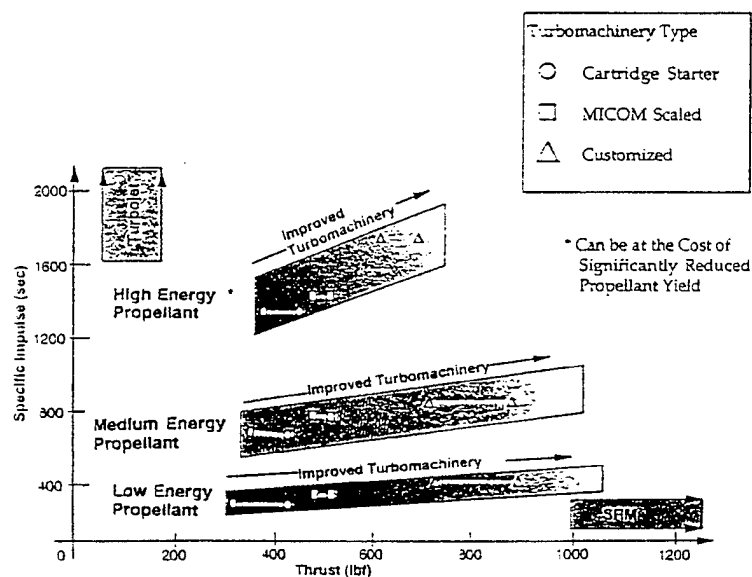
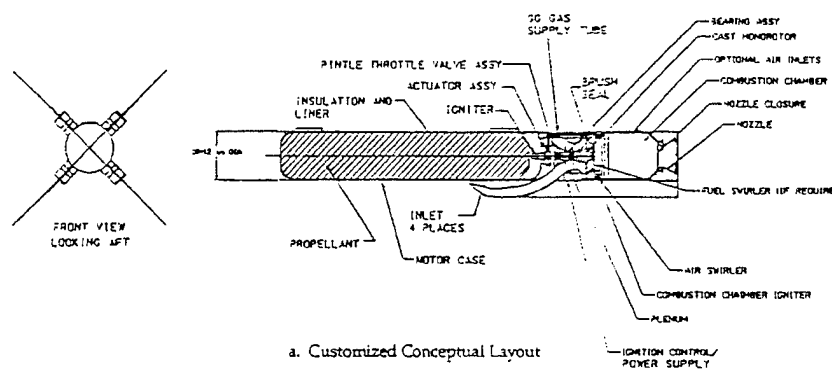


Figure 5. SPATR Performance in a Ten Inch Airframe

Under the scenarios modeled, the results in Figure 6 indicate that a solid propellant ATR can provide a 123% increase in range with a 94% increase in time of flight (TOF) in the HARM compared to the existing SRM. These results assume that:

- the ARC428 gas generator grain is suitable as a turbine drive with adequate combustion;
- vehicle aerodynamics are correctly approximated (Missile DATCOM was used to define the lift and drag coefficients);
- the flight assumed profile is practical for the AGM HARM mission; and
- baseline performance of the HARM powered by a SRM is accurate.



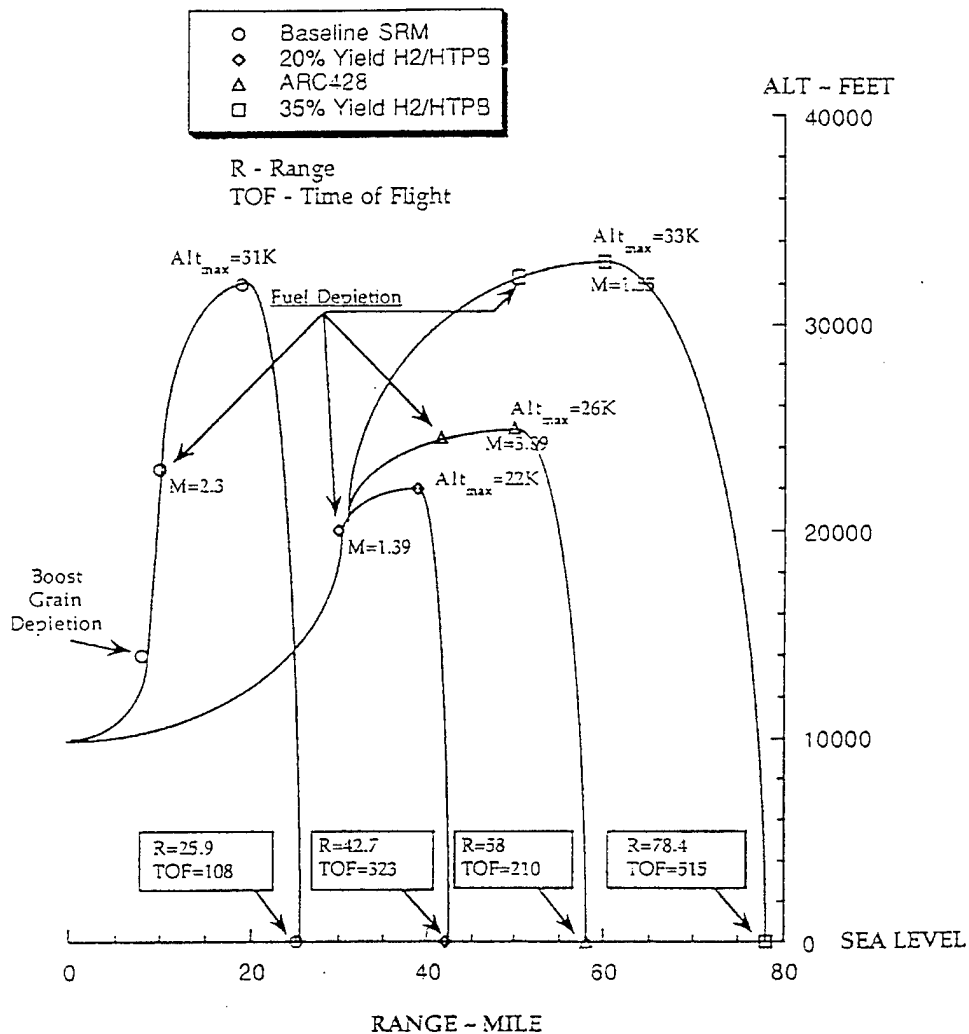


Figure 6. HARM Trajectory Results

The conceptual HARM missile propulsion layout in Figure 5 shows all critical component technologies. These components consist of:

- an end burning solid fuel propellant formulation and assembly yet to be determined;
- a solid grain burn pneumatic actuated pintle valve (currently perceived to be the most promising throttling configuration);
- a monorotor configuration integrating a radial compressor and turbine into a single assembly;
- a preliminary bearing assembly;



- e. swirl stabilized combustion chamber;
- f. single or bifurcated inlet for maximum pressure recovery, minimum spillage and minimal effect on missile aerodynamic stability; and
- g. optional integrated solid boost grain with a frangible barrier and ejectable boost nozzle.

In the case of the inlet, a quadfurcated configuration was selected as a compromise between weight, complexity, propellant load simplicity, cost, distortion to the compressor, frontal area and missile aerodynamic stabilization. Further turbomachinery assessment discussed in Sections 4 and 5 indicates a partial admission turbine and mixed flow compressor offers the best compromise on SPATR missile propulsion. For the combustion chamber, staging the air injection is anticipated to maintain a fixed geometry combustor and provide stable operation throughout the deep throttling requirements between the loiter and boost phases.

### 2.2.2 LocATR Study for Maverick

United Technologies Corporation (UTC) performed a conceptual design study of a low-cost ATR (LocATR) engine.<sup>8</sup> The study assumed the use of a solid fuel gas generator and was focused on developing a system featuring minimum cost with modest performance and life cycle cost goals. Figure 7 shows a final conceptual mechanical layout of the LocATR. Overall, the results were encouraging but lacked sufficient detail to justify further technology development at the time. In particular, there was insufficient focus on the technology interface between propellant chemistry and the turbomachinery performance.

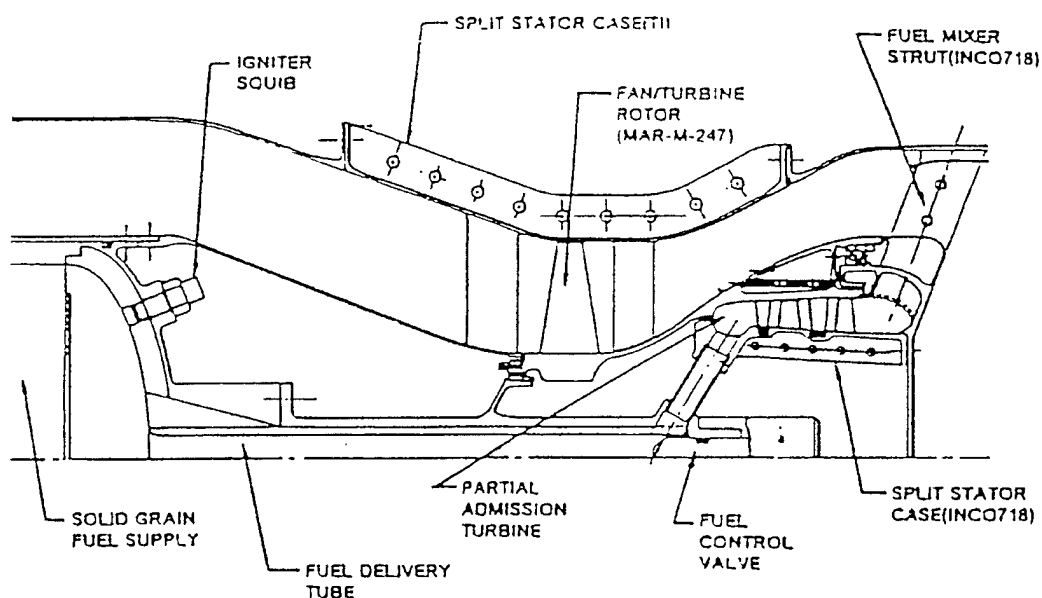


Figure 7. UTC/CSD LocATR Study Summary



Compressor and turbine efficiencies were set at levels consistent with Pratt & Whitney "near-term" technology goals, indicating a future requirement for turbomachinery technology research and development. A truly minimum cost approach would have been to use scalable performance maps of existing turbomachinery components and technology. This UTC/CSD effort recommended the use of a multi-stage axial compressor to permit a SPGG tubing configuration down the missile centerline. Although this layout offers unique system simplicity, the severe structural complications of a hollow drive shaft may preclude the possibility of this configuration becoming a reality. In addition, this study failed to provide adequate direction for solid fuel ATR technology development such as details defining the solid fuel propellant to turbomachinery interface. It continues to be CFDRC's position that with an adequate propellant/turbomachinery interface and an effluent gas with acceptable residual heat content, the SPATR is a promising propulsion plant.

### 2.2.3 U.S. Army ATR Research Activity

The primary focus of this activity was to define an ATR propulsion system of the same thrust class as the U.S. Army FOG-M, but with roughly 3 times the specific impulse (Isp) of a conventional solid propellant rocket engine.<sup>11-12</sup> This included preliminary propulsion related performance studies and demonstration of the ATR demonstrator engine shown in Figure 8. The oversized combustor is indicative of potential problems associated with combustion of low heat content fuels composed of hydrogen, carbon monoxide, inert compounds, carbon, and/or boron from potential SPATR engine propellant formulations. This ATR demonstrator engine has since completed significant testing and its performance well documented.<sup>12</sup> The results of this effort indicate a hydrazine class propellant can deliver an Isp and specific thrust approaching 600 seconds and 100 lbf-sec/lbm, respectively.

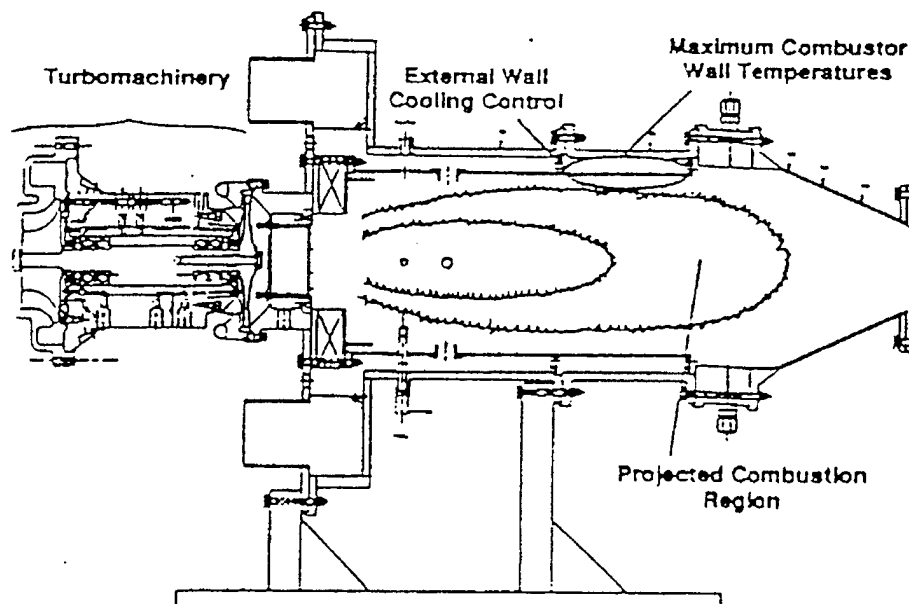


Figure 8. MICOM ATR Demonstrator Engine



The engine also demonstrated full throttleability using a personal computer-based fuel control system developed to provide closed-loop, on-demand, engine speed control. An extensive experimental evaluation included 35 successful firings with stable steady-state operation demonstrated over a rotational speed of 19 krpm to 83 krpm. Demonstrated thrust and Isp ranged from 16 lbf to 343 lbf and 445 sec to 520 sec with transient engine speed and thrust responding nearly instantaneously to changes in gas generator flow rate. The need to develop energetic solid propellants with good turbine drive capability became obvious from this effort.

MICOM concluded from this effort that:

- a. this level of performance is quite remarkable for turbomachinery that could be packaged in a 6.0 inch diameter engine (at the time the highest thrust 6.0 inch turbojet delivers 70 lbf);
- b. realistic Isp improvement to 800 seconds appears achievable with optimized turbomachinery; and
- c. major improvement in both thrust and Isp can be made by utilizing a more energetic propellant and/or customized turbomachinery.

#### **2.2.4 U.S. Navy Studies**

A recent NAVSEA mission, identified here as the Long Look<sup>15</sup>, requires a gun-launched missile speed to a distant target area, possibly slow down to look for a target of opportunity, then accelerate to attack it. Athodyds of various types (solid fuel ramjet, ducted rockets, shrouded rockets, etc.) can get to the target fast, but cannot loiter appreciably; they must maintain speed to continue operating. They must also be boosted to speeds well above acceptable muzzle velocities before the ramjet phase can begin. Muzzle velocities were limited to about 36- m/s (1200fps), and a relatively large fraction of the vehicle weight would have to be rocket propellant to boost to about 800 m/s (2700 fps). The ramjet cannot provide sufficient thrust coefficient to loiter in this type vehicle at subsonic speeds. Turbojets of 0.127-meter (5 inches) diameter have been demonstrated and could provide loiter capability, but existing designs are intended for subsonic speeds. Supersonic turbojets have been designed for missiles, but in sizes over 0.254-meter (10 inches) diameter. The 0.127-meter diameter limit would be very challenging for a low cost supersonic turbojet. If such an engine were available, the mission could be done with a very small (short) vehicle, or, for a given vehicle length, a long loiter time could be provided. However, the average speed to the target area would be relatively low because of the turbojet's limited thrust margin.

The SPATR was selected over rockets, ramjets and turbojets for further consideration since it

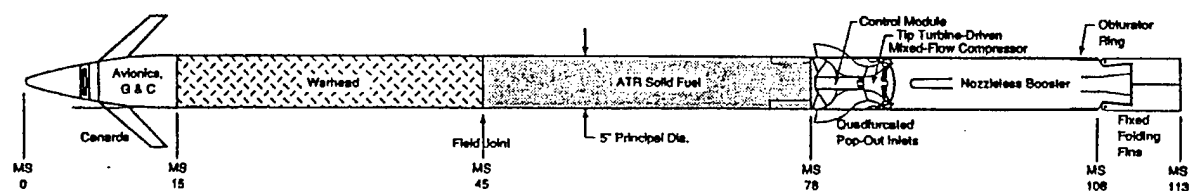
- a. has sufficient Isp to attain the ranges desired;
- b. can climb and accelerate from speeds near the allowable muzzle velocity;
- c. is simple with a light rotor which can withstand the gun setback forces;



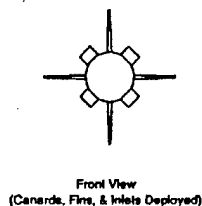
- d. can throttle from the Mach 3 cruise speed to loiter at a subsonic speed;
- e. requires only small inlets, which can be packaged more easily than those for turbojets or ramjets; and
- f. can use a solid propellant.

Figure 9 shows a preliminary version of the concept, with weight breakdown and trajectory performance estimates. The ATR propellant assumed during this assessment was an ammonium perchlorate/HTPB composite solid developed for ducted rockets. It has a moderate density and heating value and a stoichiometric ratio of 0.138 with air. It permits the use of a compressor pressure ratio exceeding 2.0 (for good thrust/frontal area and thrust/airflow) without producing fuel-rich exhaust from the ram burner. It has long shelf life, good processing and handling characteristics, is throttleable, and is well characterized. ATRs offer the best combination of time-to-target area and loiter capability, should be cheaper than a supersonic turbojet, and are readily buildable in a 0.127 meter (5 inches) diameter. For this configuration, muzzle momentum was limited to 27,000 N-s (6150 lbf-s). Higher muzzle velocities may be considered, but a vehicle designed for further in-barrel acceleration increases would be heavier, and propellant volume would be lost to thicker walls, with the net gain in performance potentially very small. The most challenging gun launch is the 5"/38, which has the shorter length, and therefore requires the greater in-barrel acceleration to provide the desired muzzle conditions. The average acceleration required for the 370 m/s (1220 f/s) muzzle velocity desired is 1466 gs; consequently 2000 gs was used as the acceleration potentially contributing to a structural yield. Maximum length of the assembled round (two "rams") is 287 m (113 inches).





### Air-Turborocket-Propelled "Long-Look" Vehicle



#### WEIGHT BREAKDOWN (lbs):

Guidance and Control	12.0	Fwd Ram	68 lbs
Warhead	56.0		
ATR Solid Fuel	28.3		
ATR Propellant Case	12.0		
Control Module	1.5		
Joint/Inlet Assembly	6.1		
ATR Engine Main Frame Assy	2.4		
ATR Engine Rotor	2.0		
Aft Case, Nozzle, & Fin Assy	17.5		
Obstructor Ring	0.7		
Boost Propellant	24.5		
Launch Weight	163.0		
Boost Propellant	-24.5		
ATR Takeover	138.5		
ATR Solid Fuel	-28.3		
Burnout	110.2		

Muzzle Velocity (Old & New Guns)	1221 fps
Muzzle Momentum	6150 lb-sec
Muzzle Energy	5.09 MJoules
Structure Yield @	> 2000 gs setback in gun
Boost Thrust (Avg)	3000 lbf
Boost Duration	1.80 sec
Assumed Gun Location	Sea Level
Assumed Gun Elevation	45°
Booster Burnout	2316 fps, Mach 2.06, 3200 ft msl
Booster Delivered Isp	220 lbf-sec/lbm
Boost Phase ΔV	1095 fps
Time to Target @ 100 nm, MS @ 50kft (no loiter)	220 sec
Loiter Time over Tgt @ 15nm (M0.7, 5kft)	331 sec

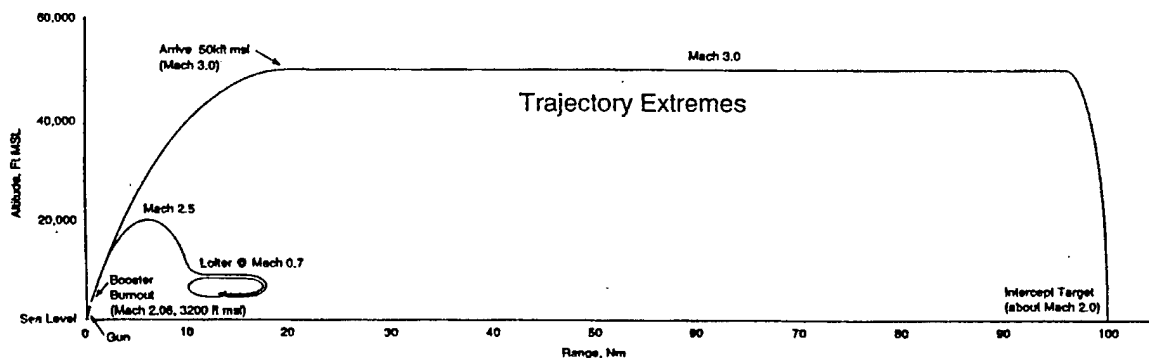


Figure 9. Long Look Conceptual Vehicle

Additional details associated with the assembled round field joints have been considered but are outside the scope of this paper. Payload and avionics weigh 256 and 50 kg (56 and 12 lbs), respectively. Folding fins and canards are used, and the inlet assembly consists of four deployable scoop inlets. The ATR ram burner will be used to house and integral, nozzleless rocket booster to fully utilize the burner volume. The integral booster could provide 333 m/s (1095 fps) of incremental speed, and be ignited by the gun launch environment. (Note that while ramjet vehicle must have such a booster, in the ATR it is merely allowable, no a necessity.) Whereas a comparable ramjet-propelled Long Look would use a staged, separable booster, the ATR is single-staged, and produces no ejects. The maximum range was estimated using a cruise flight condition of Mach 3 at an altitude of 15,000 m (50,000 ft). For closer-in targets, shorter times-to-target are obtainable at lower altitudes. Loiter time is also available for closer-in targets. Minimum loiter speed is about Mach 0.7 at 1500 m (5000 ft), as is set by the aerodynamics of the vehicle, which has a limited lift coefficient and an assumed maximum L/D of about 2.5. Over 5 minutes loiter is feasible for targets 25,000 m (15nm) out.



There is a continuing need for a supersonic sea-skimming target in the Navy<sup>16</sup> that is currently being met with existing hardware including Vandals (modified Talos missiles), AQM-37As, and a Russian variant of the SSN-22. However, the ultimate solution is probably development of a low-cost target vehicle. An ATR or solid boosted liquid fueled ramjet currently offer the potentially optimum compromise among the parameters summarized in Table 1 for this target. In the sea-skimmer target under consideration here, launch weight is to be minimized, and overall length limited to 4.7 m (185 inches) with a nominal diameter of 36.8 cm (14.5 inches). Nominal launch occurs at Mach 0.8, 1500 m (5000 ft) altitude from the center station of an F-4. Higher altitude launches violate the groundrule that the launch should be undetectable to the shooters at sea. Required range is 50 km (30 nm) although 83 km (50 nm) is desired. Minimum cruise speed is Mach 2.0 although Mach 2.5 is desired.

The SPATR-propelled Sea Skimmer concept vehicle considered here is shown in Figure 10. The airframe has a "V" tail for steering and no wings, there being sufficient lift from fuselage and tail to generate lift equal to weight at speeds down to about Mach 0.7 as sea level. The payload is in a nose section weighing 36 kg (80 lbs) (including structure) and occupying 49 liters (3000 cubic inches). This is assumed to be packaged in a nose consisting of a 3:1 fineness ratio Von Karman ogive with a 20% radius ratio blunting to provide a near-optimum tradeoff between low wave drag and high volume. The vehicle base area is nearly filled at all times by the exhaust.

The conceptual ATR presented here consists of a single-stage, axial-flow, transonic, wide-chord French compressor design which offers good characteristics for the ATR. This axisymmetric engine is under the rear of the fuselage with a nose-down incidence. The air inlet is normal-shock smile with a boundary-layer diverter, similar to that in use on the F-16. Normal-shock inlets appear to offer better transonic airflow matching with lower spillage drag than multiple-shock inlets for this application. The propellant is a high-exponent (throttleable) ammonium perchlorate/ hydrocarbon solid that yields a mixture of carbon monoxide, hydrogen, methane, and sub-micron carbon as fuel species, with a net heating value of 27,800 J/gm (12,000 Btu/lbm). It is assumed to have a density of 1.3 kg/liter (0.05 lbm/cu.in.). The end-burning fuel grain burns from the rear end forward, and is throttled by a valve at the outlet of the case. A stress-relieving liner accommodates grain expansion and contraction with temperature, and insulates the case walls from the hot fuel gases to some extent. The aft end of the case has a depression on the underside to accommodate the inlet duct and engine. The reduction of grain burning surface in this area reduces the fuel flow at the beginning of the flight (when less fuel flow is required by the engine), and assists the throttle valve in reducing the effective throttle and chamber pressure range over which it must operate.

Acceleration from launch to Mach 2 on ATR power alone requires over 16 km (10nm) of range. The propulsive impulse required for this acceleration is in effect wasted. This fact, along with the availability of free volume in the ram burner of the ATR, suggests that an integral or separable (slide-in) booster must be considered to shorten the acceleration time. While total range would be shorter, 169 km (105 nm) as opposed to over 193 km (120 nm) if unboosted, the time and range on-station is improved. The weight breakdown shows 45 kg (100 lbs) allotted to an optional booster located in the ATR's could carry about 20 kg (65 lbs) of propellant, and weight approximately 45 kg (100 lbs). The thrust from this motor would be relatively low, under 1360 kg (3000 pounds), because with an in-line exhaust nozzle, the thrust vector will be offset well



below the vehicle center of gravity, producing a large pitch-up moment. Some of this moment is desirable at low speeds to establish the high trim angle-of-attach, but must remain controllable by the aero surfaces. The booster adds about 100 m/s (335 f/s) to the launch velocity, delivering the vehicle to about Mach 1.1 at ATR takeover. At this speed, the ATR will have a large margin of thrust over drag for acceleration, and the inlet can be sized smaller, reducing spillage drag at the cruise condition.

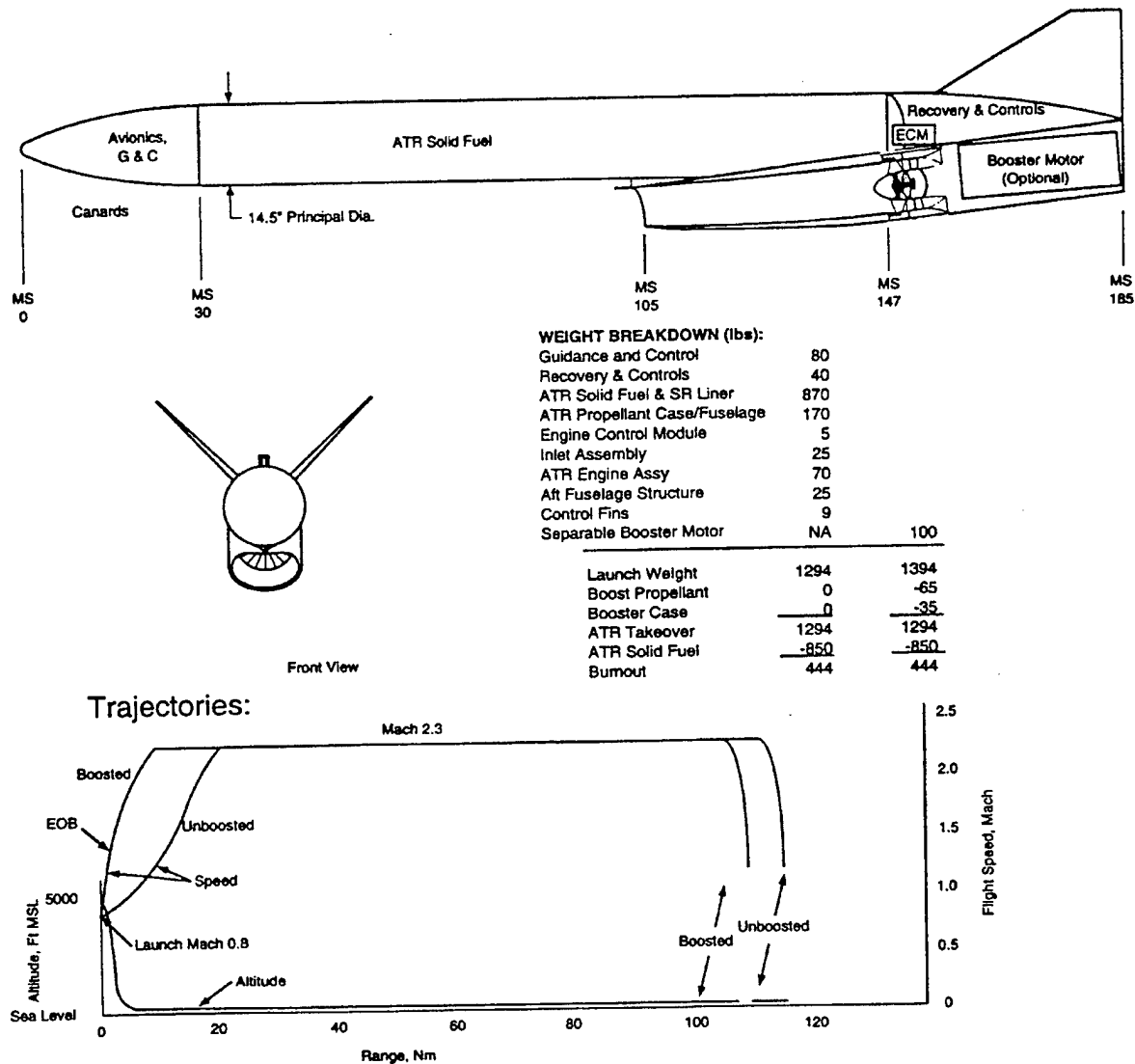


Figure 10. SPATR-Propelled Supersonic Sea-Skimmer

### 2.2.5 Background Summary

In summary, considerable research on the utility of ATR's for a wide variety of DoD missions has been conducted not only in recent years, but over most of the history of airbreathing propulsion. A fundamental question is why the ATR engine has never been developed more fully. The simple answer is that technology for the ATR comes from both the rocket and turbojet worlds, and requires an unusual amount of cooperation and interaction to develop such a cycle. This has been perhaps the biggest single reason as to why ATR development has languished.



Thus, a fundamentally motivating force behind the development work conducted during this SBIR project is to see that the great potential of the ATR is ultimately realized.

### **3.0 PHASE I TECHNICAL OBJECTIVES**

CFDRC's main Phase I objective was to offer DARPA the flexibility to select an advanced ATR system development program that best corresponds to current fiscal funding levels and development priorities. The feasibility of using CFDRC's low cost ATR propulsion concept(s) in affordable DARPA high-speed air vehicle concepts in order to maximize range, minimize time-to-target and cost (procurement and recurring), while increasing available payload, was thus evaluated. Ultimately, ATR low cost and minimal technical risk will be attained through maximum implementation of existing high volume commercial gas turbine and rocket propellant component manufacturing operations. During Phase I, design and specification of the critical propulsion components and subcomponents, with supporting mission analysis and cost was completed. This included ATR performance comparisons to other propulsion plants under consideration for multiple DARPA high-speed air vehicle concepts.

CFDRC has attempted to provide a well-balanced approach to aggressively and innovatively meet the challenges of both high speed vehicle boost operations as well as ultra low cost, flexible tactical missiles through the validation of ATR propulsion system technology readiness. Our approach ensures comprehensive advanced ATR subsystem demonstration because we draw upon CFDRC ATR experience in advanced propulsion design, analysis and testing. In addition, our Propulsion Team expertise in the design and high-volume manufacturing of low-cost, high-reliability turbine and rocket engines has enabled the integration of a sound research and development base in advanced propulsion system disciplines.

### **4.0 MISSION EVALUATION**

As stated in the original proposal, CFDRC began the mission evaluation by considering four vehicle/propulsion/mission studies: 1) ATR-boosted Scramjet, 2) the Advanced Fire Support System (AFSS), 3) Low Cost Cruise Missile Defense (LCCMD), and 4) Micro Air-Launched Decoy (MALD). Evaluation of each of these missions is detailed in the following corresponding sections. During this Phase I effort, vehicle/propulsion- /trajectory analyses associated with MALD, AFSS, and AARMD boost missions were completed using CFDRC's commercial GEMA (Global Engine Mission Analysis)<sup>12</sup> software.

During the mission evaluations, CFDRC initiated interaction between itself and major vehicle primes in an attempt to generate interest and eventual support for the use of the ATR engine in DARPA-sponsored programs that are currently underway.

#### **4.1 Scramjet Boost**

To evaluate the use of the ATR for a scramjet boost application, the basic mission definitions associated with the Advanced Rapid Response Missile Demonstrator (ARRMD) concept were used based on what few assumptions could be obtained in the open literature. The baseline missile concept consists of a set of rocket booster engines which boost the missile to flight



speeds at which a scramjet engine can begin to function. After the scramjet engine is turned on, it accelerates the vehicle to a Mach 6 cruise condition. The Vehicle then flies for 650 miles and delivers a 250 lbm payload to the target.

The analysis began by invoking Breguet's range equation to back out the total mass of the vehicle system at the start of the scramjet boost function based on the previous mission assumptions and the vehicle assumptions given below:

$$\text{Range} = \left( \frac{L}{D} \right) \cdot I_{sp} \cdot u \cdot \ln \left( \frac{m_i}{m_f} \right)$$

Where  $\left( \frac{L}{D} \right)$  is the lift-to-drag ratio of the vehicle at the mean flight velocity,  $I_{sp}$  is the specific impulse of the scramjet engine,  $u$  is the mean flight velocity,  $m_i$  is the vehicle mass at scramjet-start, and  $m_f$  is the vehicle mass at scramjet-burnout. Assuming:

$$\begin{aligned} m_f &= 350 \text{ lbm} \\ u &= 6600 \text{ ft/sec} \\ \text{Range} &= 650 \text{ stat. Miles} \\ \left( \frac{L}{D} \right) &= 0.5 \text{ for the scramjet vehicle at Mach 6} \end{aligned}$$

Solving for  $m_i$  yields a value of:

$$m_i = 550 \text{ lbm}$$

This mass thus represents the final mass for the vehicle system at the end of the ATR-boost phase. Using CFDRC's GEMA (Global Engine Mission Analysis) code, the vehicle/engine/mission definition was input, and the trajectory analysis run. The ATR engine performance was determined using CFDRC's current baseline 6-inch ATR engine configuration. A summary of the design-point definition and operating conditions for this engine is found in Appendix A. The master data file for the ATR engine off-design operating conditions are found in Appendix B. These files form the so-called engine performance maps for the ATR. During vehicle operation, these maps are queried to determine engine thrust and propellant mass flow as a function of flight speed, altitude, and rpm during the trajectory simulation. The trajectory simulation assumed the following launch and mission conditions:

Launch velocity:	Mach 0.8
Launch Altitude:	10,000 ft
Engine operation:	100% speed throughout flight
Cruise altitude:	20,000 ft

The vehicle aerodynamics were assumed to be those of the HARM missile, with a mil standard inlet. Based on these constraints and the engine performance maps, the amount of on-board propellant was iterated so as to allow the vehicle to achieve Mach 4.0 flight speed prior to ATR-



propellant depletion. Using this approach, it was found that an ATR-boosted vehicle carrying a 550 lbm payload would need to weigh about 1150 lbm at its launch condition. This total vehicle weight includes the ATR booster engine, ATR propellant, and 550 lbm payload. When the overall vehicle reached the end of the ATR-boost phase, it was assumed that the ATR booster section was jettisoned, and the scramjet engine was then started, boosting the vehicle to its Mach 6 cruise condition.

Figure 11 shows the altitude and Mach number of the vehicle as a function of time throughout the flight trajectory.

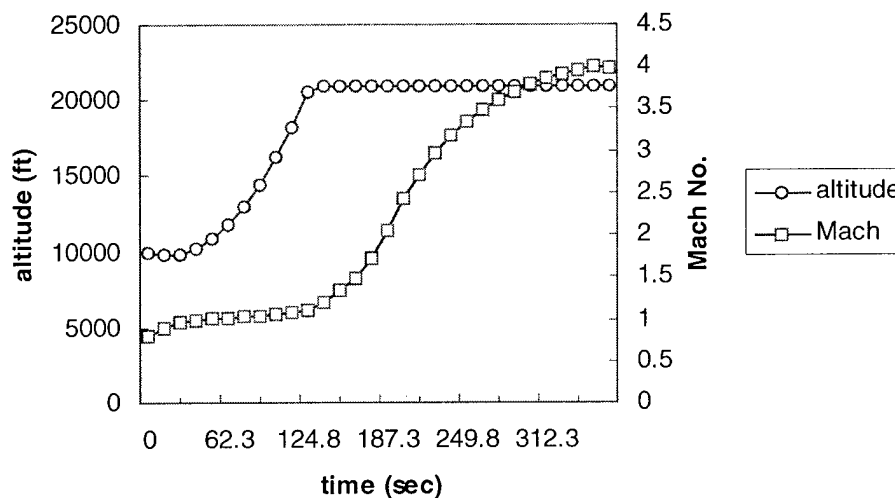


*Figure 11. Altitude and Mach Number for the ATR-boosted ARRMD Vehicle*

As can be seen in this figure, the flight mach number begins to rapidly increase once the vehicle reaches its cruising altitude.

The vehicle masses and weights are summarized as follows:

Initial Launch Mass:	1146 lbm
ATR Burnout Mass:	550 lbm
ATR Propellant Mass:	596 lbm
ATR Engine Mass:	50 lbm
Payload Mass	500 lbm

The mission and vehicle performance assumptions served as a starting point for conducting this calculation, and may not represent the actual ARRMD system. If more accurate or representative assumptions can be provided, this mission can be re-run, but it is unlikely to change the fundamental conclusion that the use of the ATR as an ARRMD boost engine will provide a considerable reduction in initial launch weight.



## 4.2 AFSS

For consideration of the ATR for the AFSS system, CFDRD initiated an interaction between itself and Lockheed Martin Vought (LMV) Systems, located in Dallas, Texas. Currently, LMV is one of two vehicle primes who are developing missile concepts for AFSS. After initiating contact, more detailed interaction resulted in the exchange of information.

LMV provided simplified constraints as to their current vehicle configuration, which included approximate vehicle launch weights, and envelope dimensions. The basic vehicle constraints are shown in Figure 12.

Secondly, they provided flight profiles, or missions, which they had identified as of particular interest to them, and which might showcase the performance benefits provided by the ATR engine. The requested flight profiles were:

1. Vertical Launch, climb to 1000 ft altitude, cruise at Mach 0.2 for 15 km, determine loiter time using remaining fuel;
2. Vertical Launch, climb to 1000 ft altitude, cruise at Mach 0.2 until fuel depletion, determine maximum range; and
3. Vertical Launch, climb to 1000 ft altitude, cruise at Mach 0.7 until fuel depletion, determine maximum range.

Based on these missions and the computed performance of the ATR engine, the performance of an ATR-powered AFSS missile could be determined and compared with alternate propulsion systems.

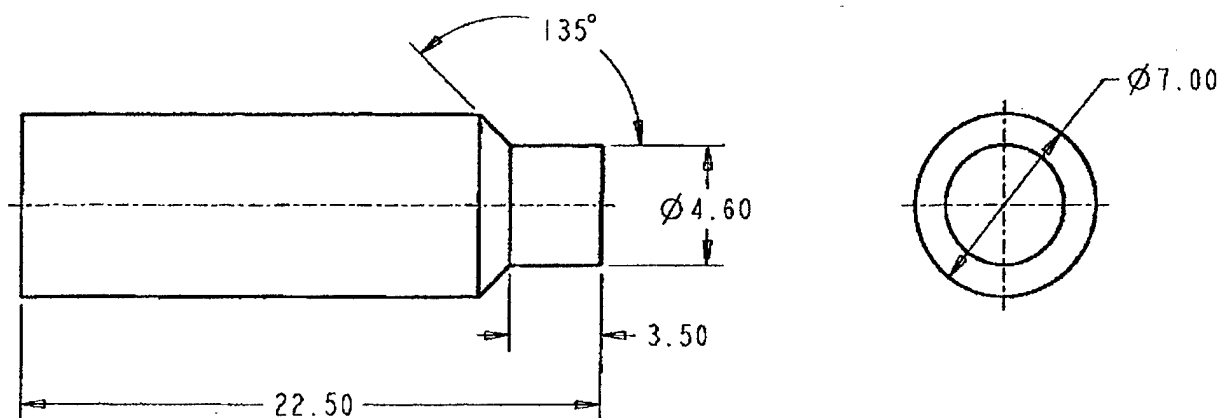


*Figure 12a. LMV AFSS Envelope Constraint*

### Baseline LAM:

Missile Length = 51 in.

Diameter = 7.0 in.



Launch Weight = 85 lb (max)  
 Non Propulsive Weight = 45 lb  
 Cg at missile center (STA = 25.5 in.)  
 (Weight available for SPATR and fuel) = 40 lb  
 Boost Thrust = 360 - 480 lbf

*Figure 12b. LMV Overall Constraints*

Based on the LMV mission profiles, the missile performance of an ATR-powered AFSS was evaluated, and compared against a pintle motor, powering the same missile geometry and mission profile. Two candidate ATR configurations were considered, and are discussed in more detail in section "Task 3 Layout Studies". The two ATR configurations consisted of a volume-constrained and a weight-constrained layout. These two ATR configurations were compared against a pintle motor geometry, details of which are also discussed in section "Task 3 Layout Studies".

A summary of the mission profiles flown is shown in Table 2.

*Table 2. Mission Summary*

- Boost Thrust              200 lbf              Isp = 800 sec  
          Cruise Thrust        60 lbf              Isp = 760 sec
  
- Horizontal Cruise Profile [TOW-2 Aero with 7" Ref. Dia.]  
          Vertical Launch  
          Boost for 7-9 sec  
          Cruise at 1000' until Burn-out  
          Ballistic until Impact
  
- Boost-Glide Profile [AFSS + Wing Aero]  
          Boost until Burn-out  
           $\gamma$  Commanded 60 deg to Burn-out  
           $\gamma$  Commanded -5 deg until Impact

Based on the respective engine performance and mission constraints, both ATR configurations showed superior range performance. In Figure 13 can be seen the respective ranges achieved by the volume-constrained and weight-constrained ATRs and the pintle motor. As can be seen, the ATRs were able to fly nearly twice as far as the pintle motor.



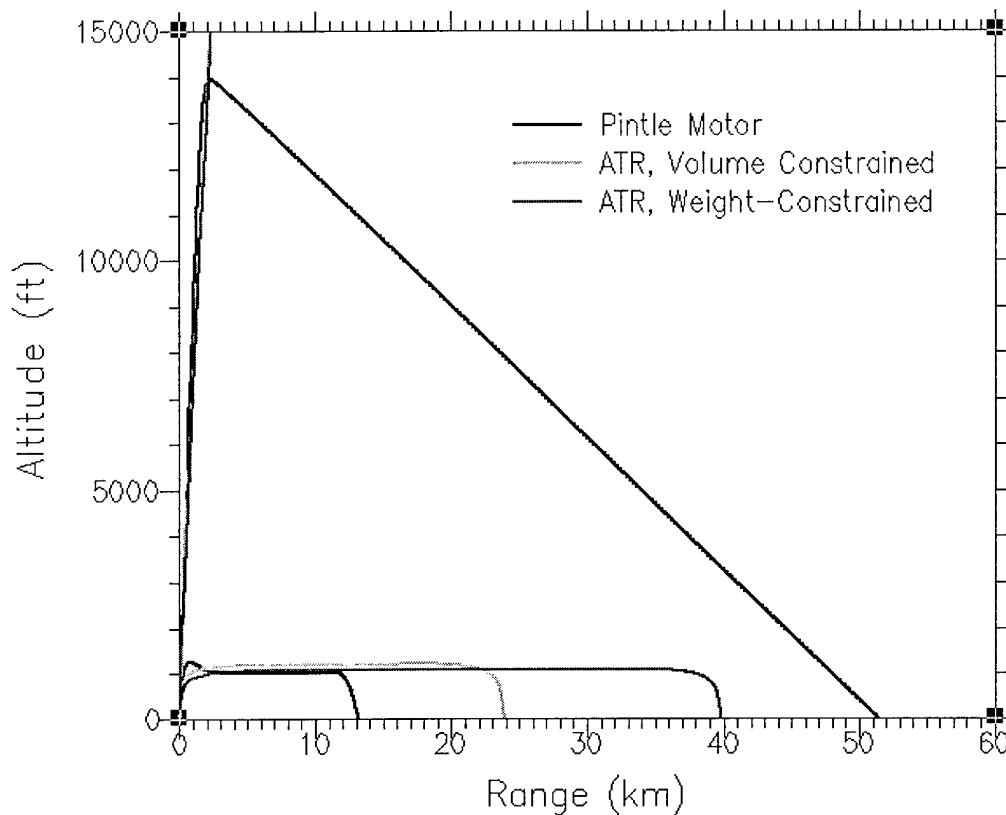


*Figure 13. Comparison of ATR with Nominal Pintle Motor for Cruise Missions*

An additional mission profile was also analyzed using the ATR configurations and the pintle motor. This mission featured a boost-glide flight profile, in which the engine boosts the vehicle up at a 45 degree angle where it continues to climb until fuel depletion. At this point, a glide-type wing on the vehicle is deployed, and the vehicle noses over and maintains a constant alpha, or pitch angle, during a long glide phase. Using this mission, the ATR powered vehicle was able to obtain some extraordinarily long ranges. As shown in Figure 14, using the boost-glide approach, the ATR powered missile was able to achieve nearly 250 km of range for the weight-constrained ATR, and almost 140 km of range with the weight-constrained system. The pintle powered vehicle only achieves around 50 km maximum range. This large increase in range is achieved by the ATRs largely because of the much longer time in which the propulsion system is making thrust relative to the pintle motor. This longer thrust time, in turn, is a result of the fact that the specific impulse of the ATR is much higher than that of the pintle motor, which has, at best, only the specific impulse of a solid propellant rocket. Thus, for a given thrust much less propellant is required to be burned to produce a given amount of thrust. For a specified amount of on-board propellant, this translates into a longer burn time. In Figure 14, fuel-depletion occurs just slightly before the vehicles reach the apogee of their flight trajectory.



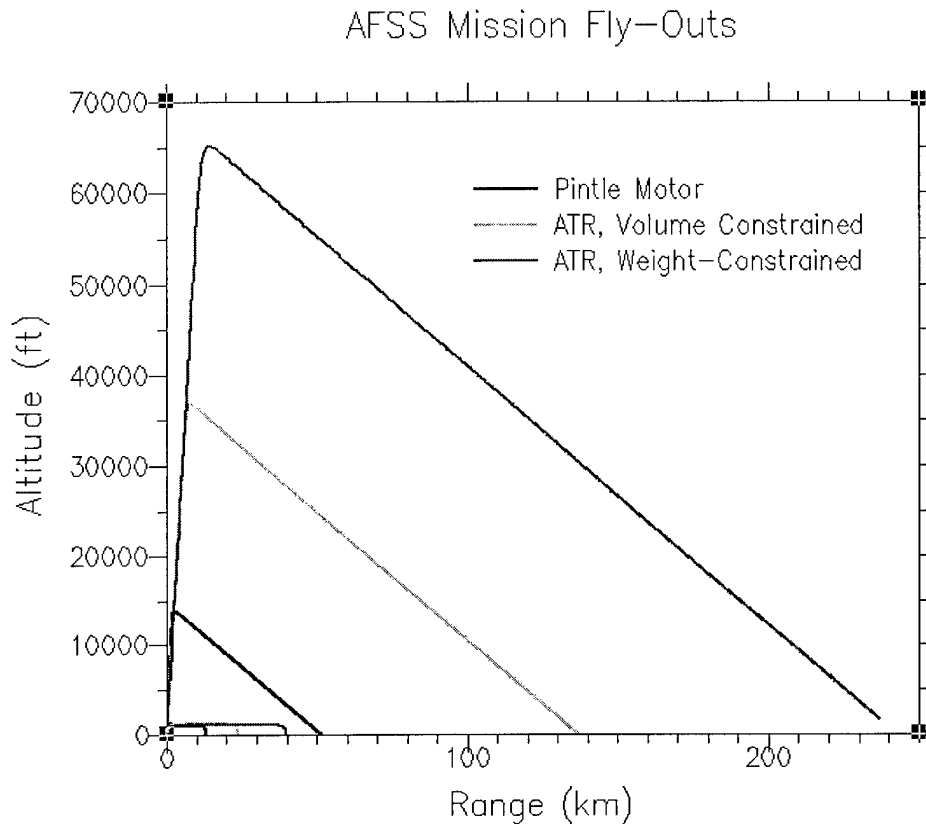


Figure 14. Comparison of ATR with Nominal Pintle Motor for Boost-Glide Mission

A summary of the pintle motor mission profiles is shown in Table 3. A summary of the maximum ranges achieved for all three systems for the cruise and boost-glide missions is shown in Table 4.

Table 3. Assumed Pintle Motor Mission Profiles

- Available Weight of Propellant = 25 lbs  
Two Thrust Levels
 

Boost	600 lbf	Isp = 245
Sustain	60 lbf	Isp = 190
- Horizontal Cruise Profile [TOW-2 Aero with 7" Ref. Dia.]
  - Vertical Launch
  - Boost for 5 sec
  - Cruise at 1000' Altitude until Burn-out
  - Ballistic until Impact
- Boost-Glide Profile [AFSS + Wing Aero]
  - Boost until Burn-out ( $t = 10.25$  sec)
  - $\gamma \sim 67$  deg at Burn-out
  - $\gamma$  Commanded -5 deg until Impact



Table 4. Mission Performance Summary

Mission	ATR Volume- Constrained	ATR Weight- Constrained	Pintle Motor
Horizontal Cruise	24 km	40 km	13.2 km
Boost/Glide	137 km	237 km	50 km

#### 4.3 Low Cost Cruise Missile Defense (LCCMD)

An ATR-powered missile would be an excellent propulsion system for a vehicle tasked with the acquisition and pursuit of a cruise missile from the rear. The rear chase would allow the use of an extremely low-cost infrared seeker. The operational plan would be for the missile to be launched in the general path of an incoming cruise missile and then loiter until the target flies past and the hot engine exhaust becomes visible. In order to overtake from the rear, the propulsion system would need to be able to quickly throttle up and generate enough thrust to overtake the target after a short chase ,and thus, destroy it.

This mission scenario is illustrated in Figure 15. The missile used in this engagement was powered by an ATR with a 3-inch engine diameter. This engine is capable of supplying in excess of 250 lbs. of thrust at flight speeds. The interceptor is assumed to be flying at Mach 0.7 and the target crosses at right angles at a distance of 10 miles and a speed of Mach 0.7. This corresponds to the first point at which a loitering missile, flying in a circular orbit, would be able to see the target. The engine throttles up and the missile accelerates to between Mach 0.9 and Mach 1.1, depending on the vehicle aerodynamics. The engagement was flown using both TOW2 and AMRAAM-type aerodynamic coefficients, and the results differ considerably. The low drag vehicle overtakes and destroys the target after a lateral chase of 10.3 miles and using slightly more than 20 pounds of propellant. The higher drag missile requires 13.6 miles distance to overtake and uses approximately 26 pounds of propellant.



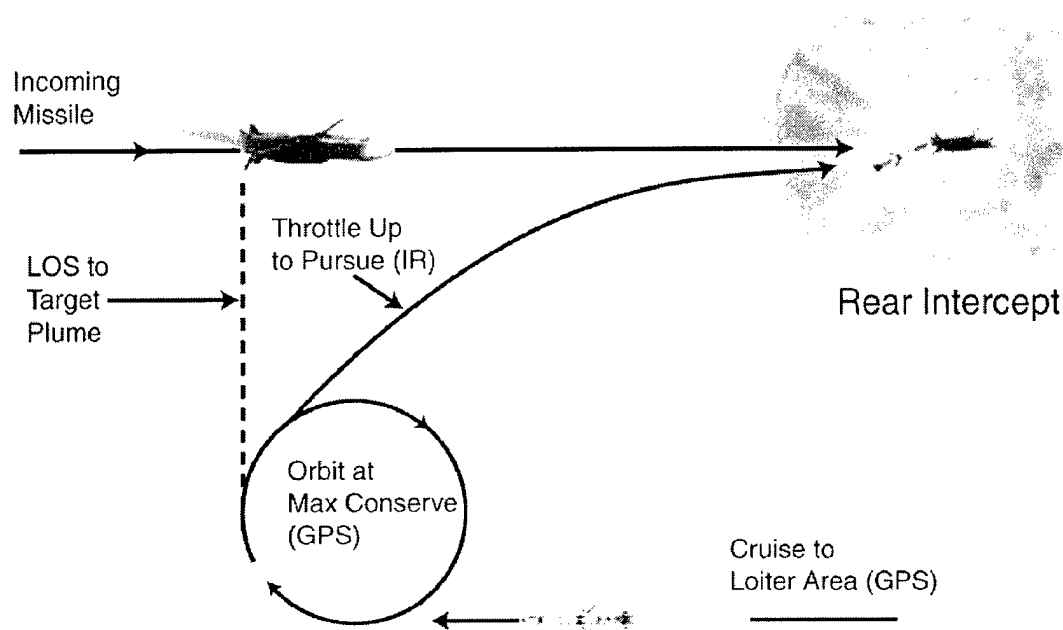


*Figure 15. ATR-Powered Supersonic MALD Offers Enhanced Cruise Missile Intercept Capabilities at Long Stand-Off Ranges*

Under optimal conditions, it may be possible to engage an enemy cruise missile in this manner at ranges exceeding 50 miles. This assessment is based on the previous end game calculations, plus cruise to acquisition point at a specific impulse of 800 seconds and Mach 0.7. Since the ATR engine is smaller and lighter than a comparable turbojet, such as the Sundstrand TJ50 (14 lb. compared to 21 lb.), a greater mass of propellant can be carried in the equivalent fuel tank volume. This is due to the higher density of the ATR propellant versus liquid JP-8 fuel, a factor of 1.8 times denser.

#### 4.4 MALD

This section discusses CFD calculations performed to evaluate the use of an ATR engine in a Micro Air Launched Decoy (MALD) vehicle. The engine size selected for integration was the 3-inch ATR engine, the performance of which given in section 5.1, and tabulated in Appendix A. With the ATR engine length of approximately 20 inches, this means that the fan face and hence the end of the inlet duct is about 65.9 inches aft of the vehicle nose. The inlet thus comes forward from that position.

Several simulations were performed, for different configurations and at two speeds. The higher speed was at Mach 3 and the low speed condition was approximately Mach 0.5. The first model was of a two-dimensional, external compression inlet designed for the high-speed condition. A representation of the flowfield is shown in Figure 16.



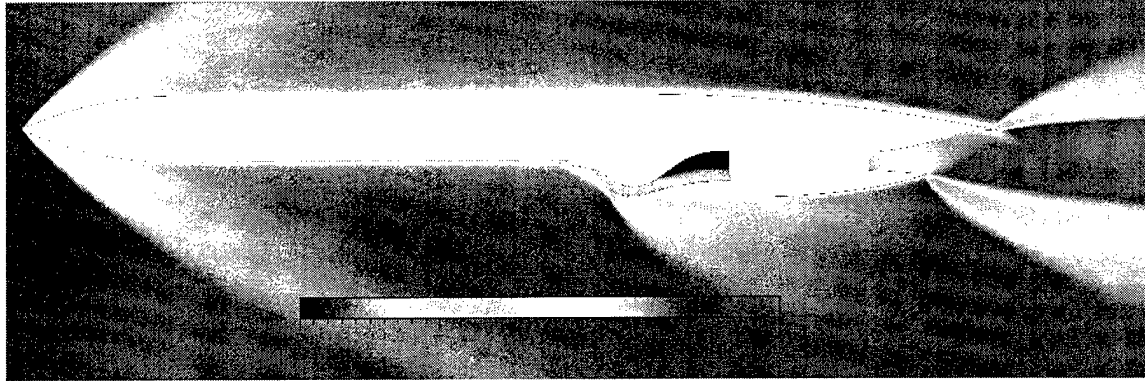


*Figure 16. Mach Number from 2D Simulation of MALD Vehicle*

A detail of this flow field is shown below for the inlet region. It can be seen that the inlet is an external compression type, with two ramps. The fixed-geometry, external compression type was selected for the sake of simplicity. A feature of note on this design is the sharp cowl leading edge.

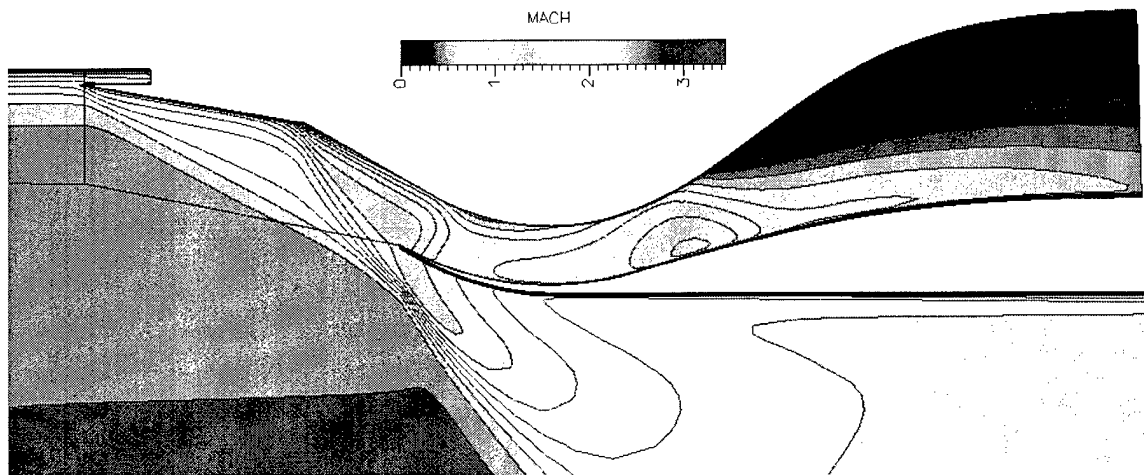


*Figure 17. Detail of Inlet Region from High-Speed Simulation*

This inlet can also be operated at subsonic speeds, as shown in Figure 18. A difference from the first configuration is that the subsonic diffuser was lengthened and the duct area expansion was made more gradual. This reduced the separation in the duct along the top wall to a great extent, although it could still be improved.



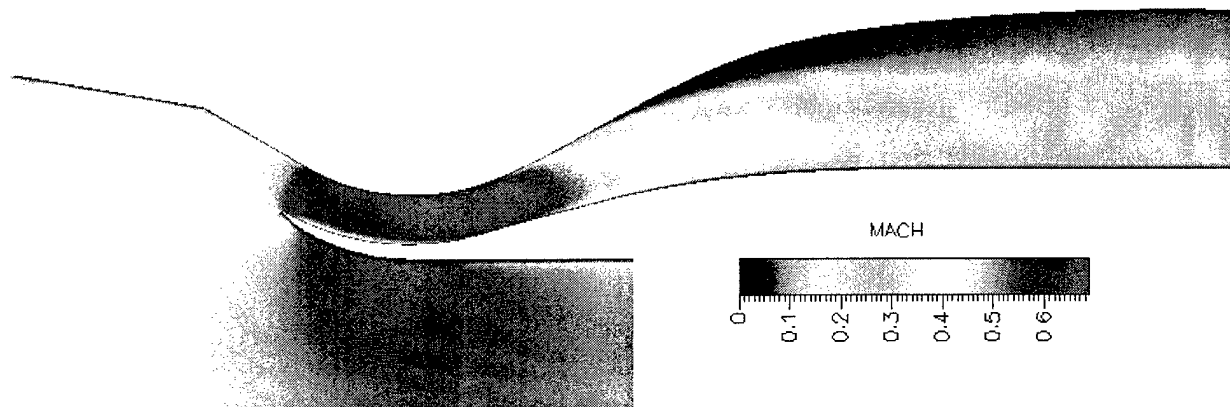


*Figure 18. Operation at Low Speed Flight Condition*

It was found that at some low-speed conditions, separation would occur behind the sharp cowl leading edge. It was thought that an inlet for a maneuvering missile over the speed range of interest might need to be a compromise between high and low-speed designs. Several configurations were examined in which the cowl leading edge was changed in both shape and position. The leading edge was blunted to an elliptical shape and oriented more horizontally. This design is shown in Figure 19.

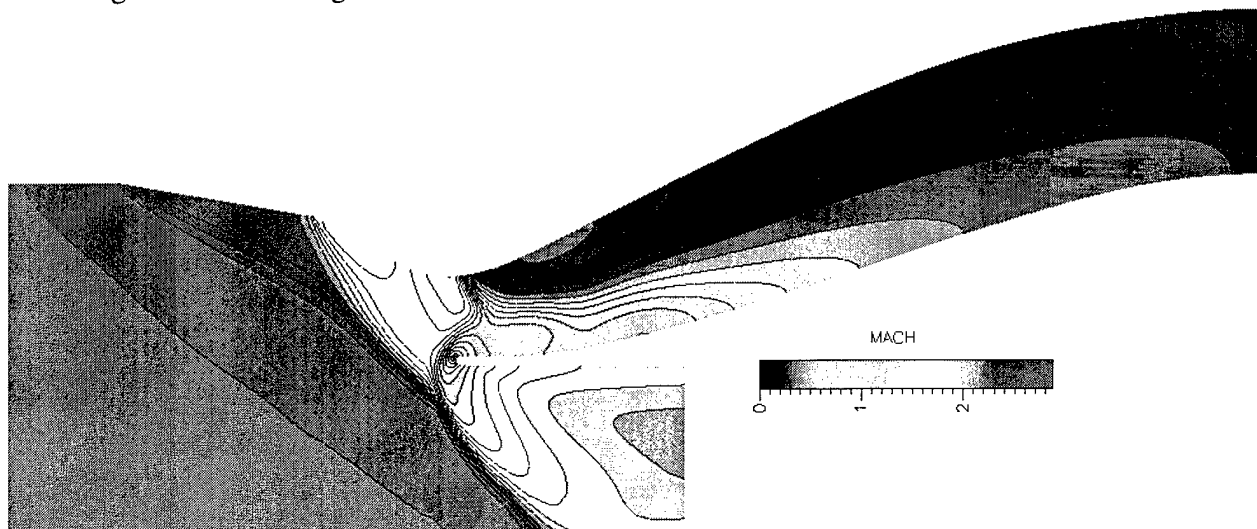


*Figure 19. Inlet Design Incorporating Modified Cowl Leading Edge*

Overall these design concepts represent an initial evaluation of the ATR integrated into a MALD-type vehicle. Based on these preliminary results, the ATR appears to offer superior speed and acceleration performance over that of a turbojet. It is also probable that the ATR will exhibit considerably less sensitivity to inlet distortion and inlet off-design operation, however, this advantage will require further analysis.



## 5.0 ATR PROPULSION ANALYSIS

### 5.1 Three-Inch ATR

Based on our baseline ATR engine, an analysis of an ATR propulsion system which could be scaled to a size appropriate for the AFFS was undertaken. Using our ATR engine models, our baseline 6-inch ATR engine was scaled to approximately a 3-inch ATR size, where the quoted dimension refers to the maximum diameter of the mixed flow compressor. This resulted in a small, compact ATR configuration capable of producing nearly 200 lbf of thrust at static conditions. A summary of the 3-inch ATR design's operating conditions is shown in Table 5.

*Table 5. Three-Inch SFATR Design Point Performance*

Propellant	428
Air flow	1.53 lb/s
Compressor pressure ratio	3.79 t-t
Gas generator flow	.28 lb/s
Turbine inlet pressure	705 psia
Turbine inlet temperature	2340 °F
Turbine pressure ratio	11.0 t-t
Combustor $\Delta P$	10% t-t
Equivalence ratio	1.23
Static thrust	193 lbf
Specific impulse	717 s

Using this set of baseline parameters, engine performance maps could be computed. The performance maps supply the engine's computed thrust and specific impulse as a function of engine rpm, flight mach number, and flight altitude. Within CFDRC's Global Engine Modeling Analysis (GEMA) code, these performance maps are automatically supplied to the trajectory calculation routines.

Figure 20 shows the predicted specific impulse performance of the 3-inch ATR engine at sea level altitude, using the ARC 428 propellant. One of the significant features illustrated is the relatively flat Isp over its throttling range, i.e. the gas mileage stays relatively constant whether at full power or partial power settings. This trend changes moderately at the higher flight speeds. It should be noted that this characteristic is very different for turbojet engines, which show considerable variation on engine specific impulse over their respective throttling range. This flat Isp curve of the ATR is a more subtle, yet still significant, characteristic of the ATR engine.



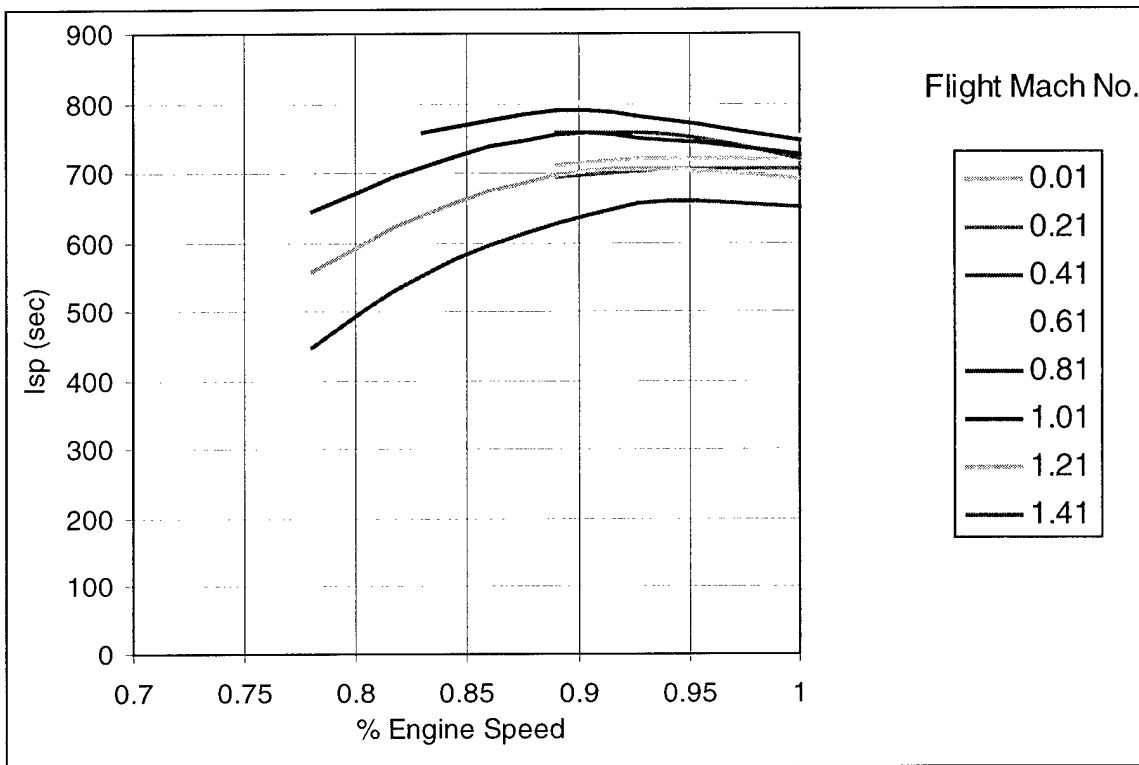


Figure 20. *Engine Specific Impulse as a Function of Engine Speed and Flight Mach Number, at Sea Level Altitude*

In Figure 21, the net thrust of the 3-inch ATR engine is shown at sea level altitude. For a given flight speed, the engine thrust is essentially linear with engine speed. The thrust calculations shown here do not demonstrate the deep throttling, i.e., large turndown ratio, that the ATR engine is actually capable of. Previous engine testing has demonstrated ATR turndown ratios in excess of 20-to-1. For the calculation results shown here, the minimum thrust computed is established by the data available from the turbomachinery performance maps. The performance maps which describe our current compressor do not extend below about 77% engine speed, which results in a computational limit on computed thrust rather than an actual limit. For these lower thrust levels, it is appropriate to merely linearly extrapolate from the existing values to the lower engine speed values.



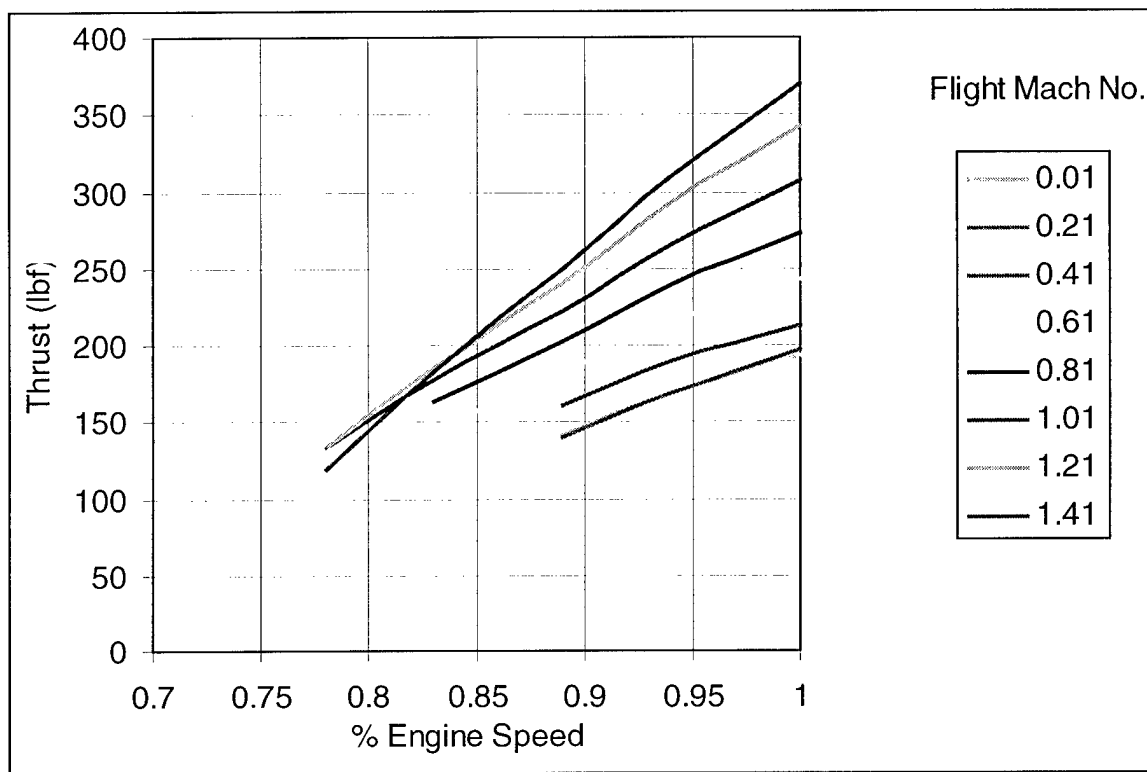


Figure 21. Engine Net Thrust as a Function of Engine Speed and Flight Mach Number, at Sea Level Altitude

An overall performance map of the current engine can be ascertained from Figure 22, which shows net engine thrust as a function of flight Mach number and altitude, all at 100% engine speed. Thus, even at static conditions, the relatively small 3-inch ATR engine should provide nearly 200 lbf of thrust.



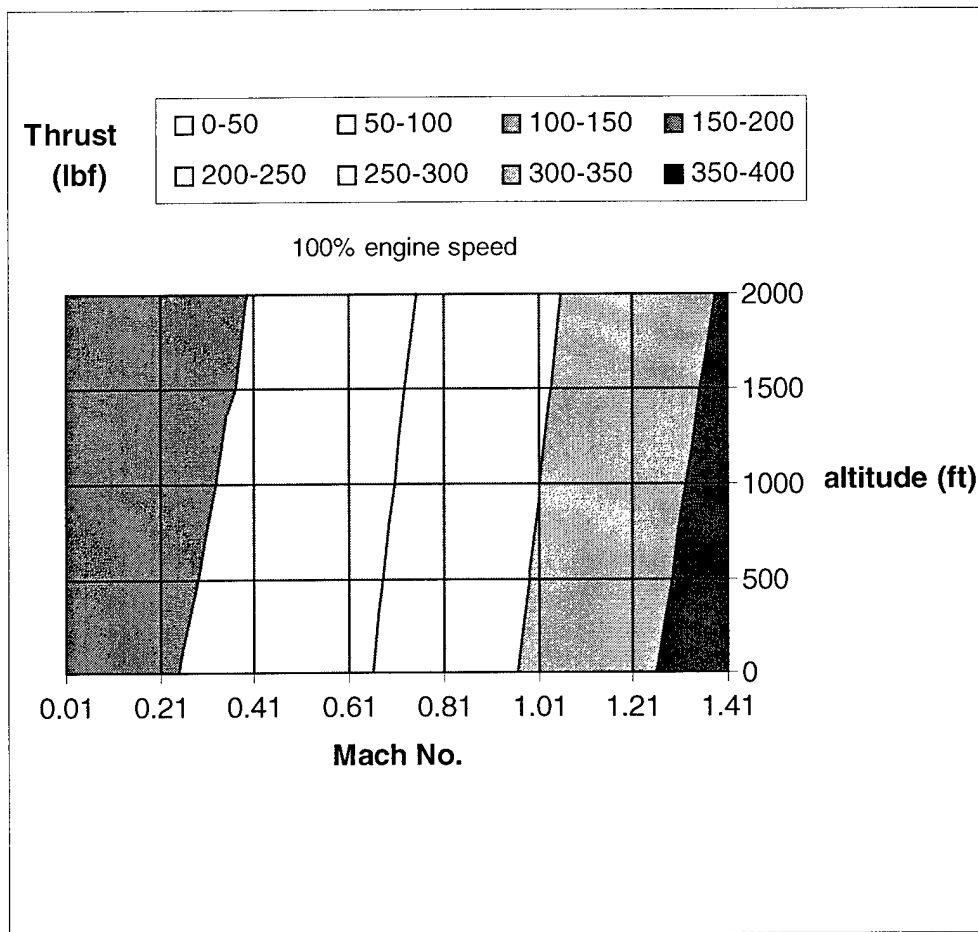


Figure 22. Engine Net Thrust as a Function of Mach Number and Altitude, at 100% Engine Speed

A map of the engine's Isp as a function of flight Mach number and altitude displays a slight reduction, or dip, in their Isp performance at the lower flight speeds, but which subsequently increase to a local extremum before dropping off again. These features result from the competition between ram drag and pressure recovery effects and their relative influence on the resulting Isp.

The ATR engine codes compute numerous other engine parameters, such as gas generator pressure, combustor stoichiometry, etc. A complete summary of the engine parameters is tabulated in Appendix A.

## 5.2 Six-Inch ATR

Additional propulsion analysis was conducted to obtain engine performance maps for the baseline 6-inch ATR when used in the scramjet-boost vehicle. This required the inclusion of an inlet definition to use with the engine performance. For this analysis, the mil-standard inlet was



used. The baseline 6-inch ATR performance at static conditions is summarized in Table 6 for the ARC-428 propellant, which was baselined for the missions analyzed here, and the ARC-246, which is a lower performance, clean-burning solid propellant.

*Table 6. Summary of 6-inch ATR Engine Performance*

<i>Propellant</i>	<b>246</b>	<b>428</b>
Air flow	5.0 lb/s	5.0 lb/s
Compressor pressure ratio	4.0 t-t	4.0 t-t
Gas generator flow	1.34 lb/s	.95 lb/s
Turbine inlet pressure	630 psia	532.6 psia
Turbine inlet temperature	2000° F	2340° F
Turbine pressure ratio	10.0 t-t	8.0 t-t
Combustor $\Delta P$	10% t-t	10% t-t
Equivalence ratio	0.85	1.26
Thrust	794 lbf	746 lbf
Specific impulse	597 s	783 s

Using this set of baseline parameters, engine performance maps could be computed. The performance maps supply the engine's computed thrust and specific impulse as a function of engine rpm, flight mach number, and flight altitude. Within CFDRC's Global Engine Modeling Analysis (GEMA) code, these performance maps are automatically supplied to the trajectory calculation routines. The complete engine performance maps for design and off-design conditions are contained in Appendices B and C.

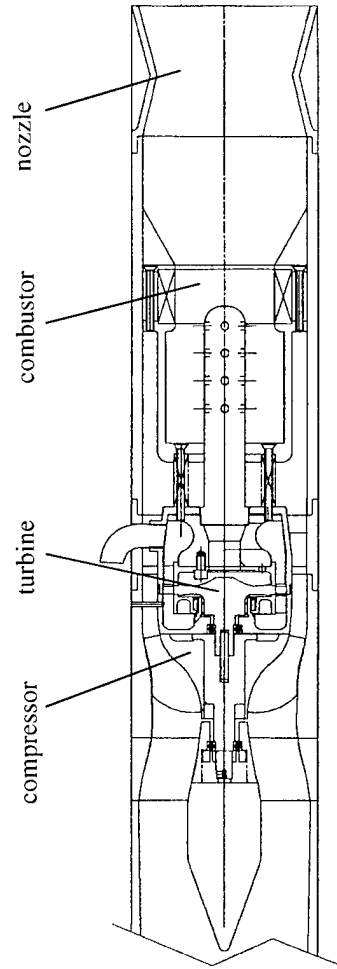
## **6.0 LAYOUT STUDIES**

### **6.1. Scramjet Boost**

Based on the 6-inch ATR engine as its associated gas generator and packaging requirements, a scramjet boost configuration was conceptualized. This configuration uses an in-line ATR engine and gas generator, with the scramjet engine section and payload located just in front of the ATR-booster section. The external vehicle aerodynamics were assumed to be similar to a HARM missile, with the scramjet engine section and payload mounted to the front. The vehicle concept is shown in Figure 23.



# ATR Engine Detail



ATR boost engine

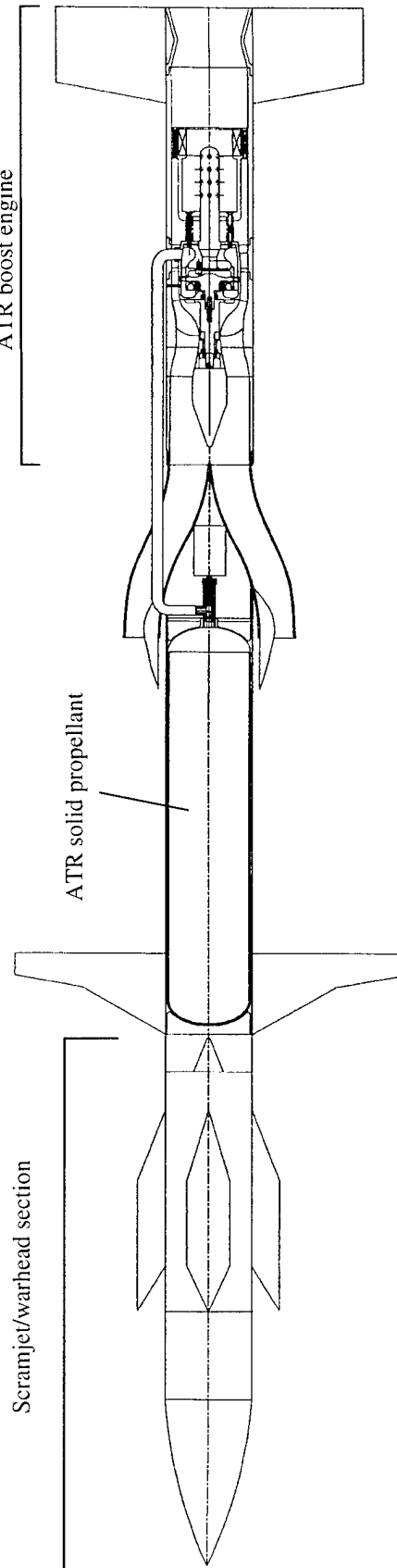


Figure 23. ATR-boosted ARRMD Vehicle



## **6.2 AFSS Layout**

In evaluating the ATR for use in the LMV concept, two general configurations were developed. These configurations evolved from the two different system constraints evaluated for the LMV missions, i.e., the volume constrained, and the weight constrained.

### **6.2.1 Volume Constrained Layout**

To stay within the prescribed LMV envelope, a concentric ATR/Gas generator configuration design was developed. This layout co-located the ATR engine within an annular gas generator configuration. Figure 24 shows a schematic of this layout.

**6.2.2 Weight-Constrained Layout:** For the weight constrained layout, the ATR engine and gas generator can be arranged in an "over-and-under" configuration, allowing more volume for the propellant and bringing the system weight up to the 85 lbm limit imposed by LMV. This configuration, illustrated schematically in Figure 25, represents a more conventional gas generator geometry than does the annular shape.

**6.2.3 Pintle Motor Configuration:** As a point of comparison to the ATR engines, a notional pintle motor concept was also evaluated, based on CFDRC's previous development work associated with this concept. In Figure 26 is shown the baseline pintle motor configuration.



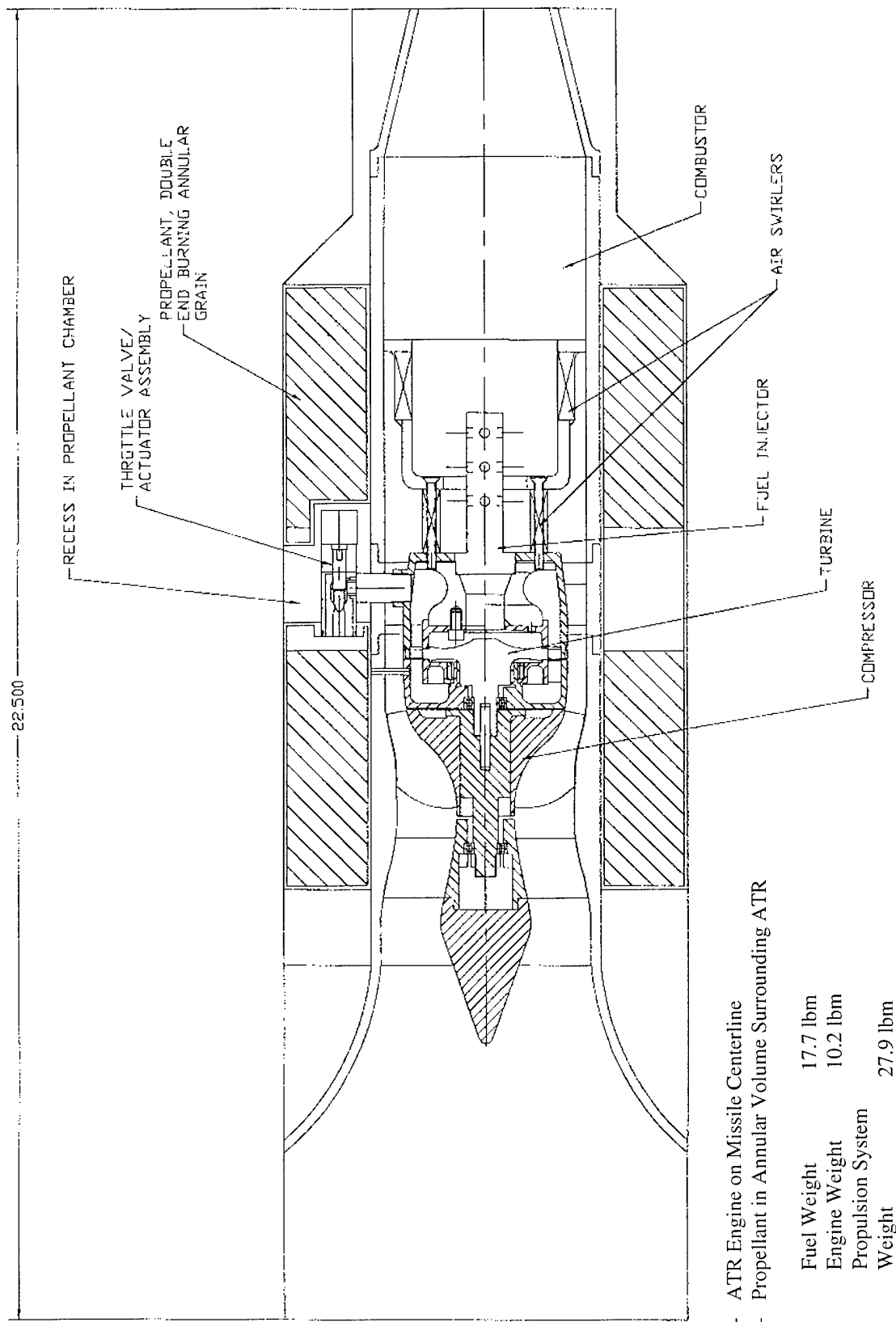
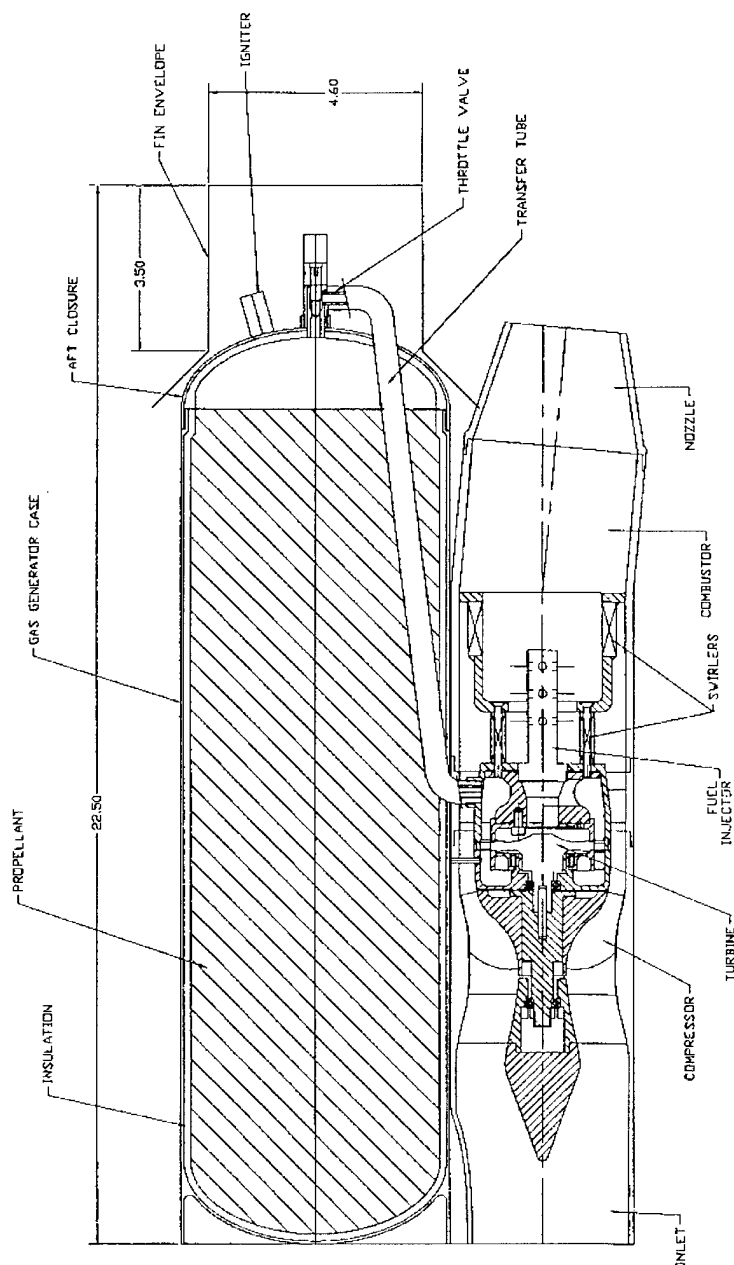


Figure 24. Volume Constrained Configuration



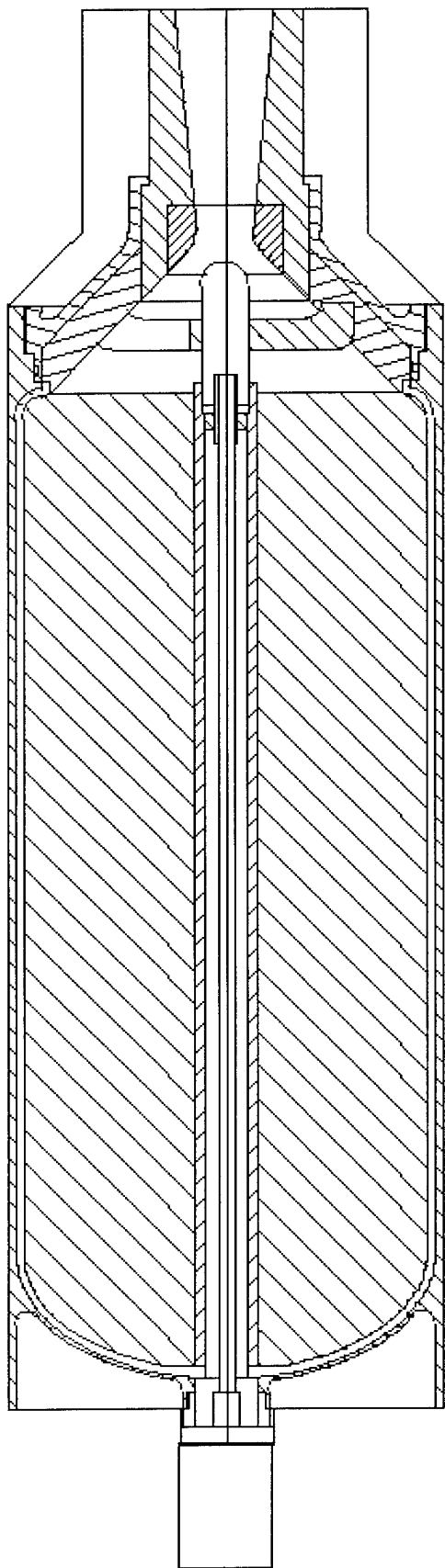


- ATR Engine Off Missile Centerline
- Propellant in the "Over-and-Under" Configuration

Fuel Weight	29.5 lbm
Engine Weight	10.2 lbm
Propulsion System Weight	39.7 lbm

Figure 25. Weight-Constrained Configuration





Propellant Weight	25 lbm
Propulsion System Weight	40 lbm

*Figure 26. Baseline Pintle Motor Configuration*



### 6.3 MALD

Layout evaluations were conducted which considered the packaging of the 3-inch ATR within the MALD vehicle. Since the 3-inch ATR has a much smaller body diameter than the TJ-50 engine (currently used by the MALD vehicle (3.5 inches vs. 4.5 inches), ATR packaging appears quite feasible. Figure 27 shows how the 3-inch ATR might package within the MALD vehicle. Placement of the solid propellant gas generator can be made independently of the ATR engine, and replaces the liquid fuel tanks of the TJ-50 in the proposed layout.

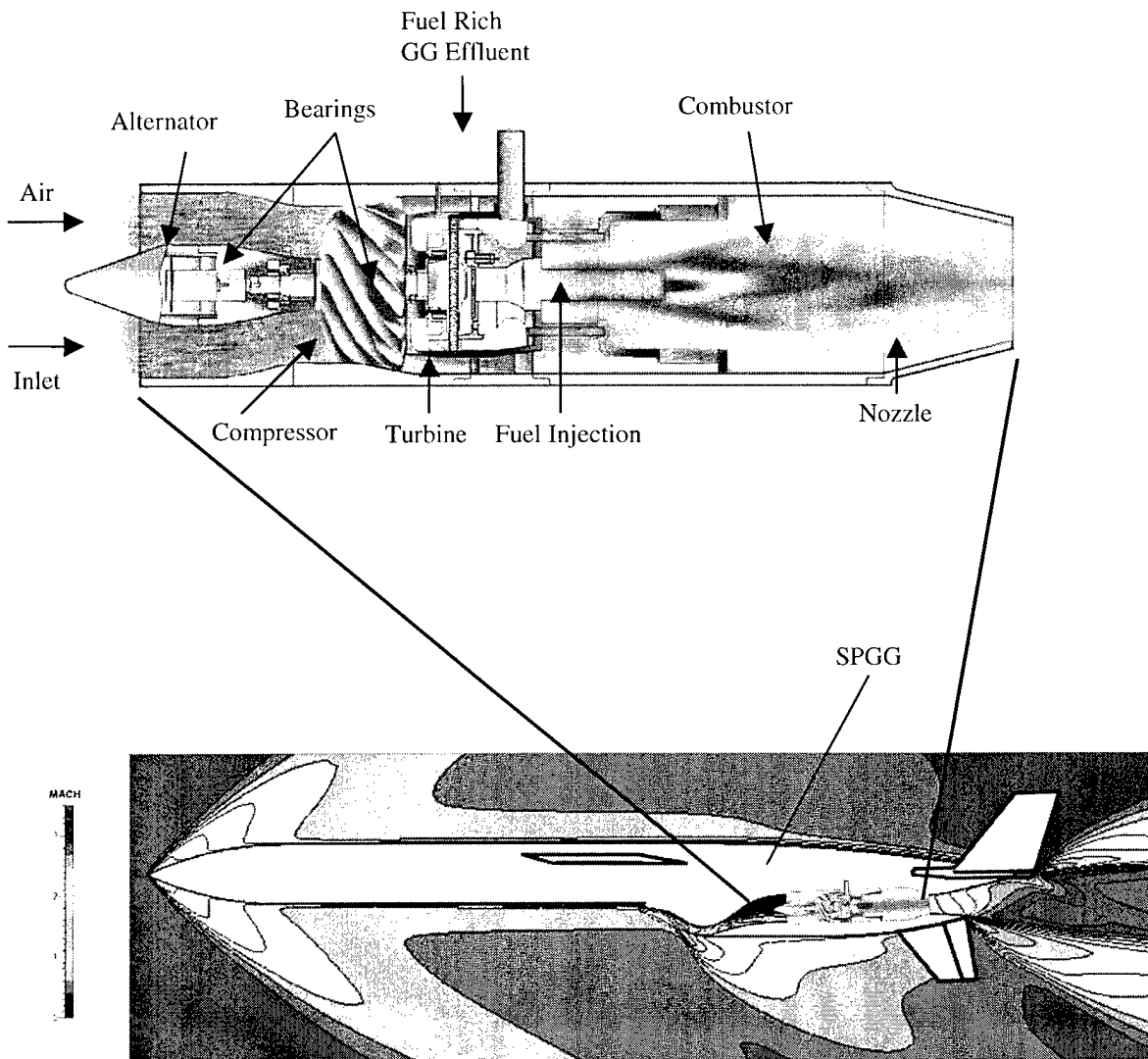


*Figure 27. ATR-Powered Supersonic MALD Layout Configuration*



#### 6.4 Engine Mockup

In addition to producing layout drawings, we have also undertaken to produce an accurate mockup of the actual engine configuration. This effort has consisted of fabricating the designed components out of polycarbonate plastic. These components were then painted and assembled into an accurate, full-size model of the 3-inch ATR engine, as shown in Figure 28. Additionally, some of the more complicated components of the engine model were produced directly from our CAD files using stereolithography. In particular, the compressor rotor, turbine wheel, and compressor diffuser vanes were fabricated using this process. These models are shown in Figure 29.

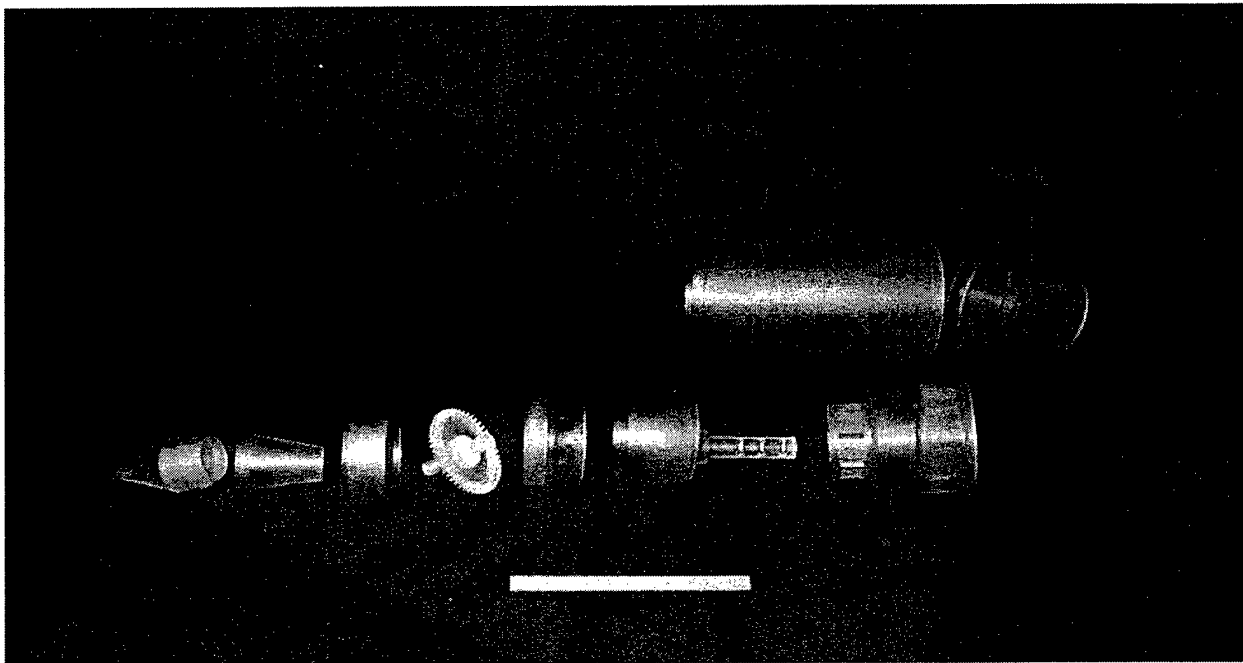
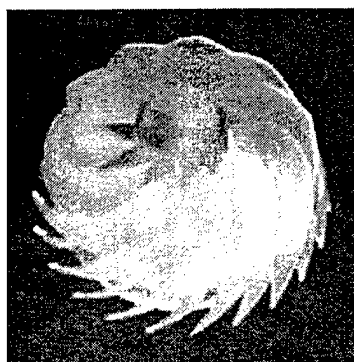
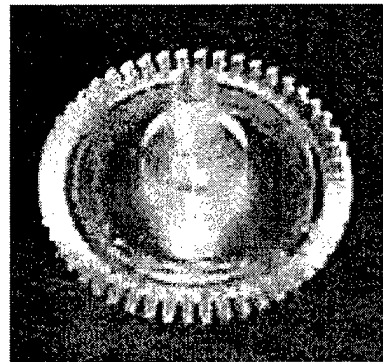


*Figure 28. Polycarbonate Model Fabrication*



3.5 inches



2.5 inches

*Figure 29. Stereolithographic Models of the Compressor Rotor and Turbine Wheel*



These individual components were then assembled into the 3-inch ATR engine. Included in the model is a small electric motor which rotates the compressor rotor and turbine wheel. This feature provides a very clear visualization of the layout and functionality of the ATR engine. A picture of the completed engine mockup is shown in Figure 30, including the speed control box for the electric motor.

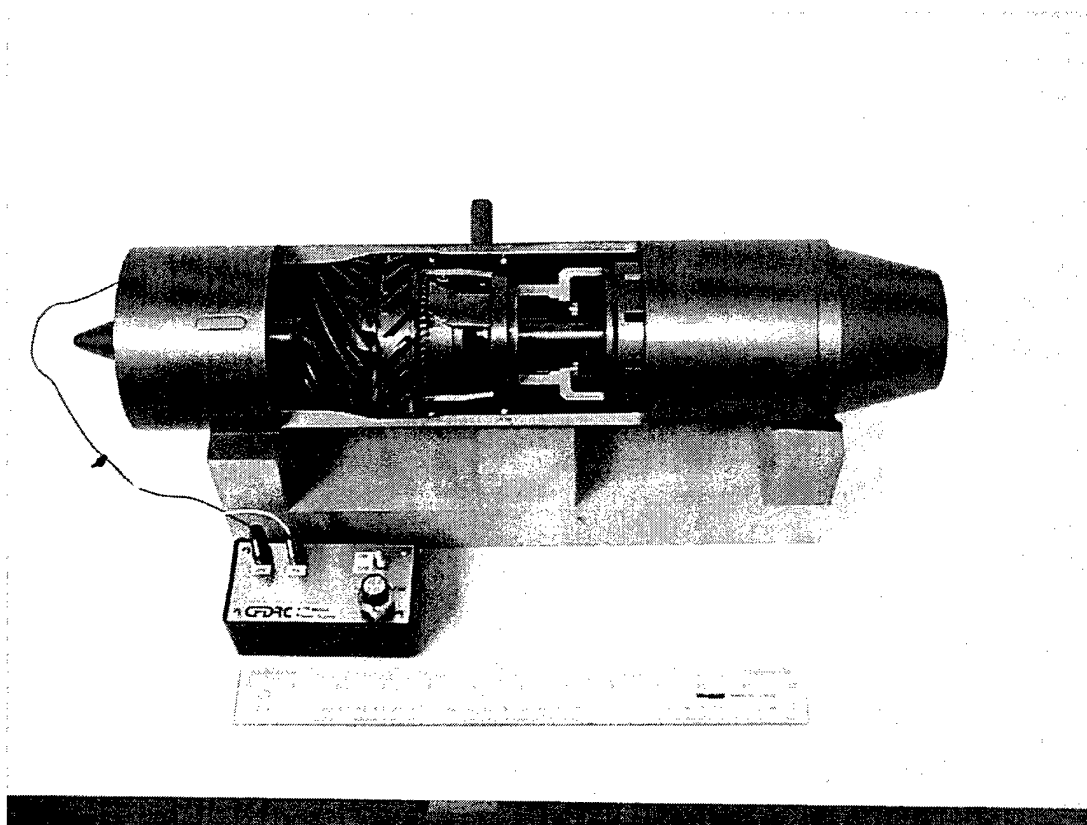


*Figure 30. Completed 3-inch ATR Engine Mockup*

## **7.0 COST/PRODUCIBILITY EVALUATION**

Previous cost studies on the ATR have been conducted by CFDRC for both Air Force and Navy applications. In "Analysis of Air Turbo Rocket Propulsion for Use in USAF Tactical Missiles", WL-TR-94-2088, the costs for ATR engines for use in HARM and Sparrow Missiles, respectively, were estimated using standard USAF costing methods specifically AFAPL-TR-77-50. A summary of the resulting cost estimates from this report is shown in Table 2.

As shown in Table 7, the biggest single cost driver is the solid propellant gas generator assembly, and throttle system. Turbomachinery component costs are significantly less. Results from these studies were then used to evaluate the cost of an ATR engine applicable to the Advanced Fire Support System (AFSS) application. The AFSS ATR engine is significantly smaller than that required for either the HARM or sparrow application and is essentially the 3-inch ATR engine



design. In this evaluation effort, the cost of the ATR engine was compared against that of a solid rocket motor, pintle motor, and expendable turbojet engine, all propulsion systems are of approximately the same thrust level (200-500 lbf). These results are summarized in Figure 31, which breaks out the cost estimates for each of the major components among the four propulsion systems.

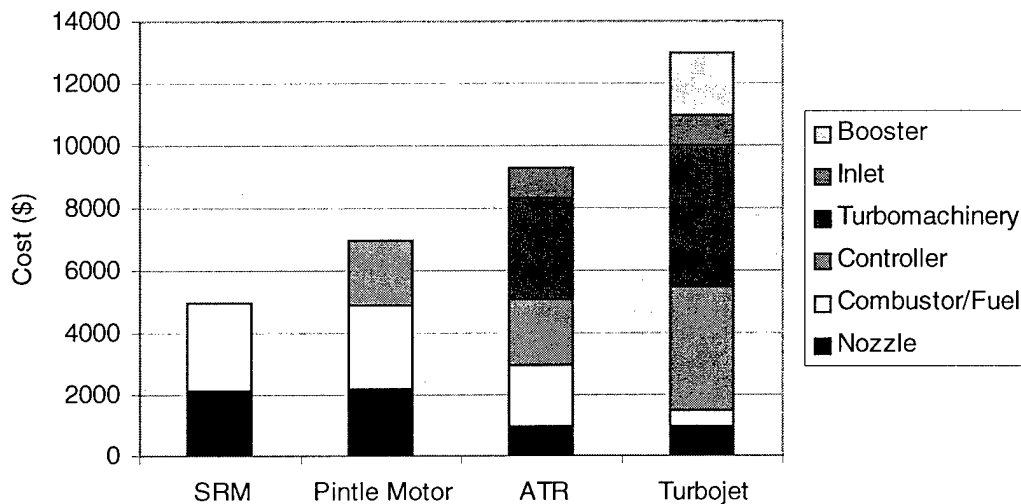


Figure 31. Cost Estimates for AFSS Propulsion Options, in Lots of 500

As might be expected, the unit cost of the ATR lies somewhere between the SRM and the turbojet engine, and is similar in cost to the pintle motor. Further cost analysis will need to be conducted to evaluate a particular ATR engine design which may emerge from this SBIR Phase I effort. After consideration of producibility issues associated with ATR manufacturing, it was concluded that the technological readiness of the ATR is not sufficiently advanced enough to meaningfully assess these issues.



Table 7. ATR Engine Costs for HARM and Sparrow Missile Propulsion, in Lots of 500

Component	Cost
HARM Cost	
Monorotor (Casting & Shaft)	1,982
Bearings	437
Misc Bearing Hardware (Springs, Supports, etc.)	172
Monostator (Casting & Assembly)	1,420
Combustor (Swirler & Chamber)	459
Fixed Inlet (Housing & Casting)	622
Outer Casing	839
Liner	657
Speed Sensor	44
Ignitor (Pyrotechnic)	355
Gas Generator Assembly	
Loaded Casing	25,249
Ignitor	1,097
Throttle Control System	17,923
Booster/Combustor Assembly	
Loaded Casing	1,717
Ignitor	1,097
Nozzle	1,473
TOTAL	\$55,543

Component	Cost
Sparrow Cost	
Monorotor (Casting & Shaft)	1,621
Bearings	358
Misc Bearing Hardware (Springs, Supports, etc.)	172
Monostator (Casting & Assembly)	1,162
Combustor (Swirler & Chamber)	460
Fixed Inlet (Housing & Casting)	600
Outer Casing	686
Liner	537
Speed Sensor	45
Ignitor (Pyrotechnic)	355
Gas Generator Assembly	
Loaded Casing	17,082
Ignitor	1,097
Throttle Control System	17,923
Booster/Combustor Assembly	
Loaded Casing	833
Ignitor	1,097
Nozzle	1,473
TOTAL	\$45,500



## 8.0 CONCLUSIONS

Based on the ATR research performed during Phase I a number of conclusions are briefly stated below. These conclusions have been categorized according to issues associated with potential DARPA vehicles and missions, engine design and systems modeling, and critical component technologies.

### 8.1 DARPA Vehicle/Missions Issues

- a. In order to fully utilize the ATR, mission studies must include a simultaneous characterization of the propulsion system and associated vehicle aerodynamic integration issues. This is particularly the case for an ATR because of its hybrid propulsion system performance nature.
- b. DoD missions, simplicity, reduced cost, and "wooden round" requirements favor the solid fuel gas generator system.
- c. Numerous next generation missile propulsion requirements dictate a compromise between time to target and range. Because of this compromise an ATR may become the preferred configuration due to the performance combination of a solid fuel gas generator combined with airbreathing turbomachinery.
- d. The inherently extensive operating flight regime of the ATR is attained at the cost of lower specific impulse, at low speed flight, compared to the turbojet. However, this particular deficiency is compensated for in many tactical missile applications by the ATR's higher thrust/weight and thrust/inlet area ratios.
- e. There are at least four major missions types for which the ATR propulsion system is optimum. They are:
  - 1) moderate range (5-200 miles) requiring boost, cruise, loiter, endgame operation;
  - 2) missions requiring copious amounts of on-board electric power;
  - 3) applications requiring a diverse array of operating conditions; and
  - 4) a single application which is intended to be used for several different types of missions.
- f. The presence of a compressor enables ATR operation at low flight speed loiter conditions throughout the flight envelope. It is this capability, and the ATR's fairly flat Isp characteristics over a wide Mach range, that makes the ATR viable for numerous missions.
- g. For selected tactical missile envelopes, the resulting boost thrust requirement is too high for initial launch and acceleration by a turbojet without a first stage solid boost. The ATR offers boost capability without the use of solid motor launch/eject capability.



## **8.2 Systems Modeling and Engine Layout**

- h. The lower the ATR combustor mixture ratio (MR), the higher the theoretically possible  $I_{sp}$ , conversely, increasing ATR combustor MR reduces  $I_{sp}$  but significantly increases specific thrust without increasing turbine inlet temperature.
- i. A solid fueled ATR represents a different ATR engine cycle. It cannot be operated as a monopropellant or bipropellant ATR. Innovative throttling and gas generator paradigms were required to compensate for nonlinearities in the gas generator operation.
- j. In a SPGG powered ATR, flow and pressure mismatch between the gas generator burn rate, turbine nozzle, compressor, and combustion chamber require very specialized system modeling techniques.
- k. An inherent advantage of the ATR engine is a cooler missile skin temperature which facilitates reduced flight signature and drag.

## **8.3 Critical Component Technologies**

- l. For U.S. Army missile installations a bifurcated inlet configuration should minimize compressor flow distortion. Mixed flow compressors offer the highest degree of tolerance to these distortions when combined with maximum performance within a given volumetric constraint.
- m. The single stage mixed flow compressor implemented in this engine provides an optimum compromise between turbine horsepower, engine massflow, combustion stoichiometry, and combustion pressure requirements.
- n. Swirl stabilized combustion offers numerous advantages associated with maximizing ATR combustor performance at Length/Diameter ratios approaching 1.0 for carbon soot laden fuels.
- o. The preferred SPGG design is a single grain, constant burn area configuration, with a pintle valve that will enable the required throttling and flowrate turndown ratio.
- p. The gas generator flow rate restrictions and burnrate exponent drive the available turbine nozzle pressure and corresponding engine turndown ratio. Higher burnrate exponent grains benefit the ATR by reducing GG pressure variation and minimizing turbine nozzle design complexity. A reduction in solid particle deposition on turbine blades and nozzles can also be anticipated.
- q. Formulation of an SPGG ATR grain received careful consideration. For maximum ATR operation, the SPGG effluent must have the following characteristics:
  - 1) low molecular weight;
  - 2) high ratio of specific heat;



- 3) high fuel heating value; and
  - 4) minimum solid particles.
- r. ATR combustion chamber design is especially unique due to lower fuel heat content, minimum available combustion chamber volume, potentially fuel rich equivalence ratio, and low combustion pressure. At this point a fundamental tradeoff between combustion efficiency and volume versus increased compressor massflow and pressure ratio is evident. All of these parameters are directly related to the turbine drive gas characteristics exiting the gas generator.

## **9.0 RECOMMENDATIONS**

A number of recommendations pertaining to future ATR technology development are presented. These recommendations are broken down into categories associated with ATR systems analysis code, critical components, and solid propellant/gas generator technologies.

### **9.1 ATR Systems Analysis Code Recommendations**

- a. Improve the trajectory analysis by implementing more advanced codes, such as the U.S. Air Force UTRAJ code or NASA OTIS code.
- b. Implement a Newton-Raphson iteration procedure where possible to reduce ATR systems analysis code run time.
- c. Install and completely debug a cold nitrogen turbine drive gas option to assist in preliminary engine speed testing.
- d. Develop and incorporate ATR system/component weight algorithm(s).
- e. Complete code development associated with SPGG throttling operation at off-design.
- f. Incorporate the NASA ODE code into the ATR code as a new subroutine to calculate gas properties within the engine, particularly the combustor and gas generator. This will eliminate the use of tables limited to single mixture ratios using a specific propellant combination.
- g. Develop an off-design output option that enables the user to generate an ATR flight map which includes engine operation and performance parameters as a function of Mach, altitude and speed.
- h. Research and modify, as required, all compressor maps to include performance data down to a minimum throttle setting.
- i. Upgrade the user interface and code algorithms to insure that both the design and off-design codes are easy to use.



- j. Repeat any ATR vehicle/mission studies using ATR SFGG propellant formulations suitable as a turbine drive gas and containing an acceptable residual heat content.
- k. For an ATR, evaluate how range and time to target are affected by the use or non-use of variable geometry nozzles and inlets.
- l. Install combustor maps similar in format to conventional airbreathing combustion performance maps.
- m. Develop a propellant tool which can perform SPGG formulation trade studies against engine performance.
- o. Develop and incorporate an inlet model that can be utilized to predict required ATR inlet size.

## **9.2 Critical ATR Components**

- a. Complete ATR rotordynamics fixes for proper operation.
- b. Fund further ATR combustor development programs, and anchor combustion performance calculations with experimental data.
- c. Develop and test variable inlet and nozzle designs for use on the SPATR.
- d. Develop a turbo-electric generator which can interface with the ATR.
- e. Evaluate alternate ignitor systems for the ATR combustor.

## **9.3 Solid Propellant/Gas Generator Technologies**

- a. Design and test alternative propellant combinations including hybrid (liquid oxidizer/solid fuel), gel-bipropellant, and liquid bi-propellant gas generators.
- b. Evaluate high burning-rate exponent solid propellant formulations.
- c. Explore "active-controlled" solid propellant gas generator formulations which possess burning rate exponents greater than 1.
- d. Examine turbine by-pass configurations to allow direct-dump fuel-injector into the ATR combustor.
- e. Evaluate alternate gas generator/ATR configurations such as the "over-and-under" arrangement, and embedded engine/gg configurations.



## 10.0 REFERENCES

1. Zarlingo, F., "Airbreathing Propulsion Concepts for High Speed Tactical Missiles," AIAA-88-3070.
2. Andrus, S.R. and Christensen, K.L., "ATR Propulsion System Sizing and Performance for Standoff Missile Applications," 1984 JANNAF Propulsion Conference, 1984 (Limited Distribution).
3. Calvo, W.C., Christensen, K.L., and Fedun, M.H., "Solid Fuel Gas Generator ATR," AIAA-86-1682, AIAA/ASME/SAE/ASEE 22nd Joint Propulsion Conference, June 16-18, 1986.
4. Bossard, J.A., Christensen, K.L., and Fedun, M.H., "Return of the Solid Fuel Gas Generator ATR," AIAA-87-1997, AIAA/SAE/ASME 23rd Joint Propulsion Conference, June 29-July 2, 1987.
5. Bossard, J.A., Christensen, K.L., and Poth, G.E., "ATR Propulsion System Design and Vehicle Integration," AIAA-88-3071.
6. Burgner, G.R. and Thomas, M.E., "Air-Turbo-Ramjet for U.S. Navy Missions," JANNAF Propulsion Meeting, Tampa, FL, December 3-5, 1995.
7. Christensen, K.L., "ATR Preliminary Design," AIAA-90-2515, AIAA/ASME/SAE/ASEE 26th Joint Propulsion Conference in Orlando, FL, July 16-18, 1990.
8. Roble, N.R., Bracey, E.D., and Caron, S.D., "Low Cost ATR-Evolving Propulsion for the AGM-130 Missile," JANNAF Propulsion Meeting, February 27, 1992.
9. Clegern, J.B. and Ostrander, M.J., "Pegasus Upgrades: A Continuing Study into an Airbreathing Alternative," AIAA 95-2806, 1995.
10. Thomas, M.E. and Christensen, K.L., "Air-Turbo-Ramjet Propulsion for Tactical Missiles," AIAA-94-2719, 1994.
11. Christensen, K.L., Pengelly, S.L., and Lilley, J.S., "Design of a 250 Lbf Thrust Hydrazine Fueled Air Turboramjet," 1990 JANNAF Propulsion Conference, 1990.
12. Lilley, J., "Experimental Evaluation of an Air-Turbo-Ramjet," AIAA-94-3395, 1994.
13. Thomas, M.E., and Christensen, K.C., "Analysis of Air-Turbo-Rockets Propulsion for use in USAF Tactical Missiles," Final Report WL-TR-99-2088, Wright Laboratory, Wright Patterson AFB, July 1994.
14. Thomas, M.E., Monorotor Turbomachinery for Air-Turbo-Rocket Engine, AIAA 95-2804, 1995.
15. Missions Office, U.S. Navy NAVSEA, Washington, D.C., August 1995.
16. Targets Office, U.S. Navy NAWCWPNS, China Lake, California, July 1995.
21. Bossard, J.A., Christensen, K.L., Fedun, M.H., "Return of the Solid Fuel Gas Generator ATR," PRA-SA-ASD/WPAFB 22 June 1987, AIAA Paper No. AIAA-87-1997, presented at AIAA/SAE/ASME 23rd Joint Propulsion Conference, June 29-July 2, 1987, San Diego, California.
22. Fedun, M.H., and Christensen, K.L., "Solid Fuel Gas Generator ATR Testing at Aerojet: Latest Results," presented at 24th AIAA/SAE/ASME/ASEE Joint Propulsion Conference held in Boston, Massachusetts, 11-14 July, 1988.
24. Fisco, K.D., Hewitt, P.W., "Program Status Report for the Air-Turbo-Rocket Solid Fuel Gas Generator Demonstration Project," August 1996, ARC Report No. TR-PL-13913-01.



25. Ostrander, M.J., "Air-Turbo-Rocket Solid-Propellant Development and Testing," AIAA 97-3258, July 1997.
26. Thomas, M.E., Ostrander, M.J., Bergmans, J.L., Christensen, K., "Air-Turbo-Rocket Vehicle/Propulsion/Mission Analysis Software and Solid Fuel Gas Generator Development," CFDRC Project 4331 Final Report, April 1997.
27. Burroughs, S.L., Michaels, R.S., Alford, W.L., Spencer, A.B., Peterson, K.L., "Demonstration of a Pintle Controlled Solid Rocket Motor in a Tactical Missile Application," 1996 JANNAF Rocket Nozzle Technology Subcommittee Meeting, Dec. 1996, CPIA Publication 649.
28. Rock, S.G., Habchi, S.D., Marquette, T.J., "Numerical Simulation of Controllable Propulsion for Advanced Escape Systems," AIAA-97-2254, 1997.
29. Thomaier, D., "Speed Control of a Missile with Throttleable Ducted Rocket Propulsion," Advances in Air-Launched Weapon Guidance and Control, AGARD-CP-431.
30. Wei, Z., Zhi-Min, S.B.C., and Zhi-Min, L., "Experimental Study of the Response of Solid Propellant Burning Rate to the Changing of Pressure and the Measurement of Transient Burning Rate," AIAA-87-1726.
31. Bossard, J.A., and Thomas, M.E., "Monorotor For Air-Turbo-Rocket (ATR) Engine," Final Report, CFDRC Project No. 4381, AFRL-PR-WP-TR-1998-2065, March 1998.
32. Lilley, J., "Experimental Evaluation of an Air-Turbo-Ramjet," AIAA-94-3395, 1994.
33. Calvo, W.C., Christensen, K.L., and Fedun, M.J., "Solid Fuel Gas Generator ATR," AIAA-86-1682, AIAA/ASME/SAE/ASEE 22nd Joint Propulsion Conference, June 16-18, 1986.
34. Kee, R.J. and Miller, J.S., "A Structural Approach to the Computational Modeling of Chemical Kinetics and Molecular Transport in Flowing Systems," SAND86-8841, Sandia National Labs, 1988.
35. Hanson, R.K. and Saliman, S., "Survey of Rate Constants in the N/H/O System," in Combustion Chemistry (W.C. Gardiner, Jr., ed.) Springer-Verlag, New York, 1984.
36. Warnatz, J., "Rate Coefficients in the C/H/O System," in Combustion Chemistry (W.C. Gardiner, Jr., ed.) Springer-Verlag, New York, 1984.
37. Drew, D., Chen, L., and Lahey, R.T., Jr., "The Analysis of Virtual Mass Effects in Two-Phase Flow," *Multiphase Flow*, Vol. 5, pp. 233-242, 1974.
38. Crow, C.T., "Two-Fluid vs. Trajectory Models; Range of Applicability," Symposium on Gas-Particle Flows, 1986.
39. Kallio, G.A. and Stock, D.E., "Turbulent Particle Dispersion: A Comparison Between Lagrangian and Eulerian Modeling Approaches," *Journal of Fluids Engineering*, Vol. 97, November 1989.



**APPENDIX A**

**3-INCH ATR ENGINE OFF-DESIGN OPERATION**



```
; ATR MASTER DATA FILE (ATR.MDF)
; Written by ATR Off-Design Code
; ATR Design Summary:
;   Fuel is ARC 428 (5-23-95)
;   Ifuel= 30
;   Design Mach is .20
;   Design Altitude (feet) is .0
;   Design Engine Speed (rpm) is 138461.5
;   Compressor is Sundstrand 4.57" Mono(1-17-96)
;   Icomp= 4
;   Turbine is SUNDSTRAND Reentry Turbine (11
;   Iturb= 7
```

## TABLE ATR THRUST

```
; ICS(1) ICS(2) ICS(3) ICS(4) ICS(5)
; 1 0 0 0 0
```

```
; NIND NMACH NALT NRPM
; 3 8 5 5
```

```
; Mach Number
; .01 .21 .41 .61 .81 1.01 1.21 1.41
```

```
; Altitude (feet)
; .0 500.0 1000.0 1500.0 2000.0
```

```
; Engine RPM
; 70000.0 75000.0 80000.0 85000.0 90000.0
```

```
; ATR Thrust (lbf)
; .00 .00 .00 .00 .00 133.40 133.60
119.30
; .00 .00 .00 .00 .00 131.50 132.60
118.80
; .00 .00 .00 .00 .00 129.20 131.50
119.30
; .00 .00 .00 .00 .00 127.00 130.50
118.80
; .00 .00 .00 .00 .00 124.80 129.90
118.00
; .00 .00 .00 145.60 163.00 177.40 185.90
183.30
; .00 .00 .00 .00 160.10 174.40 184.20
182.00
; .00 .00 .00 .00 158.00 172.70 182.60
180.70
; .00 .00 .00 .00 155.90 171.00 181.00
180.10
; .00 .00 .00 .00 153.10 169.20 179.20
178.60
141.40 140.10 161.00 182.10 202.60 221.80 240.40
249.50
138.90 138.50 158.10 180.00 198.80 219.50 237.90
247.10
137.30 136.00 155.20 177.70 196.50 215.70 233.90
244.80
; .00 134.40 153.00 174.50 194.20 213.30 231.50
242.40
; .00 .00 150.80 172.30 191.90 210.90 229.00
240.00
169.20 168.30 189.10 214.60 238.70 265.30 292.40
309.50
166.10 166.10 185.60 211.90 235.80 262.20 289.10
306.30
163.30 162.90 183.00 209.10 232.80 259.00 285.80
303.00
160.60 159.90 179.60 206.50 230.00 255.90 282.50
```



299.70						
157.60	157.50	176.50	203.80	225.70	252.80	278.40
296.40						
193.90	196.90	213.10	242.90	272.60	307.50	343.10
370.20						
189.40	193.30	210.20	239.70	269.00	303.50	339.00
366.00						
185.00	189.40	207.20	236.40	265.30	299.40	334.90
361.80						
180.70	183.00	204.40	233.30	261.80	295.50	330.90
357.60						
176.50	178.50	201.60	230.10	258.20	291.50	326.80
353.40						

## TABLE ATR ISP

ICS(1)	ICS(2)	ICS(3)	ICS(4)	ICS(5)
1	0	0	0	0

NIND	NMACH	NALT	NRPM
3	8	5	5

Mach Number	.01	.21	.41	.61	.81	1.01	1.21	1.41

Altitude (feet)	.0	500.0	1000.0	1500.0	2000.0

Engine RPM	70000.0	75000.0	80000.0	85000.0	90000.0

; ATR Specific Impulse

.00	.00	.00	.00	.00	645.50	558.50
447.50						
.00	.00	.00	.00	.00	644.40	561.90
451.50						
.00	.00	.00	.00	.00	641.60	565.20
457.00						
.00	.00	.00	.00	.00	637.70	568.50
460.80						
.00	.00	.00	.00	.00	634.90	572.30
464.60						
.00	.00	.00	749.60	757.30	710.40	639.50
553.80						
.00	.00	.00	.00	754.20	711.00	642.40
557.10						
.00	.00	.00	.00	751.50	713.40	645.10
560.40						
.00	.00	.00	.00	749.20	715.70	647.90
564.40						
.00	.00	.00	.00	745.90	718.20	650.60
567.60						
710.90	693.50	757.80	798.60	790.00	753.90	697.00
626.80						
708.30	692.60	754.00	797.00	788.40	755.80	699.30
629.50						
707.20	689.30	750.60	795.10	789.40	755.50	699.90
632.10						
.00	688.00	747.20	791.40	790.90	756.90	702.20
634.70						
.00	.00	744.10	789.30	791.80	758.20	704.40
637.30						
720.30	706.10	755.80	788.00	777.00	745.40	705.20
659.00						
717.10	703.00	751.20	788.60	777.70	746.50	706.70
660.80						
713.70	699.60	748.00	789.20	779.50	748.10	708.10
662.60						
710.40	695.90	743.70	789.80	780.20	749.10	709.50



664.00						
706.90	692.70	739.30	790.30	779.70	750.10	709.70
665.20						
717.70	705.30	721.00	751.10	745.30	726.00	692.50
650.40						
714.70	702.30	721.20	751.60	745.90	726.40	693.70
651.90						
711.20	696.80	721.90	752.00	746.50	727.30	695.30
652.90						
706.50	693.80	722.60	752.40	746.60	728.10	696.40
654.30						
703.50	689.30	722.70	752.70	747.60	728.50	697.40
655.60						

## TABLE ATR PGG

ICS(1)	ICS(2)	ICS(3)	ICS(4)	ICS(5)
1	0	0	0	0

NIND	NMACH	NALT	NRPM
3	8	5	5

Mach Number
.01 .21 .41 .61 .81 1.01 1.21 1.41

Altitude (feet)
.0 500.0 1000.0 1500.0 2000.0

Engine RPM
70000.0 75000.0 80000.0 85000.0 90000.0

ATR GG Pressure (psi)	ICS(1)	ICS(2)	ICS(3)	ICS(4)	ICS(5)
286.08	298.52	329.72	386.96	462.90	594.98
793.55					
962.73					
282.49	291.34	325.08	377.96	456.89	577.41
771.30					
937.33					
272.03	283.99	313.49	369.06	442.19	560.05
749.31					
917.16					
264.87	273.23	309.49	359.61	436.69	544.09
739.23					
905.24					
258.08	269.53	298.31	347.32	426.17	536.98
720.06					
880.02					
412.17	418.87	457.07	521.24	650.96	852.74
1134.35					
1485.33					
398.97	414.47	443.12	506.13	631.78	825.90
1119.15					
1434.40					
394.50	400.79	437.48	494.92	615.54	803.11
1077.11					
1415.50					
381.46	396.53	427.62	484.04	609.33	792.66
1035.48					
1369.40					
376.41	387.44	418.58	478.05	580.93	770.01
1021.36					
1350.81					
543.33	571.81	632.34	723.12	900.79	1177.00
1581.13					
2058.12					
535.87	556.11	613.84	705.17	873.44	1133.47
1559.65					
1991.37					
520.96	539.14	595.09	698.00	849.92	1100.44
1499.75					
1964.78					
504.53	524.25	579.51	677.97	826.45	1072.47
1479.45					
1900.26					
489.92	507.58	573.51	660.47	803.86	1031.20
1427.33					
1873.47					
767.64	790.74	854.59	996.44	1288.72	1701.31
2224.64					
2839.87					
745.64	772.25	843.81	969.97	1242.30	1644.54
2155.10					
2757.59					
725.72	749.90	823.82	943.73	1209.40	1604.34
2125.91					
2675.65					
706.09	739.96	801.08	918.28	1179.23	1566.45
2058.75					



2641.99						
696.07	721.24	791.82	905.74	1129.80	1528.87	1989.98
2564.42						
975.44	1034.78	1182.05	1419.58	1783.84	2313.56	3479.00
7992.07						
943.96	1020.71	1137.43	1368.79	1723.65	2282.01	3050.92
7665.52						
913.75	981.22	1120.02	1349.44	1681.59	2208.80	2959.87
7348.51						
898.15	939.26	1076.40	1300.52	1641.96	2137.84	2873.48
6823.11						
856.51	909.66	1034.23	1267.31	1600.59	2069.12	2833.96
6308.73						

## TABLE ATR WAIR

ICS(1)	ICS(2)	ICS(3)	ICS(4)	ICS(5)
1	0	0	0	0

NIND	NMACH	NALT	NRPM
3	8	5	5

Mach Number
.01 .21 .41 .61 .81 1.01 1.21 1.41

Altitude (feet)
.0 500.0 1000.0 1500.0 2000.0

Engine RPM
70000.0 75000.0 80000.0 85000.0 90000.0

ATR Air Flow Rate (lbm/sec)	1.16	1.18	1.24	1.35	1.49	1.68	1.98
2.30							
1.15	1.17	1.23	1.33	1.47	1.65	1.95	
2.27							
1.13	1.15	1.21	1.31	1.45	1.63	1.92	
2.23							
1.12	1.14	1.20	1.30	1.44	1.62	1.90	
2.20							
1.10	1.12	1.18	1.28	1.42	1.60	1.86	
2.17							
1.25	1.27	1.33	1.44	1.57	1.84	2.17	
2.53							
1.23	1.26	1.32	1.43	1.55	1.80	2.14	
2.50							
1.23	1.24	1.31	1.41	1.54	1.78	2.11	
2.46							
1.21	1.23	1.29	1.39	1.53	1.75	2.08	
2.42							
1.19	1.22	1.28	1.38	1.51	1.73	2.05	
2.39							
1.33	1.34	1.41	1.50	1.71	2.00	2.37	
2.76							
1.31	1.33	1.39	1.49	1.68	1.97	2.34	
2.72							
1.30	1.31	1.37	1.48	1.65	1.93	2.29	
2.69							
1.28	1.30	1.36	1.46	1.63	1.90	2.26	
2.65							
1.27	1.29	1.35	1.45	1.61	1.88	2.23	
2.61							
1.42	1.44	1.51	1.66	1.89	2.21	2.62	
3.04							
1.40	1.43	1.49	1.63	1.87	2.18	2.58	
3.00							
1.38	1.41	1.48	1.61	1.84	2.15	2.54	
2.95							
1.37	1.39	1.46	1.59	1.81	2.12	2.51	



2.91						
1.35	1.38	1.45	1.56	1.78	2.09	2.46
2.87						
1.50	1.54	1.63	1.80	2.06	2.42	2.87
3.34						
1.48	1.51	1.61	1.78	2.03	2.39	2.83
3.30						
1.45	1.50	1.58	1.75	2.00	2.35	2.79
3.25						
1.44	1.47	1.56	1.72	1.97	2.32	2.75
3.20						
1.41	1.45	1.54	1.70	1.94	2.28	2.71
3.16						

## TABLE ATR PRC

```
; ICS(1) ICS(2) ICS(3) ICS(4) ICS(5)
      1      0      0      0      0
```

```
; NIND NMACH NALT NRPM
      3      8      5      5
```

```
; Mach Number
      .01      .21      .41      .61      .81      1.01      1.21      1.41
```

```
; Altitude (feet)
      .0      500.0      1000.0      1500.0      2000.0
```

```
; Engine RPM
      70000.0      75000.0      80000.0      85000.0      90000.0
```

```
; ATR PRC
      2.32      2.30      2.27      2.22      2.15      2.06      1.91
      1.74
      2.32      2.31      2.26      2.22      2.15      2.07      1.92
      1.74
      2.33      2.31      2.27      2.23      2.16      2.07      1.92
      1.76
      2.32      2.30      2.27      2.22      2.16      2.07      1.93
      1.76
      2.33      2.31      2.28      2.23      2.15      2.07      1.95
      1.76
      2.73      2.72      2.67      2.59      2.49      2.35      2.19
      2.00
      2.74      2.72      2.66      2.59      2.50      2.36      2.19
      2.01
      2.73      2.73      2.67      2.60      2.50      2.37      2.20
      2.01
      2.74      2.72      2.68      2.61      2.51      2.38      2.21
      2.03
      2.75      2.73      2.68      2.60      2.51      2.38      2.21
      2.04
      3.13      3.11      3.04      2.95      2.81      2.64      2.47
      2.28
      3.14      3.11      3.05      2.95      2.82      2.65      2.48
      2.29
      3.14      3.12      3.06      2.96      2.83      2.66      2.49
      2.30
      3.15      3.13      3.07      2.97      2.84      2.67      2.50
      2.30
      3.15      3.14      3.07      2.98      2.85      2.68      2.50
      2.31
      3.46      3.45      3.39      3.28      3.13      2.95      2.75
      2.54
      3.47      3.45      3.40      3.29      3.14      2.96      2.76
      2.54
      3.48      3.46      3.40      3.30      3.15      2.97      2.77
      2.55
      3.48      3.47      3.41      3.31      3.16      2.98      2.78
```



2.56						
3.49	3.46	3.42	3.32	3.17	2.99	2.79
2.57						
3.76	3.79	3.71	3.59	3.42	3.25	3.04
2.81						
3.76	3.81	3.72	3.60	3.43	3.26	3.05
2.82						
3.76	3.79	3.74	3.61	3.44	3.27	3.06
2.82						
3.74	3.76	3.75	3.62	3.45	3.28	3.07
2.83						
3.74	3.74	3.76	3.63	3.46	3.28	3.08
2.84						

## TABLE ATR WF

ICS(1)	ICS(2)	ICS(3)	ICS(4)	ICS(5)
1	0	0	0	0

NIND	NMACH	NALT	NRPM
3	8	5	5

; Mach Number

.01 .21 .41 .61 .81 1.01 1.21 1.41

; Altitude (feet)

.0 500.0 1000.0 1500.0 2000.0

; Engine RPM

70000.0 75000.0 80000.0 85000.0 90000.0

; ATR WF (lbm/sec)

.14	.14	.15	.16	.18	.21	.24
.27						
.14	.14	.15	.16	.18	.20	.24
.26						
.14	.14	.15	.16	.18	.20	.23
.26						
.13	.14	.14	.16	.18	.20	.23
.26						
.13	.13	.14	.15	.17	.20	.23
.25						
.17	.17	.18	.19	.22	.25	.29
.33						
.17	.17	.18	.19	.21	.25	.29
.33						
.16	.17	.18	.19	.21	.24	.28
.32						
.16	.17	.17	.19	.21	.24	.28
.32						
.16	.16	.17	.18	.21	.24	.28
.31						
.20	.20	.21	.23	.26	.29	.34
.40						
.20	.20	.21	.23	.25	.29	.34
.39						
.19	.20	.21	.22	.25	.29	.33
.39						
.19	.20	.20	.22	.25	.28	.33
.38						
.19	.19	.20	.22	.24	.28	.33
.38						
.23	.24	.25	.27	.31	.36	.41
.47						
.23	.24	.25	.27	.30	.35	.41
.46						
.23	.23	.24	.27	.30	.35	.40
.46						
.23	.23	.24	.26	.29	.34	.40



.45						
.22	.23	.24	.26	.29	.34	.39
.45						
.27	.28	.30	.32	.37	.42	.50
.57						
.27	.28	.29	.32	.36	.42	.49
.56						
.26	.27	.29	.31	.36	.41	.48
.55						
.26	.26	.28	.31	.35	.41	.48
.55						
.25	.26	.28	.31	.35	.40	.47
.54						

## TABLE ATR PRT

```
; ICS(1) ICS(2) ICS(3) ICS(4) ICS(5)
1      0      0      0      0
```

```
; NIND NMACH NALT NRPM
3      8      5      5
```

```
; Mach Number
.01 .21 .41 .61 .81 1.01 1.21 1.41
```

```
; Altitude (feet)
.0 500.0 1000.0 1500.0 2000.0
```

```
; Engine RPM
70000.0 75000.0 80000.0 85000.0 90000.0
```

```
; ATR Turb Pressure Ratio
```

8.90	8.90	8.90	8.90	8.70	8.50	8.60
8.50						
8.90	8.90	8.90	8.80	8.70	8.50	8.60
8.50						
8.90	8.90	8.90	8.80	8.70	8.50	8.60
8.50						
8.90	8.90	8.90	8.90	8.80	8.60	8.60
8.50						
8.90	8.90	8.90	8.90	8.80	8.60	8.50
8.50						
9.40	9.40	9.30	9.20	9.00	9.20	9.20
9.30						
9.40	9.40	9.40	9.30	9.00	9.10	9.20
9.30						
9.50	9.40	9.40	9.20	9.10	9.10	9.20
9.30						
9.50	9.50	9.30	9.20	9.10	9.10	9.20
9.20						
9.50	9.50	9.40	9.30	9.10	9.10	9.20
9.20						
9.90	9.90	9.80	9.70	9.70	9.70	9.80
9.90						
9.90	9.90	9.80	9.70	9.70	9.70	9.80
9.90						
9.90	9.90	9.80	9.70	9.70	9.70	9.80
9.90						
9.90	9.90	9.90	9.70	9.70	9.70	9.80
9.90						
10.00	9.90	9.90	9.80	9.70	9.70	9.80
9.90						
10.70	10.60	10.60	10.60	10.60	10.70	10.70
10.60						
10.70	10.70	10.60	10.50	10.60	10.70	10.70
10.60						
10.80	10.70	10.60	10.50	10.60	10.70	10.70
10.60						
10.80	10.70	10.60	10.50	10.60	10.70	10.70



10.60							
10.80	10.80	10.70	10.50	10.50	10.70	10.70	
10.60							
11.50	11.50	11.60	11.60	11.70	11.70	11.70	
11.70							
11.50	11.50	11.60	11.60	11.70	11.70	11.70	
11.70							
11.40	11.60	11.50	11.60	11.70	11.70	11.70	
11.70							
11.50	11.50	11.50	11.60	11.70	11.70	11.70	
11.70							
11.50	11.50	11.50	11.60	11.70	11.70	11.70	
11.70							
TABLE            ATR EFFCMP							
;    ICS(1)    ICS(2)    ICS(3)    ICS(4)    ICS(5)							
;        1            0            0            0            0							
;    NIND NMACH NALT NRPM							
;        3            8            5            5							
;    Mach Number							
;        .01    .21    .41    .61    .81    1.01    1.21    1.41							
;    Altitude (feet)							
;        .0        500.0    1000.0    1500.0    2000.0							
;    Engine RPM							
;        70000.0    75000.0    80000.0    85000.0    90000.0							
;    ATR Comp Efficiency							
.77	.77	.77	.77	.77	.77	.77	.75
.71							
.77	.77	.76	.77	.77	.77	.77	.75
.71							
.77	.77	.76	.77	.77	.77	.77	.75
.71							
.76	.76	.77	.77	.77	.77	.77	.75
.72							
.76	.76	.77	.77	.77	.77	.77	.76
.72							
.79	.80	.80	.81	.81	.81	.80	.78
.76							
.79	.79	.80	.81	.81	.81	.80	.78
.76							
.79	.79	.80	.81	.81	.81	.80	.79
.76							
.79	.79	.80	.80	.81	.81	.80	.79
.76							
.79	.79	.79	.79	.80	.81	.81	.80
.79							
.79	.79	.79	.79	.80	.81	.81	.80
.79							
.78	.79	.79	.79	.80	.81	.81	.80
.79							
.78	.79	.79	.79	.80	.80	.80	.81
.79							
.78	.78	.79	.79	.80	.80	.80	.81
.79							
.75	.76	.76	.77	.79	.79	.79	.80
.81							
.75	.75	.76	.77	.79	.79	.79	.80
.81							
.75	.75	.76	.77	.78	.79	.79	.80
.81							
.75	.75	.76	.77	.78	.79	.79	.80



.80							
.75	.75	.76	.77	.78	.79	.80	
.80							
.72	.72	.73	.74	.75	.77	.79	
.79							
.72	.72	.73	.74	.75	.77	.79	
.79							
.72	.72	.73	.74	.75	.77	.79	
.79							
.72	.72	.73	.74	.75	.77	.79	
.79							
.72	.72	.73	.74	.75	.77	.78	
.79							
TABLE	ATR EFFTRB						
; ICS(1)	ICS(2)	ICS(3)	ICS(4)	ICS(5)			
1	0	0	0	0			
; NIND	NMACH	NALT	NRPM				
3	8	5	5				
; Mach Number							
.01	.21	.41	.61	.81	1.01	1.21	1.41
; Altitude (feet)							
.0	500.0	1000.0	1500.0	2000.0			
; Engine RPM							
70000.0	75000.0	80000.0	85000.0	90000.0			
; ATR Turb Efficiency							
.51	.51	.51	.51	.51	.51	.51	.51
.51							
.51	.51	.51	.51	.51	.51	.51	.51
.51							
.51	.51	.51	.51	.51	.51	.51	.51
.51							
.51	.51	.51	.51	.51	.51	.51	.51
.51							
.51	.51	.51	.51	.51	.51	.51	.51
.51							
.53	.53	.53	.53	.53	.53	.53	.53
.53							
.53	.53	.53	.53	.53	.53	.53	.53
.53							
.53	.53	.53	.53	.53	.53	.53	.53
.53							
.53	.53	.53	.53	.53	.53	.53	.53
.53							
.53	.53	.53	.53	.53	.53	.53	.53
.53							
.54	.55	.55	.55	.55	.55	.55	.55
.55							
.54	.54	.55	.55	.55	.55	.55	.55
.55							
.54	.54	.55	.55	.55	.55	.55	.55
.55							
.54	.54	.55	.55	.55	.55	.55	.55
.55							
.54	.54	.54	.55	.55	.55	.55	.55
.55							
.55	.55	.56	.56	.55	.55	.55	.55
.56							
.55	.55	.56	.56	.55	.55	.55	.55
.56							
.55	.55	.55	.56	.56	.55	.55	.55
.56							
.55	.55	.55	.56	.56	.55	.55	.55



.56						
.55	.55	.55	.56	.56	.55	.55
.56						
.56	.56	.56	.56	.56	.56	.56
.56						
.56	.56	.56	.56	.56	.56	.56
.56						
.56	.56	.56	.56	.56	.56	.56
.56						
.56	.56	.56	.56	.56	.56	.56
.56						
.56	.56	.56	.56	.56	.56	.56
.56						

## TABLE ATR MR

ICS(1)	ICS(2)	ICS(3)	ICS(4)	ICS(5)
1	0	0	0	0

NIND	NMACH	NALT	NRPM
3	8	5	5

Mach Number							
.01	.21	.41	.61	.81	1.01	1.21	1.41

Altitude (feet)				
.0	500.0	1000.0	1500.0	2000.0

Engine RPM				
70000.0	75000.0	80000.0	85000.0	90000.0

ATR Mixture Ratio (f/air)						
.12	.12	.12	.12	.12	.12	.12
.12						
.12	.12	.12	.12	.12	.12	.12
.12						
.12	.12	.12	.12	.12	.12	.12
.12						
.12	.12	.12	.12	.12	.12	.12
.12						
.12	.12	.12	.12	.12	.12	.12
.12						
.14	.14	.14	.14	.14	.14	.13
.13						
.14	.14	.13	.14	.14	.14	.13
.13						
.14	.14	.14	.14	.14	.14	.13
.13						
.14	.14	.14	.14	.14	.14	.13
.13						
.14	.14	.13	.13	.14	.14	.13
.13						
.15	.15	.15	.15	.15	.15	.14
.14						
.15	.15	.15	.15	.15	.15	.14
.14						
.15	.15	.15	.15	.15	.15	.15
.14						
.15	.15	.15	.15	.15	.15	.15
.14						
.17	.17	.17	.16	.16	.16	.16
.16						
.17	.17	.17	.16	.16	.16	.16
.16						
.17	.17	.17	.17	.16	.16	.16
.16						
.17	.17	.17	.17	.16	.16	.16



.16						
.17	.17	.17	.17	.16	.16	.16
.16						
.18	.18	.18	.18	.18	.17	.17
.17						
.18	.18	.18	.18	.18	.17	.17
.17						
.18	.18	.18	.18	.18	.17	.17
.17						
.18	.18	.18	.18	.18	.17	.17
.17						
.18	.18	.18	.18	.18	.17	.17
.17						

TABLE ATR ER

ICS(1)	ICS(2)	ICS(3)	ICS(4)	ICS(5)
1	0	0	0	0

NIND	NMACH	NALT	NRPM
3	8	5	5

; Mach Number

.01	.21	.41	.61	.81	1.01	1.21	1.41
-----	-----	-----	-----	-----	------	------	------

; Altitude (feet)

.0	500.0	1000.0	1500.0	2000.0
----	-------	--------	--------	--------

; Engine RPM

70000.0	75000.0	80000.0	85000.0	90000.0
---------	---------	---------	---------	---------

; ATR Equivalence Ratio

.81	.81	.82	.82	.83	.83	.82
.79						
.81	.81	.81	.82	.83	.83	.82
.79						
.81	.81	.81	.82	.83	.84	.82
.79						
.81	.81	.81	.82	.83	.83	.82
.79						
.81	.81	.81	.82	.82	.83	.82
.79						
.91	.92	.91	.92	.93	.92	.91
.89						
.91	.91	.91	.91	.93	.92	.91
.89						
.91	.91	.91	.91	.92	.92	.91
.89						
.91	.91	.91	.91	.92	.92	.91
.89						
.91	.91	.91	.91	.92	.92	.91
.89						
1.01	1.02	1.02	1.03	1.01	1.00	.98
.98						
1.01	1.01	1.02	1.02	1.02	1.00	.98
.98						
1.01	1.02	1.02	1.02	1.02	1.00	.99
.98						
1.01	1.01	1.02	1.02	1.02	1.00	.99
.98						
1.01	1.01	1.01	1.02	1.02	1.00	.99
.98						
1.12	1.12	1.12	1.11	1.10	1.09	1.07
1.05						
1.12	1.12	1.12	1.11	1.10	1.09	1.07
1.05						
1.12	1.12	1.12	1.11	1.10	1.09	1.07
1.05						
1.12	1.12	1.12	1.12	1.10	1.09	1.07



1.05						
1.12	1.12	1.12	1.12	1.10	1.09	1.08
1.05						
1.22	1.23	1.22	1.21	1.20	1.18	1.17
1.15						
1.21	1.23	1.23	1.22	1.20	1.18	1.17
1.15						
1.21	1.23	1.23	1.22	1.20	1.18	1.17
1.15						
1.21	1.22	1.23	1.22	1.20	1.18	1.17
1.15						
1.20	1.21	1.23	1.22	1.20	1.19	1.17
1.16						

## TABLE ATR PC

ICS(1)	ICS(2)	ICS(3)	ICS(4)	ICS(5)
1	0	0	0	0

NIND	NMACH	NALT	NRPM
3	8	5	5

; Mach Number

.01 .21 .41 .61 .81 1.01 1.21 1.41

; Altitude (feet)

.0 500.0 1000.0 1500.0 2000.0

; Engine RPM

70000.0 75000.0 80000.0 85000.0 90000.0

; ATR Combustor Pressure

31.70	32.50	35.00	39.20	45.60	54.60	64.40
73.50						
31.20	32.00	34.10	38.60	44.90	53.80	63.40
72.40						
30.70	31.50	33.60	38.00	44.20	52.90	62.40
71.80						
30.00	30.70	33.10	37.10	43.30	51.80	61.40
70.70						
29.50	30.20	32.60	36.50	42.30	51.00	60.90
69.60						
37.70	38.80	41.40	46.20	53.40	62.50	73.80
85.20						
37.20	38.00	40.60	45.30	52.60	61.70	72.70
83.90						
36.30	37.40	40.00	44.60	51.60	60.80	71.60
82.50						
35.80	36.60	39.40	43.90	50.70	59.80	70.50
81.90						
35.30	36.00	38.60	43.00	49.90	58.90	69.40
80.60						
43.40	44.50	47.50	52.90	60.30	70.40	83.50
97.50						
42.80	43.80	46.80	52.00	59.50	69.40	82.20
96.00						
42.00	43.10	46.10	51.20	58.60	68.50	81.10
94.50						
41.40	42.40	45.30	50.40	57.70	67.50	79.90
93.00						
40.70	41.70	44.50	49.50	56.80	66.40	78.70
91.60						
48.20	49.60	53.10	58.70	67.00	78.50	92.80
108.10						
47.50	48.60	52.30	57.80	66.00	77.30	91.50
106.50						
46.60	47.80	51.30	57.00	65.00	76.20	90.10
104.90						
45.70	47.10	50.50	56.10	64.00	75.00	88.80



103.40						
45.00	46.10	49.60	55.20	63.10	73.90	87.60
101.90						
52.40	54.50	58.00	64.20	73.20	86.20	102.70
119.40						
51.40	53.70	57.10	63.20	72.10	84.90	101.10
117.70						
50.50	52.40	56.40	62.20	71.00	83.60	99.60
115.90						
49.20	51.10	55.60	61.20	69.90	82.40	98.10
114.20						
48.30	49.80	54.70	60.30	68.80	81.10	96.60
112.50						

## TABLE ATR TTCA

ICS(1)	ICS(2)	ICS(3)	ICS(4)	ICS(5)
1	0	0	0	0

NIND	NMACH	NALT	NRPM
3	8	5	5

Mach Number
.01 .21 .41 .61 .81 1.01 1.21 1.41

Altitude (feet)
.0 500.0 1000.0 1500.0 2000.0

Engine RPM
70000.0 75000.0 80000.0 85000.0 90000.0

ATR Combustor Temp (deg R)
----------------------------

2872.70	2912.10	3047.50	3272.30	3612.70	4084.20	4069.90
4016.80						
2849.50	2888.20	3000.30	3242.30	3577.80	4053.40	4068.70
4016.20						
2825.20	2863.20	2973.50	3212.30	3542.80	4011.60	4067.60
4031.70						
2783.50	2820.30	2948.50	3159.20	3496.20	3944.30	4066.70
4031.40						
2760.40	2796.60	2922.40	3130.70	3438.80	3904.10	4077.90
4029.50						
3362.00	3424.50	3564.40	3820.70	4231.80	4284.40	4276.50
4249.20						
3336.00	3375.50	3512.00	3762.50	4188.40	4290.40	4275.30
4248.90						
3286.70	3347.60	3483.00	3729.20	4130.70	4290.40	4275.90
4248.50						
3260.90	3298.90	3454.20	3696.90	4073.10	4290.50	4274.90
4260.00						
3234.80	3272.90	3402.40	3638.10	4031.40	4289.00	4274.10
4259.00						
3834.10	3893.40	4060.40	4350.00	4454.30	4468.50	4457.40
4458.70						
3798.00	3853.80	4020.60	4305.40	4450.10	4469.90	4456.20
4456.60						
3758.80	3816.10	3981.00	4259.60	4448.40	4477.00	4463.60
4456.50						
3723.70	3777.30	3939.10	4216.80	4447.40	4475.50	4462.70
4454.50						
3684.50	3741.30	3897.60	4172.30	4445.80	4473.90	4462.00
4452.80						
4011.30	4086.40	4275.80	4360.00	4381.50	4402.40	4432.90
4474.40						
3971.40	4033.90	4231.30	4358.60	4380.00	4401.00	4431.50
4473.00						
3925.20	3992.80	4181.90	4357.10	4379.90	4400.20	4430.10
4471.50						
3879.50	3952.50	4139.20	4355.70	4378.30	4398.80	4428.60



4469.30						
3840.40	3900.40	4091.20	4354.20	4375.50	4397.30	4425.20
4467.20						
4151.80	4248.00	4257.10	4272.40	4294.80	4321.60	4348.00
4381.20						
4104.70	4209.40	4255.80	4271.20	4293.60	4319.80	4346.70
4379.80						
4057.00	4145.90	4252.90	4269.90	4292.30	4318.60	4346.00
4377.70						
3993.70	4087.10	4252.20	4268.50	4290.40	4317.40	4344.70
4376.30						
3948.50	4022.80	4250.70	4267.10	4289.70	4315.60	4343.30
4374.80						

## TABLE ATR WACORR

; ICS(1) ICS(2) ICS(3) ICS(4) ICS(5)

1	0	0	0	0
---	---	---	---	---

; NIND NMACH NALT NRPM

3	8	5	5
---	---	---	---

; Mach Number

.01	.21	.41	.61	.81	1.01	1.21	1.41
-----	-----	-----	-----	-----	------	------	------

; Altitude (feet)

.0	500.0	1000.0	1500.0	2000.0
----	-------	--------	--------	--------

; Engine RPM

70000.0	75000.0	80000.0	85000.0	90000.0
---------	---------	---------	---------	---------

; ATR Corrected Air Flow (lbm/sec)

1.80	1.79	1.74	1.68	1.59	1.49	1.43
1.37						
1.81	1.79	1.75	1.69	1.60	1.49	1.43
1.37						
1.81	1.80	1.76	1.69	1.60	1.50	1.44
1.37						
1.82	1.81	1.77	1.70	1.62	1.51	1.44
1.37						
1.83	1.81	1.77	1.71	1.63	1.52	1.44
1.38						
1.94	1.92	1.87	1.80	1.68	1.63	1.57
1.50						
1.94	1.93	1.89	1.81	1.69	1.63	1.57
1.51						
1.96	1.94	1.89	1.82	1.71	1.63	1.58
1.51						
1.97	1.96	1.90	1.82	1.72	1.64	1.58
1.51						
1.97	1.96	1.92	1.84	1.73	1.64	1.59
1.52						
2.05	2.03	1.98	1.88	1.83	1.78	1.72
1.64						
2.06	2.05	1.99	1.90	1.82	1.78	1.72
1.65						
2.08	2.05	1.99	1.91	1.83	1.77	1.71
1.65						
2.08	2.07	2.01	1.92	1.83	1.78	1.72
1.66						
2.10	2.07	2.03	1.93	1.84	1.78	1.72
1.66						
2.20	2.17	2.12	2.07	2.03	1.96	1.89
1.81						
2.20	2.19	2.12	2.08	2.03	1.97	1.90
1.81						
2.22	2.20	2.15	2.08	2.04	1.97	1.90
1.81						
2.23	2.20	2.15	2.08	2.04	1.98	1.91



1.82						
2.23	2.22	2.17	2.09	2.03	1.98	1.91
1.82						
2.33	2.32	2.29	2.25	2.21	2.15	2.07
1.99						
2.33	2.32	2.30	2.26	2.21	2.16	2.08
1.99						
2.33	2.34	2.29	2.26	2.22	2.16	2.08
2.00						
2.34	2.33	2.30	2.26	2.22	2.16	2.09
2.00						
2.34	2.34	2.30	2.27	2.22	2.17	2.09
2.00						

## TABLE ATR SM

ICS(1)	ICS(2)	ICS(3)	ICS(4)	ICS(5)
1	0	0	0	0

NIND	NMACH	NALT	NRPM
3	8	5	5

; Mach Number

.01 .21 .41 .61 .81 1.01 1.21 1.41

; Altitude (feet)

.0 500.0 1000.0 1500.0 2000.0

; Engine RPM

70000.0 75000.0 80000.0 85000.0 90000.0

; ATR Stall Margin

.00	.00	.00	.00	.00	71.90	81.20
90.60						
.00	.00	.00	.00	.00	71.90	81.20
90.60						
.00	.00	.00	.00	.00	71.90	81.20
89.10						
.00	.00	.00	.00	.00	75.00	81.30
89.10						
.00	.00	.00	.00	.00	75.00	79.70
89.10						
.00	.00	.00	59.40	50.00	59.40	68.70
81.30						
.00	.00	.00	.00	50.00	56.30	68.80
81.30						
.00	.00	.00	.00	53.10	56.30	68.70
81.30						
.00	.00	.00	.00	56.20	56.30	68.70
79.70						
.00	.00	.00	.00	56.20	56.30	68.80
79.70						
56.30	53.10	50.00	37.50	43.80	50.00	59.40
68.80						
56.30	56.20	50.00	40.60	40.60	50.00	59.40
68.80						
59.40	56.20	50.00	43.80	40.60	46.90	56.30
68.80						
.00	59.40	53.10	43.80	40.60	46.90	56.20
68.80						
.00	.00	56.20	46.90	40.60	46.90	56.20
68.70						
56.20	50.00	43.80	43.70	50.00	56.30	62.50
65.60						
56.20	56.30	43.70	43.80	50.00	56.30	62.50
65.60						
59.40	56.30	50.00	43.80	50.00	56.20	62.50
65.60						
62.50	56.30	50.00	43.80	50.00	56.30	62.50



65.60						
62.50	62.50	53.10	43.80	46.90	56.30	60.90
65.60						
56.30	50.00	53.10	56.30	62.50	65.60	68.80
73.40						
56.30	50.00	53.10	56.20	62.50	65.60	68.80
73.40						
56.30	56.30	50.00	56.20	62.50	65.60	68.80
73.40						
62.50	56.30	50.00	56.30	62.50	65.60	68.70
73.40						
62.50	62.50	50.00	56.30	62.50	65.60	68.80
73.40						

## TABLE ATR RPMCOR

ICS(1)	ICS(2)	ICS(3)	ICS(4)	ICS(5)
1	0	0	0	0

NIND	NMACH	NALT	NRPM
3	8	5	5

Mach Number
.01 .21 .41 .61 .81 1.01 1.21 1.41

Altitude (feet)
.0 500.0 1000.0 1500.0 2000.0

Engine RPM
70000.0 75000.0 80000.0 85000.0 90000.0

ATR Compressor Corrected Speed (rpm)
107722.40 107251.70 105957.80 103927.40 101285.80 98177.20 94746.70

91126.50						
107909.80	107438.30	106142.10	104108.10	101461.70	98347.60	94911.10
91284.40						
108098.10	107625.80	106327.30	104289.70	101638.60	98518.90	95076.30
91443.20						
108282.30	107809.10	106508.30	104467.10	101811.40	98686.30	95237.70
91598.40						
108467.30	107993.30	106690.20	104645.50	101985.10	98854.60	95400.00
91754.30						
115416.80	114912.60	113526.30	111350.80	108520.50	105189.80	101514.40
97635.50						
115617.60	115112.50	113723.70	111544.40	108709.00	105372.40	101690.40
97804.70						
115819.40	115313.40	113922.10	111738.90	108898.50	105556.00	101867.40
97974.90						
116016.70	115509.70	114116.00	111929.00	109083.70	105735.40	102040.40
98141.10						
116214.90	115707.10	114311.00	112120.10	109269.80	105915.70	102214.30
98308.20						
123111.30	122573.40	121094.70	118774.20	115755.20	112202.50	108282.00
104144.50						
123325.50	122786.60	121305.30	118980.70	115956.30	112397.30	108469.80
104325.10						
123540.80	123000.90	121516.90	119188.20	116158.40	112593.10	108658.60
104506.50						
123751.10	123210.40	121723.80	119391.00	116355.90	112784.40	108843.10
104683.80						
123962.60	123420.90	121931.70	119594.80	116554.40	112976.70	109028.60
104862.10						
130805.70	130234.20	128663.10	126197.60	122989.90	119215.20	115049.60
110653.60						
131033.30	130460.80	128886.80	126417.00	123203.50	119422.10	115249.20
110845.40						
131262.00	130688.50	129111.70	126637.40	123418.30	119630.10	115449.80
111038.20						
131485.60	130911.00	129331.50	126852.90	123628.10	119833.40	115645.80



[illegible][illegible][illegible][illegible][illegible][illegible][illegible][illegible]



[illegible][illegible]



[illegible]



**APPENDIX B**

**6-INCH ATR ENGINE DESIGN OPERATION**



\*\*\*\*ATR DESIGN PROGRAM V5.0\*\*\*\*

INPUT CASE DESCRIPTION: ATR DESIGN POINT DESCRIPTION

INPUT PARAMETERS 10-25-1999

VEHICLE/SYSTEM GAS GENERATOR

\*\*\*\*\*

INPUT FILE: ATRDES.INP Fuel: ARC 428 (5-23-95)  
 OUTPUT FILE: ATRDES.DBG Grain TEMP (DEG R) 530.00  
 Idebug (1 is on) 1 PGG/PSIT 5.00  
 MACH NUMBER 3.00 P Drop:gg-turb 300.0  
 ALTITUDE(FEET) 20000.0 Biprop F/O .00  
 Misc Matl Index 1 Matl Index 1

Case L/D 5.63  
 INLET Grain Mass (lbm) 15.61  
 \*\*\*\*\* Case Safety Factor 1.20

IINLET 1  
 previous HARM, but MIL PR TURBINE  
 MDF File: INLET.MDF \*\*\*\*\*  
 Lip Area (Ac) (sq in) 4.10 TYPE: SUNDSTRAND Reentry Turbine (11  
 MDF File: C:\GEMA\DIST\TURB07.MDF

COMPRESSOR TURBINE SCALE FACTOR .550  
 \*\*\*\*\* P DROP:turb-comb 10.000  
 TYPE: Sundstrand 4.57" Mono(1-17-96) BEARING HP LOSS .050  
 MDF File: COMP04.MDF INLET MACH .30  
 SCALE FACTOR: .650 % ADMISSION 100.00  
 tip diameter (in) 2.97

STALL MARGIN (%) 50.0 COMBUSTOR  
 AIR PRESS DROP (PSIA) 3.00 \*\*\*\*\*  
 BLEED AIR (%) .00 MDF File: CMB30.MDF  
 SPEED (RPM) 138461.5 Matl Index 1

Design Type No. 1  
 GEAR BOX Cooling Method Index 1  
 \*\*\*\*\* EFFICIENCY .990  
 SPEED RATIO (TURB/COMP) 1.000 Conv Length (in) 2.5  
 Div Length (in) .3  
 Mach at Entrance .3

NOZZLE  
 \*\*\*\*\*  
 Matl Index 1  
 DISCHARGE COEFF .980  
 EXIT PRESSURE (PSIA) 6.759

OUTPUT PARAMETERS 10-25-1999

VEHICLE/SYSTEM TURBINE

\*\*\*\*\*

OUTPUT FILE: ATRDES.DBG MDF File:C:\GEMA\DIST\TURB07.MDF  
 INPUT FILE: ATRDES.INP TYPE: SUNDSTRAND Reentry Turbine (11  
 THRUST (LBF) 488.9 POWER/WF(HP/LBM/SEC) 609.5  
 CF 1.485 HORSEPOWER 386.7  
 CF ALT ADDITION .000 FLOWRATE(LBM/SEC) .634  
 Isp TCA TOT FLOW(SEC) 200.9 CHK FLOW PARAMETER .3458  
 Isp RAM LOSS (SEC) 550.5 ACTUAL FLOW PAR .3458  
 Isp DEL (SEC) 770.6 CRITICAL PRESS RATIO 1.735  
 THRUST TO AIR FLOW 135.3 TOTAL INLET P(PSIA) 1688.9



AIR VELOCITY (FT/SEC)	3110.59	STATIC INLET PRESS	1604.7
ENGINE MIX RATIO	.1756	ACTUAL PRESS RATIO	8.501
FGROSS THRUST (LBF)	848.7	SPEED (RPM)	138461.5
NET THRUST (LBF)	488.9	1ST CRIT SHAFT SPEED (RPM)	97172.6
RAM DRAG (LBF)	349.2	U/CO	.208
AIR FLOW (LBM/SEC)	3.612	EFFICIENCY	.583
	CO (FT/SEC)	6083.0	
INLET	IDEAL TEMP DROP(R)	647.1	
*****CAUTION!!!*****			
MDF File:INLET.MDF	*****CHECK TURB TIP SPEED!!!*****		
TYPE: previous HARM, but MIL PR	TIP SPEED (FT/SEC)	1262.7	
Amb Density (lbm/cu in)	.00002358	TOTAL INLET T (R)	2800.0
PT1AIR	248.1	TOTAL EXIT P(PSIA)	198.7
PT2AIR	106.2	STATIC EXIT PRESS (PSIA)	198.7
Press Recovery	.428	Manifold Flow Area (sq in)	.12
TT1AIR	1252.7	THROAT AREA (SQ IN)	.19
TT2AIR	1252.7	TIP DIAMETER (IN)	3.80
STA 1 GAMMA	1.364		
STA 2 GAMMA	1.364	COMBUSTOR	
A0/Ac Critical	1.000	*****	
PR Critical	1.000	MDF File:CMB30.MDF	
A0/Ac Actual	1.000	FLOWRATE (LBM/SEC)	4.247
PR Actual	.428	PRESSURE (PSIA)	188.7
Max Inlet Air Flow (lbm/sec)	3.613	TCA MIXTURE RATIO	.176
Dynamic Pressure (psia)	42.55	MAX(IDEAL) TEMP (R)	4568.6
Cd Cowl	.0610	EFFICIENCY	.990
Cowl Drag (lbf)	10.65	ACTUAL TEMP (R)	4522.9
Cd Spillage	.0000	CHOKED FLOW PAR	.500
Spillage Drag (lbf)	.00	Cp (BTU/LBM-R)	.5253
Total Inlet Drag (lbf)	10.65	STOICH MIX RATIO (FUEL/AIR)	.148
Pressure Margin (%)	57.2	EQUIVALENCE RATIO	1.1887
Spillage Margin (%)	.0	MOLECULAR WT(LBM/LBMOLE)	29.470
Mode: supercritical	CSTAR (FT/SEC)	4350.665	
	GAMMA	1.147	
COMPRESSOR	Cyl Comb Diameter (in)	2.83	
*****		Cyl Comb Flow Area (sq in)	6.31
MDF File:COMP04.MDF	THROAT AREA (SQ IN)	3.09	
Type: Sundstrand 4.57" Mono(1-17-96)	Throat Diameter (in)	1.98	
CORR SPEED (RPM)	89122.2	Combustor Ka (sec^2*in^4/lbm^2)	1.99
MECH SPEED (RPM)	138461.5	Combustor Kb	.0091
PRESSURE RATIO	1.805	Effective air flow area (sq in)	5.42
EFFICIENCY	.762	Aero loading parameter	.0000
COMPRESSOR UNCHOKED FLOW			
HORSEPOWER	368.3	NOZZLE	
FLOWRATE (LBM/SEC)	3.612	*****	
POWER/WAIR(HP/LBM/SEC)	102.0	PR CHOKE	1.739
CORR FLOWRATE(LBM/MIN)	1.204	PRESS RATIO	27.936
PRESSURE DROP(PSIA)	3.00	P EXIT(PSIA)	6.8
EXIT PRESSURE(PSIA)	191.68	EXIT VEL (FT/SEC)	6429.9
EXIT TEMP (R)	1533.4	EXIT AREA (SQ IN)	15.43
AMBIENT GAMMA	1.400	Exit Diameter (in)	4.43
THETA	2.414	AREA RATIO	4.99
DELTA	7.224	Throat Only Isp (sec)	1089.5
	Throat P Static (psia)	108.5	
GAS GENERATOR	Throat Velocity (ft/sec)	2855.12	
*****			



MDF File:CMB30.MDF  
PRESSURE (PSIA) 1988.9230  
FLOWRATE (LB/SEC) .634  
THROAT AREA (SQ IN) .0576  
Burn Rate (in/sec) .815  
BURN AREA (SQ IN) 15.511  
Burn Dia (in) 4.444  
CHK FLOW PARAMETER .3458  
ACTUAL FLOW PAR .2929  
CRITICAL PRESS RATIO 1.735  
ACTUAL PRESS RATIO 1.239  
EXIT STATIC PRESS (IDEAL) 1604.7240  
TURBINE INLET STATIC PRESS 1604.7240  
GAMMA 1.140  
MOLECULAR WT(LBM/LBMOLE) 14.17  
TEMPERATURE (R) 2800.0  
Cp (BTU/LBM/R) 1.1418



**APPENDIX C**

**6-INCH ATR ENGINE OFF-DESIGN OPERATION**



```

; ATR MASTER DATA FILE (ATR.MDF)
; Written by ATR Off-Design Code
; ATR Design Summary:
; Fuel is ARC 428 (5-23-95)
; Ifuel= 30
; Design Mach is .50
; Design Altitude (feet) is .0
; Design Engine Speed (rpm) is 75000.0
; Compressor is Sundstrand 4.57" Mono(1-17-96)
; Icomp= 4
; Turbine is SUNDSTRAND Reentry Turbine (11
; Iturb= 7
;

```

# TABLE ATR THRUST

```

; ICS(1) ICS(2) ICS(3) ICS(4) ICS(5)
  1   0   0   0   0
; NIND NMACH NALT NRPM
  3   5   3   1
; Mach Number
  .01 .51 1.01 1.51 2.01
; Altitude (feet)
  .0 5000.0 10000.0
; Engine RPM
  90000.0
; ATR Thrust (lbf)
  677.40 788.00 922.90 1495.80 2578.80
  528.30 651.90 786.80 1281.90 2213.40
  .00 502.70 613.00 1089.40 1886.00

```

# TABLE ATR ISP

```

; ICS(1) ICS(2) ICS(3) ICS(4) ICS(5)
  1   0   0   0   0
; NIND NMACH NALT NRPM
  3   5   3   1
; Mach Number
  .01 .51 1.01 1.51 2.01
; Altitude (feet)
  .0 5000.0 10000.0
; Engine RPM
  90000.0
; ATR Specific Impulse
  729.80 748.30 739.90 765.00 765.40
  691.00 708.80 740.50 765.70 767.90
  .00 665.90 684.00 767.10 773.80

```

# TABLE ATR PG

```

; ICS(1) ICS(2) ICS(3) ICS(4) ICS(5)
  1   0   0   0   0
; NIND NMACH NALT NRPM
  3   5   3   1
; Mach Number
  .01 .51 1.01 1.51 2.01
; Altitude (feet)
  .0 5000.0 10000.0
; Engine RPM
  90000.0
; ATR GG Pressure (psi)
  904.01 1150.01 1619.62 6459.74 30605.65

```



631.98 882.22 1175.96 2766.25 22442.85  
 422.49 612.84 846.52 2011.42 14666.01

TABLE ATR WAIR

; ICS(1) ICS(2) ICS(3) ICS(4) ICS(5)  
 1 0 0 0 0

; NIND NMACH NALT NRPM  
 3 5 3 1

; Mach Number  
 .01 .51 1.01 1.51 2.01

; Altitude (feet)  
 .0 5000.0 10000.0

; Engine RPM  
 90000.0

; ATR Air Flow Rate (lbm/sec)  
 5.17 5.80 7.06 11.43 20.32  
 4.43 5.11 5.97 9.71 17.32  
 3.74 4.34 5.07 8.16 14.59

TABLE ATR PRC

; ICS(1) ICS(2) ICS(3) ICS(4) ICS(5)  
 1 0 0 0 0

; NIND NMACH NALT NRPM  
 3 5 3 1

; Mach Number  
 .01 .51 1.01 1.51 2.01

; Altitude (feet)  
 .0 5000.0 10000.0

; Engine RPM  
 90000.0

; ATR PRC  
 3.94 3.88 3.40 2.81 2.24  
 3.80 3.89 3.52 2.91 2.32  
 3.65 3.75 3.56 3.03 2.41

TABLE ATR WF

; ICS(1) ICS(2) ICS(3) ICS(4) ICS(5)  
 1 0 0 0 0

; NIND NMACH NALT NRPM  
 3 5 3 1

; Mach Number  
 .01 .51 1.01 1.51 2.01

; Altitude (feet)  
 .0 5000.0 10000.0

; Engine RPM  
 90000.0

; ATR WF (lbm/sec)  
 .93 1.05 1.25 1.96 3.37  
 .76 .92 1.06 1.67 2.88  
 .62 .75 .90 1.42 2.44

TABLE ATR PRT

; ICS(1) ICS(2) ICS(3) ICS(4) ICS(5)  
 1 0 0 0 0

; NIND NMACH NALT NRPM  
 3 5 3 1

; Mach Number  
 .01 .51 1.01 1.51 2.01

; Altitude (feet)  
 .0 5000.0 10000.0



```

; Engine RPM
90000.0
; ATR Turb Pressure Ratio
12.40 12.10 11.90 11.70 11.50
12.50 12.50 11.90 11.80 11.60
12.60 12.70 12.30 11.80 11.50
TABLE ATR EFFCMP
; ICS(1) ICS(2) ICS(3) ICS(4) ICS(5)
1 0 0 0 0
; NIND NMACH NALT NRPM
3 5 3 1
; Mach Number
.01 .51 1.01 1.51 2.01
; Altitude (feet)
.0 5000.0 10000.0
; Engine RPM
90000.0
; ATR Comp Efficiency
.76 .77 .81 .83 .80
.74 .76 .80 .82 .80
.72 .74 .78 .82 .81
TABLE ATR EFFTRB
; ICS(1) ICS(2) ICS(3) ICS(4) ICS(5)
1 0 0 0 0
; NIND NMACH NALT NRPM
3 5 3 1
; Mach Number
.01 .51 1.01 1.51 2.01
; Altitude (feet)
.0 5000.0 10000.0
; Engine RPM
90000.0
; ATR Turb Efficiency
.54 .55 .55 .55 .56
.54 .54 .55 .55 .56
.53 .54 .55 .55 .56
TABLE ATR MR
; ICS(1) ICS(2) ICS(3) ICS(4) ICS(5)
1 0 0 0 0
; NIND NMACH NALT NRPM
3 5 3 1
; Mach Number
.01 .51 1.01 1.51 2.01
; Altitude (feet)
.0 5000.0 10000.0
; Engine RPM
90000.0
; ATR Mixture Ratio (f/air)
.18 .18 .18 .17 .17
.17 .18 .18 .17 .17
.17 .17 .18 .17 .17
TABLE ATR ER
; ICS(1) ICS(2) ICS(3) ICS(4) ICS(5)
1 0 0 0 0
; NIND NMACH NALT NRPM
3 5 3 1

```



```

; Mach Number
.01 .51 1.01 1.51 2.01
; Altitude (feet)
.0 5000.0 10000.0
; Engine RPM
90000.0
; ATR Equivalence Ratio
1.22 1.23 1.20 1.16 1.12
1.17 1.22 1.21 1.17 1.13
1.13 1.18 1.20 1.18 1.13
TABLE ATR PC
; ICS(1) ICS(2) ICS(3) ICS(4) ICS(5)
1 0 0 0 0
; NIND NMACH NALT NRPM
3 5 3 1
; Mach Number
.01 .51 1.01 1.51 2.01
; Altitude (feet)
.0 5000.0 10000.0
; Engine RPM
90000.0
; ATR Combustor Pressure
55.30 65.00 79.20 129.40 231.80
44.10 54.20 66.80 109.30 195.70
34.90 42.90 53.50 92.20 165.40
TABLE ATR TTCA
; ICS(1) ICS(2) ICS(3) ICS(4) ICS(5)
1 0 0 0 0
; NIND NMACH NALT NRPM
3 5 3 1
; Mach Number
.01 .51 1.01 1.51 2.01
; Altitude (feet)
.0 5000.0 10000.0
; Engine RPM
90000.0
; ATR Combustor Temp (deg R)
3845.70 4255.40 4309.90 4386.20 4480.00
3380.60 3796.10 4295.20 4370.00 4465.10
3000.20 3325.80 3796.90 4351.90 4450.10
TABLE ATR WACORR
; ICS(1) ICS(2) ICS(3) ICS(4) ICS(5)
1 0 0 0 0
; NIND NMACH NALT NRPM
3 5 3 1
; Mach Number
.01 .51 1.01 1.51 2.01
; Altitude (feet)
.0 5000.0 10000.0
; Engine RPM
90000.0
; ATR Corrected Air Flow (lbm/sec)
8.01 7.71 7.22 6.48 5.66
8.10 8.03 7.35 6.63 5.81
8.13 8.11 7.72 6.76 5.94
TABLE ATR SM

```



```

; ICS(1) ICS(2) ICS(3) ICS(4) ICS(5)
  1   0   0   0   0
; NIND NMACH NALT NRPM
  3   5   3   1
; Mach Number
  .01 .51 1.01 1.51 2.01
; Altitude (feet)
  .0 5000.0 10000.0
; Engine RPM
  90000.0
; ATR Stall Margin
  68.70 50.00 56.30 65.60 82.80
  82.80 75.00 56.20 65.60 81.20
  .00 84.40 78.10 62.50 76.60
TABLE  ATR RPMCOR
; ICS(1) ICS(2) ICS(3) ICS(4) ICS(5)
  1   0   0   0   0
; NIND NMACH NALT NRPM
  3   5   3   1
; Mach Number
  .01 .51 1.01 1.51 2.01
; Altitude (feet)
  .0 5000.0 10000.0
; Engine RPM
  90000.0
; ATR Compressor Corrected Speed (rpm)
  74625.00 73144.20 68373.40 62177.70 55799.50
  74625.00 74431.70 69575.00 63268.50 56776.70
  74625.00 74625.00 70852.40 64429.90 57818.90
TABLE  ATR EFFINL
; ICS(1) ICS(2) ICS(3) ICS(4) ICS(5)
  1   0   0   0   0
; NIND NMACH NALT NRPM
  3   5   3   1
; Mach Number
  .01 .51 1.01 1.51 2.01
; Altitude (feet)
  .0 5000.0 10000.0
; Engine RPM
  90000.0
; ATR Inlet Recovery
  1.00 1.00 .87 .89 .94
  1.00 1.00 .85 .87 .92
  1.00 1.00 .82 .85 .90
TABLE  ISOLN
; ICS(1) ICS(2) ICS(3) ICS(4) ICS(5)
  1   0   0   0   0
; NIND NMACH NALT NRPM
  3   5   3   1
; Mach Number
  .01 .51 1.01 1.51 2.01
; Altitude (feet)
  .0 5000.0 10000.0
; Engine RPM
  90000.0
; ISOLN Values (no units)

```



1.00	1.00	1.00	1.00	1.00
1.00	1.00	1.00	1.00	1.00
3.00	1.00	1.00	1.00	1.00